Pre-clinical investigation of carnosine's anti-neoplastic effect on glioblastoma: uptake, signal transduction, gene expression and tumour cell metabolism

Der Medizinischen Fakultät

der Universität Leipzig

eingereichte

H A B I L I T A T I O N S S C H R I F T

zur Erlangung der Lehrbefugnis

doctor rerum medicinae habilitatus

Dr. rer. med. habil.

vorgelegt

von Dr. rer. med. Dipl. Chem. Henry Oppermann

geboren am 10.05.1988 in Leipzig

Tag der Verleihung: 08. 09. 2020

Zusammenfassung

Pre-clinical investigation of carnosine's anti-neoplastic effect on glioblastoma: uptake, signal transduction, gene expression and tumour cell metabolism

Dr. rer. med. Dipl. Chem. Oppermann, Henry

Universität Leipzig, Habilitation

Das Glioblastom ist der häufigste maligne Tumor des zentralen Nervensystems. Trotz leitliniengerechter Therapie, bestehend aus mikrochirurgischer Resektion, Strahlentherapie und ergänzender Chemotherapie mit Temozolomid, beträgt die 2-Jahres-Überlebensrate nur ca. 17%. Daher sind dringend neue Therapieansätze erforderlich. Dem natürlich vorkommenden Dipeptid Carnosin, welches vor über 100 Jahren erstmals isoliert wurde, konnten viele physiologische Funktionen zugeschrieben werden. Zu Beginn unserer Arbeiten war bekannt, dass das Dipeptid das Wachstum von Krebszellen inhibiert, wobei die genauen Mechanismen der antineoplastischen Wirkungsweise weitgehend unbekannt waren. Die Untersuchungen im Rahmen der vorliegenden Habilitationsarbeit setzten sich mit möglichen Wirkmechanismen des Dipeptides auseinander, wobei ebenfalls Fragestellungen zur klinischen Anwendung von Carnosin bearbeitet wurden. Im ersten Abschnitt werden die Transportmechanismen von Carnosin in Glioblastom-Zellen beschrieben. Weiterhin wird die Frage beantwortet, ob das Dipeptid die biologisch aktive Verbindung ist oder ob L-Histidin von Carnosin abgespalten werden muss, um die antineoplastische Wirkung zu entfalten. Der zweite Abschnitt beschäftigt sich mit den Einflüssen von Carnosin auf die Signaltransduktion und Genexpression. Im dritten Abschnitt wird unter anderem mit einem Metabolomics-Ansatz der Stoffwechsel von Glioblastom-Zellen charakterisiert und der Einfluss von Carnosin auf diesen bestimmt. Im vierten Abschnitt wird ein neuartiges Ko-Kultur Modell zur Untersuchung von Carnosins Einfluss auf Glioblastom-Zell-Migration und Koloniebildung vorgestellt. Weiterhin untersuchten wir die möglichen Interaktionen des Dipeptides mit der Standardtherapie von Glioblastomen.

Zusammenfassend zeigten wir, dass Carnosin durch drei verschiedene Transporter aufgenommen werden kann. Das Dipeptid hemmt sowohl Proliferation und Migration von Glioblastom-Zellen. Die Spaltung des Dipeptides ist für seine antineoplastische Wirkung nicht notwendig. In die Zelle aufgenommen, wirkt Carnosin inhibitorisch auf den Pentosephosphatweg. Eine mögliche Erklärung dafür lieferte die beobachte nicht-enzymatische Reaktion von Glycerinaldehyd-3-phosphat mit dem Dipeptid. Weiterhin zeigten unsere Experimente zum ersten Mal eine Carnosin-bedingte Veränderung der Histonacetylierung und eine damit einhergehende Beeinflussung der Genexpression. Da das Dipeptid den Effekt der Radio-/Chemotherapie verstärkt, sollte die Wirkung von Carnosin in einer klinischen Studie an Glioblastom-Patienten untersucht werden.

Abstract

Pre-clinical investigation of carnosine's anti-neoplastic effect on glioblastoma: uptake, signal transduction, gene expression and tumour cell metabolism

Dr. rer. med. Dipl. Chem. Oppermann, Henry

Universität Leipzig, Habilitation

Glioblastoma is the most common malignant tumour of the central nervous system. Only ~17% of patients undergoing standard therapy, including microsurgical resection, radiotherapy and adjuvant chemotherapy using temozolomide survive two years after diagnosis. Hence, new therapeutic approaches are urgently needed. The naturally occurring dipeptide carnosine was discovered more than 100 years ago. Since then, many physiological functions and beneficial effects have been ascribed to it. Previous studies demonstrated that carnosine inhibits growth of cancer cells. However, at the beginning of our investigations were the mechanisms behind carnosine's anti-neoplastic effect mostly unknown. The present work addresses possible modes of action of carnosine and issues regarding the clinical application of the dipeptide. In the first paragraph we describe the transport mechanisms of carnosine in glioblastoma cells. Furthermore, we deal with the problem whether carnosine is the biological active compound or release of L-histidine from the dipeptide is required to deploy its anti-neoplastic effect. The second paragraph addresses the influence of carnosine on glioblastoma cell signal transduction and gene expression. In the third paragraph we characterise the metabolism of glioblastoma cells and how it is influenced by carnosine by using a metabolomics approach. The fourth paragraph introduces a novel co-culture model which allows the analysis of carnosine's impact on glioblastoma cell migration and colony formation. Furthermore, the possible interaction of the dipeptide with the glioblastoma standard therapy is investigated.

In conclusion, we demonstrated that three different transporters are capable for the uptake of carnosine in glioblastoma cells. The dipeptide inhibited in addition to proliferation also migration of glioblastoma cells. Moreover, cleavage of carnosine was not required for its anti-neoplastic effect. After taken up by the cell, carnosine inhibits the pentose phosphate pathway. The observed non-enzymatic reaction of glyceraldehyde-3-phosphate with the dipeptide could possibly explain this effect. Furthermore, our experiments showed for the first time that carnosine influences gene expression by an effect on histone acetylation. As the administration of carnosine arguments the effects of radio-/chemotherapy, we encourage the clinical evaluation of the dipeptide for glioblastoma patients.

Table of Contents

1 Introduction

1.1 Glioblastoma

Tumours of the central nervous system (CNS) are categorized by the World Health Organisation (WHO) into four grades. The grades are based on histological and molecular properties of the tumours, on prognosis and on the response to therapy. In general, WHO grade I tumours are benign and patients have a good prospect of cure. WHO grade II to IV are malignant tumours. The median overall survival of patients suffering from these tumours is more than five years (Grade II), between two and three years (Grade III) and less than one year (Grade IV) (Louis et al. 2007). The most common malignant brain tumour of the CNS is glioblastoma with an incident of 3.21 new cases per inhabitants in the United States (Ostrom et al. 2018) and 3.91 new cases per inhabitants in Europe (Sant et al. 2012). Glioblastoma belongs to the astrocytic tumours and is categorised together with oligodendrogliomas and astrocytomas as glioma. Although it can manifest in patients of any age, persons with a median age at diagnosis of 62 years are more often diagnosed with glioblastoma. Furthermore, males are more frequently affected than females (male/female ratio: 1.26). Several risk factors for glioblastoma have been suggested, such as viral infections and environmental carcinogens (e.g. formaldehyde) but due to inconclusive and contradictory results these factors could not be validated (Ohgaki and Kleihues 2005). Deeply discussed is a possible influence of non-ionizing radiation (e.g. from cell phones) (Morgan 2015; Ostrom et al. 2014). At least, it is confirmed that ionizing radiation (IR) of head and neck increases the risk and that individuals who exhibit allergies or atopic diseases in the past have a reduced risk (Ohgaki and Kleihues 2005). Furthermore, single nucleotide polymorphisms of alleles of the genes telomerase reverse transcriptase (TERT), regulator of telomere elongation helicase 1 (RTEL1), epidermal growth factor receptor (EGFR) and tumour suppressor protein 53 (p53) have been associated with an increased risk (Ostrom et al. 2014). Approximately 5% of patients suffering from malignant glioma have a family history of gliomas. Among this family cases some rare genetic syndromes were reported, including neurofibromatosis type 1 (loss-of-function mutations of the NF1 gene which is a suppressor of Ras) and type 2, the Li−Fraumeni syndrome (germline mutations in the p53 and/or CHEK2 gene) and Turcot's syndrome (mutations in the APC gene which leads to aberrant Wnt signalling activity) (Farrell and Plotkin 2007). Glioblastomas emerging de novo exhibit different localisations. The incidence in the temporal lobe is 31%, 24% in the parietal lobe, 23% in the frontal lobe and 16% in the occipital lobe (Louis et al. 2016). Typical symptoms of

patients suffering from glioblastoma are caused by increased intracranial pressure resulting in nausea, vomiting, seizure and occasionally severe pulsing headache. Based on tumour localisation, further symptoms can occur, such as focal neurologic deficits, confusion, memory loss, and personality changes (Wen and Kesari 2008). Glioblastomas exhibit a comparable large size when first symptoms occur. In rare cases a small tumour can increase its size by several fold after two months (Ohgaki et al. 2014). Due to its rapid and infiltrative growth, supply of nutrients and oxygen of the central tumour mass is reduced, resulting in typical necrotic areas which may comprise more than 80% of the tumour. Histopathologically, glioblastomas exhibit a high cellular density, consist of poorly differentiated, pleomorphic cells, exhibit a high mitotic activity, vascular endothelial proliferation and necrosis (Kleihues et al. 1995). Furthermore, glioblastomas are composed of different cell types, including cells resembling diffuse astrocytoma, oligodendroglioma and granular components and also of small, giant and lipidized cells (Louis et al. 2016). Accompanying the histopathological heterogeneity, glioblastomas contain multiple genetic changes. Among the most important alterations are mutations of the isocitrate-dehydrogenase (*IDH*) 1/2 genes. With 89.3% the most common of them is the gain of function variant *IDH1*^{R132H} (Reitman and Yan 2010). *IDH1/2* mutations are exclusively found in secondary glioblastomas and are almost (~5%) absent in *de novo* formed primary glioblastomas. Therefore, glioblastomas are now also classified according to their *IDH1/2* mutation status (Louis et al. 2016). *IDH*-mutant glioblastomas account for ~10% of all glioblastomas, generally develop from diffuse (WHO grade II) or anaplastic (WHO grade III) astrocytoma and manifest in younger patients (mean age at diagnosis: 45 years) (Ohgaki et al. 2016). *IDH*-wild type and -mutant glioblastoma can both exhibit mutations in the *TERT* (frequency: 70% and 30%, respectively) and the p53 (frequency: 30% and 80%, respectively) gene (*TP53*) and loss of heterozygosity (LOH) on chromosome 10q (frequency: 70% and 60%, respectively). *EGFR* amplification (frequency: 35%) and mutations in the *PTEN* gene (frequency: 25%) only occur in *IDH*-wild type glioblastoma, whereas mutations in the *ATRX* Chromatin Remodeler gene (frequency: 65%) appear only in *IDH*-mutant glioblastoma (Ohgaki and Kleihues 2013).

The prognosis of patients diagnosed with glioblastoma is devastating. Without therapy the median overall survival of patients with *IDH*-wild type glioblastoma is 4.7 months and that of patients with *IDH*-mutant glioblastoma 7.8 months (Ohgaki et al. 2004). Surgical removal of the tumour and subsequent radiotherapy increases median overall survival to 11.3 (*IDH*-wild type) and 27.1 (*IDH*-mutant) months (Nobusawa et al. 2009). Current standard therapy of newly diagnosed *IDH*-mutant and *IDH*-wild type glioblastoma patients consists of 5-aminolevulinic acid supported microsurgical total gross resection (Stummer et al. 2006), followed by radiotherapy with up to 60 Gy and adjuvant chemotherapy with temozolomide (TMZ). This treatment increases the median overall survival of glioblastoma patients

(including both *IDH*-wild type and *IDH*-mutant) to 16 months (Stupp et al. 2017). An important prognostic marker, especially for the treatment with TMZ, is the methylation status of the O-6-Methylguanine-DNA methyltransferase (MGMT) promoter. Patients with tumours carrying a methylated MGMT promoter have a better prognosis compared to patients with an unmethylated MGMT promoter (median overall survival: 15.3 and 11.8 months, respectively) after resection of the tumour and radiotherapy (Hegi et al. 2005). In the same study, patients with MGMT promoter methylation have an even better prognosis when treated with TMZ (21.7 months median overall survival) compared to patient with the unmethylated promoter (12.7 months) (Hegi et al. 2005). Among the currently tested novel therapeutic approaches only treatment with alternating electric fields (tumour-treating fields) which interfere with the spindle apparatus during mitosis, appear to slightly improve median overall survival from 16 to 20.9 months (Stupp et al. 2017). In addition, new molecular and cell-therapeutic approaches have been investigated or are under investigation.

As enhanced angiogenesis is a prominent feature of glioblastoma, inhibition of the vascular endothelial growth factor receptor (VEGF) seemed to be a rational approach. Unfortunately, bevacizumab, a VEGF inhibitory antibody, only increased progression free survival and not overall survival of glioblastoma patients (Gilbert et al. 2014). Due to amplification of the epidermal growth factor receptor (EGFR) in some glioblastomas, nimotuzumab, an EGFR inhibiting antibody, was investigated in a clinical trial. Again and unfortunately, this antibody also revealed no benefit for glioblastoma patients (Westphal et al. 2015).

Recently, exploiting the human immune system became a promising approach in treating various types of cancer. Noteworthy, the discovery of checkpoint inhibitors for cancer therapy was 2018 awarded with the Nobel Prize. For example, nivolumab, a programmed death-1 inhibitor (affects T-lymphocyte activity against target cell), received marketing authorization in the United States and Europe for treatment of metastatic renal cell cancer (Ross and Jones 2017). Unfortunately, the interim analysis of a phase 3 clinical trial investigating nivolumab for treatment of recurrent glioblastoma revealed no benefits on median overall survival over bevacizumab. Nevertheless, some promising effects for long time survivors were reported (Reardon et al. 2017).

Cancer vaccine therapy, either using patient derived tumour lysates or conjugated peptides, have also been clinically evaluated for glioblastoma patients. In the DC-Vax-L clinical trial, whole tumour lysates were used to pulse dendritic cells. After surgery and radiotherapy, patients with newly diagnosed glioblastoma received TMZ and the vaccine or TMZ and placebo. Albeit the data of this study is still blinded, the median overall survival of all patients was reported to be 23.1 months (Liau et al. 2018). The adoptive cellular immunotherapy with chimeric antigen receptor (CAR) T-cells has revolutionised the treatment options for patients

suffering from B-cell non-Hodgkin's lymphoma and leukaemia (Chavez et al. 2019). In brief, this strategy utilizes genetically modified T-cells which recognize a unique extracellular tumour associated antigen which results in specific cancer cell lysis. For glioblastoma treatment interleukin-13 receptor alpha 2 (IL-13Ra2), EGFR mutation variant III (EGFRvIII) and human epidermal growth factor receptor 2 are investigated in several ongoing clinical trials as possible antigens for CAR T-cells (for a review see (Bagley et al. 2018)). In a case report of a patient with recurrent multifocal glioblastoma, injection of CAR T-cells targeting IL-13Ra2 resulted in a dramatic response, completely eliminating initial intracranial and spinal tumours. However, the disease of the patient recurred 228 days after the start of the therapy (Brown et al. 2016).

Rapid growth is a main feature of glioblastoma; requiring specific metabolic pathways which are less active in non-proliferating cells in order to build up biomass (see 1.4 Cancer metabolism). As cancer cells intensively metabolise glucose and as the enzyme expression profile of malignant gliomas does not favour growth depended on ketone bodies (Chang et al. 2013), a ketogenic diet (diet with a ratio of fat to carbohydrate and protein of 4:1) was suggested to be beneficial for glioblastoma patients. Although, the ketogenic diet can be safely applied to glioblastoma patients, no benefits in the progression free survival were observed in a pilot study (Rieger et al. 2014). However, in one case report a ketogenic diet combined with calorie restriction demonstrated the absence of recurrence after standard therapy of a glioblastoma patient until strict diet was quitted (recurrence after ten weeks). Noteworthy, due to the nutritional protocol, therapy was tolerated without using steroids (suppression of oedema resulting from radiation and chemotherapy) (Zuccoli et al. 2010). Hence, dietary treatment for glioblastoma is under further investigation with promising results after a 24-month follow-up of one patient (Elsakka et al. 2018).

Although promising approaches are under investigation to improve the outcome of glioblastoma patients, standard therapy is still restricted to neurosurgery and radio-/chemotherapy. Therefore, new therapeutic options are urgently needed to treat malignant gliomas. A potential approach to treat glioblastoma may be provided by the natural occurring dipeptide carnosine, as it was shown to inhibit aggressive tumour growth (see 1.3.2 Carnosine and cancer).

1.2 Distribution and physiology of carnosine

In 1843 the chemist Justus Liebig started to analyse the composition of meat from different animals. Over the course of his investigations he developed an extract which Liebig believed could be used as meat substitute. One decade later Liebig administered his extract to the daughter of his friend, suffering from typhus getting progressively weaker, as she couldn't take up food. Due to Liebig's meat extract the daughter of his friend was able to recover. In 1861 Georg Gilbert gained interest in Liebig's meat extract as he was looking for a use for the meat of livestock which were raised in Uruguay only for the production of pelt, animal fat, bones and horn. In cooperation with Justus Liebig, Gilbert started 1863 to sell his produced meat extract under the name: "Extractum Carnis Liebig" (Judel 2003).

In 1900 Gulewitsch and Amiradžibi analysed the composition of Liebig's meat extract and identified an organic base with the chemical formula $C_9H_{14}N_4O_3$ which they named carnosine (Gulewitsch and Amiradžibi 1900). Carnosine revealed to be a dipeptide which consists of the amino acids β-alanine and L-histidine (Gulewitsch 1911).

1.2.1 Distribution of histidine containing dipeptides in mammals

After the discovery of the dipeptide several other animal tissues were analysed for their carnosine levels. It turned out that bird muscle tissue contains mostly a methylated derivate of carnosine, anserine (β-alanyl-N3-methyl-histidine) which was named after goose (Latin: anser) wherein it was first discovered (Ackermann et al. 1929). In snake and whale muscle tissue β-alanyl-N1-methyl-histidine was abundantly found which is also known as ophidine and balenine, respectively (Suyama and Maruyama 1969). In general, skeletal muscle tissue contains an abundant amount of carnosine, anserine and/or ophidine (preference name). Therefore, carnosine, anserine and ophidine are often collectively called imidazole or histidine containing dipeptides, whereby the ratio of each dipeptide strongly varies across different species (for a comprehensive review covering the distribution, physiology and pathophysiology of carnosine see (Boldyrev et al. 2013)).

Histidine containing dipeptides are not exclusively present in skeletal muscle. In mice, carnosine reaches a concentration of ~1.8 mmol/kg tissue in the olfactory bulb which is comparable to mouse skeletal muscle (~1.15 mmol/kg tissue). Significantly lower amounts of carnosine were determined in the choroid plexus (~0.2 mmol/kg tissue), the cerebral cortex (~0.075 mmol/kg tissue), the kidney (~0.05 mmol/kg tissue) and the spleen (~0.03 mmol/kg

tissue). Blood plasma and cerebrospinal fluid exhibit with ~2.5 µM and ~8.6 µM the lowest carnosine concentrations (Kamal et al. 2009). Cardiac muscle of mammalians exhibits similar to skeletal muscle imidazole containing compounds in the millimolar range. In the case of guinea pigs, cardiac muscle contains 0.14±0.04 mmol carnosine per kg wet weight, 1.21±0.05 mmol N-acetylcarnosine and 2.31±0.01 mmol N-acetylanserine (O'Dowd et al. 1988). Unfortunately, a comprehensive profiling of the concentrations of histidine containing dipeptides in human tissue has not been performed, yet. However, multiple studies report concentrations of carnosine and its derivatives in different human tissues and body fluids. High carnosine concentrations were determined in skeletal muscle and olfactory bulb with 20.0±4.7 mmol per kg dry weight (Mannion et al. 1992) and 2.2 mmol per kg dry weight (Margolis 1974), respectively. In contrast to mice, carnosine (1.8±0.9 mmol per kg tissue) and anserine (4±2.7 mmol per kg tissue) reach concentrations in the millimolar range in human kidney tissue (Peters et al. 2015). In human brain tissue ~0.03 mmol carnosine per kg dry weigh were detected, whereas it's isomer homocarnosine (γ-aminobutyryl-L-histidine) is present at a much higher concentration with ~0.16 mmol per kg dry weight (Abraham et al. 1962). Accordingly, homocarnosine and not carnosine was detected in the human cerebrospinal fluid. Interestingly, children exhibited a higher concentration (7.9±2.6 µM) than adults (0.1±0.4 µM) (Perry et al. 1968). Regarding human blood plasma, carnosine and anserine were detected with a concentration of ~6.5 µM and ~0.27 µM, respectively (Fonteh et al. 2007). Albeit anserine is ~25-fold lower concentrated in blood plasma, carnosine and anserine are in comparable amounts present in the urine (5.5 µmol/ per mmol creatinine and 7.0 µmol/ per mmol creatinine, respectively) (Bouatra et al. 2013).

1.2.2 Transport and metabolism of histidine containing dipeptides

Tissue and plasma concentrations of carnosine are controlled by different enzymes. The central metabolism is summarized in Figure 1. The synthesis of carnosine from β-alanine and L-histidine is carried out by an ATP-consuming enzyme called carnosine synthase (CS) which is encoded by the *ATPGD1* gene (ATP-Grasp domain containing protein 1). CS (EC 6.3.2.11) features a broad substrate specificity which allows among others the synthesis of homocarnosine, anserine and ophidine (Kalyankar and Meister 1959). The synthesis of histidine containing dipeptides occurs mainly in brain, skeletal and cardiac muscle (Drozak et al. 2010). Furthermore, only specific cell types of the corresponding tissue, such as oligodendrocytes in brain (Hoffmann et al. 1996) or podocytes in kidney (Peters et al. 2015), express CS. Alongside with the cellular expression of CS, substrate availability is the rate-limiting factor for histidine containing dipeptide synthesis. It turned out that the supply of the

non-proteinogenic amino acid β-alanine and not the supply of L-histidine is curial for carnosine-synthesis (Dunnett and Harris 1999).
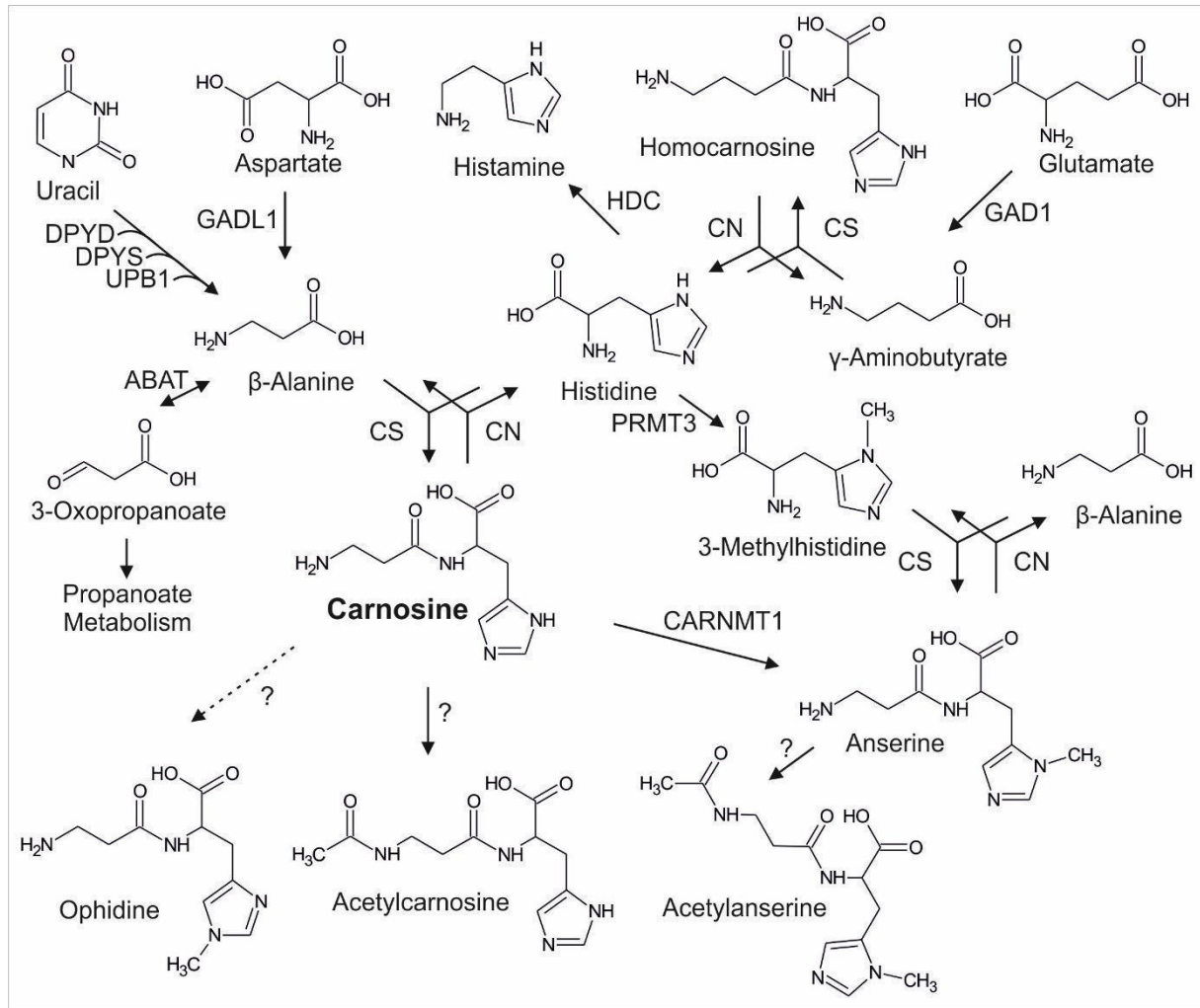

Figure 1 Metabolism of carnosine. Synthesis of carnosine, homocarnosine and anserine is catalysed by carnosine synthase (CS), whereas cleavage is carried out by carnosinase (CN). β-Alanine (substrate for carnosine and anserine synthesis) can be formed by decarboxylation of aspartate via glutamate decarboxylase like 1 (GADL1) or by the degradation of uracil via dihydropyrimidine dehydrogenase (DPYD), dihydropyrimidinase (DPYS) and beta-ureidopropionase 1 (UPB1). 4-Aminobutyrate aminotransferase (ABAT) converts β-alanine to 3-oxopropanoate which is further processed via the propanoate metabolism pathway. For homocarnosine synthesis, γ-aminobutyrate is required which is formed by decarboxylation of glutamate via glutamate decarboxylase 1 (GAD1). Histidine is decarboxylated by histidine decarboxylase (HDC) forming histamine. Anserine can either be formed from 3-methylhistidine which is produced by protein arginine methyltransferase 3 (PRMT3) via methylation of histidine or by direct methylation of carnosine via carnosine N-methyltransferase 1 (CARNMT1). ?: It is currently unknown whether acetylcarnosine and acetylanserine are formed by a specific enzyme or non-enzymatically. The formation of ophidine has not been detected in humans (dashed line). Furthermore, it is unknown whether ophidine is formed by a specific methyltransferase.

β-Alanine is an intermediate of the pyrimidine degradation pathway which occurs manly in liver (Wasternack 1978). In this pathway uracil is converted by dihydropyrimidine dehydrogenase (DPYD), dihydropyrimidinase (DPYS) and beta-ureidopropionase 1 (UPB1) to β-alanine which is further degraded in the propanoate pathway yielding acetyl-CoA. As β-alanine production by liver is comparable low, carnosine biosynthesis depends primarily on nutritional uptake of β-alanine (Artioli et al. 2010). The transport of the amino acid though cell

membranes is performed by the taurine transporter (Artioli et al. 2010). Noteworthy, β-alanine can also be generated by decarboxylation of aspartate via glutamate decarboxylase like 1 (Liu et al. 2012). In order to synthesise homocarnosine, γ-aminobutyrate is required which can be formed from glutamate by the enzyme glutamate decarboxylase 1. Due to the abundant availability of the neurotransmitter γ-aminobutyrate (GABA) in nervous tissue, homocarnosine is presumably exclusively present in the brain (Bauer 2005). The formation of anserine in the human body was unclear for a long time. Albeit its precursor 3-methylhistidine can be synthesised by protein arginine methyltransferase 3, the direct methylation of carnosine by the recently discovered human carnosine N-methyltransferase 1 which is restricted to kidney, seems to be its primary source (Drozak et al. 2015). In contrast, a specific methyltransferase which is required to produce ophidine has not been identified in humans, yet. Furthermore, the formation of ophidine in humans is unlikely, as ophidine has not been detected in human tissues and/or body fluids.

Carnosine and its related compounds contain non-proteinogenic amino acids which prevent these dipeptides from degradation by regular aminopeptidases (aminopeptidases have in general a broad substrate specificity, as these enzymes are involved in the degradation of proteins and peptide hormones – for a review see (Sanderink et al. 1988)). Nevertheless, two enzymes which belong to the M20 metalloprotease family are known to degrade carnosine in humans (for a review see (Bellia et al. 2014)). The first enzyme (EC 3.4.13.20), a homodimeric dipeptidase, is encoded by the carnosine dipeptidase 1 (*CNDP1*) gene and is exclusively present in serum of primates and the syrian golden hamster and hence, named serum carnosinase (CN1) (Jackson et al. 1991). CN1 is mainly produced in brain and liver. Noteworthy, patients suffering from liver cirrhosis (Peters et al. 2011) or glioblastoma (Gautam et al. 2012) exhibit reduced amounts of CN1 in plasma. The second enzyme (EC 3.4.13.18.) is encoded by the by the carnosine dipeptidase 2 (*CNDP2*) gene and has formerly been designated tissue carnosinase, as it is ubiquitously expressed in human tissue. Due to its broad specificity towards many dipeptides it is now named cytosolic nonspecific dipeptidase (CN2) (Teufel et al. 2003). Both dipeptidases are capable to cleave various different histidine containing dipeptides but differ with regard to specificity and activity. CN1 is able to degrade carnosine, anserine, homocarnosine and other β-alanine containing dipeptides (Jackson et al. 1991). In contrast, CN2 is not able to cleave homocarnosine. Additionally, CN2 cleaves carnosine only with low activity compared to other histidine containing dipeptides such as Met-His, Leu-His or Ala-His (Okumura and Takao 2017). Noteworthy, albeit not expressed in humans, a third dipeptidase named anserinase (EC 3.4.13.5) is known to be capable to hydrolyse carnosine, anserine and homocarnosine (Oku et al. 2012).

In order to be taken up by the cell, carnosine needs to be actively transported through biological membranes. This can be performed by membrane proteins of the proton-coupled oligopeptide transporters (POT) family. In mammals, four members of the POT family namely peptide transporter 1 (PEPT1, encoded by the *SLC15A1* gene), peptide transporter 2 (PEPT2, encoded by the *SLC15A2* gene), peptide/histidine transporter 1 (PHT1, encoded by the *SLC15A4* gene) and peptide/histidine transporter 2 (PHT2, encoded by the *SLC15A3* gene) have been identified (for a review see (Smith et al. 2013)). In general, POTs use an inwardly-directed proton gradient to transport a wide range of di- and tripeptides, which are especially formed upon protein breakdown and peptide-like drugs. While PEPT1 and PEPT2 are able to transport 400 different dipeptides and 8000 different tripeptides, it is only assumed but not confirmed that PHT1 and PHT2 are capable to transport the same range of di- and tripeptides. Nevertheless, PHT's also transport free histidine, whereas PEPT's are not able to transport amino acids (for a review see (Daniel and Kottra 2004)). PEPT1 is abundantly expressed in the small intestine, but also detected in kidney, liver, pancreas and prostate tissue (Herrera-Ruiz et al. 2001; Ogihara et al. 1996). In brain, PEPT2 is responsible for peptide uptake from of the cerebrospinal fluid (Ocheltree et al. 2004) which is of importance for fluorescence-guided neuro surgery of brain tumours (Hou et al. 2019). In contrast to PEPT's, PHT's are ubiquitously expressed across different tissues (Fagerberg et al. 2014). PHT's are supposed to perform the transport of histidine and peptides from the lysosome to the cytoplasm (Sasawatari et al. 2011) and in brain the contribution of PHT1 on cellular uptake has been demonstrated (Hu et al. 2014).

1.2.3 Molecular properties of carnosine

Since its discovery in 1900, several physiological properties of carnosine have been described. Nevertheless, the biological role of carnosine is still not completely understood. Due to the multiple functions observed, carnosine is still an enigmatic compound (Bauer 2005). The first biochemical property was discovered in 1938 by Smith (Smith 1938) observing that carnosine and anserine account for a substantial amount of the buffering capacity in muscle. This effect is due to the pK_a (6.72) of the imidazole ring. As this pK_a is close to a pH of 7 it offers a high proton sequestering capacity under physiological conditions (Sale et al. 2010). Later, it was reported that carnosine acts as a metal ion chelator as it forms complexes in the presence of Cu^{2+} (Dobbie and Kermack 1955). Subsequently, several other stable complexes consisting of carnosine and Ni^{2+}, Zn^{2+}, Co^{2+}, Ca^{2+} and Cd^{2+} were reported (Baran 2000). The metal ion chelating effect of carnosine is based on its

imidazole moiety and most complexes are present in its N^1-H tautomeric form (Gaggelli and Valensin 1990). It has been demonstrated that the complexes containing Ni^{2+} (Ueda et al. 1993), Zn^{2+} (Yoshikawa et al. 1991) or Cu^{2+} (Baran et al. 1995) exhibit antioxidant properties. More importantly, histidine containing dipeptides alone possess an antioxidant activity by metal ion chelation and scavenging of reactive oxygen species (Pavlov et al. 1993) and peroxyl radicals (Kohen et al. 1988) at physiological concentrations. Furthermore, carnosine is also a protective agent against hypochlorite and reactive nitrogen species (Hipkiss 1998a). In detail, the imidazole moiety of carnosine interacts witch reactive oxygen species such as hydroxyl radicals, forming resonance-stabilized radicals (Tamba and Torreggiani 1998). These products exhibit a lower toxicity, as resonance-stabilized radicals are less reactive compared to hydroxyl radicals. Additionally, it has been reported that histidine containing dipeptides inhibit the formation of advanced glycation end-products (AGEs) and advanced lipoxidation end-products (ALEs) by scavenging their precursors such as reducing sugars and reactive carbonyls (Hipkiss 2010). For these effects both moieties of carnosine (β-alanine and L-histidine) are required. As demonstrated for the toxic aldehyde trans-2,3-nonenal the first reaction step is the formation of an α,β-unsaturated imine via the primary amine of the β-alanyl moiety followed by ring closure through an intra-molecular Michael addition proceeding from the N3-H of the imidazole ring. Therefore, carnosine and anserine exhibit a better aldehyde quenching effectivity compared to L-histidine alone (~30% of carnosine's effect). Blocking the primary amine inhibits the scavenging effect (acetylcarnosine exhibits ~20% of carnosine's effect) which emphasizes the importance of the β-alanyl moiety for reactive aldehyde quenching (Aldini et al. 2002). Moreover, in addition to serve as sacrificial molecule to prevent glycation, carnosine and anserine can also reverse glycation of proteins. This mechanism is supposed to be similar to that reported for reactive aldehydes (Szwergold 2005). Carnosine was also reported to interact with nitric oxide. Interestingly, the dipeptide can both stimulate nitric oxide production (Takahashi et al. 2009) and scavenge free nitric oxide. L-histidine alone is also capable to scavenge nitric oxide, but the addition of the β-alanyl moiety (carnosine) strongly increases nitric oxide adduct formation (Nicoletti et al. 2007).

1.3 Carnosine in health and disease

As carnosine was initially discovered and is highly abundant in muscle tissue, its physiological role in skeletal muscle has thoroughly been investigated. High intensity muscle contractions are accompanied with anaerobic glycolysis which leads to the production of L-lactate, drop of pH values and ultimately acidosis which decreases the ability of the muscle to generate force. Carnosine's role as physiological pH-buffer was confirmed by increasing its muscular concentration via β-alanine supplementation which reduced acidosis during high intensity training (Baguet et al. 2010). Nevertheless, the average contribution of carnosine to total human muscle pH buffering amounts to only 7% (Mannion et al. 1992). Hence, it is supposed that carnosine may have additional functions in muscle. The dipeptide reduces the formation of ALEs which can be formed during exercise (Dawson et al. 2002). Furthermore, carnosine stimulates Ca^{2+} release from the sarcoplasmic reticulum and increases Ca^{2+} sensitivity for muscle contraction (Dutka et al. 2012).

In the mammalian brain, homocarnosine is the predominant histidine containing dipeptide. This is possibly due to the fact that the concentrations of γ-aminobutyrate are ~20-fold higher as those of β-alanine in different brain structures (del Rio et al. 1977). As γ-aminobutyrate is the most important inhibitory neurotransmitter in mammalian brain, β-alanine and also carnosine have been proposed to exhibit similar properties (Tiedje et al. 2010). It is assumed that carnosine interacts with glutamatergic neurotransmission as both compounds are co-localised in synaptic terminals of olfactory neurons (Sassoè-Pognetto et al. 1993). Furthermore, carnosine can stimulate glia cells to secrete neurotrophins which promotes neurite outgrowth of neurons activating cognitive function (Yamashita et al. 2018). Nevertheless, definitive evidence for carnosine's role as a neuromodulator is lacking (Marchis et al. 2000). However, unquestioned is the homoeostatic role of histidine containing dipeptides in brain due to their antioxidant properties (Bonfanti et al. 1999). Consequently, it was investigated whether treatment with carnosine could mitigate ischaemic brain damage, as oxidative stress is known to be involved in cell damage during ischaemia. In a mouse model of permanent focal cerebral ischemia, pre- or post-treatment with carnosine reduced infarct size which was also accompanied with the reduction of reactive oxygen species in ischaemic brain areas (Rajanikant et al. 2007).

Accumulation of amyloid-β is one hallmark of Alzheimer's disease. Supplementation of carnosine reduced amyloid-β induced cell toxicity in a transgenic mouse model which emphasises the neuroprotective role of the dipeptide (Corona et al. 2011). Furthermore, carnosine also inhibits the oligomerisation of α-synuclein which is known to be involved in

Parkinson's disease (Kang and Kim 2003). Using a senescence accelerated mouse model Boldyrev and co-workers impressively demonstrated the anti-ageing effect of carnosine, wherein the dipeptide increases average life span and decreased properties of the senescent phenotype such as skin ulcers and lowered reactivity (Boldyrev et al. 1999). This effect was associated with its antioxidant property, inhibited formation of AGEs and ALEs and extension of the cell division capacity (Hayflick limit) possibly by increasing telomerase activity (Ait-Ghezala et al. 2016; Hipkiss 1998b). Nevertheless, the underlying mechanism of the anti-ageing effect of carnosine are still not understood (Hipkiss 2009).

There is also a growing body of evidence that carnosine is involved in the prevention of diabetes. Due to the dipeptide's ability to scavenge reactive carbonyls, to protect from protein glycation and to chelate metal ions, it could mitigate the secondary complications of diabetes such as nephropathy and ocular damage (Hipkiss 2005). Additionally, it was demonstrated that carnosine can control blood glucose levels (Nagai et al. 2012) and insulin response (Forsberg et al. 2015). Moreover, patients suffering from diabetes mellitus type I exhibit reduced carnosine levels in erythrocytes and urine (Gayova et al. 1999). In this context, carnosine also improved wound healing in a type 2 diabetes mouse model (Ansurudeen et al. 2012). It is supposed that the activation of fibroblast proliferation is involved in its positive effect on wound healing (Perel'man et al. 1989). Histamine is known to accelerate wound healing by increasing expression of fibroblast growth factor (Numata et al. 2006). As carnosine can serve as a histamine precursor and as it is known to bind to the histamine H_1-receptor, though with low affinity (O'Dowd and Miller 1998), a histamine related mechanism of carnosine on wound healing has been proposed (Nagai et al. 1986). With regard to treatment of gastric ulcer it has been demonstrated that the Zn^{2+} complex of carnosine (polaprezinc) is more effective than zinc or carnosine alone, possibly due to the longer persistence of polaprezinc in the stomach (Furuta et al. 1995).

1.3.1 Clinical application / trials of histidine containing dipeptides

In the previous sections several functions of carnosine and its related compounds were described. Due to its multifunctional role several applications of carnosine have been discussed. In over fifteen studies the effect of increased intramuscular carnosine on exercise performance was investigated. A meta-analysis concluded that exercise capacity (volunteer individual point of volitional exhaustion) is significantly improved, when a median total of 179 g of β-alanine is supplemented over four weeks (Hobson et al. 2012). The same study also revealed that effect size consisting of different exercise performance measures such as

running and rowing performance, was especially increased when the exercise lasts between one and four minutes.

Carnosine has also been clinically evaluated for the treatment of different neurological disorders (for a review see (Schön et al. 2019)). Chengappa and co-workers reported the improved performance of carnosine treated (2 g per day for three months) adults suffering from chronic schizophrenia in some cognitive tests (Chengappa, K N Roy et al. 2012). Cognitive function was also improved by carnosine treatment (1.5 g per day for twelve weeks) of Persian Gulf War veterans who suffered of a neurological dysfunction termed Gulf War illness (Baraniuk et al. 2013). Boldyrev and co-workers suggested carnosine as adjuvant to L-DOPA therapy of Parkinson's disease patients, as combined treatment with the dipeptide (1.5 g per day) mitigated neurological symptoms such as reduced leg agility and rigidity of hands and legs (Boldyrev et al. 2008). Three clinical trials investigated the effect of carnosine on neurological symptoms of children with autistic spectrum disorder. In a pilot study the daily intake of 0.8 g carnosine improved receptive speech, social attention and behaviour (Chez et al. 2002). Employing a dose of 0.5 g carnosine per day, a later study could not confirm the results of Chez and co-workers, but a significantly reduced sleep disturbance was reported (Mehrazad-Saber et al. 2018). In a third randomized placebo-controlled trial, the daily dose of 0.8 g carnosine was combined with risperidone (atypical antipsychotic) for ten weeks. Compared to risperidone alone (placebo), carnosine significantly reduced hyperactivity and noncompliance (Hajizadeh-Zaker et al. 2018). The daily supplementation of a combination of carnosine and anserine was also reported to improve cognitive functioning in healthy elderly people (Szcześniak et al. 2014). Furthermore, carriers of the ε4 allele of apolipoprotein E, who bear a greater risk of developing Alzheimer's disease, exhibited a benefit on carnosine/anserine supplementation with regard to age related memory decline and alteration of brain blood flow (Ding et al. 2018).

It was demonstrated that polaprezinc (also known as Z-103 and promac) is able to prevent and improve healing of gastric ulcers (Seiki et al. 1990). Polaprezinc is clinically used in Japan to treat gastric ulcers since 1994 (Matsukura and Tanaka 2000) and therefore, the first approved carnosine like drug. Due to its antioxidant properties, polaprezinc was clinically evaluated to mitigate radiotherapy induced toxicity/adverse effects. As the effect of IR evolves by the formation of reactive oxygen and nitrogen species (Spitz and Hauer-Jensen 2014), the zinc carnosine complex significantly supressed the formation of radiotherapy induced oral mucositis in patients with head and neck cancer (Watanabe et al. 2010). In contrast to other antioxidant vitamins (Bairati et al. 2006), polaprezinc did not negatively affect the outcome of patients suffering from head and neck cancer (Watanabe et al. 2010)

and non-small cell lung cancer (Yanase et al. 2015). Just recently, Yehia and co-workers demonstrated in a pilot study including 65 patients that oral supplementation of carnosine (0.5 g per day for three months) protects against oxaliplatin-induced peripheral neuropathy in colorectal cancer patients (Yehia et al. 2019). Additionally to the antioxidant activity of carnosine, a large body of evidence exists on the inhibitory effect of the dipeptide on tumour growth (for reviews see (Gaunitz and Hipkiss 2012; Hipkiss and Gaunitz 2014)).

1.3.2 Carnosine and cancer

The first experimental evidence of carnosine's anti-neoplastic effect was provided by Nagai and Suda in 1986 (Nagai and Suda 1986). In their experiments they implanted tumour cells subcutaneously into mice and administered every second day carnosine by a subcutaneous injection. Carnosine treated animals exhibited reduced tumour growth and prolonged survival compared to control animals. As this work was published in Japanese, it took less attention. Ten years later, Holliday and McFarland demonstrated that carnosine selectively eliminated cervix carcinoma cells from a co-culture with fibroblasts (Holliday and McFarland 1996). After another decade, Renner and co-workers treated cells isolated from human glioblastoma with carnosine and confirmed the anti-proliferative effect of the dipeptide (Renner et al. 2008). Afterwards, the same group investigated the effect of carnosine in a nude mouse model with subcutaneously implanted NIH3T3 cells (mouse fibroblast cell line) which expressed the human epidermal growth factor receptor 2 (Renner et al. 2010b). Tumours grown in animals which received daily peritoneal injections of carnosine displayed growth retardation, were less pleomorphic and exhibited a reduced number of mitotic figures compared to tumours in mice which received NaCl. Horii and co-workers used an athymic nude mouse model with implanted human colon cancer cells to demonstrate that carnosine exerts an anti-proliferative effect also when the dipeptide is administered orally (Horii et al. 2012). In several cell culture experiments the anti-proliferative effect of carnosine was confirmed by different groups using proliferating cells originating from different tissues, namely pheochromocytoma cells (Rybakova and Boldyrev 2012), rat mesangial cells (Huijie Jia et al. 2009), human gastric cancer cells (Zhang et al. 2014), cervical gland carcinoma cells (Bao et al. 2018) and hepatocellular carcinoma cells (Tehrani et al. 2018). Furthermore, *in vitro* experiments also suggest that carnosine inhibits cancer cell invasion via inhibiting matrix metalloproteinases (Chuang and Hu 2008; Hsieh et al. 2019). Consequently, the possible use of carnosine as an anti-cancer (Gaunitz and Hipkiss 2012) agent and possible mechanisms (Hipkiss and Gaunitz 2014) had been discussed.

Due to mutations cancer cells exhibit aberrant activities of various signalling molecules which act in different signalling pathways that are important to control homeostasis, proliferation and differentiation. Different experimental observations suggest that carnosine influences such aberrant signalling pathways in cancer. Son and co-workers observed that carnosine inhibited H_2O_2 induced interleukin 8 protein synthesis which was accompanied by reduced phosphorylation of eukaryotic initiation factor (eIF) 4E, protein kinase B (Akt) and extracellular signal regulated kinase 1/2 (Erk1/2) (Son et al. 2008). The aforementioned signal molecules play key roles in the regulation of mechanistic target of rapamycin complex 1 (mTORC1) signalling which coordinates eukaryotic cell growth and metabolism and which is frequently hyper-activated in cancer (for a review see (Saxton and Sabatini 2017) and Figure 2). Further evidence of carnosine's influence on mTORC1 signalling was provided by
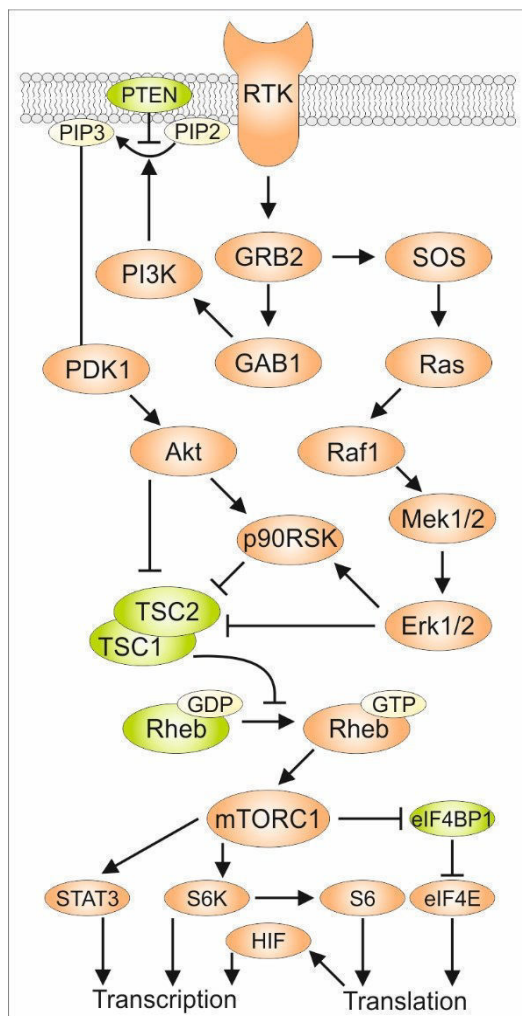

Figure 2 Signal transduction pathways related to the mechanistic target of rapamycin complex 1 (mTORC1). When receptor tyrosine kinases (RTK) are activated, binding of growth factor receptor binding protein 2 (GRB2) occurs, which can activate son of sevenless 1 (SOS). SOS activates rat sarcoma (Ras) by inducing the exchange of GDP with GTP, followed by the activation of Raf1. Active Raf1 directly phosphorylates mitogen-activated protein kinase 1/2 (Mek1/2) which in turn phosphorylates extracellular signal regulated kinase 1/2 (Erk1/2), leading to the interaction of several downstream targets including the activation of ribosomal protein S6 (S6) kinase A1 (p90RSK) and inactivation of tuberous sclerosis 2 (TSC2). GRB2 is also able to interact with the GRB2 associated binding protein 1 (GAB1) which results in the activation of the phospho-inositide 3-kinase (PI3K). PI3K catalyse the conversion of PIP2 to PIP3. Phosphatase and tensin homolog (PTEN) reverse this process. PIP3 recruits phosphoinositide-dependent protein kinase 1 (PDK1) and protein kinase B (Akt) which results in the activation of Akt. Phosphorylated Akt interacts with multiple downstream targets, including p90RSK and TSC2. As the active TSC1/2 complex inhibits phosphorylation of GDP bound to Ras homolog enriched in brain (Rheb) to GTP, inhibition of TSC1/2 results in production of Rheb:GTP, which in turn activates mTORC1. Afterwards, mTOCR1 can phosphorylate the eukaryotic initiation factor 4E (eIF4E) binding protein (eIF4BP1), S6 kinase B1 (S6K) and signal transducer and activator of transcription 3 (STAT3). STAT3 influences the transcription of several genes, including hypoxia-inducible factor 1α (HIF) which is also a key signal transducer. After phosphorylation, eIF4BP1 detaches from eIF4E, enabling cap-dependent translation. Translation is also initiated after phosphorylation of S6 by S6K, whereby S6K can also affect transcription by interfering with other signal transducers. mTORC1 initiated translation positively affects HIF activity. Red: activating nodes; green: inhibitory nodes; ↓: activation; ⊥: inhibition

Rybakova and co-workers who demonstrated the inhibitory effect of the dipeptide on Erk1/2 (Rybakova et al. 2013). More important, Zhang and co-workers suggested carnosine as a mimic of rapamycin, as the dipeptide inhibited Akt/mTORC1/S6K signalling in gastric carcinoma cells (Zhang et al. 2014).

Hypoxia-inducible factor 1α (HIF) is activated during oxygen deprivation and induces the expression of genes that enable the cell to cope with the reduced supply of oxygen and nutrients. HIF overexpression is observed in many types of cancer and thus discussed as a pharmaceutical target to supress tumour growth (for a review see (Masoud and Li 2015)). Bharadwaj and co-workers reported that carnosine inhibited HIF protein expression in cardio myoblasts (Bharadwaj et al. 2002). This observation was confirmed in colon carcinoma cells, in which the dipeptide increased the degradation of HIF (Iovine et al. 2014). At this point it should be noted that active mTORC1 signalling increases translation of HIF mRNA which in turn promotes HIF signalling. Furthermore, mTORC1 also activates the signal transducer and activator of transcription 3 (STAT3) which enhances HIF transcription and hence, strongly connects mTORC1 with HIF signalling (Dodd et al. 2015). A proteomic analysis of glioblastoma cells treated with carnosine revealed a reduction of the Hippel–Lindau binding protein 1 (VBP1) (Asperger et al. 2011) which transports the Hippel-Lindau protein (pVHL) from perinuclear granules to the nucleus or cytoplasm. pVHL itself is a tumour suppressor which initiates the degradation of HIF. Therefore, reduced expression of VBP1 may result in lower amounts of pVHL in the nucleus and the cytoplasm, which in turn will lead to decreased degradation of HIF (Kim et al. 2018). Indeed, Ditte and co-workers demonstrated that the reduced growth of cervix carcinoma xenografts under the influence of carnosine was accompanied with increased HIF protein expression (Ditte et al. 2014). In addition to carnosine's influence on cancer cell signalling, multiple studies report its impact on the cell cycle. Jia and co-workers investigated the influence of carnosine on high glucose-induced rat mesangial cell proliferation and observed cell cycle arrest in G1 phase (Huijie Jia et al. 2009). Furthermore, treatment of HCT116 human colon carcinoma cells with 50 or 100 mM carnosine also resulted in arrest in G1 phase (Iovine et al. 2012). In contrast to that, Rybakova and co-workers reported cell cycle arrest in G2 phase of U118MG glioblastoma cells, after treatment with carnosine or anserine (Rybakova et al. 2015).

Alongside with aberrant cell signalling, changes of cell metabolism are now also considered to be a hallmark of cancer (Hanahan and Weinberg 2011). In brief, a common observation in cancer and proliferating cells is the enhanced uptake of glucose and the release of L-lactate even in the presence of sufficient oxygen. This fermentation of glucose not only provides ATP. Glycolytic intermediates also serve as precursors to fuel metabolic pathways yielding nucleotides, amino acids and lipids which are building blocks for proliferation (see 1.4 Cancer metabolism). Consequently, inhibiting or diminishing glycolysis is considered as strategy to reduce tumour growth (Patra et al. 2013). As carnosine does not further reduce intracellular amounts of ATP in glioblastoma cells after inhibition of the L-lactate producing enzyme lactate dehydrogenase, it was suggested that the dipeptide inhibits glycolytic ATP production (Renner et al. 2010a). Carnosine has been shown to react non-enzymatically with glucose

and dihydroxyacetone phosphate (Hipkiss et al. 1995). Experiments with yeast cells further support carnosine's impact on glycolysis. When yeast cells grow dependent on glycolytic ATP production carnosine lowers proliferation and increases apoptosis, whereas yeast cells depending on oxidative phosphorylation become resistant to carnosine's effect (Cartwright et al. 2012). Nevertheless, two studies also demonstrate that carnosine is able to inhibit mitochondrial respiration in neoplastic cells (Bao et al. 2018; Shen et al. 2014). The pyruvate dehydrogenase complex (PDC) plays a decisive role in glucose oxidation by catalysing the formation of acetyl-CoA from pyruvate. In cancer cells PDC is frequently inhibited due to the over activation of pyruvate dehydrogenase kinases (PDK; not to be confused with phosphoinositide-dependent protein kinase) which leads to an increased formation of L-lactate (McFate et al. 2008). As carnosine was shown to induce the expression of mRNA encoding PDK4, modulation of PDC by carnosine could be responsible for its influence on oxidative metabolism (Letzien et al. 2014). Furthermore, mRNA expression of *PDK4* is controlled by signalling molecules which are known to be relevant for cancer cell growth such as Akt and estrogen-related receptors (for further details see (Gaunitz et al. 2015)). Moreover, is was also demonstrated that PDK4 can affect mTORC1 signalling (Liu et al. 2014).

In conclusion, the anti-neoplastic effect of carnosine was demonstrated by independent groups and in different cancer types both *in vitro* and *in vivo*. However, albeit different mechanisms regarding the dipeptide's anti-tumour activity were suggested, neither the precise mode of action nor a primary target is known.

1.4 Cancer metabolism

One century ago Otto Warburg, a student of Emil Fischer (developed the Fischer-projection of sugars), observed that cancer cells primarily produce L-lactate instead of CO_2 from glucose (fermentation). In general, glucose fermentation takes place under anaerobe conditions. However, Warburg detected increased L-lactate concentrations in venous compared to arterial blood of rats with Jensen sarcoma (Warburg et al. 1927). As this effect was absent in the venous blood of heathy organs, he concluded that fermentation in cancer cells is performed even when sufficient amounts of oxygen are available. This effect is also known as Warburg effect or aerobe glycolysis (Warburg 1956). As Warburg detected that two molecules of L-lactate are produced per molecule glucose, he assumed that cancer cells are forced to ferment glucose due to mitochondrial defects in cancer cells. Albeit his theory was disproved by later investigations, the discovery of the enhanced uptake of glucose remains as a major feature of cancer cells (Hanahan and Weinberg 2011). Increasing the glycolytic rate renders several advantages to support cell growth. First, glycolysis is not only used for energy production. Glycolytic intermediates also serve as precursors for important building blocks required for proliferation such as nucleotides, lipids and amino acids (for a review see (Lunt and Vander Heiden 2011)). Second, fermentation of glucose provides an enhanced ATP production rate compared to glucose oxidation, albeit only two instead of 32 moles of ATP are produced per mole glucose (Pfeiffer et al. 2001). Hence, increasing the glycolytic rate seems to be a reliable strategy for proliferating cells, as less than 7% of consumed glucose are exploited for macromolecule synthesis (DeBerardinis et al. 2007). In order to proliferate, a cell has to synthesise macromolecules which are comparable to the own biomass composition. Simplified, cells consist of carbohydrates, protein, DNA/RNA and lipids which can be synthesised from sugars, amino acids, nucleotides and fatty acids (Watson et al. 2014). As a main nitrogen source for amino acids and nucleotides serves glutamine which is the most abundant amino acid in the human plasma (Stein and Moore 1954). It turned out that glutamine possess a comparable importance for proliferating cells as glucose. Consequently, enhanced glutamine uptake and breakdown was observed to be a common feature of cancer cells (for a review see (Altman et al. 2016)). Most of the metabolic demands for proliferation can be satisfied by glycolysis and glutaminolysis. The metabolic pathways of glucose and glutamine breakdown are illustrated in Figure 3. At this point should be noted that certain cancer cells are able to overcome glutamine restriction by inducing glutamine synthetase expression (Tardito et al. 2015). Several aberrantly regulated signalling pathways have been connected to altered cancer metabolism. For example, PI3K/Akt signalling (Figure 2) increases the expression of glucose transporter GLUT1 and hexokinase 2 (catalyses the phosphorylation of glucose), whereby the latter was connected to tumour
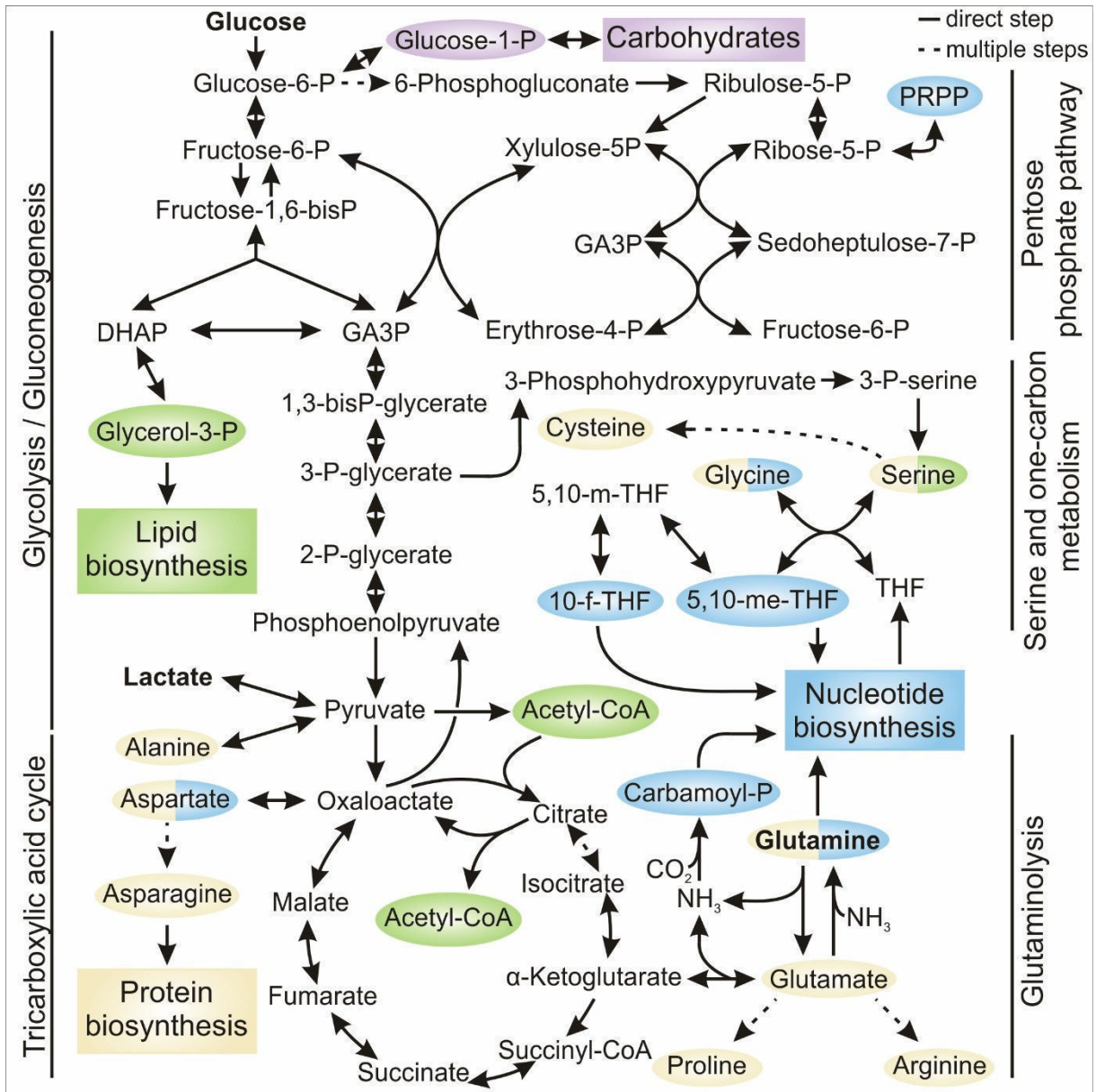
Figure 3 Metabolism of glucose and glutamine in proliferating cells. This simplified diagram shows the metabolic pathways of glucose and glutamine breakdown which are required to produce precursors of macromolecules needed for cell growth. In general, biomass is composed of proteins (yellow), lipids (green), nucleotides (blue) and carbohydrates (violet). Precursors are coloured according to their group of macromolecules. Glucose is taken up by the cell and metabolised via glycolysis yielding pyruvate. Pyruvate can be converted to alanine, lactate or further metabolised in the tricarboxylic acid (TCA) cycle which conduces to the synthesis of several amino acids. After taken up by the cell, glutamine contributes to the anaplerotic flux after conversion to glutamate. Furthermore, glutamine serves as a precursor for carbamoyl phosphate (P) and is needed for the synthesis of purines. Glucose-6-P can alternatively be consumed for carbohydrate (glycogen, maltose, etc.) synthesis via Glucose-1-P or metabolised via the oxidative pentose phosphate pathway (PPP) yielding ribulose-5-P. Fructose-6-P and glyceraldehyde-3-P (GA3P) are also metabolised in the reductive PPP to synthesise ribose-5-P which is further converted to 5-phosphoribosyl-α-pyrophosphate (PRPP). PRPP serves as an important backbone of DNA and RNA. 3-P-glycerate is an important precursor for serine synthesis which is needed for synthesis of proteins, phospholipids and one-carbon units. The latter is generated by a reaction with tetrahydrofolate (THF) yielding glycine and 5,10-methylene-THF (5,10-me-THF). 5,10-me-THF is used for pyrimidine synthesis, whereby it can also be converted to 5,10-methenyl-THF (5,10-m-THF) and further to 10-formyl-THF (10-f-THF) which is needed for purine synthesis. To generate glycerol-3-P which serves as backbone for lipids, dihydroxyacetone phosphate (DHAP) is used. Acetyl-CoA synthesised from pyruvate is conducted in the mitochondria and cannot be used for lipid biosynthesis. Therefore, citrate generated in mitochondria is cleaved by ATP-citrate lyase in the cytoplasm to produce cytoplasmic acetyl-CoA.

initiation (Patra et al. 2013). Furthermore, P53 which is frequently mutated in cancer, inhibits the transcription of several glycolytic genes, whereas HIF and protooncogene MYC induce them (Yeung et al. 2008). Aberrant activity of MYC is also associated with increased glutaminolysis via induced expression of glutaminase 1 (Wise et al. 2008). Moreover, specific expression of splice variants of pyruvate kinase muscle type (catalyses the reaction of phosphoenolpyruvate to pyruvate) can strongly influence the metabolic program of proliferating and quiescent cells (Morita et al. 2018).

Increased uptake of serine was demonstrated to accelerate cell growth. Noteworthy, the serine uptake rate can reach the level of glucose consumption (pmoles per cell per hour) (Labuschagne et al. 2014). Serine is an important intermediate for protein, phospholipid and nucleotide synthesis (for a review see (Mattaini et al. 2016)). For the latter, serine is metabolised in the folate cycle to generate one-carbon units (one-carbon metabolism), whereby an excess of glycine is generated. Albeit glycine can be converted to serine, replacement of serine by glycine inhibits proliferation (Labuschagne et al. 2014). Nevertheless, *de novo* synthesis of serine also plays a crucial role, as overexpression of enzymes required for serine synthesis is accompanied with a poor prognosis of breast and lung cancer patients (Antonov et al. 2014).

Lipids are the main components of biological membranes, which account for ~20% of total glioblastoma biomass (Yates et al. 1979). Most lipids are generated from fatty acids which require acetyl-CoA and NADPH for *de novo* synthesis. Cytosolic acetyl-CoA can be generated from citrate via ATP-citrate lyase, acetate via acetyl-CoA synthetase 2 (Schug et al. 2015) or from branched-chain amino acids catabolism (Crown et al. 2015). Biosynthesis of fatty acids and subsequently of lipids demands large amounts of NADPH (e.g. 26 molecules for cholesterol biosynthesis). Hence, production of NADPH was suggested to be rate limiting for cell proliferation (Vander Heiden et al. 2009). Malic enzyme, IDH1, the oxidative pentose phosphate pathway (PPP) and the serine/one-carbon metabolism serve as sources for NADPH, whereby the latter two pathways are the largest contributors of NADPH for proliferating cells (Fan et al. 2014). In general, fatty acid biosynthesis is restricted to liver, adipose tissue and lactating breast, but proliferating cells, such as cancer cells, reactivate expression of the required enzyme fatty acid synthase (FASN) (Kuhajda et al. 1994; Kusakabe et al. 2000). Hence, FASN was suggested as a target for cancer therapy. Interestingly, the effect of the FASN inhibitor TVB-2640 on the outcome of patients suffering from breast cancer is investigated in a clinical trial (ClinicalTrials.gov ID: NCT03179904). Although activation of *de novo* fatty acid synthesis is a common feature of cancer cells (Kinlaw et al. 2016), uptake of lipids by tumour cells during growth is strongly connected to cancer cachexia (Argilés et al. 2014). Depending on the environmental condition, fatty acids

are stored or directly used for ATP production via β-oxidation, synthesis of biological membranes or signalling molecules such as PIP3 (for a review see (Rohrig and Schulze 2016)). Especially during invasion, cancer cells can change from *de novo* fatty acid synthesis to uptake of specific fatty acids in order to adjust cell membrane fluidity for migration (Zhao et al. 2016). The rearrangement of membrane lipids of cancer cells is also highlighted by a study which identified a specific phosphatidylcholine profile in human colorectal cancer tissue using a mass spectrometry based imaging method (Kurabe et al. 2013).

In conclusion, insight into the metabolic reprograming during cancer initiation/progression offers new potential approaches to treat cancer. Additionally, cancer specific metabolism can be exploited to image tumours using specific radionuclides, such as [18F]fluoro-2-deoxy-D-glucose, 11C-acetate and 11C-methionine for positron emission tomography (Momcilovic and Shackelford 2018).

2 Publications

The following chapters summarise the own experimental efforts to elucidate the mechanisms responsible for the anti-tumour activity of carnosine. This includes the analysis of the cellular uptake and subsequent metabolism of carnosine in glioblastoma cells. Furthermore, the impact of the dipeptide on glioblastoma cell signalling, gene expression and metabolism was investigated. Using a novel co-culture system, we analysed the migratory behaviour of glioblastoma cells under the influence of carnosine. Finally, the interaction of chemo-radiotherapy and carnosine on glioblastoma cell viability was evaluated.

2.1 Uptake and possible cleavage of carnosine in glioblastoma

Previously, it was hypothesized that carnosine develops some of its effects via degradation followed by synthesis of histamine from L-histidine (Figure 1) leading to stimulation of histamine receptors (Zhang et al. 2012). As in cell cultures glioblastoma cells can degrade carnosine only intracellularly (Letzien et al. 2014; Oppermann et al. 2019c), cellular uptake of the dipeptide would be required. Although Son and co-workers demonstrated that carnosine is taken up by epithelial cells (Son et al. 2008), it was unknown which transport mechanism is responsible for uptake in glioblastoma cells. For example, adsorptive-mediated transcytosis is an alternative mechanism to transporters for drug delivery in brain (Lu 2012). As a dipeptide, carnosine could be transported across biological membranes by proton-coupled oligopeptide transporters (POTs). Four members of the POT family are known in mammalians (see 1.2.2 Transport and metabolism of histidine containing dipeptides). In a corresponding study (Oppermann et al. 2019e) we tested the hypothesis whether POTs contribute to the cellular uptake of carnosine in glioblastoma cells. Therefore, we first analysed whether mRNA encoding PEPT1, PEPT2, PHT1 or PHT2 is expressed in glioblastoma tissue and cell cultures. Furthermore, we analysed the mRNA expression of the corresponding genes (*SLC15A1/2/3/4)* in healthy brain tissue. In order to study the functional uptake of carnosine in glioblastoma cells, we used high performance liquid chromatography coupled with mass spectrometry (LC-MS) to determine the dipeptides uptake in the presence of the competitive inhibitors β-alanyl-L-alanine (taken up by all four POTs) and L-histidine (not taken up by PEPT1/2). Finally, we tested the contribution of PEPT2, PHT1 and PHT2 to carnosine uptake after transient transfection of small interfering RNA.

ORIGINAL ARTICLE

The proton-coupled oligopeptide transporters PEPT2, PHT1 and PHT2 mediate the uptake of carnosine in glioblastoma cells

Henry Oppermann[1] · Marcus Heinrich[1] · Claudia Birkemeyer[2] · Jürgen Meixensberger[1] · Frank Gaunitz[1]

Abstract

The previous studies demonstrated that carnosine (β-alanyl-L-histidine) inhibits the growth of tumor cells in vitro and in vivo. Considering carnosine for the treatment of glioblastoma, we investigated which proton-coupled oligopeptide transporters (POTs) are present in glioblastoma cells and how they contribute to the uptake of carnosine. Therefore, mRNA expression of the four known POTs (PEPT1, PEPT2, PHT1, and PHT2) was examined in three glioblastoma cell lines, ten primary tumor cell cultures, in freshly isolated tumor tissue and in healthy brain. Using high-performance liquid chromatography coupled to mass spectrometry, the uptake of carnosine was investigated in the presence of competitive inhibitors and after siRNA-mediated knockdown of POTs. Whereas PEPT1 mRNA was not detected in any sample, expression of the three other transporters was significantly increased in tumor tissue compared to healthy brain. In cell culture, PHT1 expression was comparable to expression in tumor tissue, PHT2 exhibited a slightly reduced expression, and PEPT2 expression was reduced to normal brain tissue levels. In the cell line LN405, the competitive inhibitors β-alanyl-L-alanine (inhibits all transporters) and L-histidine (inhibitor of PHT1/2) both inhibited the uptake of carnosine. SiRNA-mediated knockdown of PHT1 and PHT2 revealed a significantly reduced uptake of carnosine. Interestingly, despite its low expression at the level of mRNA, knockdown of PEPT2 also resulted in decreased uptake. In conclusion, our results demonstrate that the transporters PEPT2, PHT1, and PHT2 are responsible for the uptake of carnosine into glioblastoma cells and full function of all three transporters is required for maximum uptake.

Introduction

More than 100 years ago, Gulewitsch and Amiradžibi isolated and characterized the first dipeptide carnosine (β-alanyl-L-histidine) (Gulewitsch and Amiradzibi 1900). The formation of this naturally occurring dipeptide is catalyzed by carnosine synthase (CARNS1), whereas the degradation of carnosine is performed by serum carnosinase (CNDP1) and with a minor rate by the intracellularly expressed non-specific dipeptidase CNDP2 (Bellia et al.

✉ Frank Gaunitz
  Frank.Gaunitz@medizin.uni-leipzig.de

  Henry Oppermann
  Henry.Oppermann@medizin.uni-leipzig.de

  Marcus Heinrich
  Marcus.Heinrich@medizin.uni-leipzig.de

  Claudia Birkemeyer
  birkemeyer@chemie.uni-leipzig.de

  Jürgen Meixensberger
  Juergen.Meixensberger@medizin.uni-leipzig.de

[1] Klinik und Poliklinik für Neurochirurgie, Universitätsklinikum Leipzig AöR, Forschungslabore, Liebigstraße 19, 04103 Leipzig, Germany

[2] Institut für Analytische Chemie, Universität Leipzig, 04103 Leipzig, Germany

🖄 Springer

2014). Carnosine is highly abundant in the human skeletal muscle with around 20 ± 4.7 mmol per kg dry weight (Mannion et al. 1992). The human brain mostly contains its isomer homocarnosine (γ-aminobutyry-L-histidine) with around 0.16 mmol per kg dry weight, as mostly γ-aminobutyric acid rather than β-alanine is present in brain (Abraham et al. 1962).

Since the discovery of carnosine, several physiological properties have been ascribed to it, such as pH-buffering, scavenging of reactive oxygen species and heavy metal ions, protection from lipid peroxidation, and ischemic brain damage [for a comprehensive review see (Boldyrev et al. 2013)]. Furthermore, an anti-neoplastic effect of carnosine has been demonstrated in vitro and in vivo in different types of cancer, such as human colon carcinoma (Horii et al. 2012), gastric carcinoma (Shen et al. 2014), cervix carcinoma (Ditte et al. 2014), and glioblastoma (GBM) (Oppermann et al. 2016; Renner et al. 2008, 2010). Therefore, the dipeptide has been considered as a possible anti-cancer drug (Gaunitz and Hipkiss 2012; Hipkiss and Gaunitz 2013; Gaunitz et al. 2015).

Especially, with regard to GBM, carnosine's inhibitory effect on tumor cell growth is highly interesting, as this brain tumor is still incurable. With an incidence rate of 3.91 per 100,000 persons in Europe and 3.19 per 100,000 persons in the United States, GBM is the most common malignant primary tumor of the central nervous system (Sant et al. 2012; Ostrom et al. 2016). According to the world health organization (WHO), GBM, which relates to astrocytic tumors, is classified based on its malignancy with the highest WHO grade IV. With the current standard therapy, consisting of surgical removal of the tumor and radiotherapy with adjuvant chemotherapy using temozolomide, the 5-year overall survival of GBM patients is only 2.7% (Sant et al. 2012).

In recent years, we investigated which molecular targets and physiological mechanisms are affected by carnosine, to evaluate, whether it could be employed for the therapy of GBM. Unfortunately, the exact mechanisms by which carnosine exerts its anti-neoplastic effect are still not fully understood, although we could demonstrate that its action is associated with epigenetic regulation (Oppermann et al. 2019a) and an influence on glycolytic ATP production (Oppermann et al. 2016). In addition, we demonstrated that carnosine is also able to prevent migration of GBM cells (Oppermann et al. 2018), which is important for the high malignancy of GBM tumors.

Just recently, we could also show that the anti-neoplastic effect of carnosine is independent from its intracellular cleavage (Oppermann et al. 2019b). However, we did not know how carnosine is taken up by GBM cells which transporters are responsible.

As a dipeptide, carnosine is transported across biological membranes via proton-coupled oligopeptide transporters (POTs). In mammals, four members of the POT family including PEPT1 (encoded by *SLC15A1*), PEPT2 (encoded by *SCL15A2*), PHT1 (encoded by *SLC15A4*), and PHT2 (encoded by *SLC15A3*) have been identified [for a review, see (Smith et al. 2013)]. PEPT1 and PEPT2 are known to mediate the uptake of a wide range of di- and tri-peptides and peptide-like drugs, such as β-lactam antibiotics, angiotensin-converting enzyme inhibitors, the antiviral agent valaciclovir, 5-aminolevulinic acid, or the aminopeptidase inhibitor bestatin, in a proton gradient-dependent manner (Brandsch et al. 2008; Rubio-Aliaga and Daniel 2008). Although PHT1 and PHT2 are able to transport di- and tripeptides, L-histidine is preferably transported by these POTs, due to a high affinity for the amino acid (Yamashita et al. 1997; Sakata et al. 2001). Regarding distribution in tissue, mRNA encoding PHT1 and PHT2 is expressed in various cell types, whereas PEPT1 is mainly expressed in the small intestine, kidney, liver, pancreas, and prostate (Ogihara et al. 1996; Herrera-Ruiz et al. 2001) and PEPT2 in kidney, brain, mammary gland, and lung (Daniel and Kottra 2004).

With regard to tumor specificity, it is important to know which of the aforementioned transporters are responsible for carnosine uptake into GBM cells. In addition, this knowledge becomes therapeutically relevant when carnosine is considered to be combined with other substances that may affect a transporter system. Therefore, we investigated the four POTs known to be able to transport carnosine with regard to their significance for the dipeptides' uptake into GBM cells.

Materials and methods

Reagents

If not stated otherwise, all chemicals were purchased from Sigma-Aldrich (Taufkirchen, Germany), Merck (Darmstadt, Germany) or Carl Roth (Karlsruhe, Germany). Carnosine was kindly provided by Flamma s.p.a. (Chignolo d'Isola, Italy) and β-alanyl-L-alanine was purchased from Bachem (Bubendorf, Switzerland). cDNA samples from healthy brain tissue were obtained from BioCat ("PCR Ready First Strand cDNA"; Cat.no.: HD-201-ZY; BioCat, Heidelberg, Germany).

Cell culture and tissue samples

U87 and T98G cells were purchased from the ATCC (Manassas, USA) and LN405 cells were obtained from the DMSZ (Braunschweig, Germany). All cell lines were genotyped (Genolytic GmbH, Leipzig, Germany) to confirm their identity.

Primary GBM cell cultures were established from tumor tissue obtained after surgery as described previously

(Oppermann et al. 2018). All patients provided written informed consent according to the German law as confirmed by the local ethics committee. Surgery was performed at the Neurosurgery Department of the University Hospital Leipzig between 2014 and 2017. All samples were diagnosed as GBM and have been approved by the Neuropathology Department of the Leipzig University Hospital (Table 1).

All cells were cultivated in 75 cm² or 175 cm² culture flasks (Sarstedt AG & Co., Nümbrecht, Germany) using 10 mL or 20 mL of standard culture medium (SCM: DMEM 4.5 g/L glucose, without pyruvate, supplemented with 2 mM GlutaMAX™, 1% penicillin streptomycin (all Thermo Fisher Scientific, Darmstadt, Germany) and 10% fetal bovine serum (FBS superior, Biochrom, Berlin, Germany) at 37 °C and 5% CO_2 in humidified air in an incubator.

Transient transfection

Transient transfection was performed using 0.5 μL INTER-FERin™/pmol siRNA (Polyplus, Illkirch, France) according to the manufacturer's recommendation. For transfection, 1×10^5 LN405 cells were seeded in 2 mL of SCM in six-well plates. After an overnight incubation, old medium was removed and replaced by fresh SCM containing the transfection mix (2 mL with an equivalent of 5 pmol siRNA). 96 h later, total RNA was extracted as described below or cells

were used for uptake experiments. SiRNAs used in this study were purchased from Qiagen (Hilden, Germany): siPEPT2 (Hs_SLC15A2_5; #SI04234608), siPHT1 (Hs_SLC15A4_9; #SI04960207), siPHT2 (Hs_SLC15A3_10; #SI04362078), and negative control siRNA (#1022076).

qRT-PCR

Total cellular RNA was extracted from 10^6 cells or from 40 to 80 mg of surgically obtained tumor tissue transferred to RNA later (Qiagen, Hilden, Germany) immediately after surgical removal of tissue. Extraction was performed using a miRNeasy mini kit (Qiagen) according to manufacturer's instructions. The RNA concentration and purity were assessed photometrically using a NanoDrop spectrometer (Thermo Fisher Scientific, Wilmington, DE, USA). The RNA was stored at −80 °C until further use. For cDNA synthesis, the ImProm-II™ Reverse Transcription System (Promega, Mannheim, Germany) according to manufacturer's instructions was used, employing 500 ng of total RNA and random primer sets. DNA amplification was performed on a Rotor-Gene Q system (Qiagen), using SYBR Green (Maxima SYBR Green/ROX qPCR Master Mix, Thermo Fisher Scientific). Beta-actin was used as reference gene. Data analysis was performed using the RotorGene 6 software and

Table 1 Samples used for the experiments

	Age (years)	Gender	Diagn/Locat	Type	Passage/lot no
Patient 1	55	Male	GBM wt	T/C	2
Patient 2	59	Male	GBM wt	T/C	2
Patient 3	41	Male	GBM wt	T/C	3
Patient 4	73	Male	GBM wt	T/C	5
Patient 5	79	Female	GBM wt	T/C	3
Patient 6	63	Female	GBM wt	T/C	3
Patient 7	54	Male	GBM wt	T/C	5
Patient 8	56	Female	GBM wt	T/C	3
Patient 9	74	Male	GBM wt	T	n.a.
Patient 10	57	Male	GBM wt	T	n.a.
Patient 11	75	Male	GBM wt	C	4
Patient 12	74	Male	GBM wt	C	4
Donor 1	28	Male	Frontal lobe	cDNA	Lot no.: B811001
Donor 2	26	Male	Temporal lobe	cDNA	Lot no.: B811001
Donor 3	28	Male	Occipital lobe	cDNA	Lot no.: B811001
Donor 4	41	Male	Parietal lobe	cDNA	Lot no.: B811001
Donor 5	66	Male	Frontal lobe	cDNA	Lot no.: B209070
Donor 6	26	Male	Temporal lobe	cDNA	Lot no.: B509032
Donor 7	28	Male	Parietal lobe	cDNA	Lot no.: A403022

The table shows the samples used in the experiments with age and gender of the patients and donors. In addition, the diagnosis of patients and whether tissue (T) and cell culture (C) were available is indicated. From "donors" only cDNA from healthy brain tissue (obtained from BioCat) was available which was derived from the brain regions indicated. In the last row the passage number is indicated in case cell cultures were available and the Lot Numbers of the samples purchased from BioCat

data were processed as described previously (Letzien et al. 2014). Primer sequences are listed in Supplemental Table 1.

Uptake experiments

Ninety-six hours after transient transfection, cells were washed once with pre-warmed (37 °C) washing buffer (137 mM NaCl, 5.4 mM HCl, 0.41 mM $MgSO_4$, 0.49 mM $MgCl_2$, 0.126 mM $CaCl_2$, 0.33 mM Na_2HPO_4, 0.44 mM KH_2PO_4, 2 mM HEPES, pH 7.4). Afterwards, 1 mL of pre-warmed (37 °C) transport medium (Hanks balanced salt solution, calcium, magnesium, 1 g/L glucose, pH 7.4, Thermo Fisher Scientific, Darmstadt, Germany), containing carnosine and competitive inhibitors as indicated, was added. After 10 min of incubation, cells were washed briefly for three times with 1 mL of ice cold washing buffer and extraction was performed by the addition of ice cold methanol (1 mL per well of a six-well plate was used). The extracts were collected in 1.5 mL reaction vials after 10 min of incubation under constant shaking at 4 °C and evaporated to dryness using a SpeedVac (Thermo Fisher Scientific, Darmstadt, Germany). Extracts were stored at − 80 °C until further analysis.

The use of 1 mM carnosine and 50 mM of competitive inhibitor in transport medium resulted in maximal suppression of carnosine uptake (data not shown). Therefore, this experimental setting was used for all uptake studies. At this point, it should also be emphasized that in the uptake experiments, the cells were exposed to the compounds for only 10 min. The recently described effect of L-histidine (50 mM) on cell viability, however, was observed after 24 and 48 h exposure (Letzien et al. 2014; Oppermann et al. 2019b). In addition, β-Ala-L-Ala (50 mM) does not affect cell viability even after 48 h exposure (Oppermann et al. 2019a).

Derivatization and HPLC–MS analysis

To quantify carnosine, a modified method of Csámpai et al. was used (Csámpai et al. 2004). Extracts were dissolved in 100 μL high-quality water (Milli-Q) followed by the addition of 100 μL of 0.5% (*w/v*) *ortho*-phthalaldehyde (dissolved in methanol). Derivatization was performed at 37 °C and 1000 rpm in a thermomixer for 45 min. After adding 800 μL 0.1% formic acid (in HPLC grade water) to each sample, 200 μL of the obtained solution was transferred into 250 μL conic glass inserts of 2 mL ND10 vials (BGB Analytik, Rheinfelden, Germany), followed by high-performance liquid chromatography coupled to mass spectrometry (HPLC–MS) with 100 μL of sample.

The system used for the detection was an Agilent HPLC 1100 (Agilent, Waldbronn, Germany) consisting of a variable wave length detector (VWD), a well plate autosampler and a binary pump, coupled with a Bruker Esquire 3000 plus electrospray-ionization ion trap mass spectrometer. The employed column was a Phenomenex Gemini 5 μ C18 110 Å, 150 mm × 2 mm with a 2 mm guard column of the same material (Phenomenex Ltd., Aschaffenburg, Germany). The eluent system consisted of two solvents, with eluent A: 0.1% formic acid in acetonitrile and eluent B: 0.1% formic acid in HPLC grade water. Mobile phase flow rate was 0.5 mL/min with the following gradient for separation: 0–10 min 90% B, 90%–0% B within 15 min, 25–35 min 0% B, 0%–90% B within 5 min, and 40–47 min 90% B for column equilibration. Mass spectrometer was operated in positive mode (target mass: *m/z* 300; scan range: *m/z* 70–400), the dry gas temperature was set to 360 °C at a flow rate of 11 L/min and the nebulizer to 70 psi (both nitrogen). Carnosine was quantified by the integration of the peak area of the selective mass trace of the corresponding derivative (*m/z* 343) using Xcalibur 1.4 (Thermo Fisher Scientific, Darmstadt, Germany). The intracellular amount of carnosine was quantified using a carnosine calibration curve with concentrations from 0.1 μM to 1 mM (corresponding to an amount of 10^{-10} to 10^{-7} mol carnosine). For inter-batch correction, a carnosine reference standard (10^{-8} mol) was determined in duplicate. For normalization, protein was extracted by adding 200 μL lysis buffer (77.05 mM K_2HPO_4, 22.9 mM KH_2PO_4, 0.2% TritonX-100, pH 7.8) to the remaining cell layer in the six-well plate (which still contains the proteins), followed by incubation for 45 min on an orbital shaker. Protein concentration was determined using the Pierce 660 nm assay (Thermo Fisher Scientific) according to manufacturer's instructions. Each experiment was performed as sixfold replication.

Database analysis

Comparison of POT expression in human tissues was performed using the data provided by Fagerberg et al. which is available as fragments per kilobase of exon model per million mapped reads (FPKM) (Fagerberg et al. 2014). In addition, we also analyzed data available from the GTEx consortium (in reads per kilobase million; RPKM) (The GTEx Consortium 2015) and from "The Human Protein Atlas" (in transcripts per million; TPM) (Uhlén et al. 2015).

Statistical analysis

Statistical analysis was carried out using SPSS (IBM, Armonk, USA; Version: 24.0.0.2 64-bit). For multiple comparisons, a one-way ANOVA with the Games–Howell post hoc test was used. A significance level of $p < 0.05$ data was considered to be significant. Relative data resulting from two or more parameters (normalization to reference) with a separate mean and standard deviation are presented using

Gaussian error propagation as described before (Letzien et al. 2014).

Results

mRNA expression of peptide transporters in primary GBM cell cultures, GBM cell lines, GBM tumor tissue, and healthy brain

First, we asked whether the transporters, which are possibly responsible for the uptake of carnosine in GBM cells, are expressed on the level of mRNA. Therefore, we extracted the mRNA from ten primary GBM cell cultures and three GBM cell lines followed by the determination of the expression of PEPT1 (*SLC15A1*), PEPT2 (*SLC15A2*), PHT1 (*SLC15A4*), and PHT2 (*SLC15A3*) via qRT-PCR. In this experiment, we also included commercially available cDNA from healthy donors and RNA from tumor tissue directly isolated after surgery. As illustrated in Fig. 1, expression of PEPT1 was neither detectable in healthy brain nor in cell culture and also not in freshly isolated tumor tissue. Compared to healthy brain tissue, all other three transporters, PEPT2, PHT1, and

Fig. 1 mRNA expression of peptide transporters in healthy brain, GBM tissue, and cell cultures. Total mRNA from ten primary GBM cell cultures (C/dark grey boxes/dark diamonds), three cell lines (C/dark grey boxes/white diamonds), ten GBM tissues (GBM/light grey boxes), and healthy brain (N/white boxes) was analyzed for expression of PEPT1, PEPT2, PHT1, and PHT2 using qRT-PCR. Relative expression represents the expression of the gene of interest normalized to the expression of beta-actin. All individual measurements were performed in triplicate. Mean is shown as a small square in the box, the median is illustrated by a horizontal line, first and third quartiles are shown as box, and whiskers indicate outliers with factor 1.5. Asterisks indicate level of significance between the indicated groups as determined by one-way ANOVA with the Games–Howell post hoc test with *$p < 0.05$; **$p < 0.005$; *ns* not significant. Arrows indicate the three individual cell lines used

PHT2 were significantly upregulated in the tumor tissue (PEPT2: 21-fold; PHT1: 13-fold; PHT2:11-fold). Whereas no statistically significant difference between GBM tissue and cell culture was seen with regard to expression of PHT1 (1.6-fold lower), PHT2 exhibited a significantly lower expression in cell culture (2.3-fold lower). Most strikingly, PEPT2 expression appears to be strongly reduced during cultivation of the cells (24.8-fold lower than in GBM tissue) and statistical analysis identified no difference between expression in cell culture and healthy tissue. Comparing the mRNA expression of the detected transporters in cell cultures, PHT2 exhibited a significant 15.4-fold higher mRNA expression than PEPT2 ($p < 0.005$) and PHT1 a significant 96.2-fold higher expression than PEPT2 ($p < 0.005$). Overall, primary GBM cultures and GBM cell lines exhibited a comparable mRNA expression for each transporter.

Carnosine uptake is decreased by competitive inhibitors of peptide transporters

In the previous section, we observed that GBM cells express mRNA of the transporters encoding PEPT2, PHT1, and PHT2. To investigate whether these transporters play a role in carnosine uptake in the cultured cells, we asked whether the dipeptide β-alanyl-L-alanine (β-Ala-L-Ala), which is a substrate of all three transporters, competitively inhibits the uptake of carnosine. In addition, we used L-histidine, which is a substrate of PHT1/2 but not of PEPT2, as a competitive inhibitor to discriminate between uptake mediated by PEPT2 and/or PHT1/2. For the experiments, LN405 cells were incubated in the presence of 1 mM carnosine and 50 mM β-Ala-L-Ala, 50 mM L-histidine, or no inhibitor. After 10 min of incubation, intracellular amounts of carnosine were determined. The result of the experiment is illustrated in Fig. 2. Without any inhibitor, carnosine was taken up at a rate of 0.71 ± 0.15 nmol per mg protein and minute. The presence of 50 mM β-Ala-L-Ala significantly decreased the uptake of carnosine to 0.22 ± 0.04 nmol per mg protein and minute ($p < 0.0005$). In the presence of 50 mM L-histidine, carnosine uptake was decreased to 0.15 ± 0.04 nmol per mg protein and minute ($p < 0.0005$). Statistical analysis revealed only a $p = 0.051$ comparing the effect of both inhibitors which each other.

Carnosine uptake is decreased by knockdown of PEPT2, PHT1, and PHT2

From the experiments presented above, it is obvious that PHT1 and/or PHT2 contribute to the uptake of carnosine, as L-histidine, which does not inhibit PEPT2, significantly attenuated the uptake of the dipeptide. However, this experiment does not unequivocally tell that PEPT2 does not contribute to uptake, as it may be deduced from
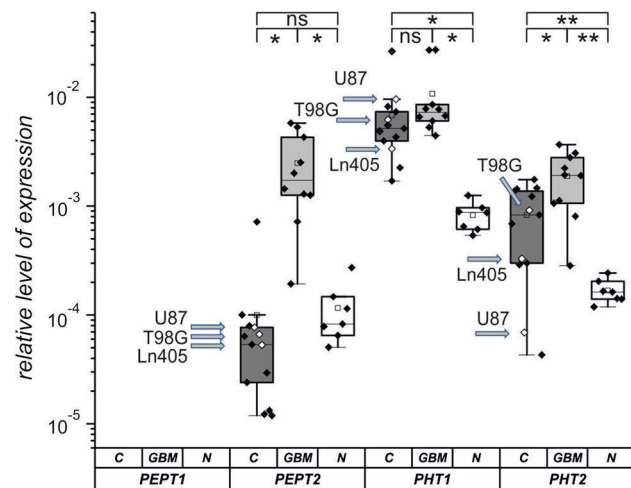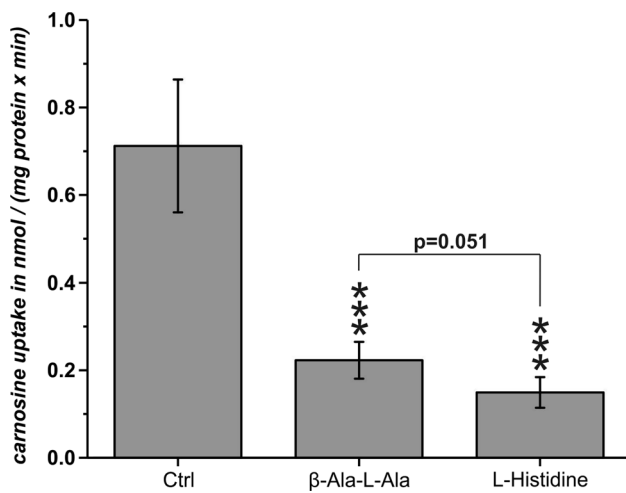
Fig. 2 Influence of competitive inhibitors on the uptake of carnosine in GBM cells from the line LN405. Uptake of carnosine in the presence of an extracellular concentration of 1 mM of the dipeptide in cells from the line LN405 was quantified by HPLC–MS in the presence of β-alanyl-L-alanine (50 mM) and L-histidine (50 mM) as competitors (Ctrl: control cells without inhibitors). All experiments were performed in sextuplicate and mean and standard deviations are presented. Statistical analysis was performed by one-way ANOVA with the Games–Howell post hoc test: ***$p < 0.0005$

the low expression of its corresponding mRNA. Therefore, we analyzed the uptake of carnosine after siRNA-mediated knockdown of PEPT2, PHT1, and PHT2 in LN405 cells. As can be seen in Fig. 3a, transfection of siRNA against
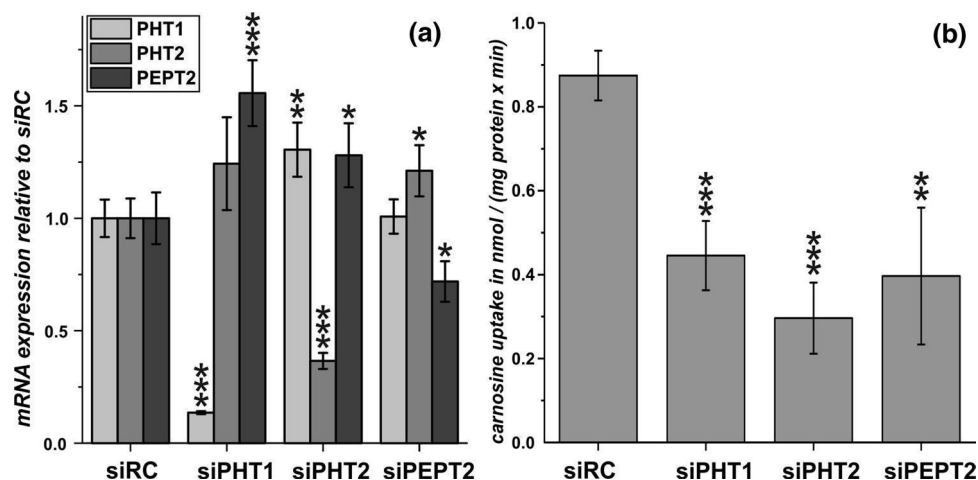
PHT1 reduced the corresponding mRNA expression by $86.4\% \pm 4.1\%$; $p < 0.0005$. Utilizing a specific siRNA targeting PHT2 resulted in a $63.4\% \pm 6.2\%$ reduction of mRNA expression ($p < 0.0005$) and expression of PEPT2 was reduced by $28.1\% \pm 3.5\%$ after transfection with siPEPT2 ($p < 0.05$). Interestingly, we also identified increases of mRNA expression of transporters not targeted by the corresponding siRNA in the single experiments: Targeting PHT1 we observed a significant increase of PEPT2 expression to $156\% \pm 15\%$; ($p < 0.0005$) and a non-significant increase of PHT2 ($124\% \pm 21\%$). In the case of siRNA directed against PHT2, both PHT1 and PEPT2 mRNA expressions were significantly increased [$131\% \pm 12\%$; ($p < 0.005$) and $128\% \pm 14\%$; ($p < 0.05$), respectively]. When PEPT2 was targeted by the specific siRNA, a significant increase of expression was observed regarding PHT2 $121\% \pm 11\%$; ($p < 0.05$) but no effect on expression of PHT1 $101\% \pm 8\%$.

More important, as illustrated in Fig. 3b, employing all three siRNAs resulted in a significant decrease of carnosine uptake [siPHT1: 0.45 ± 0.08 nmol/(mg protein × min) ($50.9\% \pm 9.4\%$) and PHT2: 0.30 ± 0.08 nmol/(mg protein × min) ($33.9\% \pm 9.7\%$), both $p < 0.0005$] compared to negative control: 0.87 ± 0.06 nmol/(mg protein × min), indicating that both PHT1 and PHT2 are responsible for uptake of carnosine in GBM cells. However, despite the low expression of mRNA encoding PEPT2, the knockdown of this transporter also resulted in a significant decrease of carnosine uptake [0.40 ± 0.16 nmol/(mg protein × min) ($44.4\% \pm 17.8\%$), $p < 0.005$].

Fig. 3 Carnosine uptake after siRNA-mediated knockdown of PEPT2, PHT1, and PHT2. Cells from the GBM line LN405 were transfected using negative control siRNA (siRC) and specific siRNAs targeting PEPT2 (siPEPT2), PHT1 (siPHT1), and PHT2 (siPHT2). 96 h after transfection, total mRNA was isolated and analyzed by qRT-PCR and uptake of carnosine was determined by HPLC–MS. **a** Relative expression of mRNA encoding PEPT2, PHT1 and PHT2 in cells transfected with siRNA targeting PEPT2, PHT1 or PHT2 was determined by normalization using expression of beta-actin mRNA as reference. Then, the relative expression of each gene under the influence of the siRNAs was compared to expression in cells transfected with negative control siRNA (set to 1). Experiments were performed in sextuplicate. **b** Quantification of intracellular carnosine 96 h after transfection followed by a 10 min incubation in the presence of 1 mM carnosine. Intracellular amounts of carnosine were normalized to the amounts of protein. Experiments were performed in sextuplicate. Statistical analysis was performed by one-way ANOVA with the Games–Howell post hoc test: *$p < 0.05$; **$p < 0.005$; ***$p < 0.0005$

Discussion

Here, we investigated the uptake of carnosine by cells derived from glioblastoma asking which transporter systems are responsible for this dipeptide. In humans and other mammals, four peptide transporters have been described. The transporters PEPT1 (encoded by *SLC15A1*), PEPT2 (encoded by *SLC15A2*), PHT1 (encoded by *SLC15A4*), and PHT2 (encoded by *SLC15A3*) are members of the evolutionary well-conserved family of proton-coupled transport systems (POTs) (Parker et al. 2017). All POTs are supposed to be able to transport carnosine, being responsible for either its uptake or its release. At the brush border membrane of intestinal epithelial cells, it is suggested that PEPT1 is the responsible transporter for luminal uptake (Son et al. 2004), but less is known about transporters mediating its observable portal release (Bauchart et al. 2007). In the kidney, PEPT2 is the most important transporter for tubular reabsorption of carnosine into epithelial cells at their apical side (Kamal et al. 2009), but a further transport into blood is very limited and probably mediated via a facilitative carrier (Jappar et al. 2009). PEPT2 is also present in the apical membrane of epithelial cells of the choroid plexus, where it is responsible for carnosine uptake from cerebrospinal fluid (CSF) (Teuscher et al. 2004) and it appears to be responsible for carnosine uptake in astrocytes (Xiang et al. 2006) and cardiomyocytes (Lin and King 2007). The physiological importance of PHT1 and PHT2 with regard to carnosine transport is less clear, although their ability to transport carnosine has been confirmed for PHT1 (Yamashita et al. 1997) as well as for PHT2 (Sakata et al. 2001). In addition, Everaert et al. suggested that PHT1 could have a role in carnosine transport in the muscle, which lacks expression of PEPT1/2 but significantly expresses mRNA encoding PHT1 (Everaert et al. 2013). As all transporters have been shown to be able to transport carnosine, the dipeptides tissue-specific transport appears to be dependent on the presence of the individual transporters.

Using the data set provided by Fagerberg et al. (2014), we compared the relative expression of the four transporters in different tissues. The analysis, which is presented in Supplemental Fig. 1, shows that according to this data set almost no expression of PEPT1 is observed in healthy brain, which is in agreement with observations made in the rat brain by Fujita et al. (2004). However, regarding to the relative expression in normal tissue, our data are in contrast to the data obtained by Fagerberg et al. (2014): In the data set of Fagerberg et al. expression of PHT1 (24.6%) and PHT2 (21.1%) almost sums up to expression of PEPT2 (54.3%), whereas in our data set, PHT1 has the highest expression in healthy brain tissue (PEPT2: 10.4%;

PHT1: 74.4%; PHT2: 15.2%). Unfortunately, the analysis of other mRNA expression data sets available, such as those provided by the GTEx consortium (The GTEx Consortium 2015) or "The Human Protein Atlas" (Uhlén et al. 2015), did not resolve this riddle, as they also revealed quite different levels of expression. At this point, it also has to be noted that in the mRNA expression data sets from "The GTEx Consortium" and "The Human Protein Atlas", high individual differences in the levels of the transporters become obvious [e.g., "The Human Protein Atlas"; Brain-Frontal Cortex, 108 samples, data in RPKM: SLC15A2 (PEPT2): range 0.9–14.6; 4.2 ± 2.6; SLC15A3 (PHT2): range 0.5–18.8; 1.4 ± 2.0; SLC15A4 (PHT1): range 1.7–10.8; 3.4 ± 1.0). Although we also encountered high deviations between our samples of RNA derived from healthy brain (PEPT2: deviation: 65.9%; PHT1: deviation: 30%; and PHT2: 25.4%), it is interesting to note that in our data, the relation between the different levels of expression was comparable between healthy brain (see above) and tumor tissue (PEPT2: 16.4%; PHT1: 71.2% and PHT2: 12.4%) despite the fact that the increase of PEPT2 expression (21-fold) was slightly higher than that of the two other transporters (PHT1: 13-fold; PHT2: 11-fold). Unfortunately, cultivation of tumor tissue-derived cells results in a small decrease of PHT1 and PHT2 expression (1.6-fold and 2.3-fold, respectively) and a high decrease in PEPT2 expression (24.8-fold) which may lead to an underestimation of PEPT2's role in carnosine uptake in intact tumor tissue as discussed below. In fact, a decrease of PEPT2 expression during cultivation has previously been reported by Zimmermann et al. investigating its expression in a primary GBM cell culture (Zimmermann and Stan 2010). It is tempting to speculate, whether a better supply with amino acids and peptides in culture compared to tumor tissue with a restricted supply, especially in bad vascularized areas of the tumor, is responsible for decreased expression in culture. This could be tested by further experiments in which the nutritional supply in culture has to be modified. However, this is beyond the scope of the present work, as these experiments would require using culture media with modified compositions of single components.

Although no kinetic data are available to discuss the individual uptake rates of carnosine by PEPT2, PHT1, or PHT2, at a first glance PEPT2 appears to be of minor importance for the uptake of carnosine into cultured glioblastoma cells, as its expression in culture is significantly lower than that of PHT1 and PHT2 (Fig. 1). However, we were able to measure uptake of carnosine in the presence of L-histidine, which competitively inhibits the transport of carnosine by PHT1 and PHT2 but not the transport by PEPT2 (Fig. 2). Therefore, we conclude that PEPT2 also contributes to the overall uptake of carnosine in the cultures. This notion is also confirmed by siRNA knockdown

of PEPT2 resulting in a significantly reduced expression of the corresponding mRNA and a significantly reduced uptake of carnosine (Fig. 3). Given the fact that PEPT2 mRNA expression decreases in cell culture compared to tumor tissue, this transporter's relevance for carnosine uptake into tumor tissue may certainly be underestimated by our uptake experiments. Unfortunately, uptake experiments with freshly isolated human cells are almost impossible to perform, as tissue material obtained by surgery is limited. Nonetheless, PHT1 and PHT2 are obviously able to transport significant amounts of carnosine. At this point, it is interesting to note that Sakata et al. reported that at least PHT2 is confined to lysosomal membranes and not present on the cell surface (Sakata et al. 2001). However, their experiments were performed with ectopic expression of rPHT2 protein in HEK-293T cells, and to our knowledge, no further data are available that shows, where this transporter is expressed in cells of human tissue. Unfortunately, as recently pointed out by Hu et al. there are currently no antibodies available to detect human PHT1 and PHT2 (Hu et al. 2018). In fact, we also tested a number of commercially available antibodies without any success (data not shown). Therefore, it is not possible to compare healthy brain tissue with GBM tissue to evaluate whether tumor cells translocate these transporters from an intracellular localization to the cell membrane.

Another aspect detected by the experiments and the analysis presented is the observation that the expression of PEPT2, PHT1, and PHT2 is increased in GBM tissue compared to healthy tissue. Of course, it should be taken into account that samples from healthy tissue have to be considered as a mixture of neurons and glia cells. Therefore, a transporter which is only present in glia cells but not in neurons may appear to be overexpressed in a tumor tissue originating from astrocytes compared to healthy brain. Unfortunately, aside from experiments with rat brain-derived cell cultures, in which PEPT2 appeared to be restricted to glial cultures (Dieck et al. 1999), to our knowledge, nothing is known about differential expression of the transporters discriminating between glia and neurons. Given the magnitude in the difference of expression between healthy tissue and GBM tissue, we think that the observed difference deserves attention because of possible pharmacological implications. At least for PEPT1 and PEPT2, it is known that they are not only responsible for proton-coupled intake of peptides consisting of 2–4 amino acids, with a preference for dipeptides; in addition, they are also able to transport other compounds, especially pharmaceutically relevant drugs [for comprehensive reviews, see (Brandsch et al. 2008; Smith et al. 2013)]. Unfortunately, the substrate specificity of PHT1/2 is less well described, but they could be alternative targets for drug delivery to target tissues such as glioblastoma. The idea to pay more attention to the "less appreciated" transporters has already been pointed out by Smith et al. as expression of

PHT1 was shown to be significantly upregulated in inflamed areas of the colon of patients with Crohn's disease and ulcerative colitis (Lee et al. 2009).

In conclusion, we show that carnosine enters glioblastoma cells via PEPT2, PHT1, and PHT2 and knockdown of one transporter cannot be compensated by one of the others, although we observed increases of mRNA encoding the transporters not targeted by a specific siRNA, which can be interpreted as a response of the cell trying to compensate the loss of one specific transporter. Nonetheless, efficient uptake of carnosine into target cells, as required for a pharmacological intervention using carnosine as an anti-cancer drug, should take into consideration that any influence on the transport efficiency of any of the transporters will result in a reduced uptake of the dipeptide.

Compliance with ethical standards

References

Abraham D, Pisano JJ, Udenfriend S (1962) The distribution of homocarnosine in mammals. Arch Biochem Biophys 99:210–213. https://doi.org/10.1016/0003-9861(62)90002-4

Bauchart C, Savary-Auzeloux I, Patureau Mirand P, Thomas E, Morzel M, Remond D (2007) Carnosine concentration of ingested meat affects carnosine net release into the portal vein of minipigs. J Nutr 137:589–593

Bellia F, Vecchio G, Rizzarelli E (2014) Carnosinases, their substrates and diseases. Molecules 19:2299–2329. https://doi.org/10.3390/molecules19022299

Boldyrev AA, Aldini G, Derave W (2013) Physiology and pathophysiology of carnosine. Physiol Rev 93:1803–1845. https://doi.org/10.1152/physrev.00039.2012

Brandsch M, Knütter I, Bosse-Doenecke E (2008) Pharmaceutical and pharmacological importance of peptide transporters. J Pharm Pharmacol 60:543–585. https://doi.org/10.1211/jpp.60.5.0002

Csámpai A, Kutlán D, Tóth F, Molnár-Perl I (2004) o-Phthaldialdehyde derivatization of histidine: stoichiometry, stability and reaction mechanism. J Chromatogr A 1031:67–78

Daniel H, Kottra G (2004) The proton oligopeptide cotransporter family SLC15 in physiology and pharmacology. Pflügers Archiv Eur J Physiol 447:610–618. https://doi.org/10.1007/s00424-003-1101-4

Dieck ST, Heuer H, Ehrchen J, Otto C, Bauer K (1999) The peptide transporter PepT2 is expressed in rat brain and mediates the accumulation of the fluorescent dipeptide derivative beta-Ala-Lys-Nepsilon-AMCA in astrocytes. Glia 25:10–20

Ditte Z, Ditte P, Labudova M, Simko V, Iuliano F, Zatovicova M, Csaderova L, Pastorekova S, Pastorek J (2014) Carnosine inhibits carbonic anhydrase IX-mediated extracellular acidosis and suppresses growth of HeLa tumor xenografts. BMC Cancer 14:358. https://doi.org/10.1186/1471-2407-14-358

Everaert I, de Naeyer H, Taes Y, Derave W (2013) Gene expression of carnosine-related enzymes and transporters in skeletal muscle. Eur J Appl Physiol 113:1169–1179. https://doi.org/10.1007/s00421-012-2540-4

Fagerberg L, Hallström BM, Oksvold P, Kampf C, Djureinovic D, Odeberg J, Habuka M, Tahmasebpoor S, Danielsson A, Edlund K, Asplund A, Sjöstedt E, Lundberg E, Szigyarto CA-K, Skogs M, Takanen JO, Berling H, Tegel H, Mulder J, Nilsson P, Schwenk JM, Lindskog C, Danielsson F, Mardinoglu A, Sivertsson A, von Feilitzen K, Forsberg M, Zwahlen M, Olsson I, Navani S, Huss M, Nielsen J, Ponten F, Uhlén M (2014) Analysis of the human tissue-specific expression by genome-wide integration of transcriptomics and antibody-based proteomics. Mol Cell Proteom 13:397–406. https://doi.org/10.1074/mcp.M113.035600

Fujita T, Kishida T, Wada M, Okada N, Yamamoto A, Leibach FH, Ganapathy V (2004) Functional characterization of brain peptide transporter in rat cerebral cortex: identification of the high-affinity type H+/peptide transporter PEPT2. Brain Res 997:52–61. https://doi.org/10.1016/j.brainres.2003.10.049

Gaunitz F, Hipkiss AR (2012) Carnosine and cancer: a perspective. Amino Acids 43:135–142. https://doi.org/10.1007/s00726-012-1271-5

Gaunitz F, Oppermann H, Hipkiss AR (2015) Carnosine and Cancer. In: Preedy VR (ed) Imidazole dipeptides. The Royal Society of Chemistry, Cambridge, pp 372–392

Gulewitsch W, Amiradzibi S (1900) Ueber das carnosin, eine neue organische Base des Fleischextraktes. Ber Dtsch Chem Ges 33:1902–1903

Herrera-Ruiz D, Wang Q, Cook TJ, Knipp GT, Gudmundsson OS, Smith RL, Faria TN (2001) Spatial expression patterns of peptide transporters in the human and rat gastrointestinal tracts, Caco-2 In Vitro cell culture model, and multiple human tissues. AAPS PharmSci 3:100–111. https://doi.org/10.1208/ps030109

Hipkiss AR, Gaunitz F (2013) Inhibition of tumour cell growth by carnosine: some possible mechanisms. Amino Acids. https://doi.org/10.1007/s00726-013-1627-5

Horii Y, Shen J, Fujisaki Y, Yoshida K, Nagai K (2012) Effects of l-carnosine on splenic sympathetic nerve activity and tumor proliferation. Neurosci Lett 510:1–5. https://doi.org/10.1016/j.neulet.2011.12.058

Hu Y, Song F, Jiang H, Nuñez G, Smith DE (2018) SLC15A2 and SLC15A4 mediate the transport of bacterially derived di/tripeptides to enhance the nucleotide-binding oligomerization domain-dependent immune response in mouse bone marrow-derived macrophages. J Immunol 201:652–662. https://doi.org/10.4049/jimmunol.1800210

Jappar D, Hu Y, Keep RF, Smith DE (2009) Transport mechanisms of carnosine in SKPT cells: contribution of apical and basolateral membrane transporters. Pharm Res 26:172–181. https://doi.org/10.1007/s11095-008-9726-9

Kamal MA, Jiang HD, Hu YJ, Keep RF, Smith DE (2009) Influence of genetic knockout of Pept2 on the in vivo disposition of endogenous and exogenous carnosine in wild-type and Pept2 null mice. Am J Physiol Regul Comp Physiol 296:R986–R991

Lee J, Tattoli I, Wojtal KA, Vavricka SR, Philpott DJ, Girardin SE (2009) pH-dependent internalization of muramyl peptides from early endosomes enables Nod1 and Nod2 signaling. J Biol Chem 284:23818–23829. https://doi.org/10.1074/jbc.M109.033670

Letzien U, Oppermann H, Meixensberger J, Gaunitz F (2014) The antineoplastic effect of carnosine is accompanied by induction of PDK4 and can be mimicked by L-histidine. Amino Acids. https://doi.org/10.1007/s00726-014-1664-8

Lin H, King N (2007) Demonstration of functional dipeptide transport with expression of PEPT2 in guinea pig cardiomyocytes. Pflgers Archiv Eur J Physiol 453:915–922. https://doi.org/10.1007/s00424-006-0171-5

Mannion AF, Jakeman PM, Dunnett M, Harris RC, Willan PL (1992) Carnosine and anserine concentrations in the quadriceps femoris muscle of healthy humans. Eur J Appl Physiol Occup Physiol 64:47–50

Ogihara H, Saito H, Shin BC, Terado T, Takenoshita S, Nagamachi Y, Inui K, Takata K (1996) Immuno-localization of H+/peptide cotransporter in rat digestive tract. Biochem Biophys Res Commun 220:848–852

Oppermann H, Schnabel L, Meixensberger J, Gaunitz F (2016) Pyruvate attenuates the anti-neoplastic effect of carnosine independently from oxidative phosphorylation. Oncotarget 7:85848–85860. https://doi.org/10.18632/oncotarget.13039

Oppermann H, Dietterle J, Purcz K, Morawski M, Eisenlöffel C, Müller W, Meixensberger J, Gaunitz F (2018) Carnosine selectively inhibits migration of IDH-wildtype glioblastoma cells in a co-culture model with fibroblasts. Cancer Cell Int 18:111. https://doi.org/10.1186/s12935-018-0611-2

Oppermann H, Alvanos A, Seidel C, Meixensberger J, Gaunitz F (2019a) Carnosine influences transcription via epigenetic regulation as demonstrated by enhanced histone acetylation of the pyruvate dehydrogenase kinase 4 promoter in glioblastoma cells. Amino Acids. https://doi.org/10.1007/s00726-018-2619-2

Oppermann H, Purcz K, Birkemeyer C, Baran-Schmidt R, Meixensberger J, Gaunitz F (2019b) Carnosine's inhibitory effect on glioblastoma cell growth is independent of its cleavage. Amino Acids. https://doi.org/10.1007/s00726-019-02713-6

Ostrom QT, Gittleman H, Xu J, Kromer C, Wolinsky Y, Kruchko C, Barnholtz-Sloan JS (2016) CBTRUS statistical report: primary brain and other central nervous system tumors diagnosed in the United States in 2009–2013. Neuro Oncol 18:v1–v75. https://doi.org/10.1093/neuonc/now207

Parker JL, Li C, Brinth A, Wang Z, Vogeley L, Solcan N, Ledderboge-Vucinic G, Swanson JMJ, Caffrey M, Voth GA, Newstead S (2017) Proton movement and coupling in the POT family of peptide transporters. Proc Natl Acad Sci USA 114:13182–13187. https://doi.org/10.1073/pnas.1710727114

Renner C, Seyffarth A, de Arriba S, Meixensberger J, Gebhardt R, Gaunitz F (2008) Carnosine inhibits growth of cells isolated from human glioblastoma multiforme. Int J Pept Res Ther 14:127–135. https://doi.org/10.1007/s10989-007-9121-0

Renner C, Zemitzsch N, Fuchs B, Geiger KD, Hermes M, Hengstler J, Gebhardt R, Meixensberger J, Gaunitz F (2010) Carnosine retards tumor growth in vivo in an NIH3T3-HER2/neu mouse model. Mol Cancer 9:2. https://doi.org/10.1186/1476-4598-9-2

Rubio-Aliaga I, Daniel H (2008) Peptide transporters and their roles in physiological processes and drug disposition. Xenobiotica 38:1022–1042. https://doi.org/10.1080/00498250701875254

Sakata K, Yamashita T, Maeda M, Moriyama Y, Shimada S, Tohyama M (2001) Cloning of a lymphatic peptide/histidine transporter. Biochem J 356:53–60

Sant M, Minicozzi P, Lagorio S, Børge Johannesen T, Marcos-Gragera R, Francisci S (2012) Survival of European patients with central nervous system tumors. Int J Cancer 131:173–185. https://doi.org/10.1002/ijc.26335

Shen Y, Yang J, Li J, Shi X, Ouyang L, Tian Y, Lu J (2014) Carnosine inhibits the proliferation of human gastric cancer SGC-7901 cells through both of the mitochondrial respiration and glycolysis pathways. PLoS One 9:e104632. https://doi.org/10.1371/journal.pone.0104632

Smith DE, Clémençon B, Hediger MA (2013) Proton-coupled oligopeptide transporter family SLC15: physiological, pharmacological and pathological implications. Mol Aspects Med 34:323–336. https://doi.org/10.1016/j.mam.2012.11.003

Son DO, Satsu H, Kiso Y, Shimizu M (2004) Characterization of carnosine uptake and its physiological function in human intestinal epithelial Caco-2 cells. BioFactors 21:395–398

Teuscher NS, Shen H, Shu C, Xiang JM, Keep RF, Smith DE (2004) Carnosine uptake in rat choroid plexus primary cell cultures and choroid plexus whole tissue from PEPT2 null mice. J Neurochem 89:375–382

The GTEx Consortium (2015) Human genomics. the genotype-tissue expression (GTEx) pilot analysis: multitissue gene regulation in humans. Science 348:648–660. https://doi.org/10.1126/science.1262110

Uhlén M, Fagerberg L, Hallström BM, Lindskog C, Oksvold P, Mardinoglu A, Sivertsson Å, Kampf C, Sjöstedt E, Asplund A, Olsson I, Edlund K, Lundberg E, Navani S, Szigyarto CA-K, Odeberg J, Djureinovic D, Takanen JO, Hober S, Alm T, Edqvist P-H, Berling H, Tegel H, Mulder J, Rockberg J, Nilsson P, Schwenk JM, Hamsten M, von Feilitzen K, Forsberg M, Persson L, Johansson F, Zwahlen M, von Heijne G, Nielsen J, Pontén F (2015) Proteomics. Tissue-based map of the human proteome. Science 347:1260419. https://doi.org/10.1126/science.1260419

Xiang J, Hu Y, Smith DE, Keep RF (2006) PEPT2-mediated transport of 5-aminolevulinic acid and carnosine in astrocytes. Brain Res 1122:18–23. https://doi.org/10.1016/j.brainres.2006.09.013

Yamashita T, Shimada S, Guo W, Sato K, Kohmura E, Hayakawa T, Takagi T, Tohyama M (1997) Cloning and functional expression of a brain peptide/histidine transporter. J Biol Chem 272:10205–10211. https://doi.org/10.1074/jbc.272.15.10205

Zimmermann M, Stan AC (2010) PepT2 transporter protein expression in human neoplastic glial cells and mediation of fluorescently tagged dipeptide derivative β-Ala-Lys-Nepsilon-7-amino-4-methyl-coumarin-3-acetic acid accumulation. J Neurosurg 112:1005–1014. https://doi.org/10.3171/2009.6.JNS08346

In summary, we detected the mRNA of the genes encoding PEPT2, PHT1 and PHT2 in glioblastoma tissue, whereas PEPT1 mRNA was absent. The comparison of tumour tissue with normal brain tissue revealed a significantly increased mRNA expression of the three POTs in glioblastoma tissue, albeit the enhanced expression of PEPT2 mRNA was lost in glioblastoma cell culture. Analysing the uptake of carnosine in glioblastoma cells, we detected an initial rate of 0.71 ± 0.15 nmol per mg protein and minute. Finally, using transient transfection of small interfering RNA we demonstrated that carnosine enters glioblastoma cells by all three POTs. Noteworthy, in contrast to PEPT1/2, PHT1/2 are comparably poorly described. As PHT2 was considered to be only present in lysosomal membranes (Sakata et al. 2001), our experiments demonstrated for the first time that PHT2 is involved in cellular uptake.

After the mechanism of cellular uptake of carnosine in glioblastoma cells was evaluated, it was of interest, whether L-histidine needs to be released from carnosine to deploy the anti-neoplastic effect of the dipeptide. In the study of Oppermann et al. (Oppermann et al. 2019c) this question is addressed. If release of L-histidine from carnosine is required to reduce glioblastoma cell viability, the amino acid should be at least as potent as the dipeptide. Therefore, we investigated the influence of different concentrations of carnosine and L-histidine on viability of ten glioblastoma cell lines and 21 primary glioblastoma cell cultures. We detected that both carnosine and L-histidine dose-dependently reduced cell viability. Furthermore, lower doses of L-histidine achieved the same quantitative effect of carnosine on viability. Analysis of *CNDP1* mRNA, which encodes the enzyme CN1 capable to cleave carnosine, revealed only a minor or undetectable expression in the analysed samples. In contrast to that, the mRNA of the intracellular isoenzyme CN2, encoded by *CNDP2* was expressed in all 31 glioblastoma cell cultures. As CN2 expression was confirmed in glioblastoma cell lines, we concluded that carnosine is presumably cleaved intracellularly to L-histidine and β-alanine. Using LC-MS we analysed the possible intracellular release of L-histidine from carnosine in five primary glioblastoma cell cultures and ten glioblastoma cell lines. Moreover, the influence of the CN2 inhibitor bestatin on the anti-neoplastic effect of carnosine was investigated.

ORIGINAL ARTICLE

Carnosine's inhibitory effect on glioblastoma cell growth is independent of its cleavage

Henry Oppermann[1] · Katharina Purcz[1] · Claudia Birkemeyer[2] · Rainer Baran-Schmidt[1] · Jürgen Meixensberger[1] · Frank Gaunitz[1]

Abstract

The naturally occurring dipeptide carnosine (β-alanyl-L-histidine) inhibits the growth of tumor cells. As its component L-histidine mimics the effect, we investigated whether cleavage of carnosine is required for its antineoplastic effect. Using ten glioblastoma cell lines and cell cultures derived from 21 patients suffering from this malignant brain tumor, we determined cell viability under the influence of carnosine and L-histidine. Moreover, we determined expression of carnosinases, the intracellular release of L-histidine from carnosine, and whether inhibition of carnosine cleavage attenuates carnosine's antineoplastic effect. We observed a significantly higher response of the cells to L-histidine than to carnosine with regard to cell viability in all cultures. In addition, we detected protein and mRNA expression of carnosinases and a low but significant release of L-histidine in cells incubated in the presence of 50 mM carnosine ($p < 0.05$), which did not correlate with carnosine's effect on viability. Furthermore, the carnosinase 2 inhibitor bestatin did not attenuate carnosine's effect on viability. Interestingly, we measured a ~40-fold higher intracellular abundance of L-histidine in the presence of 25 mM extracellular L-histidine compared to the amount of L-histidine in the presence of 50 mM carnosine, both resulting in a comparable decrease in viability. In addition, we also examined the expression of pyruvate dehydrogenase kinase 4 mRNA, which was comparably influenced by L-histidine and carnosine, but did not correlate with effects on viability. In conclusion, we demonstrate that the antineoplastic effect of carnosine is independent of its cleavage.

Keywords Carnosine · L-Histidine · Glioblastoma · Carnosinase · Pyruvate dehydrogenase kinase 4

✉ Henry Oppermann
  henry.oppermann@medizin.uni-leipzig

  Katharina Purcz
  Katharina.Purcz@medizin.uni-leipzig.de

  Claudia Birkemeyer
  birkemeyer@chemie.uni-leipzig.de

  Rainer Baran-Schmidt
  Rainer.Baran-Schmidt@medizin.uni-leipzig.de

  Jürgen Meixensberger
  Juergen.Meixensberger@medizin.uni-leipzig.de

  Frank Gaunitz
  Frank.Gaunitz@medizin.uni-leipzig.de

[1] Klinik Und Poliklinik für Neurochirurgie, Universitätsklinikum Leipzig AöR, Forschungslabore, Liebigstraße 19, 04103 Leipzig, Germany

[2] Institut für Analytische Chemie, Universität Leipzig, 04103 Leipzig, Germany

Introduction

In 1900, Gulewitsch and Amiradzibi investigated the chemical components of Liebig's meat extract (Gulewitsch and Amiradzibi 1900), discovering the first peptide, carnosine (β-alanyl-L-histidine). Carnosine is one of several imidazole-containing dipeptides such as homocarnosine (γ-aminobutyryl-L-histidine) and anserine

🖄 Springer

(β-alanyl-*N*-π-methyl-L-histidine), which are present in high concentrations in the central nervous system and the skeletal muscle of vertebrates (Boldyrev et al. 2013). In the human body, carnosine levels are controlled by three enzymes. The formation of imidazole-containing dipeptides is catalyzed by the ATP-requiring Carnosine Synthase 1 [EC 6.3.2.11, also known as ATP-Grasp Domain-Containing Protein 1 (ATPGD1)]. The enzyme is encoded by the *CARNS1* gene, which is in humans primarily expressed in skeletal muscle, heart muscle, and olfactory neurons (Drozak et al. 2013). The degradation of carnosine can be carried out by two metalloproteases. The extracellular occurring carnosine dipeptidase 1 (CN1; EC 3.4.13.20; also known as serum carnosinase and encoded by the *CNDP1* gene) is supposed to be mainly produced in brain (Jackson et al. 1991), although it may also be synthesized in the liver (Peters et al. 2011). It hydrolyses carnosine with high specificity, but is also able to cleave anserine (β-alanyl-3-methyl-L-histidine), L-alanyl-L-histidine, L-glycyl-L-histidine, and homocarnosine (deamino-3-aminomethyl-alanyl-L-histidine) (reviewed in Bellia et al. 2014). The second enzyme (CN2; EC 3.4.13.18; also known as cytosolic non-specific dipeptidase or formerly known as tissue carnosinase; encoded by the *CNDP2* gene), is expressed intracellularly and occurs ubiquitously in human tissue (Teufel et al. 2003). Although CN2 was shown to have optimum activity at pH 9.5 with regard to cleavage of carnosine (Lenney et al. 1985), the dipeptide can be hydrolyzed intracellularly, but at a much lower rate compared to other histidine containing dipeptides, as demonstrated by experiments with HEK293T cells (Okumura and Takao 2017). Since the discovery of carnosine, several physiological functions have been ascribed to it, such as Ca^{2+} regulation, pH-buffering, metal ion chelating, scavenging of reactive oxygen species, and protection against advanced glycation end products and lipid peroxidation (for a comprehensive review see Boldyrev et al. 2013). Furthermore, we and others reported the antineoplastic effect of carnosine on cancer cells from different origin such as glioblastoma (Renner et al. 2008), colon (Horii et al. 2012; Iovine et al. 2014), gastric (Shen et al. 2014), and cervix carcinoma (Ditte et al. 2014).

In Europe, glioblastoma is the most common and in the United States the second most common primary tumor of the central nervous system (Ostrom et al. 2016; Sant et al. 2012). Under the currently recommended therapy consisting of surgical removal of the tumor, radiotherapy, and adjuvant chemotherapy with temozolomide, median survival of patients is only 14.6 months (Stupp et al. 2005). Therefore, new therapeutic options are urgently needed. Although carnosine has been intensively discussed as a potential anti-tumor drug (Gaunitz et al. 2015; Gaunitz and Hipkiss 2012; Hipkiss and Gaunitz 2014), up to now, the molecular mechanisms of carnosine's antineoplastic effects are not completely understood. In addition, it is not known whether the

intact molecule or one of its moieties (β-alanine/L-histidine) is responsible for tumor growth inhibition. Previously, we reported that L-histidine is able to mimic the antineoplastic effect of carnosine in glioblastoma cell lines (Letzien et al. 2014). In these experiments, L-histidine also induced expression of pyruvate dehydrogenase kinase 4 (PDK4) in a comparable manner to carnosine. L-histidine released from the dipeptide may then become a substrate for further reactions such as decarboxylation or deamination leading to histamine or urocanate formation, respectively. In fact, both compounds are known to be able to induce gene expression (Romero et al. 2016; Kaneko et al. 2008). Therefore, we hypothesized that cleavage of the dipeptide may be required to deploy its effect.

Materials and methods

Reagents

Unless stated, otherwise, all chemicals were purchased from Sigma-Aldrich (Taufkirchen, Germany). Carnosine was kindly provided by Flamma (Flamma s.p.a. Chignolo d'Isola, Italy).

Cell lines and primary cell cultures

The glioblastoma cell lines G55T2, 1321N1, and U373 were obtained from Sigma-Aldrich (Taufkirchen, Germany), the cell lines U87, T98G, and LN229 from the American-Type Culture Collection (ATCC; Manassas, USA); MZ54 and MZ18 were originally obtained from Donat Kögel (Frankfurt, Germany) and the lines LN405 and U343 were obtained from the "Deutsche Sammlung von Mikroorganismen und Zellkulturen" (DMSZ; Braunschweig, Germany). Primary cell cultures were established from tissue samples obtained during standard surgery performed at the Neurosurgery Department of the University Hospital Leipzig during 2011 and 2015 (see Table 1 for age and gender of patients). All patients provided written informed consent according to the German laws as confirmed by the local committee. All glioblastoma samples were diagnosed and have been approved by the Neuropathology Department of the Leipzig University Hospital. Primary cultures from glioblastoma tissue were established as described before (Renner et al. 2008). Briefly, tissue specimens from the tumor were cut into approximately 1 mm³ large pieces and then separately placed into 25 mm² culture flasks (TPP, Trasadingen, Switzerland) until tumor cells grew out. When more than 90% confluence was reached, specimens were removed and primary cell cultures were transferred into 75 mm² culture flasks (TPP) for further cultivation. Cell cultures were maintained in high glucose DMEM (Dulbecco's Modified Eagle Medium with

Table 1 Patients of primary glioblastoma cell cultures

Patient	Age (years)	Gender	Passage	CBA/ qRT-PCR	HPLC-MS
P0052	69	Male	6	x	
P0076	51	Female	4	x	
P0082	52	Male	5	x	
P0086	59	Male	5	x	
P0087	76	Male	7	x	
P0091	79	Male	21	x	
P0109	55	Female	6	x	
P0138	80	Female	5–10	x	x
P0167	60	Female	4	x	
P0174	61	Female	4	x	
P0223	64	Male	3	x	
P0233	53	Male	3–4	x	x
P0240	55	Male	2	x	
P0244	63	Female	3–6	x	x
P0250	79	Female	3	x	
P0258	56	Female	3	x	
P0297	77	Female	2–3	x	x
P0306	75	Male	3–9	x	x
P0310	71	Female	5	x	
P0336	54	Male	5	x	
P0355	58	Male	4	x	

Primary cultures of glioblastoma cells established from freshly isolated tumor tissue. Table shows the patient ID with the corresponding age at time of the operation, gender and cell culture passages used for the experiments of this study. Primary cell cultures used for corresponding experiment are marked with "x"

qRT-PCR quantitative reverse transcription polymerase chain reaction, *CBA* cell based assays, *HPLC-MS* high-performance liquid chromatography coupled with mass spectrometry

4.5 g glucose/mL) supplemented with 2 mM GlutamaxTM, 1% penicillin/streptomycin (all from Gibco Life Technologies, now Thermo Fisher Scientific, Darmstadt, Germany) and 10% Fetal Bovine Serum (FBS; Biochrom GmbH, Berlin, Germany), further referred to as "culture medium", and kept in incubators (37 °C, 5% CO_2/95% air).

Cell based assays

For cell viability assays, cells were counted and seeded into sterile 96-well plates (μClear, Greiner Bio-One, Frickenhausen, Germany) at a density of 5000 cells/well in 200 μL culture medium (for passage number of primary cultured cells refer to Table 1). After 24 h of cultivation (37 °C, 5% CO_2/95% air), the medium was removed and replaced with fresh medium (100 μL/well) containing carnosine (10, 25, 50, 75 mM) or L-histidine (10, 25, 50 mM) for

the determination of viability after 48 h of incubation. For testing the effect of the CN2 inhibitor bestatin (also known as Ubenimex) on viability of cells from the glioblastoma lines G55T2 and LN405, the cells received 0 mM or 50 mM carnosine and different concentrations of bestatin (0 μM, 10 μM, 50 μM, or 100 μM). In these cells viability was determined after 24, 48, and 72 h of incubation. Cells used for the determination of viability after 48 and 72 h received fresh medium with the corresponding compounds after 24 h and 48 h to account for a possible instability of bestatin in the medium. After incubation, the CellTiter-Glo Luminescent Cell Viability Assay (CTG, Promega, Mannheim, Germany) was employed to determine viable cells by measuring ATP in cell lysates and the CellTiter-Blue Cell Viability Assay (CTB, Promega) was used to quantify the metabolic capacity in living cells. All assays were carried out according to manufacturer's protocols. Luminescence and fluorescence were measured using a SpectraMax M5 multilabel reader (Molecular Devices, Biberach, Germany).

Real-time quantitative polymerase chain reaction

Real-time quantitative polymerase chain reaction (qRT-PCR) experiments were carried out as described (Letzien et al. 2014). Briefly, 10^6 cells were seeded in 10 mL of medium into 10-cm cell culture dishes (TPP, Trasadingen, Switzerland) with 10 mL culture medium. After 24 h of incubation, cells received fresh medium without test compounds or containing 25 mM L-histidine or 50 mM carnosine. RNA was isolated after 24 h of incubation using the miRNeasy mini kit (Qiagen, Hilden, Germany) according to manufacturer's instructions. The RNA was stored at − 80 °C until further use. 500 ng of RNA was used for reverse transcription employing the ImProm-II™ Reverse Transcription System (Promega, Mannheim, Germany) according to manufacturer's instructions using random primer sets. DNA amplification was performed on a Rotor-Gene 3000 system (Qiagen) employing SYBR Green (Maxima SYBR Green/ ROX qPCR Master Mix, Thermo Scientific). Copy numbers of individual mRNAs were determined using linearized plasmid DNA (described in Letzien et al. 2014) containing the corresponding target sequence. The relative expression of pyruvate dehydrogenase kinase 4 (PDK4), serum carnosinase (CNDP1) and cytosolic non-specific dipeptidase (CNDP2) was obtained by normalization to the copy number of the mRNA encoding the TATA box-binding protein (TBP) which was used as reference gene. Data analysis was performed using the RotorGene 6 software and all amplification reactions were controlled for the appropriate products by melting curve analysis. The following primer sequences were used: For CNDP1: *CNDP1* forward primer: 5′ GAA GAA TAC CGG AAT AGC AG 3′ and *CNDP1* reverse primer: 5′ CGG CCA GGT ATG ACT GTT 3′; for CNDP2:

CNDP2 forward primer: 5′ AGA AGC CCT GCA TCA CCT AC 3′ and *CNDP2* reverse primer: 5′ CCA CCA AAG AGC CCA TC 3′; for PDK4: *PDK4* forward primer: 5′ CTG TGA TGG ATA ATT CCC 3′ and *PDK4* reverse primer: 5′ GCC TTT AAG TAG ATG ATA GCA 3′. For the reference gene TBP: *TBP* forward primer: 5′ TTG ACC TAA AGA CCA TTG CAC 3′ and *TBP* reverse primer: 5′ GCT CTG ACT TTA GCA CCT GTT 3′; (all from Biomers, Ulm, Germany).

Western blot

For isolation of protein, 10^6 glioblastoma cells were seeded into 10-cm cell culture dishes (TPP, Trasadingen, Switzerland) with 10 mL medium. After 24 h cells received fresh media and were subjected to additional 24 h of incubation. Then, cells were washed twice with ice-cold washing buffer (137 mM NaCl, 5.4 mM HCl, 0.41 mM $MgSO_4$, 0.49 mM $MgCl_2$, 0.126 mM $CaCl_2$, 0.33 mM Na_2HPO_4, 0.44 mM KH_2PO_4, 2 mM HEPES, pH 7.4) and finally collected in 1 mL washing buffer. After a brief centrifugation (5 min, 500×*g*, 4 °C), and cells were resuspended in 150 μl of ice-cold radioimmunoprecipitation assay buffer (RIPA buffer: 50 mM Tris, 150 mM NaCl, 0.25% sodium deoxy cholate, 0.1% SDS, 1% Nonidet P40) supplemented with PhosS-tOP™ and an in-house protease inhibitor cocktail (0.025 g/L aprotinin, 0.025 g/L leupeptin, 0.01 g/L pepstatin A, 1 mM dithiothreitol, 2.5 mM phenylmethylsulfonylfluoride, and 2.5 mM benzamidine). After 10 min of incubation on ice, cells were lysed by sonification (Bioruptor, Diagenode, Seraing, Belgium; settings: power: high, interval: 0.5, time: 7 min). The resulting cell fraction was centrifuged (5 min at 4 °C and 5500×*g*) and the resulting supernatant was transferred into a new 1.5 mL reaction vial and stored at − 80 °C until further use. Protein concentration was determined using the Pierce 660 nm-assay reagent according to manufacturer's instructions. Electrophoresis was performed using a vertical electrophoresis unit (Mini-Protean-Cell, Bio-Rad, Munich, Germany) and separation was carried out in 12% polyacrylamide gels. Before loading onto the gel, 30 μg protein was mixed with 4 μL sample buffer (0.5 mM Tris, 40% glycerol, 275 mM sodium dodecyl sulfate, 0.125% bromophenol blue, 20% 2-mercaptoethanol, pH 6.8) and volume was adjusted to 16 μL with double distilled water, followed by denaturation (5 min, 95 °C). Separated proteins were transferred overnight at 4 °C onto a low fluorescence polyvinylidene fluoride membrane (ab133411 Abcam, Cambridge, United Kingdom) using a wet blot system (Mini Trans-Blot Cell, Bio-Rad) with BSN-buffer (48 mM Tris, 39 mM glycine, 20% methanol). After transfer, membranes were blocked for 1 h at room temperature under constant shaking in Tris-buffered saline with Tween20 (TBST: 20 mM Tris, 134 mM NaCl, 0.1% Tween 20, pH 7.6) supplemented with 2% (w/v) bovine serum albumin. Then, the solution was exchanged,

adding primary antibodies diluted in TBST (mouse anti CNDP2 clone AT15E5 [Abnova; MAB11202] 1:1000; rabbit anti ACTB [abcam; ab8227] 1:5000) followed by incubation of 1 h at room temperature under constant shaking. The primary antibodies were removed by three washes with TBST and a mixture of two secondary antibodies (anti-rabbit-IRDye680 [LI-COR; 925-68071] 1:8000; anti-mouse-IRDye800 [LI-COR; 925-32210] 1:8000) diluted in TBST was added to the membrane. After 1 h incubation at room temperature and constant shaking, secondary antibodies were removed by three washes with TBST. The membrane was dried overnight between two Whatman filter papers. Membranes were scanned using an Odyssey Imaging System (LI-COR, Bad Homburg, Germany) and band intensities were determined by the Image Studio 5 software (LI-COR).

Determination of intracellular ʟ-histidine

To quantify intracellular amounts of histidine, a modified method of Csámpai et al. (2004) was used. Cells from ten glioblastoma lines and from five primary cultures were seeded at a density of 300,000 cells per well into a 6-well-plate in 2 mL of culture medium. After 24 h of cultivation, the culture medium was removed and replaced with fresh medium containing 50 mM carnosine or 25 mM ʟ-histidine or no compound (control). Then, cells were incubated for additional 24 h before they were washed thrice with 1 mL ice-cold washing buffer followed by extraction using 400 μL ice-cold methanol. After 10 min of gentle shaking on ice, extracts were collected in 1.5 mL Eppendorf-vials, wells were rinsed twice with 400 μL high-quality water (Milli-Q) and 800 μL obtained were combined with the first 400 μL. Samples were evaporated to dryness by lyophilization (Martin Christ Gefriertrocknungsanlagen, Osterode, Germany). For derivatization, the freeze-dried extracts were dissolved in 100 μL high-quality water (Milli-Q) and 0.5% (w/v) *ortho*-phthalaldehyde (dissolved in 100 μL methanol) was added. Derivatization was carried out at 37 °C for 45 min, followed by the addition of 800 μL 0.1% formic acid (in HPLC grade water). The obtained solution (200 μL) was transferred into 250 μL conic glass inserts of 2 mL ND10 vials, followed by high-performance liquid chromatography coupled to mass spectrometry (HPLC-MS) with 100 μL of sample.

HPLC-MS set up and data analysis

The system used for detection was an Agilent HPLC 1100 (Agilent, Waldbronn, Germany) consisting of a variable wavelength detector (VWD), a well plate auto sampler and a binary pump, coupled with a Bruker Esquire 3000 plus electrospray ionization mass spectrometer run by Esquire Control 5.3 (Bruker, Bremen, Germany). The employed column

was a Phenomenex Gemini 5 µ C18 110 Å, 150 mm × 2 mm with a 2 mm guard column of the same material (Phenomenex Ltd., Aschaffenburg, Germany). The eluent system consisted of two solvents, with eluent A: 0.1% formic acid in acetonitrile and eluent B: 0.1% formic acid in HPLC grade water. Mobile phase flow rate was 0.5 mL/min with the following gradient for separation: 0–10 min 90% B, 90–0% B within 15 min, 25–35 min 0% B, 0–90% B within 5 min and 40–47 min 90% B for column equilibration. The mass spectrometer operated in positive mode (target mass: m/z 300; scan range: m/z 70–400), the dry gas temperature was set to 360°C (with a flow rate of 11 L/min; nebulizer: 70 psi). Data were analyzed using OpenChrom version 2.0.103. v20150204-1700 (Wenig and Odermatt 2010). Histidine was identified by an authentic standard. The selective ion chromatogram of $m/z = 272$ was used for quantification by peak integration.

Data presentation and statistical analysis

If not stated otherwise, data are presented as mean ± standard deviation (SD). For pairwise comparisons, Welch's t test (unpaired two-sample test with unequal variances) was performed using the algorithm implemented in Excel (Microsoft, Redmond, USA; Version: 14.0.7212.5000 32-Bit). For multivariate statistical analysis, a Kruskal–Wallis–ANOVA was performed, followed by a Welch's t test for pairwise comparisons. To consider the false discovery rate of multiple comparisons, p values were adjusted according to Benjamini and Hochberg (1995), and a value < 0.05 was presumed to be

significant. Correlation analysis (Pearson correlation coefficient) and Kruskal–Wallis–ANOVA were carried out by OriginPro 2017G (OriginLab Corporation, Northampton, USA; Version: 2017G 64-bit SR1).

Results

Cell viability in cultured primary glioblastoma cells and cell lines derived from glioblastoma cultivated in medium with different concentrations of carnosine and L-histidine

First, we analyzed the viability of ten cell lines and 21 primary cell cultures derived from glioblastoma after 48 h of incubation in the presence of various concentrations of carnosine (0, 10, 25, 50, and 75 mM) and L-histidine (0, 10, 25, and 50 mM). As can be seen in Fig. 1, viability of glioblastoma cells was significantly reduced by a concentration of 50 ($p = 1.45 \times 10^{-9}$) and 75 ($p = 5.19 \times 10^{-22}$) mM carnosine as determined by the CTB and at a concentration of 25 ($p = 2.8 \times 10^{-2}$), 50 ($p = 7.44 \times 10^{-8}$) and 75 ($p = 3.63 \times 10^{-14}$) mM carnosine as determined by the CTG assay (for the individual responses of all cultures see supplemental Fig. 1–e). With regard to L-histidine, even the lowest concentration employed (10 mM) was able to significantly reduce the relative amount of ATP ($p = 2.13 \times 10^{-2}$) and dehydrogenase activity ($p = 6.77 \times 10^{-4}$) in the tested glioblastoma cells. In the presence of 25 mM (CTB: $p = 3.94 \times 10^{-2}$; CTG: $p = 5.53 \times 10^{-3}$) and 50 mM (CTB:
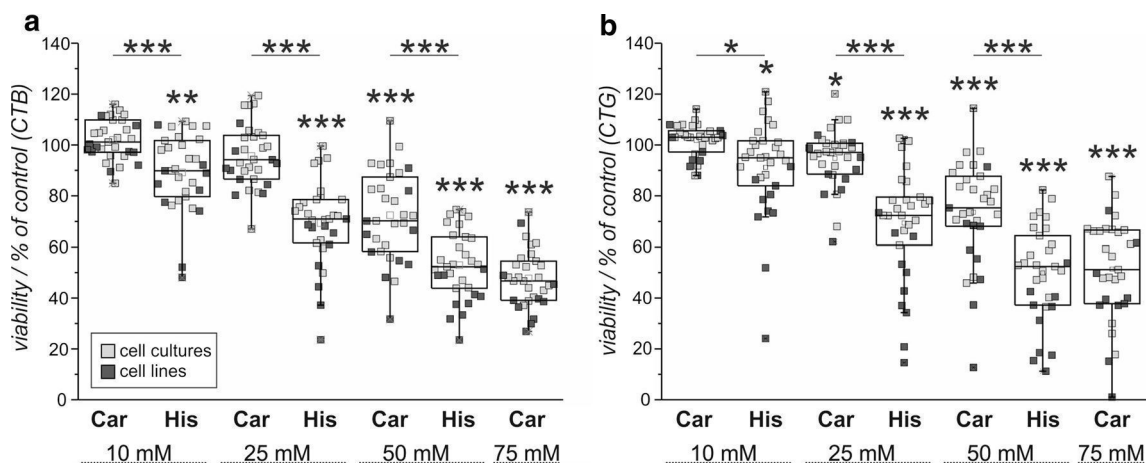

Fig. 1 Viability of primary glioblastoma cell cultures and glioblastoma cell lines under the influence of carnosine and L-histidine. Primary glioblastoma cell cultures (21) and glioblastoma cell lines (10) were exposed for 48 h to different concentrations of carnosine (0, 10, 25, 50 or 75 mM) or L-histidine (0, 10, 25, or 50 mM). Viability was determined by assessing metabolic activity (CTB; **a**) and by measuring the amount of ATP in cell lysates (CTG; **b**). Each dot within the boxplot represents the mean obtained from six independent measurements of an individual culture which was normalized to the untreated control (set to 100%). Dark gray dots represent cell lines treated with carnosine or histidine, and light gray dots represent primary cell cultures treated with carnosine or histidine. Statistical significance compared to untreated control and between equal concentrations of carnosine and L-histidine was determined by Welch's t test with: *$p < 0.05$; **$p < 0.005$; ***$p < 0.0005$. The individual results of each cell culture are presented in Supplemental Fig. 1a–e

$p = 1.49 \times 10^{-3}$; CTG: $p = 2.54 \times 10^{-3}$) of L-histidine, cells from lines revealed a significantly stronger loss of viability than primary cultured cells. Overall, comparing equal concentrations, L-histidine was 1.37 ± 0.14-fold (median) more effective than carnosine in decreasing cell viability.

Expression of serum carnosinase and cytosolic non-specific dipeptidase in human glioblastoma cells

As the experiments presented in the previous section suggest that carnosine may need first to be cleaved to L-histidine and β-alanine to deploy its effect, we asked whether the glioblastoma cells express the mRNA of the required enzymes at all. Therefore, we analyzed CNDP1 and CNDP2 expression in 31 glioblastoma cell cultures by qRT-PCR. As can be seen in Fig. 2, *CNDP2* was expressed in all analyzed samples with a relative expression ranging from 0.59 to 30.24 copy numbers per TBP copy (note that TBP mRNA has ~ 100 copies per ng RNA). In contrast to that, *CNDP1* was only weakly expressed or not detectable with a relative expression ranging from 0 to 0.14 copy numbers per *TBP* copy. Next, we asked whether the presence of *CNDP2* mRNA in glioblastoma cells also results in a corresponding protein expression. In the western blot presented in Fig. 3, it can be seen that CN2 protein was detectable in all investigated samples, suggesting the possibility that carnosine could indeed be cleaved intracellularly. Noteworthy, by quantifying CN2 band intensity, we could not find a correlation

between protein and mRNA expression (Pearson correlation; $r = -5.68 \times 10^{-4}$; $p = 0.999$).

Cell viability under the influence of carnosine and bestatin

Next, we asked, whether the CN2 inhibitor bestatin attenuates the effect of carnosine on cell viability. In Fig. 4, viability in the presence of 50 mM carnosine and different concentrations of bestatin are presented, relative to viability of cells with only the indicated concentrations of bestatin but without carnosine (set as 100% for each concentration of bestatin). As illustrated, bestatin does not attenuate the effect of carnosine in both cell lines, independent of the employed concentrations of bestatin and the time of measurement. Only at concentrations of 50 μM and 100 μM bestatin and in the case of LN405 with regard to ATP in cell lysates after 72 h of incubation, the effect of carnosine on viability was statistically not significant ($p = 0.31$ and 0.33, respectively). However, this was most likely caused by an already strong effect of bestatin on viability after 72 h exposure even in the absence of carnosine which resulted in a high standard deviation (50 μM: $42 \pm 17\%$ viability without and $27 \pm 13\%$ with carnosine, 100 μM: $26 \pm 16\%$ viability without, and $13 \pm 7\%$ with carnosine). At this point, it has to be noted that we observed a negative effect on viability with increased concentrations of bestatin and exposure time, even in the absence of carnosine (see supplemental Fig. 2). More important, comparing viability in the presence of carnosine and different concentrations of bestatin and incubation time does

Fig. 2 Expression of *CNDP1* and *CNDP2* mRNA in primary glioblastoma cell cultures and glioblastoma cell lines. Total RNA from 21 primary glioblastoma cell cultures and ten glioblastoma cell lines was extracted, reverse transcribed and analyzed by qRT-PCR. *CNDP1* and *CNDP2* mRNA copy numbers were determined using standards and relative expression was calculated by the normalization to the *TBP* mRNA copy number of each sample. Data are represented as mean and standard deviation of three measurements. An *x*-axis break has been used because of the high differences between the absolute expression of *CNDP1* and *CNDP2* mRNA
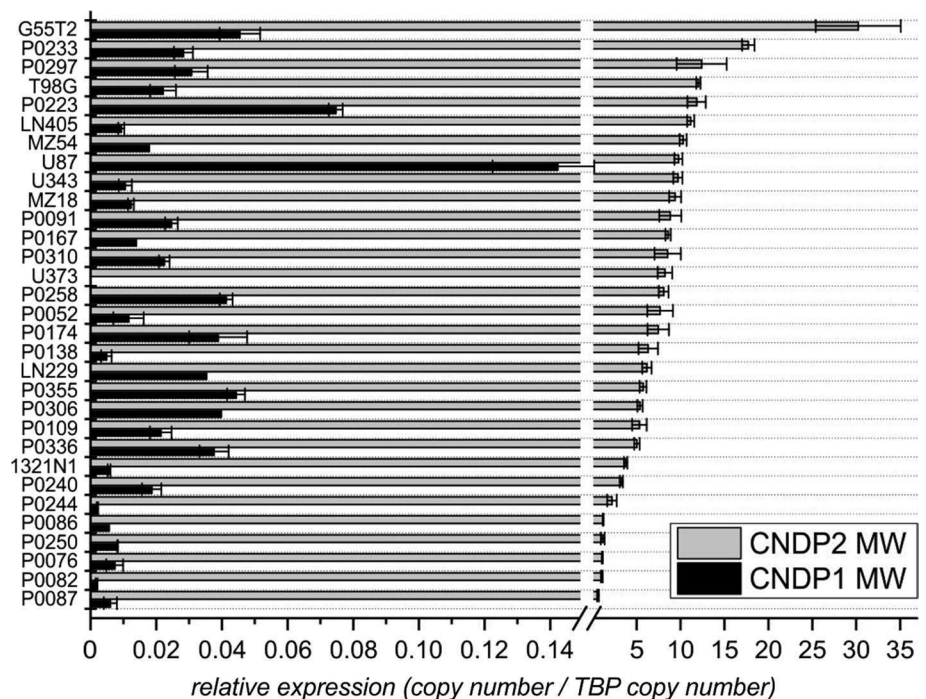
Fig. 3 Expression of CN2 protein in glioblastoma cell lines. Protein from ten glioblastoma cell lines was isolated and subjected to SDS-PAGE. Western blotting was performed using antibodies against CN2 (53 kDa) and β-actin (42 kDa). Upper panel: western blot image as analyzed by an Odyssey Imaging System. Lower panel: quantitative analysis of bands from the upper panel determined by Image Studio 5
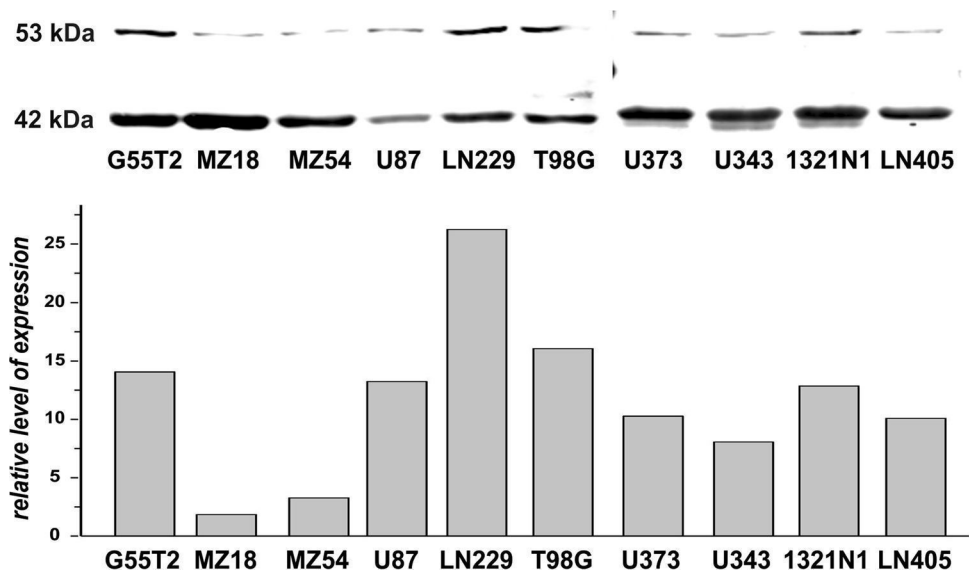
not indicate an influence of the CN2 inhibitor on carnosine's effect on viability.

Comparison of intracellular L-histidine in primary cultured glioblastoma cells and cell lines derived from glioblastoma exposed to extracellular carnosine

The experiments presented in the previous section indicated that a release of L-histidine may not be required for the antineoplastic effect of carnosine. However, as viability was obviously negatively affected by the inhibitor bestatin itself, these experiments do not unequivocally demonstrate that the antineoplastic effect of carnosine is independent of the release of L-histidine in the absence of the inhibitor. Therefore, we investigated whether the release of L-histidine and the effect of carnosine on viability show any correlation. As can be seen in Fig. 5a, except for P0297 and G55T2, treatment with 50 mM carnosine resulted in a significant 1.22 to 2.5-fold increase of the intracellular abundance of histidine (with p values reaching from 3.12×10^{-4} to 7.12×10^{-3}). This indicates that the dipeptide is cleaved to a certain amount inside the cells. However, there was no correlation between the expression of CN2 (Fig. 3) and the relative release of L-histidine. This is seen, for example, in the low expression of CN2 in MZ18 compared to its higher expression in LN229, which is not reflected by a corresponding difference in L-histidine release. More important, we did not see any significant correlation between the decrease of viability under the influence of 50 mM carnosine and the relative release of L-histidine (supplemental Fig. 3). This also indicates that the antineoplastic effect is independent of the cleavage of the dipeptide. Analyzing the intracellular abundance of L-histidine in the presence of 25 mM extracellular

L-histidine (a concentration resulting in a similar decrease of viability as observed in the presence of 50 mM carnosine, Fig. 1), we detected a ~40-fold higher abundance of intracellular L-histidine compared to incubation in the presence of 50 mM carnosine (Fig. 5). This observation also confirms the notion that cleavage of carnosine is not required for its antineoplastic effect.

Expression of PDK4 mRNA under the influence of carnosine and L-histidine and correlation between viability and influence on expression

Finally, we investigated whether the effect of L-histidine (25 mM) and carnosine (50 mM) on viability correlates with their influence on PDK4 expression. As can be seen in Fig. 6a, carnosine significantly induced the expression of PDK4 mRNA in eight samples, whereas a significantly reduced expression was found in four samples. Under the influence of L-histidine, PDK4 mRNA expression was significantly induced in 21 samples. Comparing the effect of the two compounds on PDK4 expression (Fig. 6b), 18 cell cultures responded in the same way (both carnosine and L-histidine induced or reduced PDK4 mRNA expression when treatment of at least one compound was significantly different compared to the untreated control), whereas six cell cultures responded in an opposite way. Furthermore, there was a significant correlation between the influence of carnosine and L-histidine on PDK4 mRNA expression (Pearson correlation; $r = 0.419$; $p = 0.019$). Comparing the effect on PDK4 expression with the effect on viability, no correlation was found neither for L-histidine (Fig. 6c) nor for carnosine (Fig. 6d).
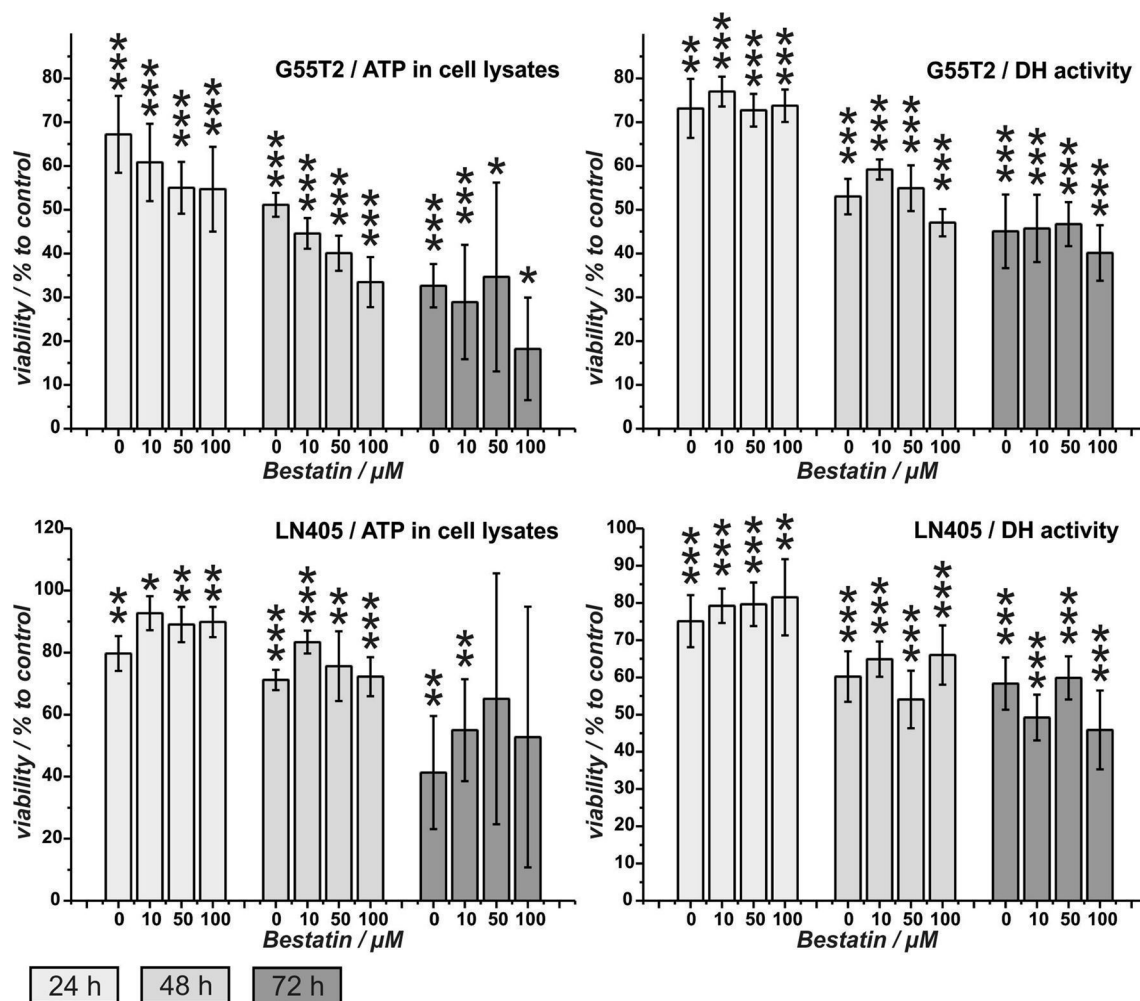
Fig. 4 Viability of G55T2 and LN405 glioblastoma cells under the influence of carnosine and the dipeptidase-inhibitor bestatin. Viability of cells from the lines G55T2 and LN405 in the presence of 50 mM carnosine and different concentrations of bestatin (0, 10, 50, or 100 μM) was compared to the viability of cells with the inhibitor bestatin but without carnosine, setting the viability without carnosine for each concentration of bestatin to 100 percent. After 24, 48, and 72 h of incubation, viability was determined by determining metabolic activity [dehydrogenase (DH) activity] and by measuring the amount of ATP in cell lysates (ATP in cell lysates). Data are represented as mean and standard deviation of six independent measurements. Statistical significance was determined by Welch's t test with: *$p < 0.05$; **$p < 0.005$; ***$p < 0.0005$

Discussion

The antineoplastic effect of carnosine, which was first described by Nagai and Suda (1986), has been confirmed in vitro (Ditte et al. 2014; Iovine et al. 2014; Renner et al. 2008; Shen et al. 2014) and in vivo (Horii et al. 2012; Renner et al. 2010) by several research groups. Hence, its potential as an anti-tumor agent has been discussed in a number of review articles (Gaunitz et al. 2015; Gaunitz and Hipkiss 2012; Hipkiss and Gaunitz 2014). As we previously demonstrated that L-histidine is able to mimic the antineoplastic effect of the dipeptide (Letzien et al. 2014), we wondered whether carnosine has to be cleaved to inhibit tumor cell growth. Comparing the viability of 21 primary cell cultures and ten cell lines originated from glioblastoma, we observed that with regard to the effector concentrations required to induce similar losses of viability, L-histidine was more effective at lower concentrations than carnosine. We also observed increased concentrations of intracellular L-histidine when cells were exposed to carnosine. As we identified the presence of CN2, we assume that this intracellular L-histidine is produced by cleavage of carnosine catalyzed by the enzyme. Comparing CN2 expression with the amount of intracellular L-histidine, we found no correlation. However, at this point, it has to be taken into account that because of different cell sizes, it is almost impossible to precisely compare the exact changes of intracellular concentrations of L-histidine between different cells. However,
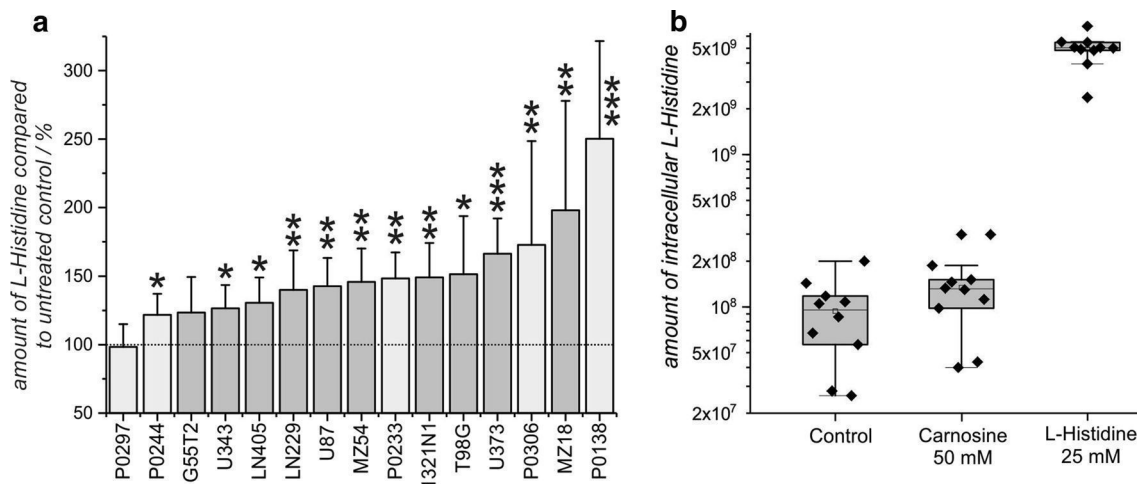
Fig. 5 Intracellular abundance of histidine in glioblastoma cells incubated in the presence of 50 mM carnosine and 25 mM histidine. **a** Cells from ten lines (dark gray) and five primary glioblastoma cell cultures (light gray) were exposed for 24 h to 50 mM carnosine. Then, amino acids were extracted and analyzed by HPLC-MS. Changes of the relative intracellular abundances of L-histidine are shown as mean percent and standard deviation (using error propagation) compared to untreated control cells from six independent experiments. Statistical significance was determined by Welch's *t* test with: *$p < 0.05$; **$p < 0.005$; ***$p < 0.0005$. **b** Relative intracellular abundance of L-histidine in cells from 10 cell lines incubated in the presence of 50 mM carnosine or 25 mM L-histidine. Each dot represents the mean obtained from six independent measurements of an individual culture

cleavage appears to be weak as the intracellular concentration of L-histidine in the presence of 25 mM L-histidine in the medium is ~40-times higher than the amount of L-histidine in cells incubated in the presence of 50 mM carnosine. At this point, it also has to be noted that Teufel et al. (2003) claimed that the intracellular pH is far from the optimal pH required for effective cleavage of carnosine by CNDP2. A very low release of L-histidine from carnosine has also been demonstrated by Son et al. (2008), investigating the intracellular concentration of amino acids of Caco-2 cells cultivated in the presence of 50 mM carnosine for 6 and 27 h. In these experiments, the intracellular amount of L-histidine in the presence of carnosine was more than 50 times lower than that observed in the presence of 50 mM L-ala-L-his.

Obviously, carnosine does not need to be cleaved into its single amino acids to deploy its antineoplastic effect, but the question remains, whether L-histidine bound to the β-alanine moiety in carnosine is sufficient to induce the antineoplastic effect of carnosine and whether β-alanine may be substituted by another moiety. This question has to be elaborated by further experiments, as it bears the interesting aspect that it could lead to the development of anti-cancer drugs which may have an advantage over carnosine. It also has to be asked whether L-histidine could be used as a supplement instead of carnosine. As demonstrated by cell injury assays with cultivated rat hepatocytes, this appears to be no good choice (Rauen et al. 2007). In these experiments, highly increased lactate dehydrogenase (LDH) release, as an indicator of cellular necrosis, was seen in the presence of 198 mM ($92 \pm 1\%$), 76 mM ($91 \pm 1\%$), and 50 mM L-histidine

($74 \pm 18\%$), whereas a concentration of 198 mM carnosine resulted in only $39 \pm 3\%$ LDH release compared to $20 \pm 5\%$ LDH release in untreated control cells. This also points to the possibility that other mechanisms are responsible for the increased toxicity of L-histidine than those responsible for the specific antineoplastic effect of carnosine. At this point, it should also be noted that we recently demonstrated that in co-cultures of tumor cells with non-tumor cells, carnosine selectively eliminated the tumor cells (Oppermann et al. 2018). In these experiments, in which the cells were incubated up to several weeks, lower concentrations of carnosine have been employed than those that were used in the experiments presented in the present study. This has to be noted, as we are aware that it may be difficult to achieve the compound concentrations employed in the present investigation in vivo. On the other hand, it is also difficult to estimate, which intracellular concentrations may be achievable when carnosine is delivered orally, as we do not know whether carnosine can efficiently be protected from degradation by CN1 (see below). We also do not know whether it can be transported to the target cells, whether it may be resynthesized from the single amino acids, and whether it may accumulate in cells which could take it up. Anyway, the most frequently discussed obstacle using carnosine as an orally given drug is its rapid degradation by serum carnosinase in humans (Lenney et al. 1982). Despite the observation that the dipeptide is effective as a drug in different diseases (Baraniuk et al. 2013; Boldyrev et al. 2008; Chengappa et al. 2012; Chez et al. 2002) and despite the fact that it may be protected by deposition in liver (Gardner et al. 1991) or erythrocytes
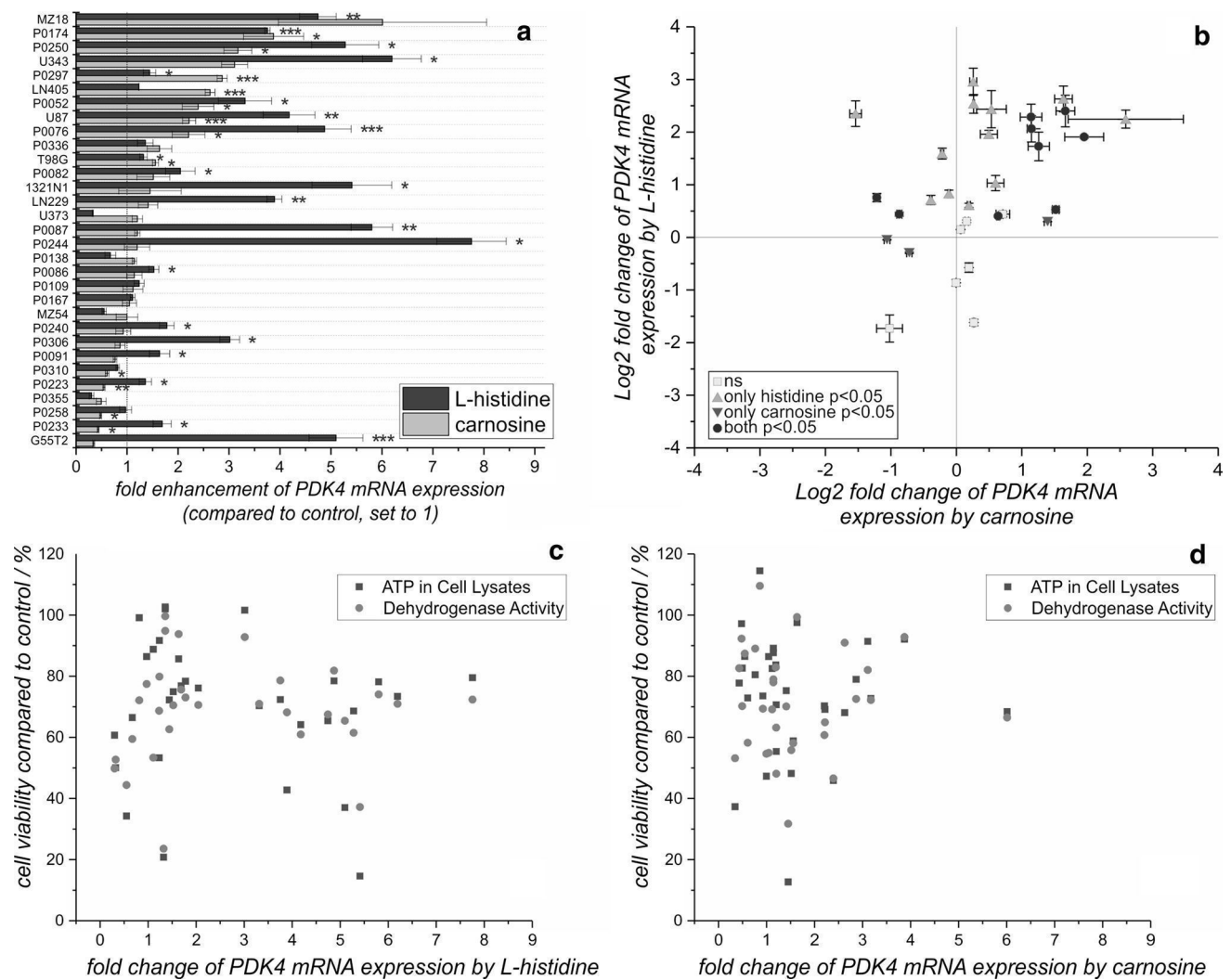
Fig. 6 Expression of *PDK4* mRNA after exposure to carnosine or L-histidine. 21 primary glioblastoma cell cultures and ten glioblastoma cell lines were incubated in the presence of 50 mM carnosine, 25 mM L-histidine, or vehicle control for 24 h. Then, total RNA was extracted, reverse transcribed and analyzed by qRT-PCR. *PDK4* mRNA copy numbers were determined using standards and relative expression was calculated by the normalization to the *TBP* mRNA copy number of each sample. **a** Fold enhancement of *PDK4* expression compared to untreated control cells. Data are represented as mean and standard deviation of three measurements compared to the untreated control (set to 1). Statistical significance was determined by Welch's *t* test with: *$p < 0.05$; **$p < 0.005$; ***$p < 0.0005$. **b** Comparison of *PDK4* mRNA expression under the influence of carnosine and L-histidine. The data presented in **a** are here depicted with fold increase of relative *PDK4* mRNA expression under the influence carnosine on the *x*-axis, and with fold increase under the influence of L-histidine on the *y*-axis. **c** Comparison between viability and *PDK4* mRNA expression under the influence of 25 mM L-histidine. **d** Comparison between viability and *PDK4* mRNA expression under the influence of 50 mM carnosine

(Chaleckis et al. 2016), the high activity of CN1 in human serum will certainly strongly affect the effective concentration achievable in a patient's tumor tissue when given orally. In addition, it has to be asked whether cleavage of carnosine by CN1 may increase serum concentrations of L-histidine to hepatotoxic concentrations. Therefore, it would be interesting to analyze whether other L-histidine- or imidazole-containing compounds which are not degradable by CN1 and are not toxic to other cells, may be useful alternatives. However, it has to be taken into account that these compounds need to be able to be taken up by tumor cells, can pass the

blood–brain barrier in case of brain tumors, and are selective in preventing cancer cell proliferation. For the purpose of further drug development, it is also of major importance to understand the molecular mechanisms responsible for the antineoplastic effect.

Aside from a plethora of reports on carnosine's influence on signaling molecules in different models (for review, see Gaunitz et al. 2015), the currently best described effect of carnosine on transcription in glioblastoma cells is its influence on transcription of *PDK4* (Letzien et al. 2014). Therefore, we also investigated whether we could see any

correlation between carnosine and L-histidine regarding their effect on *PDK4* mRNA expression (Fig. 6). As we could demonstrate that carnosine and L-histidine influence *PDK4* mRNA expression in 18 out of 31 cell cultures in the same way, this may indicate that at least in some cultures L-histidine and carnosine share similarities with regard to their influence on transcription. Although this only moderate correlation may be tempered by a limited sample size, it is at least obvious that there is no correlation between carnosine's and L-histidine's effect on viability and expression of *PDK4* mRNA. Therefore, we conclude that changes of *PDK4* expression may not be responsible for carnosine's antineoplastic effect.

In summary, we demonstrate that the cleavage of carnosine and the release of L-histidine is not required for the antineoplastic effect of the dipeptide, which can be deduced from three observations: (1) The CN2 inhibitor bestatin does not attenuate the effect of carnosine on tumor cell viability. (2) Intracellular cleavage of carnosine is observable, but has a low efficiency. (3) Roughly 40-times higher amounts of intracellular free L-histidine in the presence of 25 mM extracellular L-histidine have the same effect on tumor cell viability as concentrations of free L-histidine observed in the presence of 50 mM extracellular carnosine.

Author contributions KP performed most of the experiments with contributions of HO and RB-S. CB established the HPLC-MS method with contributions of HO and performed the HPLC-MS measurements. JM did the surgery and revised the manuscript. HO and FG designed the study and wrote the manuscript. All authors read and approved the manuscript.

Compliance with ethical standards

Conflict of interest The authors declare that they have no potential conflict of interest.

Informed consent All patients provided written informed consent according to German law as confirmed by the local committee (#144-2008) in accordance with the 1964 Helsinki declaration and its later amendments.

References

Baraniuk JN, El-Amin S, Corey R, Rayhan R, Timbol C (2013) Carnosine treatment for gulf war illness: a randomized controlled trial. GJHS 5:69. https://doi.org/10.5539/gjhs.v5n3p69

Bellia F, Vecchio G, Rizzarelli E (2014) Carnosinases, their substrates and diseases. Molecules 19:2299–2329. https://doi.org/10.3390/molecules19022299

Benjamini Y, Hochberg Y (1995) Controlling the false discovery rate: a practical and powerful approach to multiple testing. J R Stat Soc Ser B (Methodological) 57:289–300

Boldyrev A, Fedorova T, Stepanova M, Dobrotvorskaya I, Kozlova E, Boldanova N, Bagyeva G, Ivanova-Smolenskaya I, Illarioshkin S (2008) Carnosine [corrected] increases efficiency of DOPA therapy of Parkinson's disease: a pilot study. Rejuvenation Res 11:821–827. https://doi.org/10.1089/rej.2008.0716

Boldyrev AA, Aldini G, Derave W (2013) Physiology and pathophysiology of carnosine. Physiol Rev 93:1803–1845. https://doi.org/10.1152/physrev.00039.2012

Chaleckis R, Murakami I, Takada J, Kondoh H, Yanagida M (2016) Individual variability in human blood metabolites identifies age-related differences. Proc Natl Acad Sci USA 113:4252–4259. https://doi.org/10.1073/pnas.1603023113

Chengappa KR, Turkin SR, DeSanti S, Bowie CR, Brar JS, Schlicht PJ, Murphy SL, Hetrick ML, Bilder R, Fleet D (2012) A preliminary, randomized, double-blind, placebo-controlled trial of L-carnosine to improve cognition in schizophrenia. Schizophr Res 142:145–152. https://doi.org/10.1016/j.schres.2012.10.001

Chez MG, Buchanan CP, Aimonovitch MC, Becker M, Schaefer K, Black C, Komen J (2002) Double-blind, placebo-controlled study of L-carnosine supplementation in children with autistic spectrum disorders. J Child Neurol 17:833–837

Csámpai A, Kutlán D, Tóth F, Molnár-Perl I (2004) *O*-Phthaldialdehyde derivatization of histidine: stoichiometry, stability and reaction mechanism. J Chromatogr A 1031:67–78

Ditte Z, Ditte P, Labudova M, Simko V, Iuliano F, Zatovicova M, Csaderova L, Pastorekova S, Pastorek J (2014) Carnosine inhibits carbonic anhydrase IX-mediated extracellular acidosis and suppresses growth of HeLa tumor xenografts. BMC Cancer 14:358. https://doi.org/10.1186/1471-2407-14-358

Drozak J, Chrobok L, Poleszak O, Jagielski AK, Derlacz R (2013) Molecular identification of carnosine *N*-methyltransferase as chicken histamine *N*-methyltransferase-like protein (hnmt-like). PLoS One 8:e64805. https://doi.org/10.1371/journal.pone.0064805

Gardner MLG, Illingworth KM, Kelleher J, Wood D (1991) Intestinal-absorption of the intact peptide carnosine in man, and comparison with intestinal permeability to lactulose. J Physiol 439:411–422

Gaunitz F, Oppermann H, Hipkiss AR (2015) Carnosine and cancer. In: Preedy VR (ed) Imidazole dipeptides. The Royal Society of Chemistry, Cambridge, pp 372–392

Gaunitz F, Hipkiss AR (2012) Carnosine and cancer: a perspective. Amino Acids 43:135–142. https://doi.org/10.1007/s00726-012-1271-5

Gulewitsch W, Amiradzibi S (1900) Ueber das Carnosin, eine neue organische Base des Fleischextraktes. Ber Dtsch Chem Ges 33:1902–1903

Hipkiss AR, Gaunitz F (2014) Inhibition of tumour cell growth by carnosine: some possible mechanisms. Amino Acids 46:327–337

Horii Y, Shen J, Fujisaki Y, Yoshida K, Nagai K (2012) Effects of L-carnosine on splenic sympathetic nerve activity and tumor proliferation. Neurosci Lett 510:1–5. https://doi.org/10.1016/j.neulet.2011.12.058

Iovine B, Oliviero G, Garofalo M, Orefice M, Nocella F, Borbone N, Piccialli V, Centore R, Mazzone M, Piccialli G, Bevilacqua MA (2014) The anti-proliferative effect of L-carnosine correlates with a decreased expression of hypoxia inducible factor 1 alpha in human colon cancer cells. PLoS One 9:e96755. https://doi.org/10.1371/journal.pone.0096755

Jackson MC, Kucera CM, Lenney JF (1991) Purification and properties of human serum carnosinase. Clin Chim Acta 196:193–205

Kaneko K, Smetana-Just U, Matsui M, Young AR, John S, Norval M, Walker SL (2008) *cis*-Urocanic acid initiates gene transcription in primary human keratinocytes. J Immunol 181:217–224. https://doi.org/10.4049/jimmunol.181.1.217

Lenney JF, George RP, Weiss AM, Kucera CM, Chan PWH, Rinzler GS (1982) Human-serum carnosinase—characterization, distinction from cellular carnosinase, and activation by cadmium. Clin Chim Acta 123:221–231

Lenney JF, Peppers SC, Kucera-Orallo CM, George RP (1985) Characterization of human tissue carnosinase. Biochem J 228:653–660

Letzien U, Oppermann H, Meixensberger J, Gaunitz F (2014) The antineoplastic effect of carnosine is accompanied by induction of PDK4 and can be mimicked by L-histidine. Amino Acids. https://doi.org/10.1007/s00726-014-1664-8

Nagai K, Suda T (1986) Antineoplastic effects of carnosine and beta-alanine—physiological considerations of its antineoplastic effects. J Physiol Soc Jpn 48:741–747

Okumura N, Takao T (2017) The zinc form of carnosine dipeptidase 2 (CN2) has dipeptidase activity but its substrate specificity is different from that of the manganese form. Biochem Biophys Res Commun 494:484–490. https://doi.org/10.1016/j.bbrc.2017.10.100

Oppermann H, Dieterle J, Purcz K, Morawski M, Eisenlöffel C, Müller W, Meixensberger J, Gaunitz F (2018) Carnosine selectively inhibits migration of IDH-wildtype glioblastoma cells in a co-culture model with fibroblasts. Cancer Cell Int 18:111. https://doi.org/10.1186/s12935-018-0611-2

Ostrom QT, Gittleman H, Xu J, Kromer C, Wolinsky Y, Kruchko C, Barnholtz-Sloan JS (2016) CBTRUS statistical report: primary brain and other central nervous system tumors diagnosed in the United States in 2009–2013. Neuro-Oncology 18:v1–v75. https://doi.org/10.1093/neuonc/now207

Peters V, Jansen EEW, Jakobs C, Riedl E, Janssen B, Yard BA, Wedel J, Hoffmann GF, Zschocke J, Gotthardt D, Fischer C, Köppel H (2011) Anserine inhibits carnosine degradation but in human serum carnosinase (CN1) is not correlated with histidine dipeptide concentration. Clin Chim Acta 412:263–267. https://doi.org/10.1016/j.cca.2010.10.016

Rauen U, Klempt S, de Groot H (2007) Histidine-induced injury to cultured liver cells, effects of histidine derivatives and of iron chelators. Cell Mol Life Sci 64:192–205. https://doi.org/10.1007/s00018-006-6456-1

Renner C, Seyffarth A, de Arriba S, Meixensberger J, Gebhardt R, Gaunitz F (2008) Carnosine inhibits growth of cells isolated from human glioblastoma multiforme. Int J Pept Res Ther 14:127–135. https://doi.org/10.1007/s10989-007-9121-0

Renner C, Zemitzsch N, Fuchs B, Geiger KD, Hermes M, Hengstler J, Gebhardt R, Meixensberger J, Gaunitz F (2010) Carnosine retards tumor growth in vivo in an NIH3T3-HER2/neu mouse model. Mol Cancer 9:2. https://doi.org/10.1186/1476-4598-9-2

Romero SA, Hocker AD, Mangum JE, Luttrell MJ, Turnbull DW, Struck AJ, Ely MR, Sieck DC, Dreyer HC, Halliwill JR (2016) Evidence of a broad histamine footprint on the human exercise transcriptome. J Physiol (Lond) 594:5009–5023. https://doi.org/10.1113/JP272177

Sant M, Minicozzi P, Lagorio S, Børge Johannesen T, Marcos-Gragera R, Francisci S (2012) Survival of European patients with central nervous system tumors. Int J Cancer 131:173–185. https://doi.org/10.1002/ijc.26335

Shen Y, Yang J, Li J, Shi X, Ouyang L, Tian Y, Lu J (2014) Carnosine inhibits the proliferation of human gastric cancer SGC-7901 cells through both of the mitochondrial respiration and glycolysis pathways. PLoS ONE 9:e104632. https://doi.org/10.1371/journal.pone.0104632

Son DO, Satsu H, Kiso Y, Totsuka M, Shimizu M (2008) Inhibitory effect of carnosine on interleukin-8 production in intestinal epithelial cells through translational regulation. Cytokine 42:265–276

Stupp R, Mason WP, van den Bent MJ, Weller M, Fisher B, Taphoorn MJB, Belanger K, Brandes AA, Marosi C, Bogdahn U, Curschmann J, Janzer RC, Ludwin SK, Gorlia T, Allgeier A, Lacombe D, Cairncross JG, Eisenhauer E, Mirimanoff RO, van Den Weyngaert D, Kaendler S, Krauseneck P, Vinolas N, Villa S, Wurm RE, Maillot MHB, Spagnolli F, Kantor G, Malhaire JP, Renard L, de Witte O, Scandolaro L, Vecht CJ, Maingon P, Lutterbach J, Kobierska A, Bolla M, Souchon R, Mitine C, Tzuk-Shina T, Kuten A, Haferkamp G, de Greve J, Priou F, Menten J, Rutten I, Clavere P, Malmstrom A, Jancar B, Newlands E, Pigott K, Twijnstra A, Chinot O, Reni M, Boiardi A, Fabbro M, Campone M, Bozzino J, Frenay M, Gijtenbeek J, Delattre JY, de Paula U, Hanzen C, Pavanato G, Schraub S, Pfeffer R, Soffietti R, Kortmann RD, Taphoorn M, Torrecilla JL, Grisold W, Huget P, Forsyth P, Fulton D, Kirby S, Wong R, Fenton D, Cairncross G, Whitlock P, Burdette-Radoux S, Gertler S, Saunders S, Laing K, Siddiqui J, Martin LA, Gulavita S, Perry J, Mason W, Thiessen B, Pai H, Alam ZY, Eisenstat D, Mingrone W, Hofer S, Pesce G, Dietrich PY, Thum P, Baumert B, Ryan G (2005) Radiotherapy plus concomitant and adjuvant temozolomide for glioblastoma. N Engl J Med 352:987–996

Teufel M, Saudek V, Ledig JP, Bernhardt A, Boularand S, Carreau A, Cairns NJ, Carter C, Cowley DJ, Duverger D, Ganzhorn AJ, Guenet C, Heintzelmann B, Laucher V, Sauvage C, Smirnova T (2003) Sequence identification and characterization of human carnosinase and a closely related non-specific dipeptidase. J Biol Chem 278:6521–6531

Wenig P, Odermatt J (2010) OpenChrom: a cross-platform open source software for the mass spectrometric analysis of chromatographic data. BMC Bioinform 11:405. https://doi.org/10.1186/1471-2105-11-405

In summary, we observed that lower doses of L-histidine are sufficient to achieve a comparable effect on glioblastoma cell viability as carnosine. Using LC-MS we detected increased intracellular amounts of L-histidine after carnosine treatment in 13 out of 15 glioblastoma cell cultures. Nevertheless, intracellular amounts of L-histidine after carnosine treatment were ~40 times lower compared to cells treated with an L-histidine dose which leads to a comparable decrease in cell viability. Furthermore, bestatin, a CN2 inhibitor, failed to attenuate the anti-neoplastic effect of carnosine. Thus, we concluded that carnosine is the biological active compound and does not need to be cleaved or further processed to deploy its effects as it is the case for other drugs such as temozolomide.

In further studies it should be evaluated whether L-histidine or another moiety than β-alanine bound to L-histidine might have an advantage over carnosine. However, cell injury assays with cultivated rat hepatocytes demonstrated the induction of cellular necrosis after treatment with 198 mM L-histidine (92%), whereas a concentration of 198 mM carnosine resulted only in a 39% loss of viability (Rauen et al. 2007). Keeping in mind that carnosine after oral ingestion is rapidly degraded to L-histidine and β-alanine by CN1 in plasma (Park et al. 2005), it also has to be analysed whether treatment with carnosine could rise serum concentrations of L-histidine to hepatotoxic concentrations. Nevertheless, the oral administration of carnosine was demonstrated to have beneficial effects for patients with neurological disorders (see 1.3.1 Clinical application / trials of histidine containing dipeptides) and to reduce side effects of chemotherapy (Yehia et al. 2019). Considering the short half-life of carnosine in blood, Gardner and co-workers who observed release of carnosine with the urine even 3-hours after oral administration, assumed an unknown compartment which could sequester carnosine and thus, protect the dipeptide from rapid degradation in plasma (Gardner et al. 1991). Interestingly, Chaleckis and co-workers detected significant amounts of carnosine in erythrocytes (Chaleckis et al. 2016). This is an interesting observation, as red blood cells may therefore act as a protecting compartment which could also explain the delivery of the dipeptide to the brain. Therefore, we analysed whether human erythrocytes are capable of carnosine uptake using LC-MS. In these unpublished experiments the uptake of the dipeptide followed a biphasic kinetic without visible saturation in the presence of extracellular concentrations of carnosine ranging from 0.1 mM to 100 mM. Furthermore, we were also able to detect intracellular carnosine, when erythrocytes were incubated for 4 hours in the presence of human serum which otherwise completely degraded extracellular carnosine. Taken together, these observations strongly support the notion that red blood cells could serve as a depot and as a carrier for carnosine.

Nevertheless, the rapid degradation of carnosine by CN1 considerably reduces tissue availability (Qiu et al. 2019) and thus hampers the delivery of the dipeptide to the target cells.

In order to overcome this obstacle different approaches were suggested. Garofalo and co-workers used an oncolytic adenovirus as carrier to increase the delivery of carnosine. This approach resulted in an enhanced anti-tumour activity *in vivo* compared to the treatment with each component alone (Garofalo et al. 2016). Another approach would be the design of a drug which exhibits carnosine's effects but is not cleaved by CN1. Anderson and co-workers demonstrated such a carnosine derivate, carnosinol which possesses the dipeptides property to scavenge reactive aldehydes without being cleaved by CN1 (Anderson et al. 2018). However, whether carnosinol exhibits a comparable anti-cancer activity as carnosine still needs to be addressed by further experiments. Hipkiss suggested the intra-nasal administration of carnosine to overcome degradation by CN1 in plasma which would be applicable for the treatment of neurodegenerative diseases and brain tumours (Hipkiss et al. 2013). Interestingly, Bermúdez and co-workers compared the intra-nasal and oral administration of carnosine in a Thy1-aSyn mouse model (Parkinson's disease model). They found that intra-nasal application of carnosine increases mitochondrial function and restores genetic alterations caused by aSyn overexpression and thus, recommended the intra-nasal route of administration of the dipeptide (Bermúdez et al. 2018). In order to increase the serum concentration of carnosine, Qiu and co-workers performed a screening of 6080 different protease-directed small-molecules to discover a selective inhibitor against human CN1 (Qiu et al. 2019). They identified carnostatine (SAN9812) which inhibits human recombinant CN1 with a K_i of 11 nM. Most importantly, subcutaneous injection of carnostatine reduced CN1 activity and increased carnosine concentration in renal tissue after administration of the dipeptide in transgenic mice overexpressing human CN1 (Qiu et al. 2019).

2.2 The influence of carnosine on glioblastoma cell signalling and gene expression

Previously, we demonstrated that the anti-neoplastic effect of carnosine is accompanied by the induction of mRNA expression of the gene encoding PDK4 (Letzien et al. 2014). As the expression of *PDK4* has intensively been studied in different tissues and organisms, several pathways and transcription factors are known which regulate its expression (for a review see (Jeong et al. 2012)). Analysing the influence of carnosine on the transcription of *PDK4* may reveal possible molecular targets of the dipeptide. Among the factors known to interact with specific elements within the ~ 850 bp long 5'-upstream region of the human *PDK4* gene are the estrogen-related receptor (Wende et al. 2005) and the forkhead box proteins FOXO1 and FOXO3a (Kwon et al. 2004). Induction of *PDK4* expression by FOXO1 and FOXO3a is

reversed by Akt (Puthanveetil et al. 2010), which plays a central role in stimulation of growth and evasion of apoptosis in cancer (Peng et al. 2016). Additionally, the downstream target of Akt, mTORC1, conduces the suppression of transcription of *PDK4* via peroxisome proliferator-activated receptors (Laplante and Sabatini 2013; Muoio et al. 2002). As it was demonstrated that carnosine is able to reduce phosphorylation of Akt and mTORC1 (Son et al. 2008; Zhang et al. 2014), the dipeptide could induce *PDK4* expression via inhibition of the PI3K/Akt/mTORC1 signalling pathway. In the study of Oppermann et al. (Oppermann et al. 2019b) we evaluated the relevance of the PI3K/Akt/mTORC1 signalling pathway for the carnosine-dependent induction of the *PDK4* gene and the anti-neoplastic effect of the dipeptide. To do this, we treated T98G and U87 glioblastoma cells with rapamycin (inhibitor of mTORC1), Ly-294,002 (inhibitor of PI3K), carnosine or a combination of these compounds and determined *PDK4* mRNA expression. Furthermore, we investigated which transcription factors possibly lead to the induction of *PDK4* expression using a reporter gene whose activity is controlled by the *PDK4* promoter. To test whether the PI3K/Akt/mTORC1 signalling pathway is affected at the level of phosphorylation of Akt and mTORC1 by carnosine, we treated T98G and U87 cells with the dipeptide and a combination of rapamycin and Ly-294,002 and performed Western blot experiments. Finally, we analysed the impact of the inhibitors on carnosine-dependent reduction of glioblastoma cell viability, to estimate the contribution of the PI3K/Akt/mTORC1 signalling pathway on the anti-neoplastic effect of the dipeptide.

Carnosine inhibits glioblastoma growth independent from PI3K/Akt/mTOR signaling

Henry Oppermann☯**, Helene Faust**☯**, Ulrike Yamanishi, Jürgen Meixensberger, Frank Gaunitz**[ID] *

Klinik und Poliklinik für Neurochirurgie, Universitätsklinikum Leipzig AöR, Leipzig, Germany

☯ These authors contributed equally to this work.
* Frank.Gaunitz@medizin.uni-leipzig.de

Abstract

Glioblastoma is a high-grade glioma with poor prognosis even after surgery and standard therapy. Here, we asked whether carnosine (β-alanyl-L-histidine), a naturally occurring dipeptide, exert its anti-neoplastic effect on glioblastoma cells via PI3K/Akt/mTOR signaling. Therefore, glioblastoma cells from the lines U87 and T98G were exposed to carnosine, to the mTOR inhibitor rapamycin and to the PI3K inhibitor Ly-294,002. Pyruvate dehydrogenase kinase (PDK4) expression, known to be a target of PI3K/Akt/mTOR, and which is also affected by carnosine, was analyzed by RT-qPCR, and reporter gene assays with the human PDK4 promoter were performed. Cell viability was assessed by cell-based assays and mTOR and Akt phosphorylation by Western blotting. Rapamycin and Ly-294,002 increased PDK4 mRNA expression in both cell lines but significance was only reached in U87. Carnosine significantly increased expression in both lines. A significant combinatorial effect of carnosine was only detected in U87 when the dipeptide was combined with Ly-294,002. Reporter gene assays revealed no specific effect of carnosine on the human PDK4 promoter, whereas both inhibitors increased reporter gene expression. Rapamycin reduced phosphorylation of mTOR, and Ly-294,002 that of Akt. A significant reduction of Akt phosphorylation was observed in the presence of carnosine in U87 but not in T98G, and carnosine had no effect on mTOR phosphorylation. Cell viability as determined by ATP in cell lysates was reduced only in the presence of carnosine. We conclude that carnosine's anti-neoplastic effect is independent from PI3K/Akt/mTOR signaling. As the dipeptide reduced viability in tumor cells that do not respond to PI3K or mTOR inhibitors, it appears to be worth to further investigate the mechanisms by which carnosine exerts its anti-tumor effect and to consider it for therapy, especially as it is a naturally occurring compound that has already been used for the treatment of other diseases without indication of side-effects.

Introduction

The most common and aggressive primary tumor of the brain is designated Glioblastoma (GBM). It is classified by the WHO (World Health Organization) as grade IV glioma. In the

United States it accounts for 46.6 percent of all malignant tumors of the central nervous system (CNS) and for 55.4 percent of gliomas. Its incidence is 3.21 per 100.000 population which accounts for 13,010 cases projected in 2018 and 13,310 cases projected in 2019 [1]. Current standard of medical treatment after maximal safe resection is radiotherapy and adjuvant chemotherapy with the alkylating agent temozolomide. Unfortunately, in patients with newly diagnosed GBM the median survival under this treatment is only 12 to 15 month [2,3] and there is urgent need for new strategies for treatment including targeted and immunotherapy strategies (for recent reviews see [4,5]). Among the intracellular pathways, which are intensively investigated as potential targets for treatment strategies, is the PI3K/AKT/mTOR pathway (Phosphoinositide 3-kinase/Ak strain transforming/mechanistic target of rapamycin pathway) (for review see [6]). The more than 50 PI3K inhibitors that have been designed for cancer treatment are classified into pan-PI3K, isoform selective or dual PI3K/mTOR inhibitors (for a recent review see [7]). The drugs MK-2206 and perifosine (KRX-0401) are used as inhibitors of Akt and there is a number of inhibitors of mTOR currently investigated, including temsirolimus, sirolimus (rapamycin), everolimus and ridaforolimus (for review see: [5]).

In recent years our group investigated whether the dipeptide carnosine (β-alanyl-L-histidine) is a candidate for glioblastoma therapy. Carnosine has originally been isolated from Liebig's meat extract almost 120 years ago by Gulewitsch and Amiradzibi [8]. The dipeptide is highly abundant in skeletal muscle with around 20±4.7 mmol per kg dry weight [9], and since its discovery several physiological properties have been ascribed to it, such as pH-buffering, scavenging of reactive oxygen species and heavy metal ions, protection from lipid peroxidation and ischemic brain damage (for a comprehensive review see [10]). Furthermore, an anti-neoplastic effect of carnosine has been demonstrated in vitro and in vivo in a number of cancer models, such as human colon carcinoma [11], gastric carcinoma [12], cervix carcinoma [13], and GBM [14,15]. Interestingly, the dipeptides effect is not limited to proliferation and cell cycle control, but it is also able to decrease the migration of glioblastoma cells [16]. In fact, migration and invasive behavior are hallmarks of glioblastoma, leading to recurrence of tumors only a few months after surgical removal of the primary tumor mass.

Unfortunately, not much is known about the molecular targets of carnosine in cancer cells. Among the mechanisms discussed are an influence on ATP production from glucose [17], and there are observations that depending on the model investigated, hypoxia inducible factor 1 (HIF1) [18], the signal transducer and activator of transcription 3 (STAT3) [19], the mitogen-activated protein kinase (MAPK) [20], and the Kirsten rat sarcoma viral oncogene (KRAS) [21] might be influenced. In addition, there have been hints that the Akt/mTOR/Ribosomal protein S6 kinase beta-1 pathway is involved in carnosine's anti-neoplastic effect [22]. At this point, it is noteworthy, that other observations also point towards the possibility that carnosine may be a mimic of rapamycin, which is an inhibitor of mTORC1 (mTOR complex 1) [23]. In addition, carnosine's anti-neoplastic effect in glioblastoma cells was shown to be accompanied by increased expression of pyruvate dehydrogenase kinase 4 (PDK4) [24]. As PDK4 expression is regulated by transcription factors, such as FOXO1a and FOXO3a (Forkhead box protein O1a and O3a) [25], which are downstream effectors of PI3K/AKT/mTOR signaling, we hypothesized that carnosine's anti-neoplastic effect may be mediated by an influence on this pathway. Therefore, we compared the effect of carnosine on glioblastoma cell viability, PDK4 expression and signaling molecule phosphorylation with the PI3K inhibitor Ly294,002 and the mTOR inhibitor rapamycin in two cell lines derived from glioblastoma.

Materials and methods

Reagents

If not stated otherwise, all chemicals were purchased from Sigma Aldrich (Taufkirchen, Germany) including the PI3K inhibitor Ly-294,002, and the carnosine employed in this study (Cat.-Nr.: C9625/ Lot: BCBK4678V). The mTOR inhibitor rapamycin was purchased from Santa Cruz Biotechnology (Heidelberg, Germany).

Cell culture

U87 (ATCC HTB-14) and T98G (ATCC CRL-1690) cells were obtained from the American Type Culture Collection (ATCC, Manassas, USA) and genotyped (Genolytic GmbH, Leipzig, Germany) to confirm their identity prior to the experiments. Cells were propagated in 250 ml culture flasks (Sarstedt AG & Co., Nümbrecht, Germany) using 10 ml of standard culture medium (SCM) consisting of DMEM (Dulbecco's Modified Eagle Medium) with 4.5 g/l glucose, and without pyruvate (Life Technologies, Darmstadt, Germany), supplemented with 10% fetal bovine serum (FBS superior, Biochrom, Berlin, Germany), 2 mM GlutaMAX (Life Technologies) and Penicillin-Streptomycin (Life Technologies) at 37°C and 5% CO_2 in humidified air in an incubator.

Reporter gene construction

The human PDK4 promoter (-3968/+319 bp relative to the transcription start site) was obtained by PCR (polymerase chain reaction) employing the GoTaq Long PCR Master Mix (Promega, Mannheim, Germany) using genomic DNA extracted from T98G cells (QIAamp DNA mini Kit, Qiagen) as template using the following primers: *hPDK4_(-)3968*: 5'-CAT GGC GGG ATC CTT TCT TAT GGG CTG C-3'; (forward) and *hPDK4_(+)319*: 5'-CGC CTC CAT GGT GAC GCC CAC CC-3' (reverse). *hPDK4_(-)3968* was designed containing a *Bam*HI recognition site and *hPDK4_(+)319* containing an *Nco*I recognition site (both underlined in the primer sequences presented). These recognition sites allowed subcloning of the amplification product into the reporter gene *pT81_GauIII* (containing the secreted luciferase from *Gaussia princeps* [26]) after restriction digestion of both the PCR product and the vector. In this way the reporter gene *hPDK4_GauIII* was obtained in which a ~4000 bp 5'-region (-3986/+319) from the PDK4 gene controls the luciferase from *Gaussia princeps* with the endogenous PDK4 start codon matching the start codon of the luciferase gene.

Reverse transcription–quantitative real time polymerase chain reaction experiments

For the quantification of mRNA, RT-qPCR (reverse transcription–quantitative real time polymerase chain reaction) experiments were carried out as described [24]. Briefly, 10^6 cells were seeded into 100-mm cell culture dishes (TPP, Trasadingen, Switzerland) with 10 ml of medium. After 24 hours of incubation, cells received fresh medium containing the compounds to be tested. Cells were harvested 24 hours later and RNA was isolated using a miRNeasy mini kit (Qiagen, Hilden, Germany) according to manufacturer's instructions. The RNA was stored at -80°C until further use. 500 ng of RNA were used for reverse transcription employing the ImProm-II Reverse Transcription System (Promega, Mannheim, Germany) according to manufacturer's instructions using random primer sets. DNA amplification was performed on a Rotor-Gene 3000 system (Qiagen) employing SYBR Green (Maxima SYBR Green/ROX qPCR Master Mix, Thermo scientific). Copy numbers of individual mRNAs were determined using linearized plasmid DNA (described in [24]) containing the corresponding target

52

sequence. Data analysis was performed using the Rotor-Gene 6 software, and data was processed as described [24]. For reference, the transcript encoding the TATA-box binding protein (TBP) was used. Primer sequences: *PDK4_forward*: 5'-CTG TGA TGG ATA ATT CCC-3'; *PDK4_reverse*: 5'-GCC TTT AAG TAG ATG ATA GCA-3'; *TBP_forward*: 5'-TGA CCT AAA GAC CAT TGC AC-3'; *TBP_reverse*: 5'-GCT CTG ACT TTA GCA CCT GTT-3'.

Cell viability assays

For the determination of ATP production the CellTiter-Glo Assay (CTG) and for the determination of dehydrogenase activity the CellTiter-Blue Assay (CTB) were employed (all from Promega, Mannheim, Germany) according to the instructions of the manufacturer, and as described previously [27]. All measurements of luminescence and fluorescence were performed using either a Mithras LB 940 Multimode Microplate reader (Berthold Technologies, Bad Wildbad, Germany) or a Spectra Max M5 reader (Molecular Devices, Biberach, Germany).

Transfection experiments

Transient transfection was performed using TurboFect transfection reagent (Thermo scientific, Dreieich, Germany) according to manufacturer's instructions. The ratio of DNA to TurboFect employed was 2 µg DNA per 4 µl transfection reagent. For transfection, cells were first seeded in 96-well plates at a density of 10,000 cells per well in 200 µl of medium. After 24 hours, old medium was removed and fresh medium containing the DNA/Polymer complexes was added (100 µl with an equivalent of 25 ng DNA). Three hours later, medium was exchanged and the cells received fresh medium with the supplements to be tested. *Gaussia* luciferase activity was determined from the supernatant 24 hours after the start of the transfection as described before [26]. Briefly, cell supernatant (5 µl) was transferred into a well of a white 96-well plate (Greiner bio-one, Frickenhausen, Germany). After an incubation of 20 minutes at room temperature, *Gaussia* luciferase activity was determined using a Mithras LB 940 Multimode reader (Berthold Technologies, Bad Wildbad, Germany) by injecting 50 µl of luciferase assay reagent (20 mM MOPS (3-(N-morpholino)propanesulfonic acid); 0.75 M KBr; 5 mM $MgCl_2$; 5 mM $CaCl_2$; 1 mM EDTA (ethylenediaminetetraacetic acid); 10 µM Coelenterazine; pH 7.8) to the cell supernatant, followed by a 1.6 second delay until luminescence was determined within a 0.5 s integral.

Western Blot analysis

Western Blot experiments were performed with cells cultivated at a density of 10^6 cells per dish in 100-mm cell culture dishes for 24 hours in the presence of the test compounds. Briefly, cells were washed twice with ice-cold washing buffer (137 mM NaCl; 5.4 mM HCl; 0.41 mM $MgSO_4$, 0.49 mM $MgCl_2$; 0.126 mM $CaCl_2$; 0.33 mM Na_2HPO_4; 0.44 mM KH_2PO_4; 2 mM HEPES (4-(2-hydroxyethyl)-1-piperazineethanesulfonic acid); pH 7.4), and were then transferred to a 1.5 ml reaction vial using a cell scraper (TPP, Trasadingen, Switzerland), and 1 ml of ice-cold washing buffer. Cells were collected by centrifugation (500xg; 4 min; 4˚C), and resuspended in 150 µl of ice-cold RIPA buffer (50 mmol/l Tris (tris(hydroxymethyl)amino-methane); 150 mmol/l NaCl; 1% Nonidet P40; 0.25% Natriumdesoxycholat; 0.1% SDS; pH 8.0) containing a combination of protease inhibitors (0.025 mg/ml Aprotinin; 0.025 mg/ml Leupeptin; 2.5 mmol/l Benzamidin; 0.01 mg/ml Pepstatin A; 2.5 mmol/l phenylmethylsulfonyl-fluorid), phosphatase inhibitors (PhosSTOP, Sigma) and 1 mmol/l DTT (Dithiothreitol). Cells were sonified using a Bioruptor system (Diagenode, Seraing, Belgium) at highest energy

53

setting using a "30 s on/ 30 s off" protocol for 7.5 min. After sonification debris was removed by centrifugation (5500xg; 5 min; 4°C) and the supernatant containing the proteins was transferred to fresh reaction vials. Proteins were either immediately used for Western blotting or frozen at -80°C for long term storage.

SDS-PAGE (sodium dodecyl sulfate–polyacrylamide gel electrophoresis) was performed with 30 µg of protein per lane using a Mini-PROTEAN System (Bio-Rad, Munich, Germany). For the detection of Akt, gels with a concentration of 12% acrylamide were used, and for the detection of mTOR, gels with an acrylamide concentration of 6%. After electrophoresis, proteins were transferred to PVDF (polyvinylidene difluoride) membranes (Low Fluorescence Membrane Opti Blot, Abcam, Cambridge, GB) using a Mini Trans-Blot Cell (Bio-Rad). Then, the membranes were incubated with antibodies diluted in TBST (Tris-buffered saline with Polysorbate 20: 20 mM Tris, 134 mM NaCl, 0.1% Tween 20 and 2% (w/v) bovine serum albumin; pH 7.6) at the dilutions indicated below.

The primary antibodies used were: mouse anti-pan-AKT [Cell Signaling; #2920] 1:2000 in TBST; rabbit anti-PSer473-AKT [Cell Signaling; #4058] 1:1000 in TBST; mouse-anti-mTOR [Millipore; # 05–1564] 1:1000 in TBST; rabbit anti-PSer2448-mTOR [Cell Signaling; #2971] 1:1000 in TBST. The secondary antibodies employed (red fluorescent IRDye 680RD Goat anti-Mouse and green fluorescent IRDye 800CW Goat anti-Rabbit; both diluted 1:5000 in TBST) were purchased from LI-COR (LI-COR Biosciences, Lincoln, USA). Membranes were scanned using an Odyssey Imaging System (LI-COR, Bad Homburg, Germany), and band intensities were determined by the Image Studio 5 software (LI-COR).

Statistical analysis

Statistical analysis was carried out using SPSS (IBM, Armonk, USA; Version: 24.0.0.2 64-bit). For multiple comparisons, a one-way ANOVA with the Games-Howell post hoc test was used. A significance level of $p < 0.05$ was considered to be significant. Relative data resulting from two or more experiments or parameters (normalization to reference) with a separate mean and standard deviation are presented using Gaussian error propagation as described before [24]. For the comparison of data obtained from the densitometric analysis of different Western Blot experiments, a least square method was employed in order to calculate means and standard deviations [28].

Results

PDK4 expression under the influence of carnosine, rapamycin and Ly-294,002

In a first series of experiments, we asked whether the effect of carnosine on the expression of PDK4 in U87 and T98G glioblastoma cells, that was described by Letzien et al. [24], can also be detected using inhibitors of PI3K/Akt/mTOR signaling. Therefore, cells from the two lines were exposed for 24 hours to carnosine (50 mM), the PI3K inhibitor Ly-294,002 (5 µM), the mTORC1 inhibitor rapamycin (25 nM), and to combinations of the compounds. Then, mRNA was isolated and subjected to RT-qPCR. The result of the experiment is presented in Fig 1. The concentration of rapamycin employed in the experiments (25 nM) has been determined to result in a maximal effect on PDK4 expression in U87 cells, whereas that of Ly-294,002 (5 µM) resulted in an increase of 60% compared to the maximal achievable effect at a concentration of 10 µM in U87 cells (S1 Fig). The rational for using Ly-294,002 at a concentration of 5 µM instead of 10 µM was based on suppliers information that the compound has an IC50 of 0.5 µM/0.57 µM/0.97 µM for PI3Kα/δ/β (Selleckchem, Munich, Germany), but that
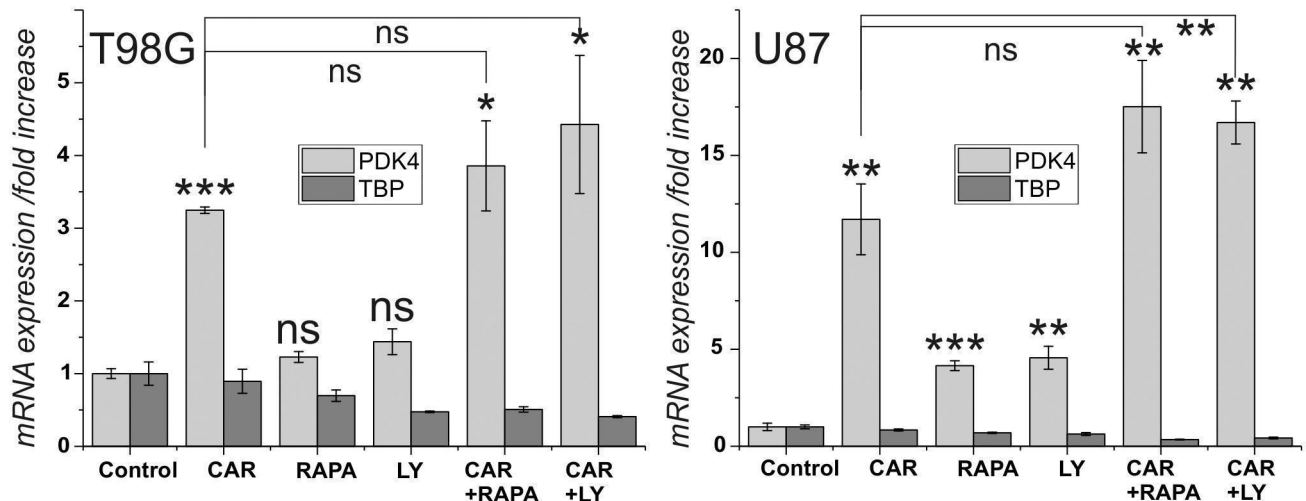
54

Fig 1. Influence of carnosine, rapamycin and Ly-294,002 on the expression of PDK4 and TBP in cells from the glioblastoma cell lines U87 and T98G. Cells from the lines U87 and T98G were cultivated for 24 hours in the presence of carnosine (Car; 50 mM), rapamycin (Rapa; 25 nM), Ly-294,002 (Ly; 5 μM) or a combination of the compounds. Afterwards expression of PDK4 and TBP was measured and the fold change of expression under the influence of the compounds was determined. Asterisks above the columns indicate a significantly increased expression under the influence of the test compound compared to untreated control cells and the asterisks at the lines connecting columns indicate significant differences between the connected columns: ns: not significant; *: p<0.05; **: p<0.005; ***: p<0.0005.

the compound may also affect targets seemingly unrelated to the PI3K family with an IC50>50 μM (Abcam). Therefore, we preferred to have a concentration as low as possible, but resulting in a reproducible significant effect. As can be seen in Fig 1, carnosine significantly increased the expression of PDK4 in both cell lines, but only in U87 cells a significant increase is seen under the influence of rapamycin and Ly-294,002. Combining Ly-294,002 with carnosine resulted in a higher expression of PDK4, compared to expression with carnosine alone, but only for U87 cells significance was confirmed (p<0.005). Although, the combination of carnosine with rapamycin did also result in a higher expression, compared to that in carnosine alone, this effect was not significant in both cell lines.

Expression of a PDK4 reporter gene under the influence of carnosine, rapamycin and Ly-294,002

As rapamycin and Ly-294,002 were both able to increase expression of PDK4 in the two cell lines investigated (although significance was only confirmed for U87), we wondered whether carnosine exerts its effect on PDK4 expression via PI3/Akt/mTOR signaling. In order to prove this hypothesis, reporter gene assays were performed. The experiments were based on the observation that the effect of PI3K/Akt/mTOR signaling on expression of PDK4 is mediated by elements in the 5'-upstream region of the gene, e.g. by binding sites for transcription factors of the FOXO family [25]. Therefore, we asked whether the effect of carnosine is also mediated by elements located in the promoter of the gene. To answer this question, a reporter gene was constructed that covered a region from the human PDK4 gene (hPDK4) encompassing 3968 bp upstream from the transcriptional start point and 319 bp downstream of it, including the start codon of hPDK4 controlling a luciferase gene with a secretion signal from *Gaussia princeps*. The construct designated "*hPDK4_GauIII*" was transfected into U87 and T98G cells. After 3 hours of exposure to the DNA/transfection complexes, medium was exchanged and the cells were exposed to carnosine (50 mM), rapamycin (25 nM) and Ly-294,002 (5 μM). Twenty-four hours later, luciferase activity was determined from the supernatant. As
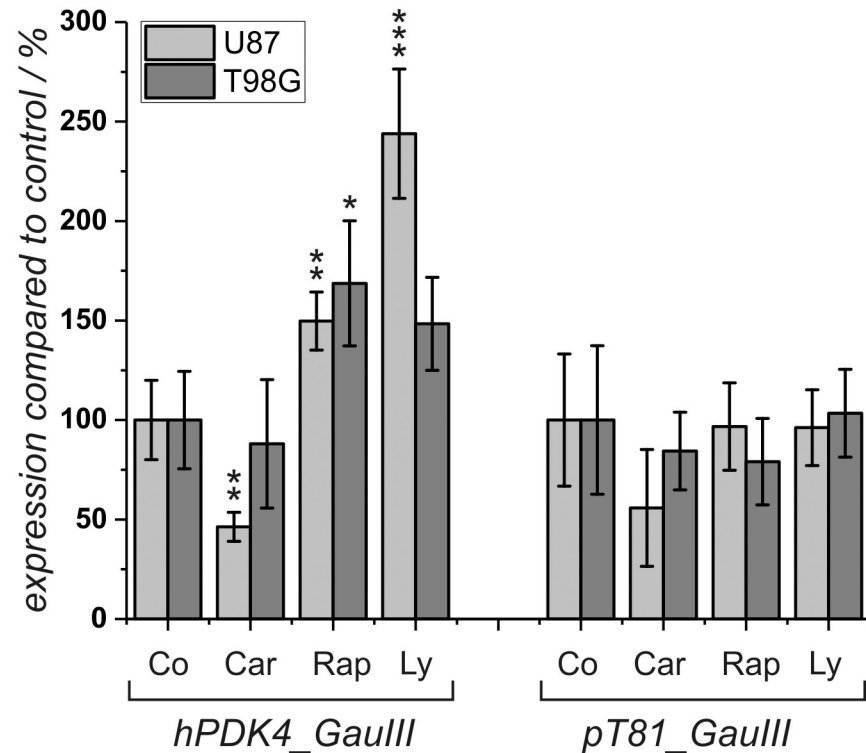
55

Fig 2. Expression of a reporter gene with human PDK4 5'-region after exposure to different compounds. The reporter gene *hPDK4_GauIII* with the 5'-region from the human PDK4 promoter and the control vector *pT81_GauIII* were transfected into U87 and T98G cells. Cells were exposed to carnosine (Car; 50 mM), rapamycin (Rap; 25 nM), Ly-294,002 (Ly; 5 μM) or to vehicle control (Con) and luciferase activity was determined after 24 hours of incubation (6 independent wells). *: $p < 0.05$; **: $p < 0.005$, and ***: $p < 0.0005$.

reference, cells were also transfected with the reporter gene "*pT81_GauIII*" used for the construction of "*hPDK4_GauIII*" which only contained a minimal promoter from the thymidine kinase of *Herpes simplex*. The result of a corresponding experiment is presented in Fig 2. The experiment demonstrates a significant response of the PDK4 reporter gene to the presence of rapamycin in both cell lines. In the presence of Ly-294,002, we also observed increased expression in both cell lines but statistical significance could only be confirmed for U87 cells. Regarding expression of the corresponding control vector, no statistically significant influence of carnosine, rapamycin, and Ly-294,002 was obtained. In the presence of carnosine, the reporter gene and the control plasmid exhibited a comparable reduced expression in U87 cells (statistically significant only for the reporter gene) and no response in cells from the line T98G. Note: The negative response in the presence of carnosine, which becomes significant in U87 cells transfected with the reporter gene, is a result of reduced viability under the influence of the dipeptide (compare Fig 3). Therefore, we conclude that carnosine's effect on expression of the endogenous PDK4 gene is independent from an interaction of transcription factors within the tested cis-elements and also different from the effects exhibited by rapamycin and Ly-294,002.

Cell viability under the influence of carnosine, rapamycin and Ly-294,002

As the reporter gene assay performed indicated a strong influence of carnosine on viability of cells from the line U87, which was not observed in the presence of rapamycin and Ly-294,002, we decided to study the effect of the three compounds on viability in more detail. Therefore,
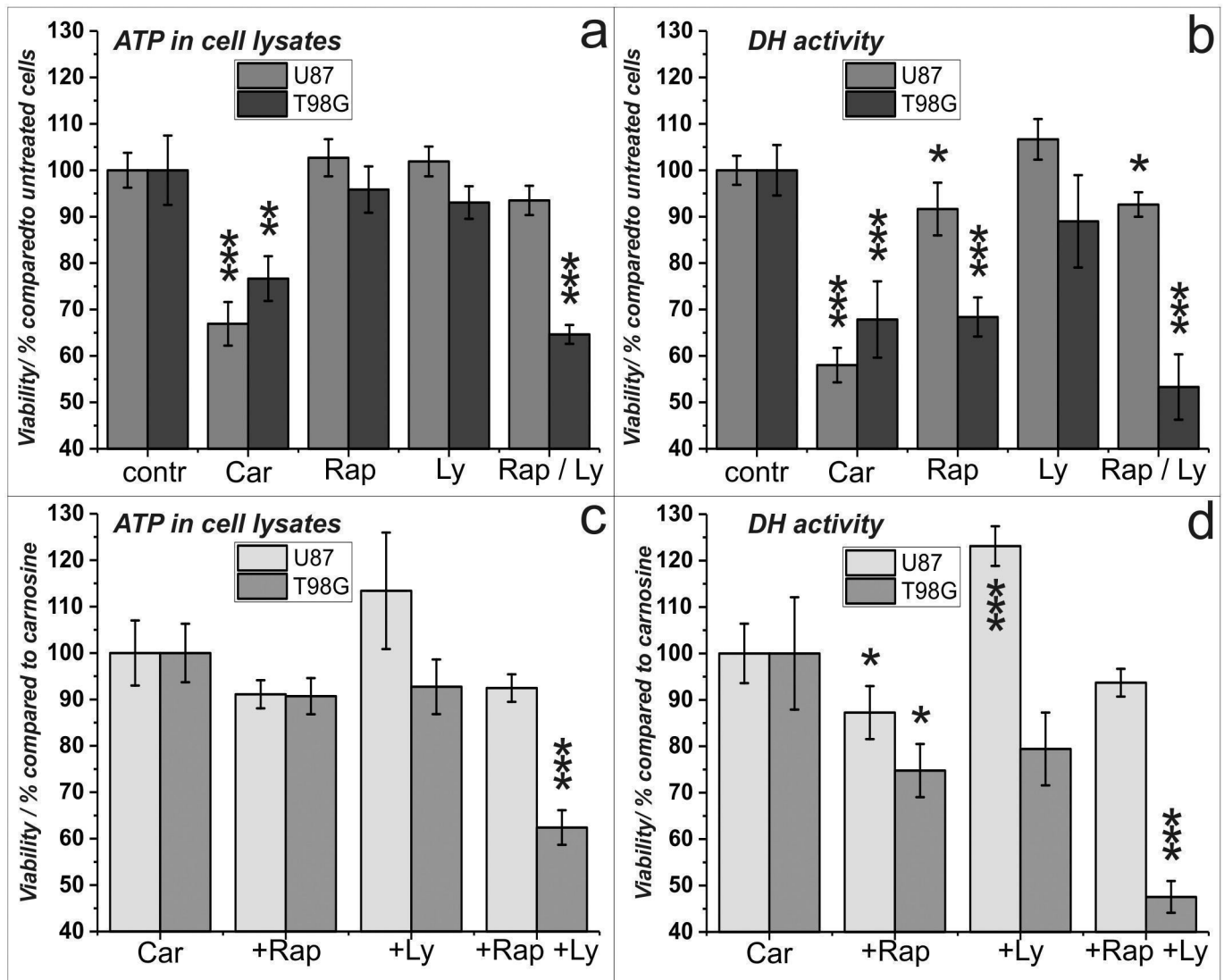
Fig 3. Viability of U87 and T89G cells under the influence of carnosine, rapamycin and Ly-294,002. Cells from the lines U87 and T98G were cultivated for 24 hours in the presence of carnosine (Car; 50 mM), rapamycin (Rap; 25 nM), Ly-294,002 (Ly; 5 μM) or vehicle control (contr). Then, the amount of ATP in cell lysates (left panels) and dehydrogenase activities (right panels) as a measure of cell viability were determined. Upper panels show the influence of each compound on viability compared to untreated cells. In the lower panels the effect of rapamycin and Ly-294,002 on the viability of cells treated in combination with carnosine (cells treated with carnosine only set as 100%) is shown. Mean and standard deviation are presented from 8 independently treated wells for each condition. *: $p < 0.05$; **: $p < 0.005$, and ***: $p < 0.0005$.

https://doi.org/10.1371/journal.pone.0218972.g003

U87 and T98G cells were cultivated in 96-well plates and exposed to carnosine (50 mM), rapamycin (25 nM) and Ly-294,002 (5 μM). Twenty-four hours later, cell viability was determined measuring ATP in cell lysates using the CellTiter-Glo assay and dehydrogenase activity using the CellTiterBlue assay. The result of an experiment in which 5000 cells per well were used is presented in Fig 3. As can be seen, carnosine had a significant effect on viability of both cell lines as determined by ATP production (Fig 3a) and dehydrogenase activity (Fig 3b). The determination of ATP in cell lysates did not show an influence of rapamycin on viability, but the determination of dehydrogenase activity clearly indicated that rapamycin affects dehydrogenase activity as a measure of viability, which is more prominent in cells from the line T98G than in cells from the line U87. Analyzing effects by combination of carnosine with the other

compounds (Fig 3c/3d), a significant reduction of viability compared to cells treated with carnosine alone was detected by combination with rapamycin in both cell lines but only regarding dehydrogenase activity. Interestingly, dehydrogenase activity was increased in U87 cells treated with Ly-294,002 and carnosine compared to carnosine alone, and we identified a reduction of dehydrogenase activity in T98G cells combining Ly-294,002 with carnosine relative to cells treated with carnosine alone, which was not significant.

Phosphorylation of Akt and mTOR under the influence of carnosine, rapamycin and Ly-294,002

The experiments presented in the preceding paragraphs indicated that carnosine's effect on PDK4 expression is different from that of rapamycin and Ly-294,002. To finally analyze whether PI3K/Akt/mTOR pathway signaling in U87 and T98G cells is affected at the level of Akt and mTOR phosphorylation, when the cells are exposed to carnosine and the inhibitors, we performed Western Blot experiments. Therefore, U87 and T98G cells were cultivated for 24 hours in the presence of carnosine (50 mM), rapamycin (25 nM) and Ly-294,002 (5 μM), and combinations of the compounds. Then, proteins were extracted, subjected to SDS-PAGE and Western Blotting was performed with antibodies directed against mTOR and Akt and their phosphorylated forms. In Fig 4 representative Blots and a densitometric analysis from six (U87), and three (T98G) independent experiments with each pair of antibodies are presented. Whereas rapamycin was able to reduce mTOR phosphorylation in both cell lines, Ly-294,002 did affect phosphorylation of mTOR only in T98G cells but not in U87 cells. Most importantly, carnosine had no effect on phosphorylation of mTOR. Analyzing the phosphorylation of Akt we did not detect an effect of rapamycin on its phosphorylation, but a significant one by Ly-294,002 in both cell lines. Interestingly, carnosine significantly reduced phosphorylation of Akt in cells from the line U87 but not in T98G.

Discussion

Here, we investigated, whether carnosine has an influence on the PI3K/Akt/mTOR pathway. Ample laboratory studies suggest that this pathway is vital to the growth and survival of cancer cells, including glioblastoma with hyperactivated PI3K/Akt/mTOR [7]. In our experiments, the PI3Kα/δ/β inhibitor Ly294,002 significantly inhibited phosphorylation of Akt in T98G and U87 cells, but an effect on phosphorylation of mTOR after 24 hours of treatment was only detected in T98G and not in U87 cells. More importantly, we found no indication of reduced viability after treatment with Ly294,002 in both cell lines. This appears to be in contrast to results obtained by others [29]. These authors observed enhanced survival of nude mice with intracranially implanted U87 cells after oral administration of the pan-class I PI3K inhibitor NVP-BKM120 (buparsilib; 5 times a week for a total of 20 treatments). In addition, they also detected enhanced apoptosis, as detected by Annexin V staining, in cultured U87 cells after 72 hour treatment with NVP-BKM120 [29]. We assume that it may be that the 24-hour incubation period employed in our experiments is too short to see effects of PI3K inhibition on tumor cell viability. This assumption is supported by data obtained with the glioblastoma cell lines LN229 and U251, which did significantly respond to 10 μM Ly294,002 only when they were incubated in its presence for more than one day [30]. It also should be noted that other authors point out that in the range of 4 to 8 μM Ly294,002 does not discernibly affect cell cycle progression, at least in U251 MG glioblastoma cells [31]. Carnosine, which also reduced phosphorylation of Akt in U87 cells, although not as strong as Ly294,002, had a strong effect on viability already after 24-hour exposure. We currently do not know why phosphorylation of Akt under the influence of carnosine is not observed in T98G cells. However, it has to be taken
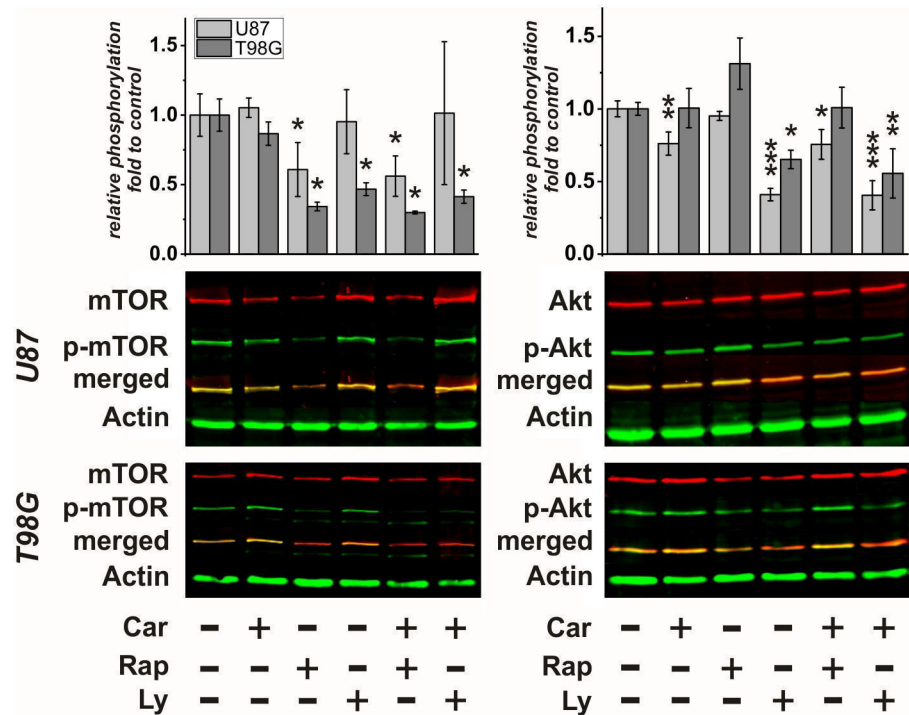
58

Fig 4. Phosphorylation of mTOR and Akt under the influence of carnosine, rapamycin and Ly-294,002. Cells from the lines U87 and T98G were incubated in the presence of carnosine (Car; 50 mM), rapamycin (Rap; 25 nM), Ly-294,002 (Ly; 5 μM) or vehicle control or a combination of the compounds. Proteins were isolated, subjected to SDS-PAGE and Western Blotting was performed using antibodies for mTOR and mTOR phosphorylation at serine 2448 (mTOR and p-mTOR; left) and antibodies against Akt and Akt phosphorylation at serine 473 (Akt and p-Akt right). In the lower part, representative blots are presented in which the total amount of each signaling molecule is detected by red fluorescence and its corresponding phosphorylated form by green fluorescence. Below the combined bands are shown (merged) in yellow. Actin served as loading control (green fluorescence). A densitometry analysis from six (U87) and three (T98G) independent experiments was performed with each set of the two primary antibodies. Data is presented as "relative phosphorylation", indicating the ratio of the signal obtained with the phospho-specific antibody compared to the signal with the antibody direct against total protein of the factor under the influence of a compound, compared to this ratio in untreated control cells (set as 1). Statistical significance was calculated by one-way ANOVA with the Games-Howell post hoc test: *: $p<0.05$; **: $p<0.005$, and ***: $p<0.0005$.

into account, that the status of phosphorylation is also dependent on the activity of phosphatases and other mechanisms such as subcellular localization (for a recent review see [32]).

Rapamycin (also known as Sirolimus) did reduce phosphorylation of mTOR in both cell lines, as it had to be expected, but it had no effect on viability as determined by ATP in cell lysates. Measuring dehydrogenase activity, a minor effect of rapamycin on viability was detected in U87 cells. In T98G cells the effect of rapamycin was comparable to the effect of carnosine, when measuring dehydrogenase activity. From these data, we conclude that the anti-neoplastic effect of carnosine is certainly not mediated via an effect on PI3K, and also unlikely to be mediated via mTOR. However, as demonstrated by the data presented in Fig 3, a small combinatorial effect of carnosine and rapamycin can be observed in both cell lines with regard to dehydrogenase activity, and not with regard to the amount of ATP in cell lysates.

The influence of Ly294,002 and rapamycin on PDK4 expression is known to be mediated by 5'-elements in the PDK4 gene, which we confirmed by our reporter gene assay. As carnosine did not increase the expression of the reporter gene, this observation supports the assumption resulting from the viability assays, that carnosine must mediate its physiological effects without influencing PI3K/Akt/mTOR in the glioblastoma cells used. At this point it may be

59

hypothesized that elements which were not present in our reporter gene, such as intronic or 3'-elements, could be responsible for the induction of the PDK4 gene under the influence of carnosine. In fact, we just recently demonstrated that the effect of carnosine on PDK4 expression is linked to epigenetic mechanisms [33]. At this point it is also interesting to note, that a recent report, comparing PDK4 mRNA expression under the influence of carnosine and L-histidine in 21 primary glioblastoma cultures and 10 glioblastoma cell lines, revealed that no correlation exists between increased mRNA expression and the compounds influence on viability [34].

As already outlined in the introduction, there is evidence, that carnosine's effect on tumor cell viability is accompanied by effects on signal transduction and on tumor cell metabolism. However, the question remains, whether the effects on signal transduction detected in other tumor models, as outlined in the introduction, are resulting from a direct effect on a single transduction molecule or on a receptor. In fact, we recently demonstrated that increased expression of PDK4 is accompanied by epigenetic regulation [33], and the possibility cannot be ruled out that the primary target of carnosine is an unknown Histone Deacetylase. In that case, the observed changes in signal transduction may be a secondary response. As carnosine is able to react non-enzymatically with aldehydes [35], one could also imagine that its primary target is a metabolite, such as an aldehyde of the glycolytic pathway, which might explain its effect on ATP production from glucose [17]. Any influence on metabolism will in turn also feed-back on signal transduction [36].

Although, carnosine's primary targets have still not been revealed, we consider it worth to further investigate them, as understanding carnosine's mode of action could pave the way to the discovery of novel therapeutic interventions. In this context, it should be emphasized, that the present investigation demonstrates, that tumors, which do not or less respond to drugs targeting pathways, such as the PI3K/Akt/mTOR pathway, are still sensitive to carnosine. This could offer the opportunity for new strategies for the treatment of tumors in general and glioblastoma in particular, that are resistant to currently employed drugs. However, these interventions may include the design of novel drugs, targeting the primary targets of carnosine, as we are aware, that the concentrations employed in the in vitro experiments in the present study may not be reached in a patient by oral administration of the dipeptide. On the other hand, dose response studies demonstrated that lower concentrations are also effective [14,24], especially after prolonged incubation [16]. In addition, the great advantage of carnosine is, that it is a naturally occurring compound, which has already been used for the treatment of other diseases, without having side-effects [37–39]. In addition, we just recently demonstrated that the dipeptide does not decrease the viability of fibroblasts [16], and does even have neuroprotective effects [40].

Supporting information

S1 Fig. Relative PDK4 expression after exposure to different concentrations of rapamycin and Ly-294,002. Cells from the line U87 were cultivated at a density of 10^6 cells per culture plate and exposed for 24 hours to different concentrations of rapamycin and Ly-294,002. The fold of enhancement of PDK4 mRNA expression was calculated from the relative expression of PDK4 (compared to the expression of mRNA encoding TBP) and compared to the corresponding control cells treated with vehicle.
(TIF)

Acknowledgments

Author Contributions

Conceptualization: Henry Oppermann, Frank Gaunitz.

Data curation: Henry Oppermann, Helene Faust, Ulrike Yamanishi, Frank Gaunitz.

Formal analysis: Henry Oppermann, Helene Faust, Frank Gaunitz.

Funding acquisition: Jürgen Meixensberger, Frank Gaunitz.

Investigation: Henry Oppermann, Helene Faust, Ulrike Yamanishi, Frank Gaunitz.

Methodology: Henry Oppermann, Helene Faust.

Project administration: Jürgen Meixensberger, Frank Gaunitz.

Resources: Frank Gaunitz.

Supervision: Jürgen Meixensberger, Frank Gaunitz.

Validation: Jürgen Meixensberger, Frank Gaunitz.

Writing – original draft: Henry Oppermann, Helene Faust, Frank Gaunitz.

Writing – review & editing: Frank Gaunitz.

References

1. Ostrom QT, Gittleman H, Truitt G, Boscia A, Kruchko C, Barnholtz-Sloan JS. CBTRUS Statistical Report: Primary Brain and Other Central Nervous System Tumors Diagnosed in the United States in 2011–2015. Neuro-Oncology. 2018; 20: iv1–iv86. https://doi.org/10.1093/neuonc/noy131 PMID: 30445539

2. Stupp R, Mason WP, van den Bent M. J., Weller M, Fisher B, Taphoorn MJB, et al. Radiotherapy plus concomitant and adjuvant temozolomide for glioblastoma. New England Journal of Medicine. 2005; 352: 987–996. https://doi.org/10.1056/NEJMoa043330 PMID: 15758009

3. Wen PY, Kesari S. Malignant gliomas in adults. N Engl J Med. 2008; 359: 492–507. https://doi.org/10.1056/NEJMra0708126 PMID: 18669428

4. Bush NAO, Chang SM, Berger MS. Current and future strategies for treatment of glioma. Neurosurg Rev. 2017; 40: 1–14. https://doi.org/10.1007/s10143-016-0709-8 PMID: 27085859

5. Alifieris C, Trafalis DT. Glioblastoma multiforme. Pathogenesis and treatment. Pharmacol Ther. 2015; 152: 63–82. https://doi.org/10.1016/j.pharmthera.2015.05.005 PMID: 25944528

6. Li X, Wu C, Chen N, Gu H, Yen A, Cao L, et al. PI3K/Akt/mTOR signaling pathway and targeted therapy for glioblastoma. Oncotarget. 2016. https://doi.org/10.18632/oncotarget.7961 PMID: 26967052

7. Zhao H-F, Wang J, Shao W, Wu C-P, Chen Z-P, To S-ST, et al. Recent advances in the use of PI3K inhibitors for glioblastoma multiforme. Current preclinical and clinical development. Mol Cancer. 2017; 16: 100. https://doi.org/10.1186/s12943-017-0670-3 PMID: 28592260

8. Gulewitsch W, Amiradzibi S. Ueber das Carnosin, eine neue organische Base des Fleischextraktes. Ber Dtsch Chem Ges. 1900; 33: 1902–1903.

9. Mannion AF, Jakeman PM, Dunnett M, Harris RC, Willan PL. Carnosine and anserine concentrations in the quadriceps femoris muscle of healthy humans. Eur J Appl Physiol Occup Physiol. 1992; 64: 47–50. PMID: 1735411

10. Boldyrev AA, Aldini G, Derave W. Physiology and pathophysiology of carnosine. Physiol Rev. 2013; 93: 1803–1845. https://doi.org/10.1152/physrev.00039.2012 PMID: 24137022

11. Horii Y, Shen J, Fujisaki Y, Yoshida K, Nagai K. Effects of l-carnosine on splenic sympathetic nerve activity and tumor proliferation. Neurosci Lett. 2012; 510: 1–5. https://doi.org/10.1016/j.neulet.2011.12.058 PMID: 22240100

12. Shen Y, Yang J, Li J, Shi X, Ouyang L, Tian Y, et al. Carnosine inhibits the proliferation of human gastric cancer SGC-7901 cells through both of the mitochondrial respiration and glycolysis pathways. PLoS ONE. 2014; 9: e104632. https://doi.org/10.1371/journal.pone.0104632 PMID: 25115854

13. Ditte Z, Ditte P, Labudova M, Simko V, Iuliano F, Zatovicova M, et al. Carnosine inhibits carbonic anhydrase IX-mediated extracellular acidosis and suppresses growth of HeLa tumor xenografts. BMC Cancer. 2014; 14: 358. https://doi.org/10.1186/1471-2407-14-358 PMID: 24886661

14. Renner C, Seyffarth A, de Arriba S, Meixensberger J, Gebhardt R, Gaunitz F. Carnosine Inhibits Growth of Cells Isolated from Human Glioblastoma Multiforme. Int J Pept Res Ther. 2008; 14: 127–135. https://doi.org/10.1007/s10989-007-9121-0

15. Renner C, Zemitzsch N, Fuchs B, Geiger KD, Hermes M, Hengstler J, et al. Carnosine retards tumor growth in vivo in an NIH3T3-HER2/neu mouse model. Mol Cancer. 2010; 9: 2. https://doi.org/10.1186/1476-4598-9-2 PMID: 20053283

16. Oppermann H, Dietterle J, Purcz K, Morawski M, Eisenlöffel C, Müller W, et al. Carnosine selectively inhibits migration of IDH-wildtype glioblastoma cells in a co-culture model with fibroblasts. Cancer Cell Int. 2018; 18: 111. https://doi.org/10.1186/s12935-018-0611-2 PMID: 30123089

17. Oppermann H, Schnabel L, Meixensberger J, Gaunitz F. Pyruvate attenuates the anti-neoplastic effect of carnosine independently from oxidative phosphorylation. Oncotarget. 2016; 7: 85848–85860. https://doi.org/10.18632/oncotarget.13039 PMID: 27811375

18. Iovine B, Oliviero G, Garofalo M, Orefice M, Nocella F, Borbone N, et al. The Anti-Proliferative Effect of L-Carnosine Correlates with a Decreased Expression of Hypoxia Inducible Factor 1 alpha in Human Colon Cancer Cells. PLoS One. 2014; 9: e96755. https://doi.org/10.1371/journal.pone.0096755 PMID: 24804733

19. Wang J-P, Yang Z-T, Liu C, He Y-H, Zhao S-S. L-carnosine inhibits neuronal cell apoptosis through signal transducer and activator of transcription 3 signaling pathway after acute focal cerebral ischemia. Brain Res. 2013; 1507: 125–133. https://doi.org/10.1016/j.brainres.2013.02.032 PMID: 23454231

20. Kulebyakin K, Karpova L, Lakonsteva E, Krasavin M, Boldyrev A. Carnosine protects neurons against oxidative stress and modulates the time profile of MAPK cascade signaling. Amino Acids. 2012; 43: 91–96. https://doi.org/10.1007/s00726-011-1135-4 PMID: 22101981

21. Iovine B, Iannella ML, Nocella F, Pricolo MR, Baldi MR, Bevilacqua MA. Carnosine inhibits KRas-mediated HCT-116 proliferation by affecting ATP and ROS production. Cancer Lett. 2011; 315: 122–128. https://doi.org/10.1016/j.canlet.2011.07.021 PMID: 22137144

22. Zhang Z, Miao L, Wu X, Liu G, Peng Y, Xin X, et al. Carnosine Inhibits the Proliferation of Human Gastric Carcinoma Cells by Retarding Akt/mTOR/p70S6K Signaling. J Cancer. 2014; 5: 382–389. https://doi.org/10.7150/jca.8024 PMID: 24799956

23. Hipkiss AR. Energy metabolism, proteotoxic stress and age-related dysfunction–Protection by carnosine. Mol Aspects Med. 2011; 32: 267–278. https://doi.org/10.1016/j.mam.2011.10.004 PMID: 22020113

24. Letzien U, Oppermann H, Meixensberger J, Gaunitz F. The antineoplastic effect of carnosine is accompanied by induction of PDK4 and can be mimicked by L-histidine. Amino Acids. 2014. https://doi.org/10.1007/s00726-014-1664-8 PMID: 24398899

25. Kwon H-S, Huang B, Unterman TG, Harris RA. Protein kinase B-alpha inhibits human pyruvate dehydrogenase kinase-4 gene induction by dexamethasone through inactivation of FOXO transcription factors. Diabetes. 2004; 53: 899–910. https://doi.org/10.2337/diabetes.53.4.899 PMID: 15047604

26. Braun S, Oppermann H, Mueller A, Renner C, Hovhannisyan A, Baran-Schmidt R, et al. Hedgehog signaling in glioblastoma multiforme. cbt. 2012; 13: 487–495. https://doi.org/10.4161/cbt.19591 PMID: 22406999

27. Gaunitz F, Heise K. HTS compatible assay for antioxidative agents using primary cultured hepatocytes. Assay.Drug Dev.Technol. 2003; 1: 469–477. https://doi.org/10.1089/154065803322163786 PMID: 15090184

28. Degasperi A, Birtwistle MR, Volinsky N, Rauch J, Kolch W, Kholodenko BN. Evaluating strategies to normalise biological replicates of Western blot data. PLoS ONE. 2014; 9: e87293. https://doi.org/10.1371/journal.pone.0087293 PMID: 24475266

29. Koul D, Fu J, Shen R, LaFortune TA, Wang S, Tiao N, et al. Antitumor activity of NVP-BKM120—a selective pan class I PI3 kinase inhibitor showed differential forms of cell death based on p53 status of glioma cells. Clinical Cancer Research. 2012; 18: 184–195. https://doi.org/10.1158/1078-0432.CCR-11-1558 PMID: 22065080

30. Nan Y, Guo L, Song Y, Le Wang, Yu K, Huang Q, et al. Combinatorial therapy with adenoviral-mediated PTEN and a PI3K inhibitor suppresses malignant glioma cell growth in vitro and in vivo by regulating the PI3K/AKT signaling pathway. J Cancer Res Clin Oncol. 2017; 143: 1477–1487. https://doi.org/10.1007/s00432-017-2415-5 PMID: 28401302

31. Nakamura JL, Karlsson A, Arvold ND, Gottschalk AR, Pieper RO, Stokoe D, et al. PKB/Akt mediates radiosensitization by the signaling inhibitor LY294002 in human malignant gliomas. J Neurooncol. 2005; 71: 215–222. https://doi.org/10.1007/s11060-004-1718-y PMID: 15735908

32. Yudushkin I. Getting the Akt Together: Guiding Intracellular Akt Activity by PI3K. Biomolecules. 2019; 9. https://doi.org/10.3390/biom9020067 PMID: 30781447

33. Oppermann H, Alvanos A, Seidel C, Meixensberger J, Gaunitz F. Carnosine influences transcription via epigenetic regulation as demonstrated by enhanced histone acetylation of the pyruvate dehydrogenase kinase 4 promoter in glioblastoma cells. Amino Acids. 2018. https://doi.org/10.1007/s00726-018-2619-2 PMID: 30030619

34. Oppermann H, Purcz K, Birkemeyer C, Baran-Schmidt R, Meixensberger J, Gaunitz F. Carnosine's inhibitory effect on glioblastoma cell growth is independent of its cleavage. Amino Acids. 2019: 761–772. https://doi.org/10.1007/s00726-019-02713-6 PMID: 30863889

35. da Silva Bispo V, Di Mascio P, Medeiros M. Quantification of Carnosine-Aldehyde Adducts in Human Urine. Free Radic Biol Med. 2014; 75 Suppl 1: S27. https://doi.org/10.1016/j.freeradbiomed.2014.10.751 PMID: 26461323

36. Metallo CM, Vander Heiden MG. Metabolism strikes back: metabolic flux regulates cell signaling. Genes Dev. 2010; 24: 2717–2722. https://doi.org/10.1101/gad.2010510 PMID: 21159812

37. Chez MG, Buchanan CP, Aimonovitch MC, Becker M, Schaefer K, Black C, et al. Double-blind, placebo-controlled study of L-carnosine supplementation in children with autistic spectrum disorders. J Child Neurol. 2002; 17: 833–837. https://doi.org/10.1177/08830738020170111501 PMID: 12585724

38. Boldyrev A, Fedorova T, Stepanova M, Dobrotvorskaya I, Kozlova E, Boldanova N, et al. Carnosine [corrected] Increases Efficiency of DOPA Therapy of Parkinson's Disease: A Pilot Study. Rejuvenation Res. 2008; 11: 821–827. https://doi.org/10.1089/rej.2008.0716 PMID: 18729814

39. Baraniuk JN, El-Amin S, Corey R, Rayhan R, Timbol C. Carnosine Treatment for Gulf War Illness: A Randomized Controlled Trial. GJHS. 2013; 5. https://doi.org/10.5539/gjhs.v5n3p69 PMID: 23618477

40. Devyatov AA, Fedorova TN, Stvolinsky SL, Ryzhkov IN, Riger NA, Tutelyan VA. Issledovanie neĭroprotektornykh mekhanizmov deĭstviia karnozina pri éksperimental'noĭ fokal'noĭ ishemii/reperfuzii. Biomed Khim. 2018; 64: 344–348.

In summary, we have shown that inhibition of the PI3K/Akt/mTORC1 pathway also induces the expression of the *PDK4* gene in glioblastoma cells. However, carnosine's influence on *PDK4* mRNA expression was independent from this pathway and possibly also independent from any other transcription factor binding within the ~ 4000 bp long 5'-upstream region of the human PDK4 gene. Aside from a reduction of Akt phosphorylation in U87 cells, the dipeptide did not affect mTORC1 or Akt phosphorylation in glioblastoma cells. As carnosine reduced cell viability of glioblastoma cells which were resistant to treatment with Ly-294,002 and rapamycin, we conclude that the PI3K/Akt/mTORC1 pathway is of less importance for the anti-neoplastic effect of the dipeptide.

Further studies should address the identification of signalling pathways which are influenced by carnosine in different cancer cells equally. Indeed, previous studies suggested different signalling molecules to be associated with carnosine's effect. Among them are HIF (Forsberg et al. 2015), prohibitin-1 which controls the expression of mitochondrial proteins (Cheng et al. 2019), the oncogene c-myc (Bao et al. 2018) and Erk1/2 (Rybakova et al. 2013). Unfortunately, the published observations are sometimes controversial, as for example in the case of HIF. There are reports demonstrating increased HIF signalling (cervix carcinoma cells (Ditte et al. 2014)) under the influence of carnosine whereas other reports show decreased HIF signalling (colon cancer cells (Iovine et al. 2014)). Hence, care has to be taken transferring observations of carnosine's action on cancer cell signalling from one cancer model to another.

2.3 The influence of carnosine on epigenetic regulation in glioblastoma cells

As outlined in the preceding chapter, we ruled out that increased expression of *PDK4* mRNA under the influence of carnosine is mediated by the interaction of transcription factors within the promoter region of the gene and known upstream signalling pathways controlling their activity. As it was known that *PDK4* mRNA expression is also controlled by microRNAs (Deng et al. 2018) we also investigated whether carnosine induces *PDK4* mRNA expression via microRNAs. Therefore, a reporter gene containing the 3'- untranslated region (binding sites for microRNAs) of the PDK4 mRNA was employed. This experiment did not reveal an effect of carnosine on reporter gene expression. Therefore, we next focussed on the possibility that carnosine may affect histone acetylation as it was previously demonstrated that *PDK4* expression can also be controlled by epigenetic mechanisms, such as DNA methylation (Barrès et al. 2012) or histone acetylation (Kwon et al. 2006). First, we compared

the effect of different histone deacetylase inhibitors, including trichostatin A which was shown to induce *PDK4* expression (Kwon et al. 2006), with the dipeptides effect on *PDK4* mRNA expression. In addition, we performed chromatin immunoprecipitation experiments to analyse the acetylation of lysine residues of *PDK4* promoter associated histones under the influence of carnosine. We also tested whether carnosine may reduce glioblastoma cell viability by an effect on histone acetylation. Therefore, the dipeptides effect on cell viability was compared to that of other histone deacetylase inhibitors on viability. In addition, an analysis of a potential general effect of carnosine on histone acetylation was investigated by Western blot.

ORIGINAL ARTICLE

CrossMark

Carnosine influences transcription via epigenetic regulation as demonstrated by enhanced histone acetylation of the pyruvate dehydrogenase kinase 4 promoter in glioblastoma cells

Henry Oppermann[1] · Athanasios Alvanos[1] · Christiane Seidel[1] · Jürgen Meixensberger[1] · Frank Gaunitz[1]

Abstract

Carnosine (β-alanyl-L-histidine) affects a plethora of signaling pathways and genes in different biological systems. Although known as a radical scavenger, not all of these effects can simply be ascribed to its chemical nature. As previous experiments pointed towards the possibility that carnosine affects epigenetic regulation via histone acetylation, we investigated this hypothesis using the glioblastoma cell lines U87 and T98G in which carnosine's anti-neoplastic effect is accompanied by increased expression of pyruvate dehydrogenase kinase 4. Viability and expression of PDK4 was analyzed after incubation in carnosine and different histone deacetylase inhibitors (HDACi) using cell-based assays and qRT-PCR. In addition, chromatin immunoprecipitation (ChIP) experiments were performed and the global influence of carnosine on histone H3 acetylation was analyzed by Western blot. Carnosine as well as the HDACi used increased expression of PDK4. In addition, all compounds reduced cell viability, although differences were observed with regard to magnitude and required concentrations. ChIP analysis revealed increased acetylation of histone H3 in the PDK4 promoter of U87 and T98G cells (~1.3- and ~1.7-fold, respectively) 6 h after the addition of carnosine (50 mM) followed by increased expression of PDK4 mRNA. Western blots did not detect a general increase of H3 acetylation at a genome-wide scale under the influence of carnosine. Our experiments for the first time demonstrate that carnosine influences epigenetic regulation via increased histone acetylation.

Keywords Glioblastoma · Histone deacetylase · Chromatin immune precipitation

---

Handling Editor: W. Derave.

Henry Oppermann and Athanasios Alvanos contributed equally to this publication (shared first authorship).

✉ Frank Gaunitz
  Frank.Gaunitz@medizin.uni-leipzig.de

  Henry Oppermann
  Henry.Oppermann@medizin.uni-leipzig.de

  Athanasios Alvanos
  Athanasios.Alvanos@medizin.uni-leipzig.de

  Christiane Seidel
  Christiane.Seidel@medizin.uni-leipzig.de

  Jürgen Meixensberger
  Juergen.Meixensberger@medizin.uni-leipzig.de

1 Klinik und Poliklinik für Neurochirurgie, Universitätsklinikum Leipzig AöR, Liebigstraße 20, 04103 Leipzig, Germany

Introduction

Carnosine (β-alanyl-L-histidine) was first described by Gulewitsch and Amiradzibi (Gulewitsch and Amiradzibi 1900) more than 100 years ago. It is a naturally occurring dipeptide which is especially abundant in human skeletal muscle. In gastrocnemius, for example, basal concentrations of 7.2 ± 2.5, 7.2 ± 1.6 and 7.3 ± 1.6 mM (each from a group of 10 volunteers) have been reported (Blancquaert et al. 2017). Since its discovery, different physiological roles have been considered (for review, see Boldyrev et al. 2013). Many functions described such as its pH-buffering potential (Smith 1938), its potential to chelate metal ions (Baran 2000) or the aspect that it has a role as a scavenger of radical oxygen species (Kohen et al. 1988) are based on the assumption that the dipeptides' functions are simply based on their chemical properties. After the discovery that carnosine also has anti-neoplastic effects (for review, see Gaunitz and Hipkiss 2012 and Hipkiss and Gaunitz 2014), several groups identified different influences of the dipeptide on molecular

🍀 Springer

mechanisms that point towards specific effects on signal transduction, gene expression and metabolism. Briefly, there is evidence that carnosine affects a number of signaling molecules and pathways including HIF (Iovine et al. 2014), Akt/mTOR/p70S6 K (Zhang et al. 2014), STAT3 (Wang et al. 2013), MAPK (Kulebyakin et al. 2012) and KRAS signaling (Iovine et al. 2011). It also affects the transcription of a number of genes including RUNX2/Cbfa1 (Ito-Kato et al. 2004), pyruvate dehydrogenase kinase 1 and 4 (PDK1/4) and glucokinase (Letzien et al. 2014) and it interferes with glycolytic production of ATP in tumor cells (Oppermann et al. 2016). Some of the observations may be retraceable to carnosine's effect on radical oxygen species (ROS), such as it was suggested for KRAS and MAPK signaling. In addition, effects on signaling in turn affect gene expression and influence metabolism (or vice versa). However, there is a growing body of evidence that the dipeptide exerts its physiological functions by more sophisticated mechanisms than simply by detoxifying ROS. This assumption is underlined by the fact that the enantiomer D-carnosine, which shares the chemical properties of L-carnosine, fails to provoke some of the effects observed under L-carnosine, such as the rejuvenation of fibroblasts in vitro (McFarland and Holliday 1994). The multitude of the responses observable in single cells, tissues and organisms points towards the possibility that carnosine's primary molecular target is high in the hierarchy of signaling or that the physiological mechanism affected is of such a general importance that its modulation results in a plethora of biological effects.

Among the best described effects of carnosine on gene expression is the enhancement of mRNA expression of PDK4 in cells derived from glioblastoma (Letzien et al. 2014), which is a tumor of the central nervous system. The regulation of PDK4 mRNA expression has been studied since many years and several pathways and transcription factors modulating its expression have been described. Within a ~850-bp-long 5′-promoter region, functional transcription factor-binding sites for glucocorticoids, transcription factors from the FOXO family, retinoic acid receptors, estrogen-related receptors, SP1 and p300/CBP have been identified (Kwon and Harris 2004). In addition, there is evidence that regulation controlled by these binding sites can be influenced by PGC-1α and PPARα (Araki et al. 2007), by PPAR-δ (Barrès et al. 2012) and by PPARγ (Way et al. 2001). It has also been shown that PDK4 mRNA is induced in the presence of the histone deacetylase inhibitor trichostatin A (TSA) (Kwon et al. 2006) and driven down by promoter methylation at a single cytosine residue located within a non-CpG site in its promoter (Barrès et al. 2012). In addition, influences on expression by miRNAs were described (Han et al. 2016). As reporter gene assays performed with reporter genes either carrying a ~4000-bp-long 5′-region (−3986/+319) from the human PDK4 gene or a ~3700-bp-long 3′-end from the gene

did not reveal any effect of carnosine on their expression (Supplement 1), we hypothesized that enhanced expression of the endogenous PDK4 gene may result from an effect of carnosine on histone acetylation of the PDK4 promoter which may not be detectable by the plasmid-based reporter genes used in our experiments. To test this hypothesis, we compared the effect of carnosine on viability and on expression of PDK4 in U87 and T98G glioblastoma cells with the effect of different histone deacetylase (HDAC) inhibitors using qRT-PCR and cell-based assays. Finally, we analyzed PDK4 histone acetylation at the promoter of the gene by chromatin immunoprecipitation (ChIP).

Materials and methods

Reagents

Carnosine was kindly provided by Flamma (Flamma s.p.a. Chignolo d'Isola, Italy) and β-alanyl-L-alanine was purchased from Bachem (Bubendorf, Switzerland). If not stated otherwise all chemicals were purchased from Sigma-Aldrich (Taufkirchen, Germany) and Carl Roth (Karlsruhe, Germany).

Cell culture

U87 and T98G cells were obtained from the ATCC (Manassas, USA) and genotyped (Genolytic GmbH, Leipzig, Germany) to confirm their identity. Cells were propagated in 250-ml culture flasks (Sarstedt AG & Co., Nümbrecht, Germany) using 10 ml of DMEM/4.5 g/l glucose, without pyruvate (Life Technologies, Darmstadt, Germany) supplemented with 10% fetal bovine serum (FBS superior, Biochrom, Berlin, Germany), 2 mM GlutaMAX (Life Technologies) and Penicillin–Streptomycin (Life Technologies) at 37 °C and 5% CO_2 in humidified air in an incubator.

qRT-PCR experiments

qRT-PCR experiments were carried out as described (Letzien et al. 2014). Briefly, 10^6 cells were seeded in 10-mm cell culture dishes (TPP, Trasadingen, Switzerland) with 10 ml of medium. After 24 h of incubation, cells received fresh medium containing the compounds to be tested. Cells were harvested at the times specified in each experiment and RNA was isolated using a miRNeasy mini kit (Qiagen, Hilden, Germany) according to the manufacturer's instructions. The RNA was stored at − 80 °C until further use. 500 ng of RNA was used for reverse transcription employing the ImProm-II™ Reverse Transcription System (Promega, Mannheim, Germany) according to the manufacturer's instructions using random primer sets. DNA amplification was

performed on a Rotor-Gene 3000 system (Qiagen) employing SYBR Green (Maxima SYBR Green/ROX qPCR Master Mix, Thermo Scientific, Dreieich, Germany). Copy numbers of individual mRNAs were determined using linearized plasmid DNA (described in Letzien et al. 2014) containing the corresponding target sequence. Data analysis was performed using the Rotor-Gene 6 software and the data were processed as described (Letzien et al. 2014). Primer sequences used: *PDK4_forward*: 5′-CTG TGA TGG ATA ATT CCC-3′; *PDK4_reverse*: 5′-GCC TTT AAG TAG ATG ATA GCA-3′; *TBP_forward*: 5′-TGA CCT AAA GAC CAT TGC AC-3′; *TBP_reverse*: 5′-GCT CTG ACT TTA GCA CCT GTT-3′; *β-actin_forward*: 5′-CCG GGA CCT GAC TGA CTA CCT-3′; *β-actin_reverse*: 5′-CCT AGA AGC ATT TGC GGT GGA-3′. TATA box-binding protein (TBP) was used as reference gene in Fig. 4 for normalizing expression of PDK4 and β-actin under the influence of carnosine as it is not affected by carnosine. However, we identified an effect of trichostatin A (TSA) on TBP expression. Therefore, when TSA was used (Fig. 3), β-actin, which was not effected by TSA, was used as reference gene to normalize PDK4 expression.

Cell-based assays

Viability was determined by measuring ATP in cell lysates using the CellTiter-Glo Assay and by the determination of dehydrogenase activity using the CellTiter-Blue Assay (all from Promega, Mannheim, Germany) according to the instructions of the manufacturer and as described previously (Gaunitz and Heise 2003). All measurements of luminescence and fluorescence were performed using either a Mithras LB 940 Multimode Microplate reader (Berthold Technologies, Bad Wildbad, Germany) or a Spectra Max M5 reader (Molecular Devices, Biberach, Germany).

Chromatin immunoprecipitation

For chromatin immunoprecipitation, four culture flasks were used for each condition tested. Briefly, 5×10^6 cells were seeded in culture flasks (250 ml) in 10 ml of medium. After 19 h, cells received fresh medium with or without 50 mM carnosine. After 3, 6, 9, 12, 15, 18, 21 and 24 h of incubation, cells from one flask (with or without carnosine) were harvested for the determination of cell number and for the analysis of PDK4 mRNA expression. Cells from the remaining flasks (three treated with carnosine and three without carnosine) were used for ChIP analysis. To each flask 20 ml fresh serum-free culture medium with 0.5% formaldehyde was added after the old medium was removed. After 10-min incubation at room temperature, glycine was added to a final concentration of 125 mM. After 5 min at room temperature, medium was removed and the flasks were transferred

to ice. Now, cells were washed three times with 20 ml ice-cold phosphate-buffered saline (PBS; Gibco Thermo Fisher Scientific) and finally 1 ml of PBS with a protease inhibitor cocktail was added (aprotinin: 10 µg/ml; benzamidine: 2.5 mM; leupeptin: 10 µg/ml; pepstatin A: 10 µg/ml, phenylmethylsulfonyl fluoride (PMSF): 2.5 mM; dithiothreitol (DTT): 1 mM). Now, cells were mechanically removed using a cell scraper (TPP, Trasadingen, Switzerland) and transferred into 2 ml reaction vials. To transfer all cells, the last step was repeated with another 1 ml PBS with inhibitor cocktail. Then the suspensions were centrifuged (700×g; 4 °C; 5 min) and after removal of medium, the pellets were stored at − 80 °C if not directly processed further. For shearing, pellets were dissolved in SDS lysis buffer (10 mM EDTA; 1% SDS (sodium dodecyl sulfate); 50 mM Tris/HCl; pH 8.1) containing protease inhibitors in the concentrations given above. The amount of SDS lysis buffer was adjusted to have 20×10^6 cells (as estimated from the culture flask that was used to determine the cell number) in 1 ml of buffer. Suspensions were then distributed into 1.5 ml reaction vials (each with 150 µl suspension) and sonicated for 4 cycles (30 s on/30 s off) using a Bioruptor (Diagenode, Liège, Belgium) set at high intensity. Then, suspensions were centrifuged (10,000×g; 4 °C; 10 min) and the supernatants from cells treated with each condition were collected in one vial. After success of fragmentation was confirmed by gel electrophoresis of a small sample (fragmentation size 500–1200 bp), comparable amounts of DNA were obtained from cells under each condition, using a Nano Drop 1000 (ThermoFisher Scientific), 800 µl of fragmented DNA was mixed with 1200 µl of ChIP-Dilution Buffer (1.2 mM EDTA; 167 mM NaCl; 16.7 mM Tris/HCl; 0.01% SDS; 1.1% Triton X-100; pH 8.1) containing protease inhibitors as stated above. An aliquot of the mixture (10 µl) was stored at − 20 °C to be used as "input sample" and 500 µl was transferred to new 1.5-ml reaction vials. One vial (with 500 µl) received 2 µl of rabbit IgG (#2729; Cell Signaling Technologies, Danvers, USA) for negative control and one vial received 10 µl anti-acetyl-histone H3 antibody directed against acetyl K9, K14, K18, K23, and K27 (ab47915; Abcam, Cambridge, UK). The vials were incubated at 4 °C overnight using a tube rotator (SB3 Rotator; Cole-Parmer Ltd; Staffordshire; UK) and the next day ChIP-Grade Protein G Magnetic Beads (30 µl; Cell Signaling Technology) were added to each vial. Tubes were again continuously mixed for 2 h at 4 °C using the tube rotator before the beads were collected for 3 min using a magnetic stand. Then the supernatant was carefully removed and the pellets were washed three times with 1 ml of low-salt buffer (2 mM EDTA; 150 mM NaCl; 0.1% SDS; 20 mM Tris/HCl; 1.1% Triton X-100; pH 8.1) for 5 min at 4 °C using the rotator. After the last collection and removal of residual low-salt buffer 1 ml of high-salt buffer (2 mM EDTA; 350 mM NaCl; 0.1% SDS; 20 mM Tris/HCl; 1.1%

Triton X-100; pH 8.1) was added and the beads were again incubated for 5 min at 4 °C using the rotator. After the final removal of the high-salt buffer, ChIP-elution buffer (150 µl; 1% SDS; 100 mM $NaHCO_3$) was added to each pellet and to the pre-thawed 10 µl of "input sample". Pellets dissolved in ChIP-elution buffer were incubated for 30 min at 65 °C and 1200 rpm using a thermomixer. Finally, the magnetic beads were collected using a magnetic stand (3 min) before supernatants were transferred to 1.5-ml reaction vials. To each supernatant and the "input sample", 6 µl of NaCl solution (5 M) was added before overnight incubation at 65 °C and 700 rpm using a thermomixer. After overnight incubation, 1 µl of RNase A (10 mg/ml), 2 µl of Proteinase K (20 mg/ml), 4 µl EDTA (0.5 M) and 17 µl of Tris/HCl (0.5 M; pH 7.4) were added to each vial and incubation proceeded for 3 h at 37 °C and 800 rpm in a thermomixer. Finally, DNA for PCR was extracted using a PCR-extraction Kit (Qiagen). Then, qRT-PCR was performed using "ChIP-primers" for PDK4 and β-actin with the following primer sequences: *ChiP_PDK4 forward: 5'-TCA CTG GAA CTT GGA AAC GC-3';ChiP_PDK4_reverse: 5'-TCC GTG GTC ACC GTG CC-3';ChiP_β-actin_forward: 5'-GGC CAC TTA GAA GTC GCA GGA 3'-3';ChiP_β-actin_reverse: 5'-GGC TGG GCG TGA CTG TT -3'.*

To calculate the relative change of histone acetylation (for β-actin in triplicate and for PDK4 expression in quintuplicate), measurements were normalized to the signal of the corresponding input sample.

Western blot analysis

Western blot experiments were performed with cells cultivated at a density of 10^6 cells per dish in 10-cm culture dishes. For total protein isolation, cells were washed twice with ice-cold washing buffer (137 mM NaCl, 5.4 mM HCl, 0.41 mM $MgSO_4$, 0.49 mM $MgCl_2$, 0.126 mM $CaCl_2$, 0.33 mM Na_2HPO_4, 0.44 mM KH_2PO_4, 2 mM HEPES, pH 7.4) and finally collected in 1 ml of washing buffer. After a centrifugation (5 min, 500×g, 4 °C), cells were suspended in 150 µl of ice-cold RIPA buffer (50 mM Tris, 150 mM NaCl, 0.25% sodium deoxycholate, 0.1% SDS, 1% Nonidet P40) supplemented with PhosSTOP and a protease inhibitor cocktail (0.025 g/L aprotinin, 0.025 g/L leupeptin, 0.01 g/L pepstatin A, 1 mM dithiothreitol, 2.5 mM phenylmethylsulfonylfluoride and 2.5 mM benzamidine). After 10 min of incubation on ice, cells were lysed by sonification (Bioruptor, Diagenode, Seraing, Belgium; settings: power: high, interval: 0.5, time: 7 min), the debris removed by centrifugation (5500×g at 4 °C for 5 min) and the supernatant was transferred into new 1.5-ml reaction tubes. The protein concentration was determined using the Pierce 660 nm assay reagent according to the manufacturer's instructions. Proteins were stored at − 80 °C or immediately used for SDS

polyacrylamide gel electrophoresis (SDS-PAGE). For histone isolation, cells were washed three times with ice-cold histone extraction buffer (5 mM sodium butyrate in phosphate-buffered saline; pH 7.4). After addition of 1 ml histone extraction buffer, cells were transferred to a 1.5-ml reaction vial using a cell scraper. Cells were collected by centrifugation (500×g; 5 min; 4 °C) and resuspended in 100 µl of ice-cold Triton buffer (histone extraction buffer containing 0.5% Triton X-100; 2 mM PMSF and 0.02% NaN_3). After mincing by ten strokes using a 1-ml Dounce tissue grinder with PTFE pestle (Wheaton/Fisher Scientific), cells were put on ice for 10 min. Then, the lysate was centrifuged (10,000×g; 10 min; 4 °C) and the pellet was washed once with 50 µl of ice-cold Triton buffer, followed by a second centrifugation step (10,000×g; 10 min; 4 °C). The pellet was resuspended in 25 µl 0.2 N HCl and the solution was incubated overnight at 4 °C and 950 rpm using a thermomixer. The next day, debris was pelleted by centrifugation (10,000×g; 10 min; 4 °C) and the supernatant was transferred to a 1.5-ml reaction vial. After the determination of their concentration, proteins were stored at − 20 °C or immediately used for SDS-PAGE. SDS-PAGE was performed according to standard protocols using a Mini-PROTEAN® System (Bio-Rad, Munich, Germany). A concentration of 12% acrylamide was used to separate proteins and a concentration of 20% to separate histone extracts. After electrophoresis, proteins were transferred to PVDF membranes (Low-Fluorescence Membrane 0.2 µm, Biozym, Oldendorf, Germany) using a Mini Trans-Blot® Cell (Bio-Rad). The membrane was blocked using Odyssey® Blocking Buffer for 1 h at room temperature. Then, the membranes were incubated with antibodies diluted 1:1000 in TBST (20 mM Tris, 134 mM NaCl, 0.1% Tween 20). The primary antibodies used were mouse anti-PDK4 (Abcam; ab110336), rabbit anti-GAPDH (1:5000; Cell Signaling; #2118), mouse anti-histone H3 (Cell Signaling; #3638) and rabbit anti-acetyl-histone H3 (Abcam; ab47915). The secondary antibodies employed (red fluorescent IRDye® 680RD Goat anti-Mouse and green fluorescent IRDye® 800CW Goat anti-Rabbit; both diluted 1:5000 in TBST) were purchased from LI-COR (LI-COR Biosciences, Lincoln, USA). Membranes were scanned using an Odyssey Imaging System (LI-COR, Bad Homburg, Germany) and band intensities were determined by the Image Studio 5 software (LI-COR).

Determination of oxygen consumption rate

For the determination of the oxygen consumption rate (OCR), 2500 cells were seeded in 80 µl of medium in an XF96 cell culture microplate (Seahorse Bioscience, Billerica, MA). After 19 h, cells received fresh medium containing 20 or 50 mM carnosine or vehicle control. After additional 24 h of incubation, cells were washed twice with

Seahorse XF DMEM medium containing 4.5 g/L glucose and 2 mM L-glutamine and OCR was determined in the same medium using an XF96 Extracellular Flux Analyzer according to the instructions of the manufacturer. After completion of the assay, cells were lysed in 20 µl of lysis buffer (77.05 mM K_2HPO_4, 22.9 mM KH_2PO_4, 1 mM dithiothreitol, 0.2% Triton X-100, pH 7.8) and the amount of protein was determined using the Pierce 660-nm assay.

Statistical analysis

One-way and two-way ANOVA analyses with post hoc Tukey test have been performed using OriginPro 2017GS (OriginLab Corporation, Northampton, USA). When applicable, an unpaired Student's t test with unequal variances was performed using the algorithms implemented in Excel (Microsoft, Richmond, USA). Relative data resulting from two or more experiments or parameters (normalization to reference) with a separate mean and standard deviation are presented using Gaussian error propagation as described before (Letzien et al. 2014).

Results

PDK4 mRNA expression in U87 cells under the influence of carnosine and different HDAC inhibitors

Previous experiments demonstrated that PDK4 mRNA expression is increased when cells from the glioblastoma cell line U87 are exposed to carnosine (Letzien et al. 2014). As we hypothesized that this effect is mediated via increased histone acetylation, we compared the effect of carnosine on PDK4 mRNA expression with the effect of other known HDAC inhibitors. For the experiment, U87 cells were incubated for 24 h in the presence of carnosine (Car; 50 mM), belinostat (Bel; 4 µM), valproate (Val; 4 mM), TSA (1.6 µM) or SAHA (4 µM). In addition, we also included resveratrol (Res; 100 µM) in our experiments although it is not a classical HDAC inhibitor, but was also shown to affect histone acetylation (Venturelli et al. 2013). In Fig. 1, expression of PDK4 mRNA under the influence of the compounds is presented. All compounds significantly increased expression of PDK4 mRNA compared to untreated control cells. The greatest increase was obtained with carnosine (4.3 ± 0.7-fold; $p < 0.005$) followed by belinostat (2.9 ± 0.2-fold; $p < 0.0005$), TSA (2.5 ± 0.1-fold; $p < 0.0005$), valproate (2.2 ± 0.0-fold; $p < 0.0005$), SAHA (2.1 ± 0.2-fold; $p < 0.0005$) and resveratrol (1.7 ± 0.2-fold; $p < 0.0005$). In addition, statistical analysis revealed that expression under the influence of carnosine was significantly strongly increased compared to any other HDACi ($p < 0.05$–$p < 0.005$) at the concentrations employed
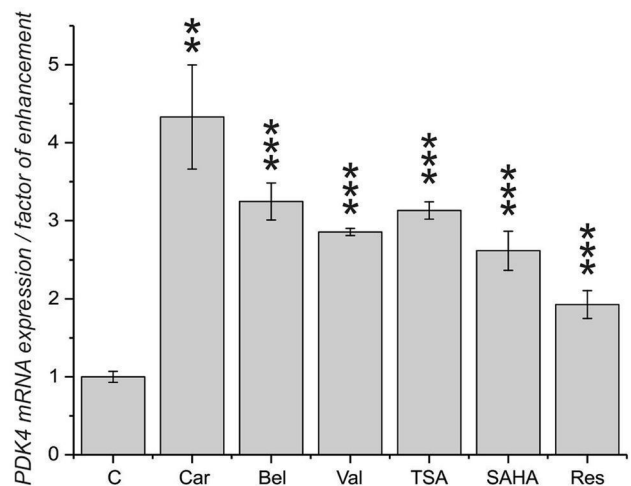

Fig. 1 PDK4-mRNA expression in U87 cells incubated in the presence of different compounds after 24-h exposure. U87 cells were exposed to carnosine (Car; 50 mM), belinostat (Bel; 4 µM), valproate (Val; 4 mM), TSA (1.6 µM), SAHA (4 µM) or resveratrol (Res; 100 µM) and the relative level of expression of PDK4 mRNA was determined after 24 h of incubation from five individually treated cultures for each compound. The increase of PDK4 mRNA expression under the influence of the test compounds was calculated in relation to PDK4 mRNA expression in untreated control cells and statistically analyzed by pairwise comparison of treated cells to untreated control cells using Student's t test. **$p < 0.005$; ***$p < 0.0005$

in the experiment. At this point, it may also be interesting to note that none of the compounds had a significant effect on the expression of the reference gene β-actin (data not shown).

Viability of U87 glioblastoma cells under the influence of carnosine and different HDAC inhibitors

Next, we asked whether the HDAC inhibitors used in the previous experiments have an effect on viability comparable to that described for carnosine (Letzien et al. 2014). Therefore, U87 cells were incubated for 24 and 48 h in the presence of the compounds used in the previous experiment. In Fig. 2, the result of the determination of cell viability is presented and statistical significance is indicated by a pairwise statistical analysis using Student's t test comparing cells treated with a compound to untreated cells. As can be seen, carnosine at a concentration of 50 mM significantly reduced viability after 24 and 48 h of incubation (all: $p < 0.0005$) and all compounds employed inhibited tumor cell viability after 48-h exposure and at the highest concentration employed aside from valproate when measuring dehydrogenase activity after 48 h. Although the high variation of response to the different concentrations employed and the inhibitors used makes it difficult to compare the effect of carnosine on any
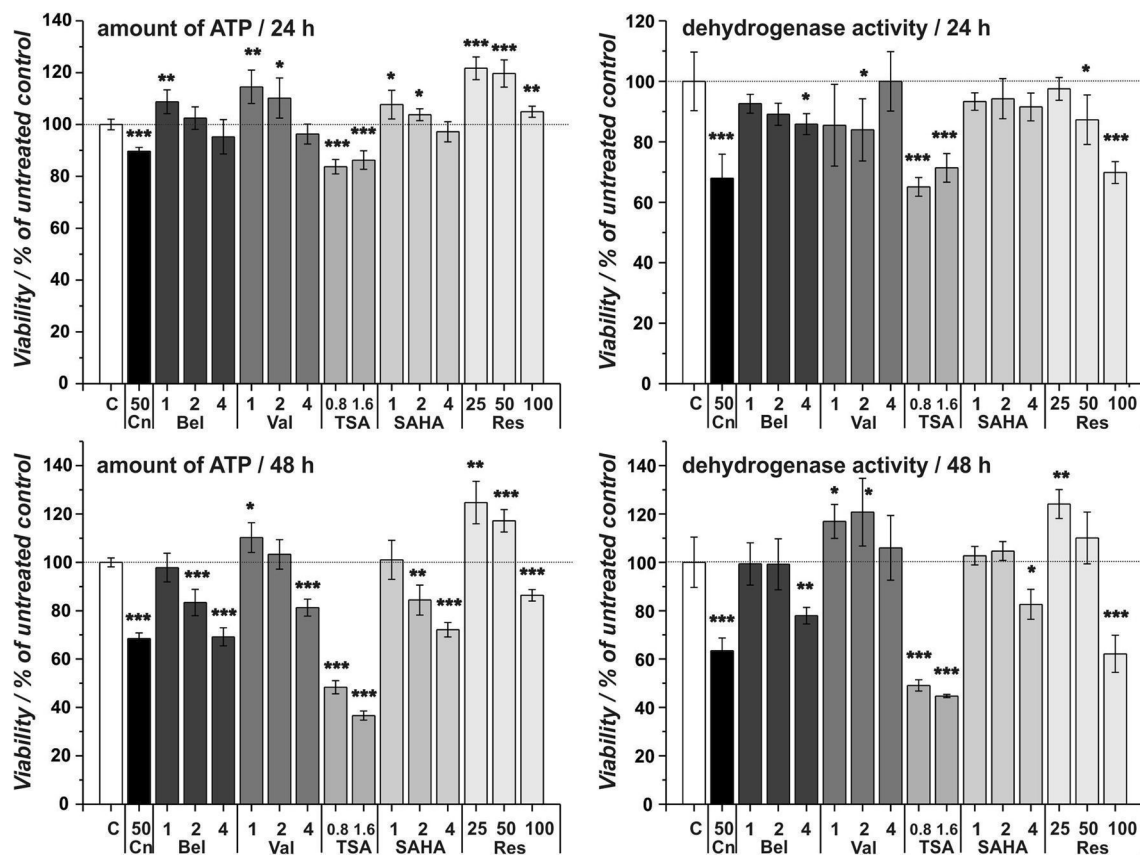
Fig. 2 Viability of U87 cells incubated in the presence of different compounds after 24- and 48-h exposure. Cells from the line U87 were cultivated in the presence of 50 mM carnosine, belinostat (1, 2 or 4 μM), valproate (1, 2, 4 mM), TSA (0.8 and 1.6 μM), SAHA (1, 2 or 4 μM) or resveratrol (25, 50 or 100 μM). For control, cells received fresh medium without any compound. After 24 (upper panels) and 48 h (lower panels), viability was determined by measuring the amount of ATP in cell lysates (left panels) and by determining dehy-drogenase activities (right panels). The values obtained were normalized to those obtained analyzing cells treated without supplement set as 100%. All experiments were performed in sextuplicate and the means and standard deviations are presented. Statistical analysis was determined by pairwise comparison of cells treated with compound at the indicated concentration to untreated cells using Student's t test: *$p < 0.05$; **$p < 0.005$; ***$p < 0.0005$

other HDACi, it is obvious that all HDAC inhibitors negatively influenced tumor cell viability as does carnosine.

Expression of PDK4 mRNA in U87 cells combining different concentrations of carnosine and TSA indicates that both compounds have common molecular targets

Next, we performed an experiment exposing cells to the HDAC inhibitor TSA together with carnosine for 24 h. We hypothesized that in case both compounds exert their effect on PDK4 mRNA expression by the same mechanism (e.g., histone acetylation) no additive effect of a compound should be visible when the other compound already shows a maximum effect. The result of a corresponding experiment is presented in Fig. 3. As can be seen, at a concentration of 20 mM carnosine, expression of PDK4 mRNA can significantly be increased with increasing concentrations of TSA (for p values, refer to

Fig. 3), whereas at a concentration of 50 mM carnosine, an increase in the concentration of TSA from 0.8 to 1.6 μM does not result in a further significant increase in expression (Fig. 3, left panel). In addition, PDK4 mRNA expression at a concentration of 0, 0.4 and 0.8 μM TSA can be further increased by increasing concentrations of carnosine (for p values, refer to the figure), whereas at a concentration of 1.6 μM, TSA expression is not significantly different between 20 mM carnosine and 50 mM carnosine. This observation points towards the possibility that carnosine and TSA may in fact affect PDK4 mRNA expression via a common mechanism.
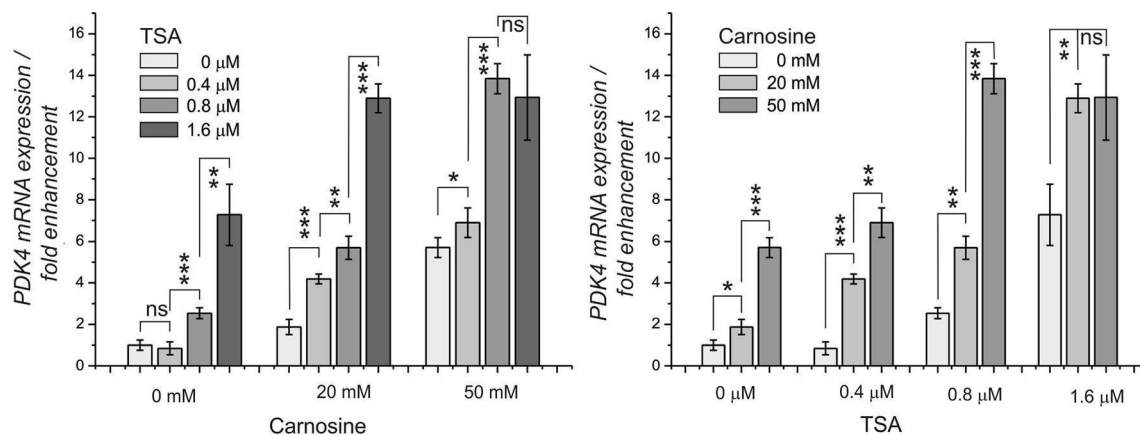
Fig. 3 PDK4-mRNA expression in U87 cells incubated in the presence of carnosine and TSA after 24-h exposure. U87 cells were exposed to different concentrations of carnosine (Car: 20, 50 mM) and TSA (0.4, 1.6 μM). After 24 h, the increase of PDK4 mRNA expression under the influence of the test compounds was analyzed by the comparison of expression in the presence of the compounds to expression in untreated control cells (all in quintuplicate). Pairwise statistical analysis was performed by Student's *t* test. *$p < 0.05$; **$p < 0.005$; ***$p < 0.0005$. n.s.: not significant

Chromatin immune precipitation identifies increased histone acetylation of the PDK4 promoter after exposure to carnosine followed by enhanced mRNA expression

The experiments described in the preceding chapters pointed towards the possibility that the effect of carnosine on PDK4 expression may be caused by increased histone acetylation. To test this notion, we decided to investigate the acetylation of PDK4 promoter-associated histones by chromatin immunoprecipitation (ChIP) using U87 and T98G cells treated with 50 mM carnosine. As acetylation is known to be a highly dynamic process, we performed the experiments with cells incubated for 3, 6, 12, 18 and 24 h. In addition, we also determined the amount of mRNA encoding PDK4 by qRT-PCR after 3, 6, 9, 12, 15, 18, 21 and 24 h of incubation in the presence or absence of 50 mM carnosine. The result of the experiment is presented in Fig. 4. For control, we also determined the amount of mRNA encoding β-actin as well as histone acetylation of the corresponding gene. As can be seen in Fig. 4, we identified increased acetylation of PDK4-associated histones at 6-h exposure in both cell lines, followed by an increase in mRNA expression. This demonstrates that exposure to carnosine results in enhanced histone acetylation at the PDK4 promoter followed by induction of its expression. In addition, no statistically different expression of β-actin was observed under the influence of carnosine in T98G cells and only a small but significant reduction of β-actin mRNA expression (as revealed by two-way Anova) was seen in U87 cells after 9- ($p < 0.05$) and 21-h exposure ($p < 0.0005$).

Histone acetylation under the influence of carnosine and Trichostatin A determined by Western blot of histone extracts

The experiments of the preceding section indicated that carnosine does increase histone acetylation of the PDK4 gene and there was no indication of enhanced histone acetylation of the gene encoding β-actin. We now asked whether we could detect a general influence on histone acetylation under the influence of carnosine as it is the case with HDACs such as TSA or valproate for which acetylation of H3 can be detected in Western blots (He et al. 2014). For the experiment, U87 and T98G cells were incubated for 6 h in the presence of 50 mM carnosine or 1.6 μM TSA and Western blots using antibodies directed against histone 3 and against histone H3 acetylated at K9; K14; K18; K23 and K27 were performed. Representative Western blots are presented in Fig. 5. Whereas a strong increase in the amount of acetylated H3 was detectable in the presence of TSA in both cell lines, the amount of detectable acetylation of H3 was even slightly reduced in the presence of carnosine, although the effect was in no case significant as deduced by one-way ANOVA. This demonstrates that the effect of carnosine on histone acetylation is obviously different from TSA which has a broad-spectrum inhibiting class I and class II deacetylases in mammals.

Discussion

Since its discovery, many different physiological functions have been ascribed to carnosine. With the advent of modern techniques allowing the analysis of signal transduction
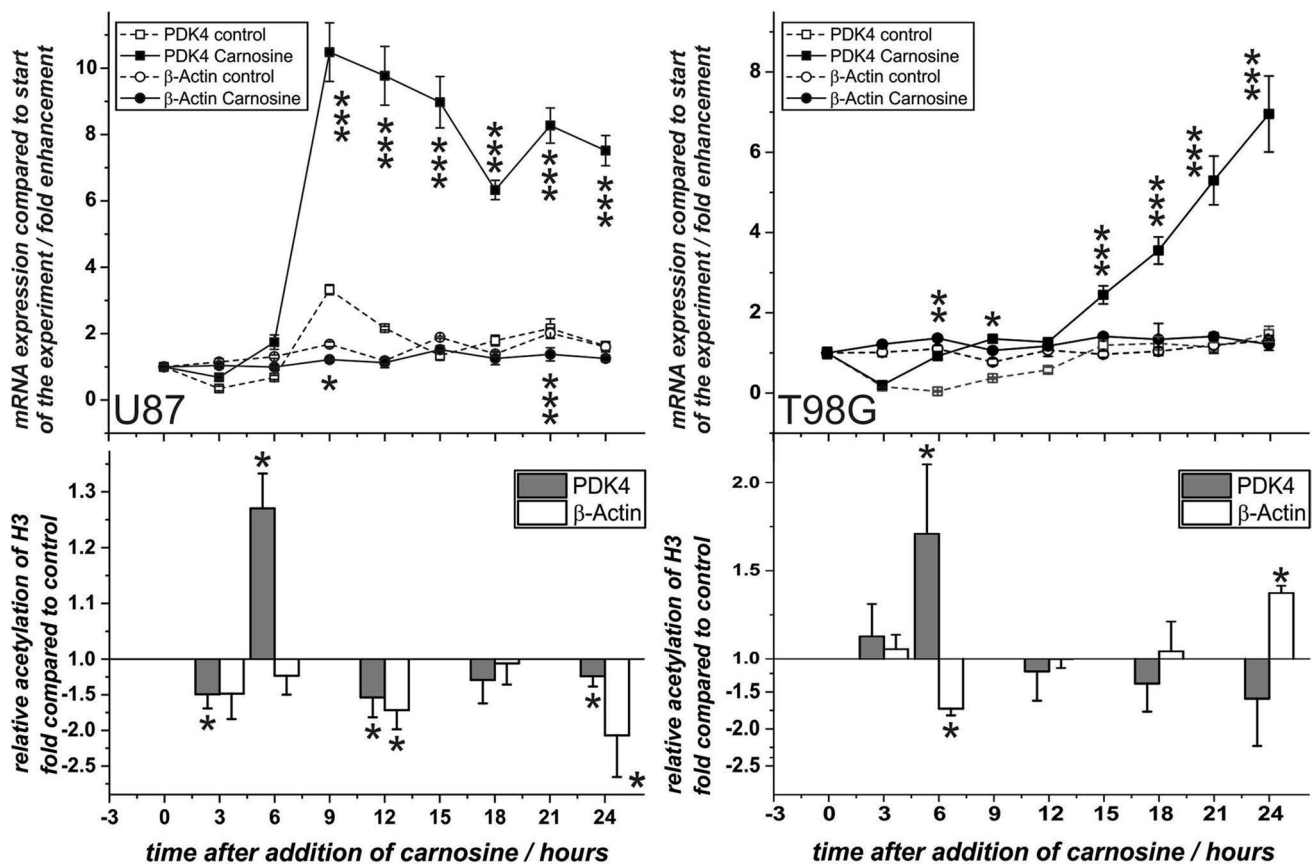
Fig. 4 PDK4 and β-actin mRNA expression in relation to histone acetylation of their corresponding genes after treatment with carnosine. Cells from the lines U87 (left panels) and T98G (right panels) were incubated in the absence and presence of carnosine. ChIP analysis and expression analysis of mRNA encoding PDK4 and β-actin were performed before the addition of carnosine (0 h control) and after 3, 6, 9, 12, 15, 18, 21 and 24 h of incubation. The upper panels show the relative mRNA expression of cells treated with carnosine and of untreated control cells (in fold, relative to the level of expression before the addition of carnosine). qRT-PCR of β-actin was performed in triplicate and of PDK4 expression in quintuplicate. Stars in the upper panels indicate significant differences (as determined by pairwise Student's t test between treated and untreated cells at each individual time point) in the expression mRNA either encoding β-actin or PDK4. $*p < 0.05$; $**p < 0.005$; $***p < 0.0005$

pathways and gene expression profiles, it became evident that the broad range of different physiological and pharmacological observations made are also reflected by a broad range of cellular responses. The high pleiotropy of effects observed and the fact that different biological models respond differently to the dipeptide already led to the notion that carnosine may have specific functions aside from effects based on its chemical nature, e.g., having buffer or metal-chelating capacity.

Previous experiments performed in our group identified an increase in mRNA expression of PDK4 under the influence of carnosine. Analyzing the known regulatory mechanisms responsible for increased PDK4 expression by reporter gene assays, including interactions in the 5′-upstream and the 3′-downstream region, we were not able to identify interactions with transcription factors or miRNAs with regulatory sequences of the PDK4 gene as responsible for the effect of carnosine on endogenous PDK4 expression

(Supplemental Fig. 1). As it was known that PDK4 mRNA expression can also be increased by increased histone acetylation (Kwon et al. 2006) we asked whether carnosine may be able to influence histone acetylation.

The results presented for the first time provide evidence that carnosine influences the acetylation of histones. The acetylation of lysine residues in core histones by histone acetyl transferases (HATs) neutralizes the positive charge of side chains, promoting a less dense chromatin structure which allows transcriptional activation, whereas deacetylation by HDACs promotes a less relaxed state, inhibiting transcription (Kuo and Allis 1998). The ChIP assay described in the present manuscript is in good agreement with the notion that carnosine does in fact influence histone 3 acetylation at least within the PDK4 promoter. However, it appears that the effect of carnosine on acetylation is different from that of other classical HDAC inhibitors. We could clearly demonstrate increased histone acetylation of the PDK4 promoter
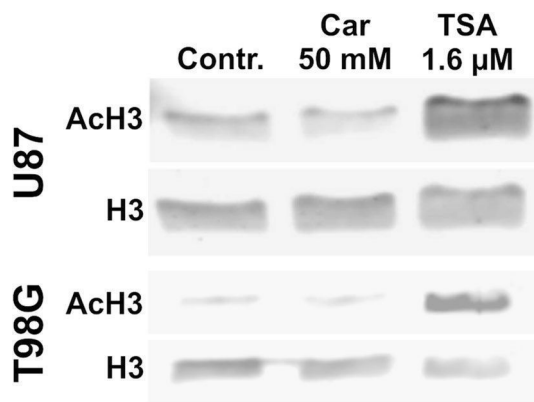
Fig. 5 Abundance of histone 3 and acetylated histone 3 in U87 glioblastoma cells after treatment with carnosine and TSA. Cells from the line U87 and T98G were exposed to carnosine (50 mM) or TSA (1.6 μM) for 24 h. For control, cells received fresh medium without compound. After 6 h, histones were extracted and Western blot was performed with 5 μg of protein. The membranes were probed with an antibody directed against total histone 3 and histone 3 acetylated at K9, K14, K18, K23 and K27

by ChIP, but no general effect on histone 3 acetylation in Western blots, which we observed under the influence of TSA. General effects have also been described for SAHA (Xu et al. 2014), belinostat [previously known as PXD101 (Mackay et al. 2010)] and valproate (Chavez-Blanco et al. 2005). At this point it should also be taken into account that we cannot rule out the possibility that instead of inhibiting HDACs carnosine may positively influence the activity of HATs, although its anti-neoplastic effect points towards its function as an inhibitor of deacetylation (Cohen et al. 2011). However, this is highly speculative and further experiments will be required to resolve the exact mechanisms by which carnosine influences histone acetylation. The same holds true for the question whether carnosine may directly interact with a histone-modifying enzyme or whether its effect is of secondary nature, e.g., influencing the NAD/NADH ratio or the supply with acetyl-CoA.

Although the focus of our work was to analyze whether carnosine affects histone acetylation, we also wondered whether increased expression of PDK4 influences pyruvate dehydrogenase activity and in turn mitochondrial oxidative phosphorylation. By performing Western blot analysis we were not able to detect PDK4 protein expression in U87 cells independent of whether cells were treated with carnosine or not. In T98G cells, PDK4 protein was detectable, but no change in PDK4 protein expression under the influence of carnosine was observed (Supplement 2 a). In addition, when we analyzed the oxygen consumption rate (OCR) of U87 and T98G cells by a Seahorse XF analyzer, we did not see a change in the OCR after 24 h of incubation in the presence of 20 or 50 mM carnosine (Supplement 2b). This obvious discrepancy between protein expression and mRNA

expression and the absence of an effect of carnosine on the OCR after 24-h exposure to the dipeptide raise the interesting question of whether the tumor cells are able to prevent enhanced protein expression of PDK4 by a mechanism that counteracts the enhanced expression of mRNA encoding PDK4. As the activity of a reporter gene, which contained the 3′UTR of the PDK4 gene, was not influenced by carnosine (Supplemental Fig. 1), we rule out the possibility that a miRNA is responsible for the effect.

An interesting question that also has to be asked is whether the high concentrations of carnosine (up to 50 mM) used in our experiments do reflect physiological doses. This is certainly not the case although it is difficult to tell which concentrations are reached at a specific site in an organism. It should also be kept in mind that cell culture experiments are always far away from the physiological situation and can only help to get an idea of which mechanism is affected in an individual. With regard to carnosine, the situation is especially difficult as carnosine administered to humans is prone to rapid degradation by serum carnosinase. On the other hand, it has been discussed that there must be some kind of depot where carnosine is protected from degradation. In experiments with volunteers that orally ingested carnosine, it was demonstrated that the dipeptide is secreted with the urine even 5 h after ingestion. At this time the concentrations in serum are already below the detection level (Gardner et al. 1991). Therefore, a certain tissue may be able to pick up significant amounts of carnosine, accumulating the dipeptide in amounts much higher as supposed by measuring serum concentrations. At this point it should also be noted that we currently rule out the possibility that osmotic effects are responsible for the effects observed, as dipeptides such as β-Ala-L-Ala (also at a concentration of 50 mM) do not influence viability of tumor cells (Supplement 3).

In conclusion, under the experimental condition used by our group, we could for the first time demonstrate that carnosine influences histone acetylation which could well be one key to understand the multiple and different effects carnosine has in different model systems, tissues and organisms. It would be highly interesting to investigate which other genes in addition to PDK4 are activated by histone acetylation under the influence of carnosine. This could, for example, be done by ChIP followed by next-generation sequencing. In addition, the question how transcription is influenced under physiological concentrations of carnosine and in other tissues and whether in other tissues enhanced expression of PDK4 mRNA may be followed by enhanced protein expression and changes of PDH enzyme activity should be answered.

Author contributions AA and HO performed the experiments presented in the manuscript. CS performed the experiments presented in Supplement 3. HO, JM and FG supervised the experiments. All authors read and contributed to writing the manuscript. FG supervised and planned the experiments, analyzed the data together with AA and HO and wrote the manuscript.

Compliance with ethical standards

Conflict of interest The authors declare that they have no potential conflict of interest.

References

Araki M, Nozaki Y, Motojima K (2007) Transcriptional regulation of metabolic switching PDK4 gene under various physiological conditions. Yakugaku Zasshi 127:153–162

Baran EJ (2000) Metal complexes of carnosine. Biochemistry (Mosc.) 65:789–797

Barrès R, Yan J, Egan B, Treebak JT, Rasmussen M, Fritz T, Caidahl K, Krook A, O'Gorman DJ, Zierath JR (2012) Acute exercise remodels promoter methylation in human skeletal muscle. Cell Metab 15:405–411. https://doi.org/10.1016/j.cmet.2012.01.001

Blancquaert L, Everaert I, Missinne M, Baguet A, Stegen S, Volkaert A, Petrovic M, Vervaet C, Achten E, de Maeyer M, de Henauw S, Derave W (2017) Effects of histidine and β-alanine Supplementation on human muscle carnosine storage. Med Sci Sports Exerc 49:602–609. https://doi.org/10.1249/MSS.0000000000001213

Boldyrev AA, Aldini G, Derave W (2013) Physiology and pathophysiology of carnosine. Physiol Rev 93:1803–1845. https://doi.org/10.1152/physrev.00039.2012

Chavez-Blanco A, Segura-Pacheco B, Perez-Cardenas E, Taja-Chayeb L, Cetina L, Candelaria M, Cantu D, Gonzalez-Fierro A, Garcia-Lopez P, Zambrano P, Perez-Plasencia C, Cabrera G, Trejo-Becerril C, Angeles E, Duenas-Gonzalez A (2005) Histone acetylation and histone deacetylase activity of magnesium valproate in tumor and peripheral blood of patients with cervical cancer. A phase I study. Mol Cancer 4:22. https://doi.org/10.1186/1476-4598-4-22

Cohen I, Poręba E, Kamieniarz K, Schneider R (2011) Histone modifiers in cancer: friends or foes? Genes Cancer 2:631–647. https://doi.org/10.1177/1947601911417176

Gardner MLG, Illingworth KM, Kelleher J, Wood D (1991) Intestinal-absorption of the intact peptide carnosine in man, and comparison with intestinal permeability to lactulose. J Physiol 439:411–422

Gaunitz F, Heise K (2003) HTS compatible assay for antioxidative agents using primary cultured hepatocytes. Assay Drug Dev Technol 1:469–477

Gaunitz F, Hipkiss AR (2012) Carnosine and cancer: a perspective. Amino Acids 43:135–142. https://doi.org/10.1007/s00726-012-1271-5

Gulewitsch W, Amiradzibi S (1900) Ueber das Carnosin, eine neue organische Base des Fleischextraktes. Ber Dtsch Chem Ges 33:1902–1903

Han H, Li W, Shen H, Zhang J, Zhu Y, Li Y (2016) microRNA-129-5p, a c-Myc negative target, affects hepatocellular carcinoma progression by blocking the Warburg effect. J Mol Cell Biol. https://doi.org/10.1093/jmcb/mjw010

He Y, Cai C, Tang D, Sun S, Li H (2014) Effect of histone deacetylase inhibitors trichostatin A and valproic acid on hair cell regeneration in zebrafish lateral line neuromasts. Front Cell Neurosci 8:382. https://doi.org/10.3389/fncel.2014.00382

Hipkiss AR, Gaunitz F (2014) Inhibition of tumour cell growth by carnosine: some possible mechanisms. Amino Acids 46:327–337

Howitz KT, Bitterman KJ, Cohen HY, Lamming DW, Lavu S, Wood JG, Zipkin RE, Chung P, Kisielewski A, Zhang L-L, Scherer B, Sinclair DA (2003) Small molecule activators of sirtuins extend Saccharomyces cerevisiae lifespan. Nature 425:191–196. https://doi.org/10.1038/nature01960

Iovine B, Iannella ML, Nocella F, Pricolo MR, Baldi MR, Bevilacqua MA (2011) Carnosine inhibits KRas-mediated HCT-116 proliferation by affecting ATP and ROS production. Cancer Lett 315:122–128. https://doi.org/10.1016/j.canlet.2011.07.021

Iovine B, Oliviero G, Garofalo M, Orefice M, Nocella F, Borbone N, Piccialli V, Centore R, Mazzone M, Piccialli G, Bevilacqua MA (2014) The anti-proliferative effect of L-carnosine correlates with a decreased expression of hypoxia inducible factor 1 alpha in human colon cancer cells. PLoS ONE 9:e96755. https://doi.org/10.1371/journal.pone.0096755

Ito-Kato E, Suzuki N, Maeno M, Takada T, Tanabe N, Takayama T, Ito K, Otsuka K (2004) Effect of carnosine on runt-related transcription factor-2/core binding factor alpha-1 and Sox9 expressions of human periodontal ligament cells. J Periodontal Res 39:199–204

Kohen R, Yamamoto Y, Cundy KC, Ames BN (1988) Antioxidant activity of carnosine, homocarnosine, and anserine present in muscle and brain. Proc Natl Acad Sci USA 85:3175–3179

Kulebyakin K, Karpova L, Lakonsteva E, Krasavin M, Boldyrev A (2012) Carnosine protects neurons against oxidative stress and modulates the time profile of MAPK cascade signaling. Amino Acids 43:91–96. https://doi.org/10.1007/s00726-011-1135-4

Kuo M-H, Allis CD (1998) Roles of histone acetyltransferases and deacetylases in gene regulation. BioEssays 20:615–626

Kwon H-S, Harris RA (2004) Mechanisms responsible for regulation of pyruvate dehydrogenase kinase 4 gene expression. Adv Enzyme Regul 44:109–121. https://doi.org/10.1016/j.advenzreg.2003.11.020

Kwon H-S, Huang B, Ho Jeoung N, Wu P, Steussy CN, Harris RA (2006) Retinoic acids and trichostatin A (TSA), a histone deacetylase inhibitor, induce human pyruvate dehydrogenase kinase 4 (PDK4) gene expression. Biochim Biophys Acta 1759:141–151. https://doi.org/10.1016/j.bbaexp.2006.04.005

Letzien U, Oppermann H, Meixensberger J, Gaunitz F (2014) The antineoplastic effect of carnosine is accompanied by induction of PDK4 and can be mimicked by L-histidine. Amino Acids. https://doi.org/10.1007/s00726-014-1664-8

Mackay HJ, Hirte H, Colgan T, Covens A, MacAlpine K, Grenci P, Wang L, Mason J, Pham P-A, Tsao M-S, Pan J, Zwiebel J, Oza AM (2010) Phase II trial of the histone deacetylase inhibitor belinostat in women with platinum resistant epithelial ovarian cancer and micropapillary (LMP) ovarian tumours. Eur J Cancer 46:1573–1579. https://doi.org/10.1016/j.ejca.2010.02.047

McFarland GA, Holliday R (1994) Retardation of the senescence of cultured human diploid fibroblasts by carnosine. Exp Cell Res 212:167–175

Oppermann H, Schnabel L, Meixensberger J, Gaunitz F (2016) Pyruvate attenuates the anti-neoplastic effect of carnosine independently from oxidative phosphorylation. Oncotarget 7:85848–85860. https://doi.org/10.18632/oncotarget.13039

Smith EC (1938) The buffering of muscle in rigor; protein, phosphate and carnosine. J Physiol 92:336–343

Venturelli S, Berger A, Böcker A, Busch C, Weiland T, Noor S, Leischner C, Schleicher S, Mayer M, Weiss TS, Bischoff SC, Lauer UM, Bitzer M (2013) Resveratrol as a pan-HDAC inhibitor alters the acetylation status of histone corrected proteins in

human-derived hepatoblastoma cells. PLoS ONE 8:e73097. https://doi.org/10.1371/journal.pone.0073097

Wang J-P, Yang Z-T, Liu C, He Y-H, Zhao S-S (2013) L-carnosine inhibits neuronal cell apoptosis through signal transducer and activator of transcription 3 signaling pathway after acute focal cerebral ischemia. Brain Res 1507:125–133. https://doi.org/10.1016/j.brainres.2013.02.032

Way JM, Harrington WW, Brown KK, Gottschalk WK, Sundseth SS, Mansfield TA, Ramachandran RK, Willson TM, Kliewer SA (2001) Comprehensive messenger ribonucleic acid profiling reveals that peroxisome proliferator-activated receptor gamma activation has coordinate effects on gene expression in multiple insulin-sensitive tissues. Endocrinology 142:1269–1277. https://doi.org/10.1210/endo.142.3.8037

Xu G, Wang J, Wu Z, Qian L, Dai L, Wan X, Tan M, Zhao Y, Wu Y (2014) SAHA regulates histone acetylation, butyrylation, and protein expression in neuroblastoma. J Proteome Res 13:4211–4219. https://doi.org/10.1021/pr500497e

Zhang Z, Miao L, Wu X, Liu G, Peng Y, Xin X, Jiao B, Kong X (2014) Carnosine inhibits the proliferation of human gastric carcinoma cells by retarding Akt/mTOR/p70S6 K signaling. J Cancer 5:382–389. https://doi.org/10.7150/jca.8024

In summary, we have shown that carnosine induces the mRNA expression of the *PDK4* gene by increasing acetylation of *PDK4*-promoter associated histones. To our knowledge, this is the first report demonstrating that the dipeptide is able to affect transcription by an epigenetic mechanism. As a general effect on histone acetylation by the dipeptide, as determined by Western blot, was not detected, we concluded that carnosine does not conduct its effects like a classical histone deacetylase inhibitor such as trichostatin A. This notion was supported by determining cell viability. In these experiments only one out of five histone deacetylase inhibitors could mimic carnosine's effect on viability.

In further studies it has to be evaluated whether carnosine's effect on histone acetylation may affect the expression of other genes. These investigations could potentially reveal clues understanding mechanisms responsible for carnosine's other effects, such as those on ageing, on the mitigation of symptoms of neurological disorders and on wound healing (see 1.3 Carnosine in health and disease).

2.4 The influence of carnosine on glioblastoma cell metabolism

Previously, our group demonstrated that carnosine inhibits glycolytic ATP production in glioblastoma (Renner et al. 2010a) which was confirmed also in other tumour entities (Bao et al. 2018; Shen et al. 2014). However, the mechanisms behind carnosine's effect on glucose metabolism are far from being understood. In the study of Oppermann et al. (Oppermann et al. 2016a) we investigated the response of glioblastoma cells, when glucose supply is reduced or glycolysis is bypassed via substitution of glucose by pyruvate. For these experiments we omitted the use of foetal bovine serum which influences metabolic fluxes in an undefined manner, as serum contains more than 2000 different compounds (Psychogios et al. 2011). By determining L-lactate, methylglyoxal which arises by non-enzymatic elimination of phosphate from GA3P and DHAP, and its detoxification product D-lactate, we analysed how different glucose concentrations or pyruvate in medium contribute to the glycolytic flux. Furthermore, the amount of ATP in cell lysates was determined to monitor energy balance of glioblastoma cells after treatment. In order to investigate how metabolites are affected by different supply of glucose, we analysed the associated metabolic changes using gas chromatography coupled to mass spectrometry (GC-MS).

CrossMark

Metabolic response of glioblastoma cells associated with glucose withdrawal and pyruvate substitution as revealed by GC-MS

Henry Oppermann[1*] (iD), Yonghong Ding[2], Jeevan Sharma[2], Mandy Berndt Paetz[1], Jürgen Meixensberger[1], Frank Gaunitz[1†] and Claudia Birkemeyer[2†]

Abstract

Background: Tumor cells are highly dependent on glucose even in the presence of oxygen. This concept called the Warburg effect is a hallmark of cancer and strategies are considered to therapeutically exploit the phenomenon such as ketogenic diets. The success of such strategies is dependent on a profound understanding of tumor cell metabolism. With new techniques it is now possible to thoroughly analyze the metabolic responses to the withdrawal of substrates and their substitution by others. In the present study we used gas chromatography coupled to mass spectrometry (GC-MS) to analyze how glioblastoma brain tumor cells respond metabolically when glucose is withdrawn and substituted by pyruvate.

Methods: Glioblastoma brain tumor cells were cultivated in medium with high (25 mM), medium (11 mM) or low (5.5 mM) glucose concentration or with pyruvate (5 mM). After 24 h GC-MS metabolite profiling was performed.

Results: The abundances of most metabolites were dependent on the supply of glucose in tendency but not in a linear manner indicating saturation at high glucose. Noteworthy, a high level of sorbitol production and release was observed at high concentrations of glucose and high release of alanine, aspartate and citrate were observed when glucose was substituted by pyruvate. Intermediates of the TCA cycle were present under all nutritional conditions and evidence was found that cells may perform gluconeogenesis from pyruvate.

Conclusions: Our experiments reveal a high plasticity of glioblastoma cells to changes in nutritional supply which has to be taken into account in clinical trials in which specific diets are considered for therapy.

Keywords: Cancer, Glucose, Pyruvate, Metabolite profiling, Glioblastoma, Warburg effect

Background

In many studies published in recent years the analysis of tumors predominately focused on gene and protein expression as well as on signal transduction in order to draw conclusions about the biology of cancer. Compared to the high amount of literature focusing on these topics much less has been investigated with regard to cancer cell metabolism despite the fact that the peculiarities of energy metabolism in tumors have already been investigated at the beginning of the last century [1].

The most prominent feature of tumor cell metabolism is the so-called Warburg effect which describes a strong dependence on glycolytic production of ATP accompanied by the conversion of pyruvate to lactate even in the presence of oxygen (aerobic glycolysis). In his article from 1956 which was a translation of a lecture delivered in 1955, Warburg still proposed that "respiration" (OxPhos) must be irreversibly injured in cancer cells [2]. Although the concept has been refined, it is still common sense that in many cancer cell lines as well as in solid tumors the production of lactate is more pronounced than the production of pyruvate. Pyruvate accounts for 60–75 % of the metabolic consumption of external glucose whereas the production of acetyl-CoA from pyruvate accounts for ~10 to 25 % of the glycolytic flux [3, 4]. At this point it should

* Correspondence: henry.oppermann@medizin.uni-leipzig.de
†Equal contributors
[1]Klinik und Poliklinik für Neurochirurgie, Universitätsklinikum Leipzig AöR, Liebigstraße 19, Leipzig 04103, Germany
Full list of author information is available at the end of the article

Oppermann *et al. Nutrition & Metabolism* (2016) 13:70

Page 2 of 11

also be kept in mind that only a fraction of the acetyl-CoA produced from pyruvate is used for the production of ATP [3, 4].

Aerobic glycolysis is still considered to be a hallmark of cancer [5] and up to now no breakthrough therapeutic strategy exploiting this potential Achilles heel of cancer has been developed. Aside from research on drugs that could possibly be used for a "metabolic therapy" (for review see [6]), several authors and clinicians focused on the development of diets especially high in fat and low in carbohydrates. These so-called ketogenic diets were considered having beneficial effects by forcing cells to utilize fatty acids as their primary energy source [7–10]. Aside from the increasing amount of data implying that the ketogenic diet is an effective adjuvant cancer therapy (for a summary of current mouse models and clinical trials see [11]), the underlying mechanisms might be more complex involving also anti-angiogenic, anti-inflammatory and pro-apoptotic processes [12]. However, it is without question that the development of successful strategies targeting tumor-specific metabolism requires a thorough understanding of the underlying mechanisms, especially of the mechanisms that enable tumor cells to switch from one substrate to another under defined dietary constraints. Unfortunately, up to now, most investigations focused on proteins required for the glycolytic flux and much research has been committed to the analysis of their activity [6, 13]. In addition, a number of transcription factors and pathways involved in the up-regulation of the corresponding genes have frequently been identified to be aberrantly regulated in cancer such as c-Myc, Hif-1α or mTOR [14]. Much less research has been done on the metabolites and their concentration as the available methods have been cumbersome and mostly out of fashion. With the advent of improved technologies such as liquid or gas chromatography (GC) coupled to mass spectrometry (MS) the biochemical analysis of pathway fluxes and changes of single metabolite concentrations under different physiological conditions became possible in an elegant and precise manner.

In the present work we used GC coupled to MS to analyze the metabolic response of glioblastoma cells to the presence of different concentrations of glucose and in a situation when glucose is substituted by pyruvate. Glioblastoma is the most aggressive and most frequent primary brain tumor in adults with a median survival after biopsy and standard therapy of only 14.6 months [15]. As previous experiments pointed towards the importance of glycolysis for the survival of cells derived from this highly malignant tumor and the possibility that pyruvate may become important under conditions of impaired glycolysis [16], we analyzed metabolite abundances under different concentrations of glucose and in

medium in which glucose was substituted by pyruvate. In addition, we omitted medium supplements commonly used such as fetal bovine serum or glutamine which significantly influence metabolic fluxes and in the case of serum in an even undefined manner.

Methods

Chemicals and reagents
If not stated otherwise all chemicals were purchased from Sigma-Aldrich (Taufkirchen, Germany).

Cell culture
U87 cells were originally obtained from the ATCC (Manassas, USA) and cultured in 250 mL culture flasks (Sarstedt AG & Co., Nümbrecht, Germany) using DMEM/25 mM glucose, without pyruvate (Life Technologies, Darmstadt, Germany) supplemented with 10 % fetal bovine serum (FBS superior, Biochrom, Berlin, Germany), 2 mM GlutaMAX and antibiotics (Life Technologies) at 37 °C and 5 % CO_2 in humidified air in an incubator. In order to confirm identity over long culture periods, cells were genotyped by STR analysis at the Genolytic GmbH (Leipzig, Germany) using a PowerPlex® 21 System (Promega, Mannheim, Germany) and cells were confirmed as the U87MG cell line from the ATCC [17]. For starvation experiments, U87 cells were seeded in 6-well plates (TPP, Trasadigen, Switzerland) at a density of 10^6 cells per well in 2 mL full supplemented DMEM (10 % FBS, GlutaMAX, antibiotics) and incubated for 3 h before receiving fresh medium (1 mL) without a carbon source and without GlutaMAX and FBS (DMEM [0]). Cells were incubated for 20 h before replacing the culture medium with medium (1 mL) containing either different concentrations of glucose or medium without glucose but pyruvate at a concentration of 5 mM.

Determination of extracellular lactate
After incubation, media were collected for lactate determination and cells were lysed in 200 μL lysis buffer (77 mM K_2HPO_4, 23 mM KH_2PO_4, 0.2 % TritonX-100, pH 7.8) and the protein content was determined using the Pierce 660 nm Protein Assay (Thermo Scientific, Braunschweig, Germany). For D-lactate determination collected medium (100 μL) was evaporated to dryness and dissolved in H_2O_{dd} (25 μL). For the determination of L-lactate, H_2O_{dd} (20 μL) was added to collected medium (5 μL). Then, prepared samples (20 μL) were incubated in the wells of a black 96 well plate (Greiner Bio One, Frickenhausen, Germany) in the presence of enzyme mix (224 μL) consisting of 430 mM glycine, 340 mM hydrazine sulfate, 5 mM NAD and 10 U L-lactate dehydrogenase (Megazyme, Wicklow, Ireland) (pH 9) for L-lactate and 490 mM glycine, 200 mM

Oppermann *et al. Nutrition & Metabolism* (2016) 13:70

Page 3 of 11

hydrazine sulfate, 1 mM DETAPAC, 5 mM NAD and 100 U D-lactate dehydrogenase (pH 9.2) for D-lactate (Megazyme) (final concentration for all formulations) for 90 min at room temperature. Production of NADH was observed by fluorometric detection (excitation/ emission = 340/ 460 nm) using a SpectraMax M5 Microplate Reader (Molecular Devices, Biberach, Germany) [18]. A standard curve was prepared using 0.375 to 10 μg D/L-lactate.

Determination of free MGO
U87 cells were seeded as described above. After 20 h in medium without a carbon source and without serum, cells received fresh medium (1 mL) supplemented with the compounds to be tested. After 24 h of incubation, cells were washed with ice cold washing buffer (1 mL of 100 mM Tris/HCl, pH 8.0) and then 70/30 methanol/ H_2O (*v/v*; 430 μL) containing 1.16 mM *O*-(2,3,4,5,6-pentafluorobenzyl)hydroxylamine (PFBHA) was instantly added to each well. After shaking for 10 min at room temperature, the plates were placed on a shaking incubator at 40 °C for 1 h derivatization. Afterwards, the solution was transferred into a 1.5 mL reaction vial. Then, 9 M H_2SO_4 (10 μL) and cyclohexane (200 μL) was added to each sample. The solution was vortex mixed, followed by a brief centrifugation. The upper organic phase was transferred into a clean conical glass insert. This extraction procedure was performed three times in total. The collected extract was evaporated to dryness using a gentle stream of air, analytes were dissolved in cyclohexane (60 μL) containing suberic acid dimethyl ester as internal standard (cyclohexane: internal standard = 10000:1, *v/v*) and analyzed by GC-MS.

GC-MS analysis of intracellular MGO samples
Free MGO from cell extracts was analyzed on an Agilent 6890 N gas chromatograph equipped with a 7683 Series auto sampler and a 30-m J&W Fisher DB-35 ms capillary column (250-μm I.D. and 0.25 μm film) coupled with a 5973 N mass selective detector (all modules and columns from Agilent Technologies, Waldbronn, Germany). Samples (2 μL) were injected at 250 °C in splitless mode with helium as carrier gas with a flow rate of 1 mL/min. Initial GC oven temperature was set to 50 °C, held for 2 min, then increased at a rate of 15 °C/ min up to 320 °C and held for 10 min. The electron impact ionization source operated at 230 °C, 70 eV and a scan range of *m/z* 50 to 550. For MGO quantitation, the peak area of *m/z* 181 of the corresponding derivative was integrated.

Metabolic profiling via GC-MS
For the determination of extracellular metabolites, medium (10 μL) was collected from each well and immediately frozen at −80 °C until further use. For the

determination of intracellular metabolites, cells were briefly washed with pre-cooled (4 °C) washing buffer on ice. Immediately after washing, pre-cooled (-20 °C) methanol (1 mL) was added to each well and metabolites were extracted for 24 h on an orbital shaker at 8 °C. Then, the extracts were transferred to 1.5 mL reaction vials and additional pre-cooled (4 °C) methanol (500 μL) was used to rinse the remaining metabolites from each well and combined with the extract. Samples were evaporated to dryness using a speed vac (Maxi-Dry Lyo, Heto-Holten, Allerød, Denmark) and stored at -80 °C until further use.

Derivatization and GC-MS analyses were performed as described previously [19]. Data evaluation was carried out using AMDIS 2.71 [20] for peak picking and creation of a customer library of detected peaks. Quantitation with Xcalibur 1.4 (Thermo Scientific) was based on the integration of selective mass traces. Tentative identifications were achieved by spectra comparison with NIST14 (National Institute of Standards and Technologies [NIST], Gaithersburg, USA) and a customer library of reference spectra under consideration of related Kovac retention time indices [21]. Metabolite profiling experiments were repeated once with a similar result, whereas representative data is presented. If not stated otherwise, the abundance of a metabolite is defined by the peak area determined from the selected ion chromatogram of an experiment normalized to total cellular protein (μg).

Statistical analysis
Student's *t*-test was performed using the algorithm implemented in Excel (Version: 14.0.7128.5000; Microsoft, Redmond, USA) (unpaired two-sample test with unequal variances). Principal component analysis was performed using the Excel add-in Multibase package (Numerical Dynamics, Japan). All experiments were carried out in 6-tuplicate.

Results
D-lactate, L-lactate and MGO production at different concentrations of glucose and supply of pyruvate
In order to investigate how different concentrations of glucose in the medium contribute to the glycolytic flux in U87 glioblastoma cells, we determined the production of L-lactate in medium with different concentrations of glucose and in the presence of 5 mM pyruvate instead of glucose. In addition, we also determined the production of methylglyoxal (MGO) and D-lactate. MGO arises by non-enzymatic elimination of phosphate from glyceraldehyde-3-phosphate and dihydroxyacetone phosphate, two intermediates of glycolysis, and is finally converted to D-lactate by the glyoxalase system [22]. We expected to get a more comprehensive picture of the glycolytic flux than just by the determination of L-lactate, which only appears as long

Oppermann *et al. Nutrition & Metabolism* (2016) 13:70

Page 4 of 11

as glycolytic produced pyruvate is not used for the production of acetyl-CoA. For the experiment, cells were cultivated for 20 h in the absence of glucose and pyruvate in medium which did not contain any glutamine source or fetal bovine serum. Then, fresh medium was added containing 25, 11 and 5.5 mM glucose or 5 mM pyruvate without glucose, followed by incubation for 24 h. The used concentrations of glucose are commonly employed in cell culture experiments. With regard to physiological concentrations, 5 mM has to be considered as a physiological blood concentration at starvation and 11 mM as the blood concentration after a meal, whereas 25 mM is only reached in diabetic conditions. Blood concentrations of pyruvate are supposed to be around 0.05 mM (0.44 mg/100 ml) in fasted individuals [23]. The rational to use an almost 100-fold higher concentration is based on control experiments in which we determined that at this concentration (5 mM) the relative ATP concentration is saturated and was comparable to that obtained with all three concentrations of glucose used (Additional file 1: Figure S1). Finally, media were collected for the determination of extracellular D- and L-lactate. In addition, the intracellular MGO was determined from the cells and normalized to the total extracted protein.
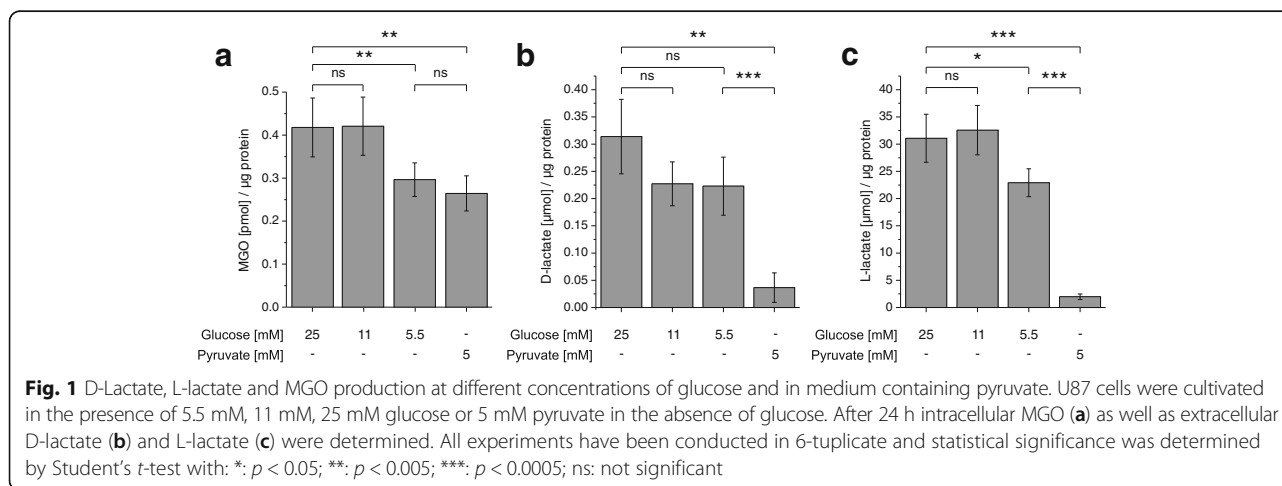
As can be seen in Fig. 1, there was no significant difference neither in L/D-lactate production nor in MGO production between cells either incubated in the presence of 25 mM or 11 mM glucose. This may indicate that there was almost the same glycolytic flux at both concentrations of glucose. Only when the concentration of glucose was further decreased down to 5.5 mM, a significant reduction was detected in the production of L-lactate (fold change to: 0.74 ± 0.08; $p < 0.05$) which was very low in the absence of glucose and the presence of pyruvate (fold change to: 0.06 ± 0.02; $p < 0.0005$). Although a significant reduction of MGO was observed at a concentration of 5.5 mM glucose compared to higher

glucose concentrations (fold change in 5.5 compared to 25 mM glucose: 0.71 ± 0.09; $p < 0.005$) the abundance of MGO was almost equal to the one measured in the absence of glucose (fold change in 5 mM pyruvate compared to 25 mM glucose: 0.63 ± 0.09; $p < 0.005$) indicating that the highly reactive MGO is a poor indicator of the glycolytic flux. The same holds true for D-lactate although compared to MGO it was strongly reduced in the absence of glucose (fold change in 5 mM pyruvate compared to 25 mM glucose: 0.12 ± 0.09; $p < 0.005$).

Metabolites in glioblastoma cells at different supply with glucose and pyruvate

In order to analyze how metabolites are affected by a different supply of glucose we analyzed the associated metabolic changes using GC-MS profiling. Therefore, U87 cells were cultivated as described in the previous section and after 24 h of incubation the intra-and extracellular metabolites were extracted, derivatized and analyzed by GC-MS. After automated peak deconvolution by AMDIS, 194 peaks were manually selected and quantified using Xcalibur. Finally, 106 metabolites were identified by comparison of mass spectra and Kovac retention time indices with mass spectral libraries. The resulting relative intracellular abundances are presented in Fig. 2 as logarithmically transformed fold-changes compared to the samples obtained from the cells treated with 25 mM glucose.

Among the most prominent changes associated with a reduced supply of glucose was an expected reduction in the amount of different mono- and disaccharides and sugar phosphates that already became prominent when the concentration of glucose was reduced from 25 mM to 11 mM. In contrast to the results obtained with the analysis of MGO and lactate in the previous section, the metabolic profile of 11 mM glucose samples was more

Fig. 1 D-Lactate, L-lactate and MGO production at different concentrations of glucose and in medium containing pyruvate. U87 cells were cultivated in the presence of 5.5 mM, 11 mM, 25 mM glucose or 5 mM pyruvate in the absence of glucose. After 24 h intracellular MGO (**a**) as well as extracellular D-lactate (**b**) and L-lactate (**c**) were determined. All experiments have been conducted in 6-tuplicate and statistical significance was determined by Student's *t*-test with: *: $p < 0.05$; **: $p < 0.005$; ***: $p < 0.0005$; ns: not significant

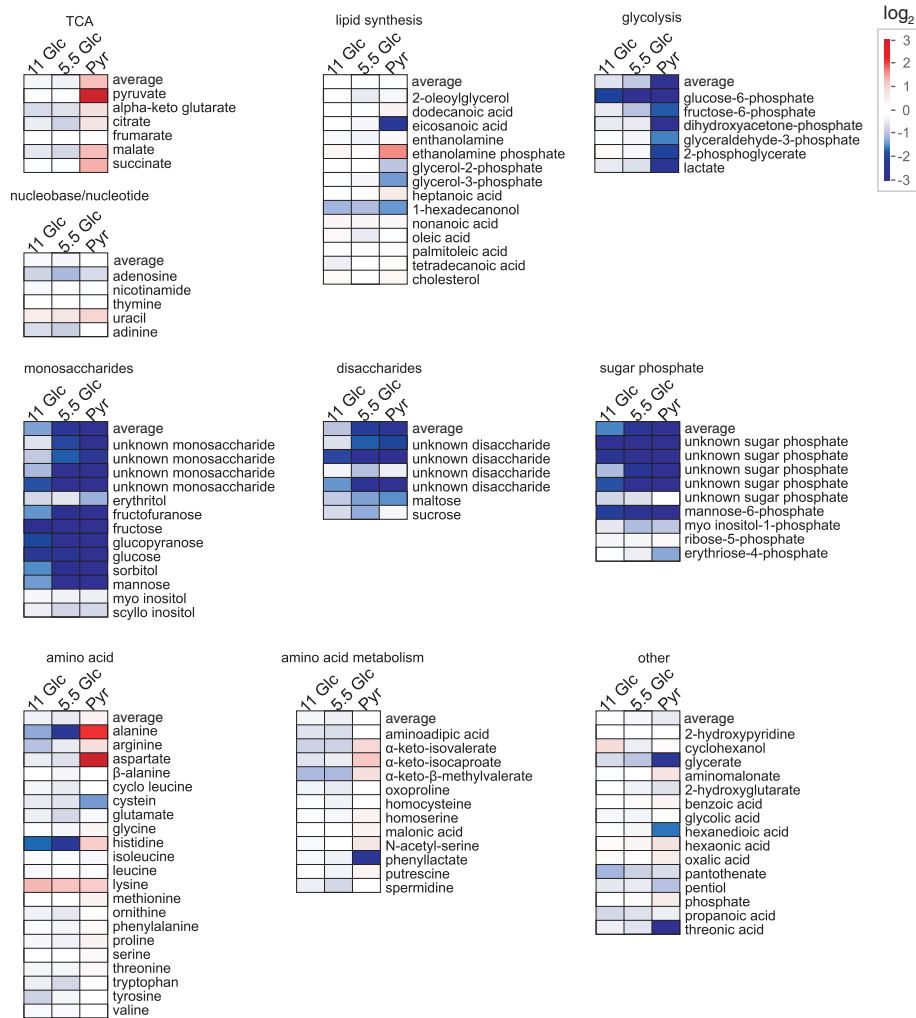Oppermann *et al. Nutrition & Metabolism* (2016) 13:70

Page 5 of 11

Fig. 2 Comparative metabolic profiling of U87 cells cultivated in the presence of glucose and pyruvate. Fold changes (log$_2$-transformed) of intracellular metabolite abundances are indicated with regard to the highest concentration of glucose employed (25 mM; set to log$_2$(1) = 0) for glucose concentrations of 11 mM (11 Glc), 5.5 mM (5.5 Glc) or for medium without glucose containing 5 mM pyruvate instead (Pyr). Identified metabolites were grouped in dependence on their metabolic role: TCA: metabolites associated with the tricarboxylic acid cycle; lipid synthesis: metabolites associated with lipid synthesis; glycolysis: glycolytic metabolites; nucleobase/nucleotides; monosaccharides; disaccharides; sugar phosphates; amino acids; amino acid metabolism: metabolites associated with amino acid metabolism; other: other metabolites not unequivocally associated with the other pathways indicated. The average of the fold changes from the metabolites in each group is indicated as "average"

similar to 5.5 mM glucose than to 25 mM glucose samples, which was confirmed by multivariate analysis (Additional file 2: Figure S2). Possibly, this may be related to the fact that the glycolytic flux appeared to enter saturation from 11 mM glucose supplement on. A complete overview of the metabolites detected and quantified and their relation to other metabolites is depicted in Fig. 3 (for an extended version see Additional file 3: Figure S3). Based on the data presented in Fig. 3, a number of different features of tumor metabolism in U87 cells under different nutritional supply was analyzed and is presented in the following paragraphs.

Glucose and the glycolytic flux

As can be seen in Fig. 3 the intracellular abundance of glucose increases with increased supply, but does not follow it in a linear manner as the intracellular abundance of glucose was more than 5 times higher at an extracellular concentration of 25 mM than at 11 mM. We presume that the transport of glucose is mainly carried out by GLUT1 as this is the main transporter in brain [24] and we found its mRNA to be ~ 25 times more abundantly expressed than that encoding GLUT3 or GLUT4 whereas mRNA encoding GLUT2 was almost not present in the U87 cells used in the experiment (Additional file 4: Figure S4a). As the K$_m$ of GLUT1 for
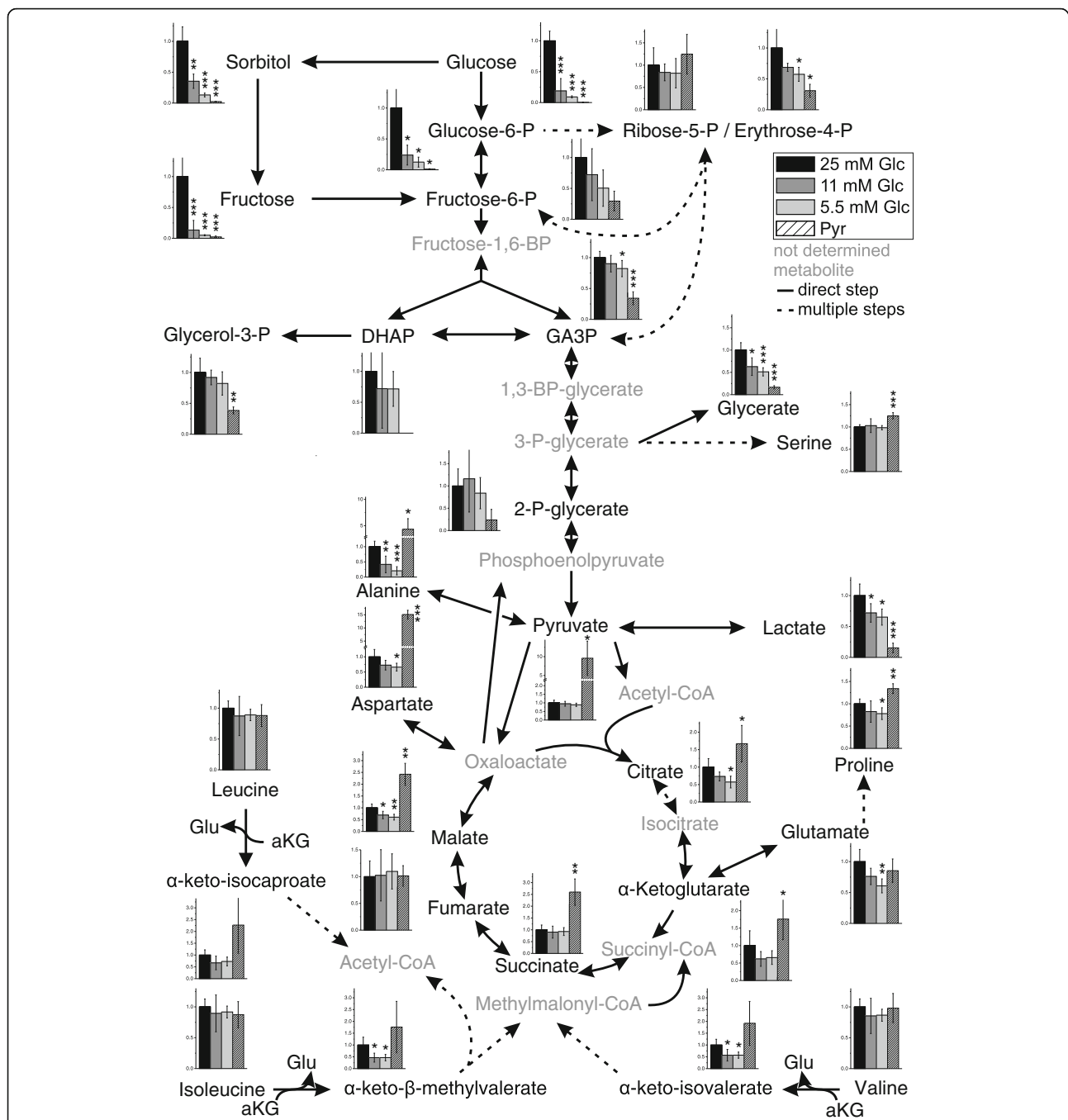
Oppermann *et al. Nutrition & Metabolism* (2016) 13:70

Page 6 of 11

Fig. 3 Metabolic pathway of U87 cells profiling data. A combined metabolic pathway is presented, including glycolysis, the pentose-phosphate pathway, the TCA cycle and branched chain amino acid degradation. Intracellular metabolite abundances (Fig. 2) are shown as bar diagrams depicting the relative abundance which is the: ratio between the abundance of a metabolite (the peak area) normalized to total protein (μg) compared to the abundance at 25 mM glucose (normalized to protein) set as 1. Direct reactions without intermediates are presented as straight lines and reactions involving several steps are presented as dotted lines. Metabolites which were not determined are labeled in Grey. All experiments have been conducted in 6-tuplicate and statistical significance was determined by Student's *t*-test with: *: $p < 0.05$; **: $p < 0.005$; ***: $p < 0.0005$. An extended version of the figure including extracellular metabolite concentrations is available in the (Additional file 2: Figure S2). Abbreviations: GA3P: glyceraldehyde-3-phosphate; DHAP: dihydroxyacetone phosphate; Glu: glutamate; aKG: α-ketoglutarate

glucose is around 1.5 mM, uptake should already be saturated at the lowest concentration of glucose (5.5 mM). Consequently, phosphorylation to glucose-6-phosphate

becomes important for a continuous uptake of glucose. This phosphorylation should be catalyzed by hexokinase 2 and hexokinase 1 which at the level of the mRNA is

Oppermann *et al. Nutrition & Metabolism* (2016) 13:70

Page 7 of 11

three times stronger expressed than isoform 2 as revealed by qRT-PCR (Additional file 4: Figure S4b). At this point, it is interesting to note, that in normal brain tissue hexokinase 2 is only negligibly expressed and its expression in glioblastoma was already considered to contribute to the Warburg effect and the malignity of the tumor [25].

When glucose in the medium was reduced from 25 mM to 11 mM the abundances of intracellular glucose (fold change to: 0.22 ± 0.19; $p < 0.0005$) and glucose-6-phosphate (fold change to: 0.24 ± 0.16; $p < 0.05$) were significantly reduced. In the case of fructose-6-phosphate (fold change to: 0.72 ± 0.42) and glyceraldehyde-3-phosphate (fold change to: 0.9 ± 0.13) only weak and non-significant effects were observed. A further reduction of glucose supply to 5.5 mM did also not significantly reduce fructose-6-phosphate (fold change to: 0.5 ± 0.29) and 2-phospho-glycerate (fold change to: 0.84 ± 0.35), but we observed a significant reduction in intracellular glucose (fold change to: 0.15 ± 0.02; $p < 0.0005$), glucose-6-phosphate (fold change to: 0.12 ± 0.08; $p < 0.05$) and glyceraldehyde-3-phosphate (fold change to: 0.82 ± 0.13; $p < 0.05$). Comparing glucose concentrations 11 mM and 5.5 mM in medium, no significant changes of the aforementioned metabolites were detected. Therefore, it has to be assumed that the glycolytic flux downstream from glucose-6-phosphate is similar under the different external glucose concentrations. As the amount of ribose-5-phosphate was also not significantly affected by different concentrations of extracellular glucose it may be assumed that the pentose-phosphate pathway has the same activity at all concentrations of glucose, although we observed a significant reduction of erythrose-4-phosphate comparing its amounts at 25 mM glucose and 5.5 mM (fold change to: 0.57 ± 0.11; $p < 0.05$).

Fructose and sorbitol
Aside from a steep raise of the intracellular abundances of glucose and glucose-6-phosphate when the extracellular concentration of glucose was increased from 11 mM to 25 mM, we also observed a significant raise in the abundances of intracellular sorbitol (fold change to: 2.86 ± 0.98; $p < 0.005$) and fructose (fold change to: 7.69 ± 9.46; $p < 0.005$). Moreover, raising glucose concentrations from 5.5 mM to 11 mM in medium also resulted in a significant enhancement of sorbitol abundances (fold change to: 2.69 ± 0.62; $p < 0.05$). Interestingly, sorbitol produced by the cells was significantly released into the extracellular medium whereas the extracellular abundance of fructose did not follow its enhanced intracellular production (Additional file 3: Figure S3).

Glucose and the tricarboxylic acid cycle
The data presented in Fig. 3 shows that the abundance of intracellular lactate (fold change in 5.5 mM compared to 25 mM glucose: 0.65 ± 0.13; $p < 0.05$) followed in tendency the abundance of glyceraldehyde-3-phosphate (fold change in 5.5 compared to 25 mM glucose: 0.82 ± 0.13; $p < 0.05$) which is the metabolite at the entry of the second (three carbon) part of the glycolytic pathway. Although this appears to be in accordance with the Warburg effect, we also observed a significant reduction (fold change) in 5.5 mM glucose compared to 25 mM glucose in the amounts of citrate (0.57 ± 0.17; $p < 0.05$), malate 0.61 ± 0.12; $p < 0.005$) and α-ketoglutarate (0.71 ± 0.18). This clearly indicates that at a high glucose concentration (25 mM), glucose-derived pyruvate is metabolized by the TCA cycle.

Metabolic flux under substitution of glucose by pyruvate: lactate and metabolites associated with the TCA cycle
When glucose was substituted by pyruvate a strong increase of the intracellular amount of pyruvate was observed (5 mM pyruvate compared to 25 mM glucose: 9.85 ± 4.54; $p < 0.05$) which clearly indicates that the compound is readily taken up by the tumor cells. The high intracellular amount of pyruvate was not accompanied by a corresponding raise of intracellular lactate. As the formation of lactate requires $NADH + H^+$, that in the presence of a glycolytic flux is produced by the conversion of glyceraldehyde-3-phosphate to glycerate 1,3-bisphosphate, a lack of reduced NADH may be the reason for the non-appearance of increased lactate production in the absence of glucose. We also observed a significantly higher abundance of the TCA cycle metabolites citrate (1.67 ± 0.52; $p < 0.05$), α-ketoglutarate (1.76 ± 0.59; $p < 0.05$), succinate (2.60 ± 0.56; $p < 0.005$) and malate (2.42 ± 0.46; $p < 0.005$) following the higher abundance of intracellular pyruvate when glucose was substituted by pyruvate (fold change in cells exposed to 5 mM pyruvate compared to cells exposed to 25 mM glucose). Therefore, pyruvate in the absence of glucose can obviously be metabolized by the TCA cycle and it has to be expected that at least two mitochondrial $NADH + H^+$ producing steps (from isocitrate to α-ketoglutarate and from α-ketoglutarate to succinyl-CoA) are active. Provided that we found no evidence of enhanced production of lactate in the absence of glucose and high levels of intracellular pyruvate, these reduction equivalents are most likely used for the production of ATP by OxPhos rather than shuttled out of the mitochondria. An intensive use of pyruvate for the production of ATP under the extracellular concentrations employed (5 mM) is also in accordance to the observation that at this concentration

Oppermann *et al. Nutrition & Metabolism* (2016) 13:70

Page 8 of 11

ATP production was comparable to the production in medium containing glucose (Additional file 1: Figure S1).

We also observed a significantly higher abundance of extracellular citrate when glucose was substituted by pyruvate (5 mM pyruvate compared to 25 mM glucose: 2.01 ± 0.33; $p < 0.05$). Most likely this citrate originates in the mitochondria by the reaction of acetyl-CoA with oxaloacetate. Under normal conditions this reaction precedes the export of citrate which is then cleaved by cytosolic ATP/citric acid lyase in order to provide acetyl-CoA for lipid synthesis by the cytosolic lipid acid synthase. It may be presumed that in the absence of glucose not enough NADPH for lipid synthesis is available which can be gained from the pentose-phosphate pathway or from the conversion of malate to pyruvate by malic enzyme [EC 1.1.1.40] [26]. This notion is in contrast to the fact that the amount of ribose-5-phosphate was still high in the absence of glucose and the presence of pyruvate. On the other hand, the high abundance of malate in the presence of high concentrations of pyruvate may indicate that its conversion to pyruvate by malic enzyme and the associated production of NADPH is impaired.

Metabolic flux under substitution of glucose by pyruvate: gluconeogenesis

As pointed out in the introduction several metabolites from the glycolytic pathway are building blocks required for growth and proliferation of tumor cells. Therefore, the question was whether a substitution of glucose by pyruvate contributes to gluconeogenesis sufficient for their supply. As demonstrated in Fig. 3, abundances of 2-phosphoglycerate (fold change to: 0.24 ± 0.24) and fructose-6-phosphate (fold change to: 0.29 ± 0.16) were obviously reduced, whereas reduction of abundances in glyceraldehyde-3-phosphate (fold change to: 0.34 ± 0.1; $p < 0.0005$), glycerol-3-phosphate (fold change to: 0.38 ± 0.06; $p < 0.005$) and erythrose-4-phosphate (fold change to: 0.31 ± 0.1; $p < 0.05$) was detected as statistically significant when glucose was substituted by pyruvate (comparing cells exposed to 5 mM pyruvate to cells exposed to 25 mM glucose). Interestingly, the abundance of ribose-5-phosphate did not appear to be affected in a comparable manner as the aforementioned metabolites of the glycolytic pathway when glucose was substituted by pyruvate. This may indicate that the gluconeogenic pathway is active in the absence of glucose and the presence of pyruvate [27].

Metabolic flux under substitution of glucose by pyruvate: amino acids

Substituting glucose with pyruvate resulted in a strong increase of alanine (significant fold change to: 4.33 ± 2.01;

$p < 0.05$) which is most likely catalyzed by the transamination of pyruvate supplied in high amounts in the medium. A second prominent effect was a strong raise in the concentration of aspartate (significant fold change to: 15.09 ± 1.62; $p < 0.0005$). As aspartate is mainly synthesized by a transamination reaction from oxaloacetate it has to be assumed that under our experimental conditions more oxaloacetate was produced by pyruvate carboxylase than is needed for anaplerosis and gluconeogenesis. As both amino acids are released in significantly higher amounts into the medium (alanine: fold change to: 3.51 ± 0.32; $p < 0.0005$; aspartate fold change to: 9.6 ± 5.63; $p < 0.05$), the cells seem to continuously loose amino groups. Although speculative, we presume that the observed increase in the amounts of branched chain keto acids (BCKA) such as α-keto-isocaproate (4-Methyl-2-oxopentanoate) (fold change compared to 25 mM glucose intracellular: 2.27 ± 1.19; extracellular: 2.18 ± 0.13; $p < 0.0005$), α-keto-β-methylvalerate ((S)-3-Methyl-2-oxopentanoate) (fold change compared to 25 mM glucose intracellular: 1.76 ± 1.09; extracellular: 1.53 ± 0.1; $p < 0.0005$) and of α-keto-isovalerate (3-Methyl-2-oxobutanoate) (fold change compared to 25 mM glucose intracellular: 2.07 ± 1.13; extracellular: 1.69 ± 0.09; $p < 0.0005$) may indicate that the amino groups originate from transamination reactions catalyzed by branched-chain amino acid (BCAA) aminotransferase [EC:2.6.1.42] using L-leucine, L-isoleucine and L-valine as substrates (Additional file 3: Figure S3). This notion is supported by the observation that BCAAs are a major source of amino groups for transamination reactions in the brain [28].

Discussion

The central aim of this study was to obtain a more comprehensive understanding of the metabolic contribution of glucose and pyruvate in tumor cells. In accordance with the concept of Krall and Christofk [21], who pointed out that metabolic mechanisms that are imperative for tumor growth may be uncovered by subjecting tumor cells to nutrient limitations [29], we used different concentrations of glucose in our experiments and we also substituted glucose by pyruvate. The rational to use pyruvate to replace glucose goes back to the observation that cancer cells proliferate rapidly in the presence of exogenous pyruvate [30]. It was also demonstrated that exogenous pyruvate is required to sustain proliferation of both cancer and non-cancer cells that cannot utilize oxygen [31]. In this work the authors also propose that exogenous pyruvate may be released by tumor adjacent cells. Although, to our knowledge there is no experimental confirmation that non-tumor cells can release pyruvate into the tumor microenvironment, the high expression of monocarboxylate

Oppermann *et al. Nutrition & Metabolism* (2016) 13:70

Page 9 of 11

transporters (which transport lactate and pyruvate) in many tumors has led to the assumption that tumor cells may use these transporters for the uptake of metabolically important molecules [30].

Analyzing the dependence of the abundance of glycolytic intermediates from glucose we found no strict linear correlation between the extracellular supply of glucose and the abundance of glycolytic intermediates, but there was a general tendency that most metabolites of the glycolytic and associated pathways are more abundant at a higher concentration of glucose than at a lower concentration.

An interesting observation is the high increase in the abundance of sorbitol in the medium.

The polar character of sorbitol usually should prevent its release by diffusion, which in the case of diabetes results in the so-called diabetic cataract [32]. As intracellular sorbitol does induce osmotic stress [33] it is tempting to speculate whether tumor cells may have acquired mechanisms for the effective removal of sorbitol such as the sorbitol permease described to be present in the rabbit papillary epithelial cell line PAP-HT25 [34]. In conclusion, we consider that the high level of sorbitol produced under conditions of high glucose supply and especially the ability to release this metabolite should be studied in more detail as it may be a possible unique target for therapeutic intervention.

Our data clearly demonstrates that at a glucose concentration of 25 mM glycolytically derived pyruvate is metabolized by the TCA cycle. This may at a first glace appear to be in contrast to the Warburg effect but is in agreement with its present day understanding. As pointed out by DeBerardinis et al. [35], the reduction of substrate oxidation by glioblastoma and other tumor cells can simply be secondary to the metabolic activities needed for biosynthesis rather than being an impairment of oxidative metabolism. At this point it has to be taken into account that the TCA cycle also delivers acetyl-CoA which is required for lipid biosynthesis. In fact, using the paediatric glioma cell line SF188 DeBerardinis et al. [35] could demonstrate that 10 % of total glucose metabolism is utilized for the biosynthesis of fatty acids and nucleotides as well as for other processes such as glycosylation.

In conclusion, our data demonstrates that in human U87 glioblastoma cells, pyruvate derived from glucose can be shuttled into the TCA cycle as previously demonstrated for paediatric glioma cells [35], A549 lung carcinoma cells [4] and rat C6 glioma cells [3]. From our data we cannot estimate the percentage of glucose entering the TCA cycle as we did not use isotopically labeled glucose. This will be the next step in future experiments in which we will also investigate how other

energy-rich metabolites such as ketone bodies can be utilized as substrates for glioma cell metabolism.

More experiments are required to solve the interesting question whether the high extracellular concentration of citrate, under the withdrawal of glucose and its substitution by pyruvate, indicates that the cell produces more citrate than needed for the production of fatty acids or whether the conversion of citrate to acetyl-CoA and oxaloacetate is impaired as this would finally prevent tumor cell proliferation. The high amount of citrate released into the medium also raises a question about anaplerosis: it should be kept in mind that the removal of citrate and other metabolites from the TCA cycle that are used as precursors for biosynthetic reactions outside the mitochondria, requires anaplerotic reactions that refill the pool of precursor molecules. In glioblastoma and other transformed cell lines, glutamine is the preferred anaplerotic precursor when it is supplied by the medium, contributing up to 90 % to the oxaloacetate pool [35]. As in our experiments glutamine is not supplied with the medium, the synthesis of oxaloacetate via pyruvate carboxylase becomes important and may compensate the loss of glutamine-dependent anaplerosis, which is a mechanism previously proposed by Cheng et al. who investigated glioblastoma growth under deprivation of glutamine [36]. A high flux of pyruvate through the pyruvate carboxylase reaction is also in agreement with the assumption that the cells perform gluconeogenesis when glucose is substituted by pyruvate in order to provide ribose-5-phosphate (or other metabolites of the glycolytic pathway). At this point it is also interesting to note that gluconeogenesis in tumor cells under low glucose conditions has also been reported in lung cancer cells [27] although in this study glutamine served as substrate for the gluconeogenic pathway.

Conclusions

Overall the data in the present study demonstrates that i) there is no strict correlation between the extracellular supply of glucose and abundance of glycolytic intermediates, ii) sorbitol is highly produced and released into the medium under high glucose supply, iii) U87 cells metabolize a significant amount of glucose derived pyruvate in the mitochondria and iv) gluconeogenesis is most likely activated when glucose is substituted by pyruvate. These observations suggest a high plasticity of glioblastoma cells to changes in nutritional supply which should be taken into account with regard to the prescription of special diets for the treatment of tumor patients or when considering to use specific inhibitors of glycolysis.

Oppermann *et al. Nutrition & Metabolism* (2016) 13:70

Page 10 of 11

Additional files

Additional file 1: Figure S1. Relative intracellular ATP concentration at different concentrations of glucose and pyruvate. U87 cells were seeded at a density of 5000 cells per well in 96 well microplates and received medium without a carbon source and without GlutaMAX and FBS for 20 h. Then, fresh medium was added containing different concentrations of glucose (5.5 mM, 11 mM and 25 mM), pyruvate (1 mM, 2.5 mM, 5 mM, 10 mM and 20 mM) or without any carbon source (0 mM). 24 h later the relative intracellular ATP concentration was determined by the CellTiterGlo Assay (for method description see Additional file 5: Methods). Results are represented as mean and standard deviation of 6 independently measured wells compared to the signal of 25 mM glucose set to 1. Statistical significance was determined by Student's *t*-test with: *: $p < 0.05$; **: $p < 0.005$; ***: $p < 0.0005$; ns: not significant. (TIF 949 kb)

Additional file 2: Figure S2. Multivariate analysis of metabolite profiles. Principal component analysis (PCA) of metabolite profiles from U87 cells cultivated in the presence of 5.5 mM (5.5 Glc), 11 mM (11 Glc), 25 mM glucose (25 Glc) or 5 mM pyruvate in the absence of glucose (Pyr) for 24 h. 25 Glc and Pyr appear clearly separated from each other, whereas 11 Glc and 5.5 Glc have a similar profile separated from 25 Glc and Pyr. PC1 includes 34.7 % of variability (responsible for separation of Pyr), PC2 16.2 % (differences between the glucose treated cells). $n = 6$ for each condition, all identified metabolites were included ($n = 106$). (TIF 69 kb)

Additional file 3: Figure S3. Extended metabolic pathway of U87 cells profiling data. A combined metabolic pathway is presented, including glycolysis, the pentose-phosphate pathway, the TCA cycle and the branched chain amino acid degradation with the subcellular localization (mitochondrial, cytoplasm and extra cellular—methodically it can only be distinguished between intra- and extracellular metabolites). Intracellular metabolite abundances (Fig. 2) are shown as bar diagrams depicting the ratio between the abundance of a metabolite (the peak area) normalized to total protein (μg) compared to the abundance at 25 mM glucose (normalized to protein) set to 1. The consumption of extracellularly present metabolites was determined by the comparison of signals obtained from medium without cells to those after incubation with cells. Thus, a value of 0 indicates the same abundance of a metabolite in medium with and without cells (no consumption) and a value of -1 indicates that the metabolite is completely consumed. Abundances of metabolites released from the cells are expressed as the abundance of a metabolite in medium after incubation compared to its abundance in medium with 25 mM glucose set to 1. All experiments have been conducted in 6-tuplicate and statistical significance was determined by Student's *t*-test with: *: $p < 0.05$; **: $p < 0.005$; ***: $p < 0.0005$. The statistical analysis for intracellular and released metabolites was performed by comparing the abundance of a metabolite in an experiment (11 mM or 5 mM glucose or 5 mM pyruvate) to the abundance in 25 mM glucose. For consumed metabolites, each metabolite's abundance was compared to its abundance in medium without cells. Direct reactions are presented as straight lines and reactions involving several steps are presented as dotted lines. Metabolites which were not determined are labeled Grey. Abbreviations: GA3P: glyceraldehyde-3-phosphate; DHAP: dihydroxyacetone phosphate; Glu: glutamate; aKG: α-ketoglutarate; PEP: phosphoenolpyruvate. (JPG 3880 kb)

Additional file 4: Figure S4. mRNA expression of glycolytic genes in U87 cells. Expression of mRNA encoded by the genes GLUT1/2/3/4 (glucose transporters 1/2/3/4) (a) and HK1/2 (hexokinase 1/2) (b) in U87 cells as revealed by qRT-PCR (for method description see Additional file 5). The relative expression was determined using standard curves normalized to the expression of TATA box binding protein (TBP). (TIF 655 kb)

Additional file 5: Methods. (DOCX 16 kb)

Abbreviations
aKG: α-ketoglutarate; BCAA: Branched-chain amino acid; BCKA: Branched chain keto acids; DHAP: Dihydroxyacetone phosphate; GA3P: Glyceraldehyde-3-phosphate; GC-MS: Gas chromatography coupled to mass spectrometry; Glc: Glucose; Glu: Glutamate; MGO: Methylglyoxal; NIST: National Institute of Standards and Technologies; PCA: Principal component analysis; PEP: Phosphoenolpyruvate; PFBHA: *O*-(2,3,4,5,6-pentafluorobenzyl) hydroxylamine; Pyr: Pyruvate; TCA: Tricarboxylic acid

Availability of data and materials
The datasets generated in this study are available from the corresponding author on reasonable request.

Authors' contributions
HO, JS, MBP, CB and YD performed the experiments. HO and CB analyzed the data. HO created the figures with support of CB and FG. JM supported the project and revised the manuscript. CB, FG and HO designed the study and wrote the manuscript. All authors read and approved the final manuscript.

Authors' information
Not applicable.

Competing interests
The authors have not declared any conflict of interest relevant to this work.

Author details
[1]Klinik und Poliklinik für Neurochirurgie, Universitätsklinikum Leipzig AöR, Liebigstraße 19, Leipzig 04103, Germany. [2]Institut für Analytische Chemie, Fakultät für Chemie & Mineralogie der Universität Leipzig, Linnéstraße 3, Leipzig 04103, Germany.

References
1. Warburg O, Wind F, Negelein E. The metabolism of tumors in the body. J Gen Physiol. 1927;8:519–30.
2. Warburg O. On the origin of cancer cells. Science. 1956;123:309–14.
3. Portais JC, Schuster R, Merle M, Canioni P. Metabolic flux determination in C6 glioma cells using carbon-13 distribution upon 1-13Cglucose incubation. Eur J Biochem. 1993;217:457–68.
4. Metallo CM, Walther JL, Stephanopoulos G. Evaluation of 13C isotopic tracers for metabolic flux analysis in mammalian cells. J Biotechnol. 2009;144:167–74. doi:10.1016/j.jbiotec.2009.07.010.
5. Hanahan D, Weinberg RA. Hallmarks of cancer: the next generation. Cell. 2011;144:646–74. doi:10.1016/j.cell.2011.02.013.
6. Rodriguez-Enriquez S, Marin-Hernandez A, Gallardo-Perez JC, Carreno-Fuentes L, Moreno-Sanchez R. Targeting of cancer energy metabolism. Mol Nutr Food Res. 2009;53:29–48. doi:10.1002/mnfr.200700470.
7. Branco AF, Ferreira A, Simoes RF, Magalhaes-Novais S, Zehowski C, Cope E, et al. Ketogenic diets: from cancer to mitochondrial diseases and beyond. Eur J Clin Invest. 2016;46:285–98. doi:10.1111/eci.12591.
8. Strowd RE, Cervenka MC, Henry BJ, Kossoff EH, Hartman AL, Blakeley JO. Glycemic modulation in neuro-oncology: experience and future directions using a modified Atkins diet for high-grade brain tumors. Neurooncol Pract. 2015;2:127–36. doi:10.1093/nop/npv010.
9. Seyfried TN, Flores R, Poff AM, D'Agostino DP, Mukherjee P. Metabolic therapy: a new paradigm for managing malignant brain cancer. Cancer Lett. 2015;356:289–300. doi:10.1016/j.canlet.2014.07.015.
10. Woolf EC, Scheck AC. The ketogenic diet for the treatment of malignant glioma. J Lipid Res. 2015;56:5–10. doi:10.1194/jlr.R046797.
11. Vidali S, Aminzadeh S, Lambert B, Rutherford T, Sperl W, Kofler B, Feichtinger RG. Mitochondria: The ketogenic diet—A metabolism-based therapy. Int J Biochem Cell Biol. 2015;63:55–9. doi:10.1016/j.biocel.2015.01.022.

Oppermann *et al. Nutrition & Metabolism* (2016) 13:70

Page 11 of 11

12. Wright C, Simone NL. Obesity and tumor growth: inflammation, immunity, and the role of a ketogenic diet. Curr Opin Clin Nutr Metab Care. 2016;19: 294–9. doi:10.1097/MCO.0000000000000286.

13. Marin-Hernandez A, Rodriguez-Enriquez S, Vital-Gonzalez PA, Flores-Rodriguez FL, Macias-Silva M, Sosa-Garrocho M, Moreno-Sanchez R. Determining and understanding the control of glycolysis in fast-growth tumor cells. Flux control by an over-expressed but strongly product-inhibited hexokinase. FEBS J. 2006;273:1975–88. doi:10.1111/j.1742-4658. 2006.05214.x.

14. Wouters BG, Koritzinsky M. Hypoxia signalling through mTOR and the unfolded protein response in cancer. Nat Rev Cancer. 2008;8:851–64. doi:10.1038/nrc2501.

15. Stupp R, Mason WP, van den Bent MJ, Weller M, Fisher B, Taphoorn MJB, et al. Radiotherapy plus concomitant and adjuvant temozolomide for glioblastoma. N Engl J Med. 2005;352:987–96. doi:10.1056/NEJMoa043330.

16. Renner C, Asperger A, Seyffarth A, Meixensberger J, Gebhardt R, Gaunitz F. Carnosine inhibits ATP production in cells from malignant glioma. Neurol Res. 2010;32:101–5. doi:10.1179/016164109X12518779082237.

17. Allen M, Bjerke M, Edlund H, Nelander S, Westermark B. Origin of the U87MG glioma cell line: Good news and bad news. Sci Transl Med. 2016;8:354re3. doi:10.1126/scitranslmed.aaf6853.

18. McLellan AC, Phillips SA, Thornalley PJ. Fluorimetric assay of d-lactate. Anal Biochem. 1992;206:12–6. doi:10.1016/S0003-2697(05)80004-1.

19. Hutschenreuther A, Kiontke A, Birkenmeier G, Birkemeyer C. Comparison of extraction conditions and normalization approaches for cellular metabolomics of adherent growing cells with GC-MS. Anal Methods. 2012;4:1953. doi:10.1039/c2ay25046b.

20. Stein SE. An integrated method for spectrum extraction and compound identification from gas chromatography/mass spectrometry data. J Am Soc Mass Spectrom. 1999;10:770–81. doi:10.1016/S1044-0305(99)00047-1.

21. Kopka J, Schauer N, Krueger S, Birkemeyer C, Usadel B, Bergmuller E, et al. GMD@CSB.DB: the Golm Metabolome Database. Bioinformatics. 2005;21:1635–8. doi:10.1093/bioinformatics/bti236.

22. Allaman I, Bélanger M, Magistretti PJ. Methylglyoxal, the dark side of glycolysis. Front Neurosci. 2015;9:23. doi:10.3389/fnins.2015.00023.

23. Landon J, Fawcett JK, Wynn V. Blood pyruvate concentration measured by a specific method in control subjects. J Clin Pathol. 1962;15:579–84.

24. Vannucci SJ, Maher F, Simpson IA. Glucose transporter proteins in brain: delivery of glucose to neurons and glia. Glia. 1997;21:2–21.

25. Wolf A, Agnihotri S, Micallef J, Mukherjee J, Sabha N, Cairns R, et al. Hexokinase 2 is a key mediator of aerobic glycolysis and promotes tumor growth in human glioblastoma multiforme. J Exp Med. 2011;208:313–26. doi:10.1084/jem.20101470.

26. Lunt SY, Vander Heiden MG. Aerobic glycolysis: meeting the metabolic requirements of cell proliferation. Annu Rev Cell Dev Biol. 2011;27:441–64. doi:10.1146/annurev-cellbio-092910-154237.

27. Leithner K, Hrzenjak A, Trotzmuller M, Moustafa T, Kofeler HC, Wohlkoenig C, et al. PCK2 activation mediates an adaptive response to glucose depletion in lung cancer. Oncogene. 2015;34:1044–50. doi:10.1038/onc.2014.47.

28. Yudkoff M, Nissim I, Daikhin Y, Lin Z, Nelson D, Pleasure D, Erecinska M. Brain Glutamate Metabolism: Neuronal-Astroglial Relationships. Dev Neurosci. 2004;15:343–50. doi:10.1159/000111354.

29. Krall AS, Christofk HR. Rethinking glutamine addiction. Nat Cell Biol. 2015;17:1515–7. doi:10.1038/ncb3278.

30. Diers AR, Broniowska KA, Chang C, Hogg N. Pyruvate fuels mitochondrial respiration and proliferation of breast cancer cells: effect of monocarboxylate transporter inhibition. Biochem J. 2012;444:561–71. doi:10.1042/BJ20120294.

31. Yin C, He D, Chen S, Tan X, Sang N. Exogenous pyruvate facilitates cancer cell adaptation to hypoxia by serving as an oxygen surrogate. Oncotarget 2016. doi: 10.18632/oncotarget.10202.

32. Pollreisz A, Schmidt-Erfurth U. Diabetic cataract-pathogenesis, epidemiology and treatment. J Ophthalmol. 2010;2010:608751. doi:10.1155/2010/608751.

33. Wehner F, Olsen H, Tinel H, Kinne-Saffran E, Kinne RKH. Cell volume regulation: osmolytes, osmolyte transport, and signal transduction. Rev Physiol Biochem Pharmacol. 2003;148:1–80. doi:10.1007/s10254-003-0009-x.

34. Garty H, Furlong TJ, Ellis DE, Spring KR. Sorbitol permease: an apical membrane transporter in cultured renal papillary epithelial cells. Am J Physiol. 1991;260:F650–6.

35. DeBerardinis RJ, Mancuso A, Daikhin E, Nissim I, Yudkoff M, Wehrli S, Thompson CB. Beyond aerobic glycolysis: transformed cells can engage in glutamine metabolism that exceeds the requirement for protein and nucleotide synthesis. Proc Natl Acad Sci U S A. 2007;104:19345–50. doi:10.1073/pnas.0709747104.

36. Cheng T, Sudderth J, Yang C, Mullen AR, Jin ES, Mates JM, DeBerardinis RJ. Pyruvate carboxylase is required for glutamine-independent growth of tumor cells. Proc Natl Acad Sci U S A. 2011;108:8674–9. doi:10.1073/pnas. 1016627108.

88

In summary, our experiments demonstrate that glioblastoma cells exhibit a high metabolic flexibility which enables adjustments to maintain cell growth under restricted conditions. As inhibition of glycolytic flux appeared not to be accompanied by reduced intracellular ATP, we conclude that glioblastoma cells shift metabolism in response to reduced supply with glucose.

After we demonstrated that glioblastoma cells can metabolise pyruvate, we further investigated the hypothesis of Holliday and McFarland regarding the attenuation of carnosine's anti-neoplastic effect by pyruvate (Holliday and McFarland 1996). In their study carnosine selectively eliminated cervix carcinoma cells from a co-culture with fibroblasts which was attenuated by the presence of 1 mM pyruvate. The authors assumed that treatment with carnosine reduces the production of pyruvate from glucose and therefore inhibits the ATP produced by glycolysis, TCA cycle and subsequent oxidative phosphorylation (OxPhos). Hence, the supplementation of pyruvate could reverse this effect by increasing aerobic ATP production (Holliday and McFarland 1996). In the study of Oppermann et al. (Oppermann et al. 2016b) we investigated whether the anti-neoplastic effect of carnosine can be antagonised by ATP production via OxPhos fuelled by pyruvate. To do that, we tested the influence of carnosine on glioblastoma cell viability after pre-starvation and the availability of only glucose, galactose or pyruvate during cultivation. With this strategy, we expected to minimize possible unintended effects from serum which is present during long term cultivation and contains compounds of undefined nature. To investigate the significance of aerobe metabolism of pyruvate when this compound is added to the medium to attenuate carnosine's growth inhibiting effect, we used the inhibitors 2,4-dinitrophenol (DNP) and CPI-613. The latter is a lipoate analogue which blocks the entry of pyruvate into the TCA cycle by inducing PDKs which in turn inhibit the PDC via phosphorylation (Zachar et al. 2011). DNP inhibits mitochondrial ATP production by uncoupling electron transport from phosphorylation without affecting oxygen uptake (Loomis and Lipmann 1948).

Pyruvate attenuates the anti-neoplastic effect of Carnosine independently from oxidative phosphorylation

Henry Oppermann[1,*], Lutz Schnabel[1,*], Jürgen Meixensberger[1], Frank Gaunitz[1]

[1]Klinik und Poliklinik für Neurochirurgie, Universitätsklinikum Leipzig AöR, 04103 Leipzig, Germany

[*]These authors contributed equally to this work

Correspondence to: Frank Gaunitz, **email:** Frank.Gaunitz@medizin.uni-leipzig.de

ABSTRACT

Here we analyzed whether the anti-neoplastic effect of carnosine, which inhibits glycolytic ATP production, can be antagonized by ATP production via oxidative phosphorylation fueled by pyruvate. Therefore, glioblastoma cells were cultivated in medium supplemented with glucose, galactose or pyruvate and in the presence or absence of carnosine. CPI-613 was employed to inhibit the entry of pyruvate into the tricarboxylic acid cycle and 2,4-dinitrophenol to inhibit oxidative phosphorylation. Energy metabolism and viability were assessed by cell based assays and histochemistry.

ATP in cell lysates and dehydrogenase activity in living cells revealed a strong reduction of viability under the influence of carnosine when cells received glucose or galactose but not in the presence of pyruvate. CPI-613 and 2,4-dinitrophenol reduced viability of cells cultivated in pyruvate, but no effect was seen in the presence of glucose. No effect of carnosine on viability was observed in the presence of glucose and pyruvate even in the presence of 2,4-dinitrophenol or CPI-613.

In conclusion, glioblastoma cells produce ATP from pyruvate via the tricarboxylic acid cycle and oxidative phosphorylation in the absence of a glycolytic substrate. In addition, pyruvate attenuates the anti-neoplastic effect of carnosine, even when ATP production via tricarboxylic acid cycle and oxidative phosphorylation is blocked. We also observed an inhibitory effect of carnosine on the tricarboxylic acid cycle and a stimulating effect of 2,4-dinitrophenol on glycolytic ATP production.

INTRODUCTION

The anti-neoplastic effect of carnosine has been described for a number of tumor derived cells *in vitro* including gastric [1, 2], colon [3], ovarian [4] and brain cancer cells [5]. In addition, effects were demonstrated *in vivo* [6, 7] and the number of examples is still increasing (for reviews see [8, 9, 10]). The primary molecular targets responsible for carnosine's action on tumor cells are still not known. Although, its influence on glycolytic ATP production, recognized to be crucial for tumor cell energy metabolism, has been suggested by previous experiments [11]. The dependence of tumor cells on glycolysis is known as the so-called Warburg effect. It describes that ATP production in cancer cells is frequently dependent on glycolysis resulting in the production of lactate even in the presence of oxygen. In normoxic conditions non-

tumor cells produce ATP by oxidative phosphorylation (OxPhos) using reduction equivalents derived from the metabolization of pyruvate entering the tricarboxylic acid (TCA) cycle (for reviews see [12, 13]). The Warburg effect has originally been attributed to defects in the mitochondria of cancer cells. According to current knowledge this only holds true for a minority of tumors [14]. More recent data point towards variants of glycolytic enzymes that may specifically be expressed in tumors such as pyruvate kinase M2 [15]. Unfortunately, this knowledge has up to now not resulted in the development of new therapeutic strategies to fight cancer. Thus, a thorough investigation of the inhibitory effect of carnosine on tumor cell specific ATP production will greatly help to develop new strategies which can exploit the Warburg effect. This is especially pertinent for malignancies, for those chances of recovery are poor under present-day

treatment strategies. Tumor cells may adapt to changes in nutritional supply by switching metabolic fluxes and/ or become fed by compounds supplied by neighbor cells [16]. Hence a possible inhibition of glycolysis, attenuated by metabolic adaptation, has to be taken into account (for recent reviews see [17, 18]). More than 20 years ago, Holiday and McFarland suggested that carnosine's anti-neoplastic effect might be inhibited by the presence of pyruvate [19]. As carnosine inhibits glycolytic ATP production [11] the most straight interpretation of the observation of Holiday and McFarland would be a tumor cell switch to OxPhos when glycolysis is inhibited and pyruvate is supplied. Therefore, we analyzed the response of tumor cell viability measuring ATP in cell lysates and dehydrogenase activities (NAD(P)H) in living cells. We used cells from human glioblastoma (GBM) which is the most common primary tumor of the adult brain [20]. According to the classification of the world health organization (WHO), GBM is one of the most malignant diffuse astrocytic tumors and classified as WHO grade IV [21]. Currently, the median overall survival of patients receiving standard therapy after surgery of the tumor is 14.6 month [22]. Consequently, there is urgent need to develop alternative treatment strategies. These may include a metabolic intervention at the level of glycolysis as glucose is the central metabolic fuel of this tumor. Our experiments were mainly performed with cells cultivated in the presence of glucose. We also tested galactose as a nutritional substitute for glucose in a first series of experiments. The cells were cultivated in the absence and presence of carnosine and we analyzed the influence of pyruvate on carnosine's anti-neoplastic effect. In order to determine the influence of the TCA cycle and of OxPhos the experiments were also performed in the absence and presence of inhibitors for the pyruvate dehydrogenase complex and for ATP production by OxPhos. In addition, we established a protocol in which the cells were pre-starved in the absence of glucose, glutamine and serum. Effects from the presence of compounds the cells were exposed to during long term cultivation were thus avoided. This appeared to be especially important with regard to serum that was omitted throughout the experiments because it contains compounds of undefined nature.

RESULTS

Viability, amount of ATP and NAD(P)H production in glioblastoma cells cultivated in glucose, galactose or pyruvate under the influence of serum and GlutaMax

In previous experiments, in which the anti-neoplastic effect of carnosine on glioblastoma cells was analyzed, a high variation of viability was encountered [23]. Comparing eight independent experiments, in which the effect of 50 mM carnosine in U87 cells after 24 hours of incubation

was determined, we found a reduction of ATP in cell lysates between 44% and 89% (75 ± 15%; data not shown) compared to the untreated control. In these experiments cells received medium supplemented with carnosine after they had been grown in medium with 4.5 g/L glucose, 10% FBS and 2 mM GlutaMax. Therefore, it cannot be ruled out that the effect of carnosine on ATP production was concealed by intracellular metabolites, contributing to ATP production, downstream of carnosine's target.

This question was addressed by firstly investigating the viability of cells cultivated for 24 hours in medium without the supplements glucose, GlutaMax and FBS. The result of one representative experiment is presented in Figure 1. In addition, we investigated whether galactose and pyruvate are able to substitute glucose. As can be seen in Figure 1, only the absence of FBS from the culture medium prominently decreased viability as revealed by reduced dehydrogenase activity and ATP in cell lysates. Additionally, no signs of apoptosis or necrosis were observed. Galactose as well as pyruvate could substitute glucose to a large extent. More importantly, the viability of cells that were cultivated in the absence of glucose, galactose or pyruvate did not severely differ from that of cells cultivated in the presence of the nutrients or did exhibit morphological change (data not shown). The experiment indicates an influence of FBS on viability and demonstrates that a 24 hour starvation in the absence of glucose, galactose or pyruvate had only minor effects on viability. The determination of lactate dehydrogenase release into the medium, as a marker of necrotic loss of membrane integrity, did not reveal cell death by necrosis (data not shown). Further experiments with cells cultivated without glucose, galactose or pyruvate and without FBS and GlutaMax prior to the addition of carnosine were hence decided.

Viability, amount of ATP and NAD(P)H production of pre-starved glioblastoma cells under the influence of carnosine and different nutrients

The cultivation of cells for 24 hours in the absence of FBS, GlutaMax and the specified nutrients did not result in a pronounced reduction of viability. Therefore, experiments with carnosine were performed with cells pre-cultivated for 20 hours in the absence of the aforementioned supplements. This avoids effects which could flaw the experiments as described in the introduction. Cells from the glioblastoma cell line U87 were transferred to 96-well plates at a density of 5000 cells per well, seeded for 3 hours in fully supplemented medium and then cultivated in the absence of glucose, galactose or pyruvate and without FBS and GlutaMax for 20 hours. Then, fresh medium was added containing glucose, galactose, pyruvate or without any of these compounds and supplemented with or without

50 mM carnosine. Twenty-four and forty-eight hours later viability was determined by measuring ATP in cell lysates and dehydrogenase activity in living cells. As can be seen in Figure 2A, cells cultivated in glucose, galactose and pyruvate exhibited a comparable amount of ATP in cell lysates after 24 and 48 hours in the absence of carnosine. Whereas carnosine strongly reduced viability in cells cultivated in the presence of glucose and galactose (down to $3.6 \pm 5.6\%$ at 48 hours), but not in those cells incubated in the presence of pyruvate ($94.0 \pm 15.5\%$ at 48 hours). This demonstrates strong inhibition of the glycolytic ATP production by carnosine. In addition, it indicates that the tumor cells can compensate insufficient production of ATP by glycolysis by fueling pyruvate into the TCA cycle resulting in ATP production by OxPhos. As there was a distinctively measurable amount of ATP in cell lysates of cells cultivated without any supplement and in the absence of carnosine ($47.3 \pm 42.9\%$ at 24 hours + 20 hours of starvation and $29.3 \pm 31.7\%$ at 48 hours + 20 hours of starvation compared to cells in the presence of glucose), but not in the presence of carnosine ($0.2 \pm 0.1\%$ at 44 and 68 hours of total starvation time), this ATP may be generated from metabolites that are present even after 44 and 68 hours of starvation. This ATP production, however, is clearly inhibited by carnosine. Comparing the production of NAD(P)H in living cells (Figure 2B) it becomes obvious that pyruvate does not completely substitute galactose or glucose. The glycolytic production of redox equivalents appears to be higher than that from pyruvate, but this may be caused by a rapid mitochondrial

metabolization of TCA cycle derived redox equivalents. The minor difference between production of NAD(P)H in medium containing pyruvate with or without carnosine may indicate that there are still metabolites present which account for the production of NAD(P)H. Moreover, this notion is substantiated by the observation that there is still some NAD(P)H production in medium containing either glucose or galactose and carnosine. It also has to be taken into account that the CellTiter-Blue assay also measures the production of reduced reduction equivalents from other dehydrogenases aside from the glyceraldehyde-3-phosphate dehydrogenase reaction. However, as the production of NAD(P)H is higher in medium containing pyruvate than in the medium without any supplement there is an obvious production of NAD(P)H via pyruvate. As revealed in Figure 7 and Table 1 no necrosis does occur in cells treated with carnosine in the presence of pyruvate.

Viability and the amount of ATP in glioblastoma cells in the presence of the pyruvate dehydrogenase inhibitor CPI-613

The experiments presented in Figure 2 demonstrate that cells from the line U87 are viable in the absence of a glycolytic substrate, when pyruvate is present. This indicates that the cells can produce ATP from pyruvate via the TCA cycle and OxPhos in the absence of glucose, which we just recently demonstrated by the analysis of metabolic profiles, determined by gas chromatography coupled to mass spectrometry (GC-MS) [24]. Hence, it
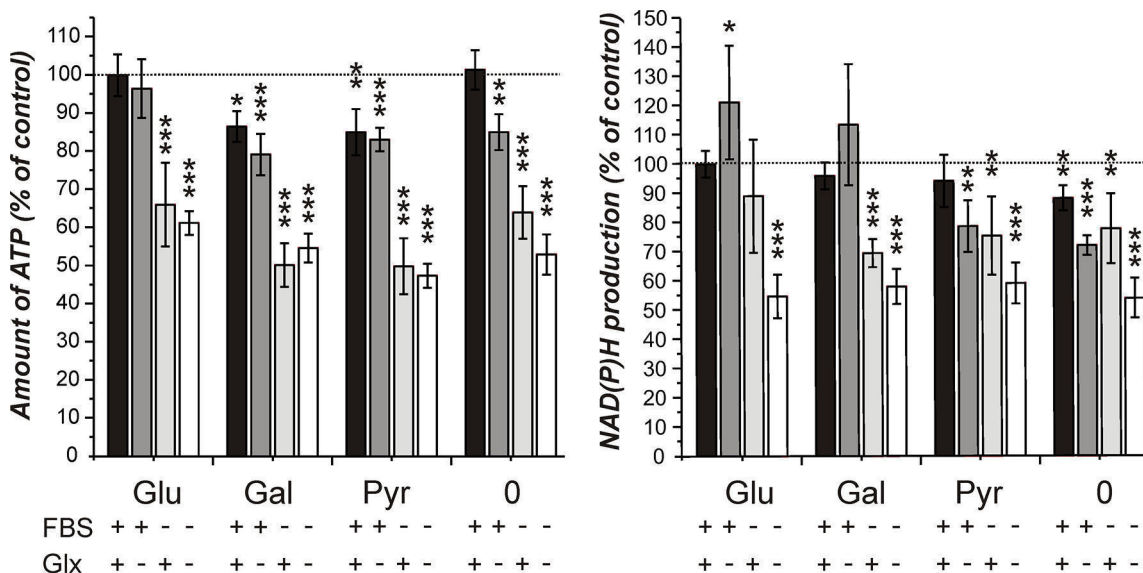

Figure 1: Amount of ATP in cell lysates and NAD(P)H production in cells from the line U87 under different culture conditions. Cells from the line U87 were cultivated for 20 hours at a density of 5000 cells per well in 96-well microplates in DMEM standard culture medium before they received fresh medium with different supplements: FBS: fetal bovine serum, 10%; Glx: GlutaMax, 2 mM; Glu/Gal/Pyr: glucose, galactose, pyruvate: each 25 mM; 0: no Glu/Gal/Pyr. 24 hours later the CellTiter-Glo assay (measuring ATP in cell lysates, left part of the panel) and the CellTiter-Blue assay (measuring NAD(P)H production, right part of the panel) were employed to assess cell viability. Signals obtained from cells cultivated in 25 mM glucose, 10% FBS and 2 mM GlutaMax were set as 100%. Results are presented as mean and standard deviation of 6 wells. Statistical significance was determined by Student's *t*-test with: *$p < 0.05$; **$p < 0.005$; ***$p < 0.0005$.

was asked whether the flux of metabolites through the TCA cycle can antagonize the effect of carnosine on ATP production. Therefore, the pyruvate dehydrogenase inhibitor CPI-613 was used to block the initial step that converts pyruvate to acetyl-CoA fueling the TCA cycle [25]. CPI-613 is a lipoic acid analog which activates the lipoate-responsive regulatory phosphorylation of the E1α pyruvate dehydrogenase subunit and was shown to be selective for tumor cells in culture [25]. The experiments were performed with cells from the glioblastoma lines LN405 and T98G in addition to U87 in order to analyze a cell line dependent difference. For the experiment, cells from the three lines were pre-starved for 20 hours as described above, before they received medium with either 25 mM glucose or 5 mM pyruvate and different concentrations of CPI-613 for 24 hours. A concentration of 5 mM pyruvate was chosen, as experiments revealed that this concentration is sufficient for the maximum amount of ATP determined in cell lysates in the presence of 50 mM carnosine (Supplementary Data S1). As shown in Figure 3, the amount of ATP in cell lysates in the presence of CPI-613 was progressively reduced with increasing concentrations of the inhibitor when pyruvate was supplied as nutrient. This supports the notion that pyruvate can be metabolized by the TCA cycle and that OxPhos is not impaired in these cells. Furthermore, cells from the lines U87 and LN405 did not show any significant change in the amount of ATP in the presence of glucose and CPI-613, whereas ATP of cells from the line T98G was strongly reduced. This demonstrates that T98G cells are dependent on the TCA cycle and OxPhos. At this point

it is interesting to note, that in the absence of glucose, pyruvate does differently contribute to the amount of ATP (in the absence of the inhibitor) in the three lines (data not shown in the graph): Whereas ATP in U87 and T98G cells is not significantly different between cells either supplied with glucose or pyruvate (glucose to pyruvate in U87: $100 \pm 15.1\%$ and $120.2 \pm 31\%$, in T98G: $100 \pm 12.4\%$ and $83 \pm 28.6\%$), pyruvate does less efficiently contribute to ATP in cells from the line LN405 (glucose to pyruvate: $100 \pm 14.3\%$ and $39 \pm 13\%$; $p < 0.005$).

Viability and amount of ATP in glioblastoma cells under the influence of carnosine in the presence of glucose and glucose plus pyruvate

The experiments in the previous sections demonstrated that the production of ATP via pyruvate is possible in glioblastoma cells (although not required when glucose is abundant - at least in cells from the lines U87 and LN405), but may become important in the absence of glucose. To consider using carnosine's capacity to block the glycolytic flux from glucose in tumor cells for the treatment of human tumors, it had to be asked whether the anti-neoplastic effect of the dipeptide may be attenuated by pyruvate. Therefore, cells from the glioblastoma lines U87, LN405 and T98G were incubated in the presence of either glucose (25 mM) or a mixture of glucose (25 mM) and pyruvate (5 mM) and in the absence and presence of different concentrations of carnosine determined to equal an inhibitory concentration of IC20, IC50 and IC80 (see Supplementary Data S2). The data presented in
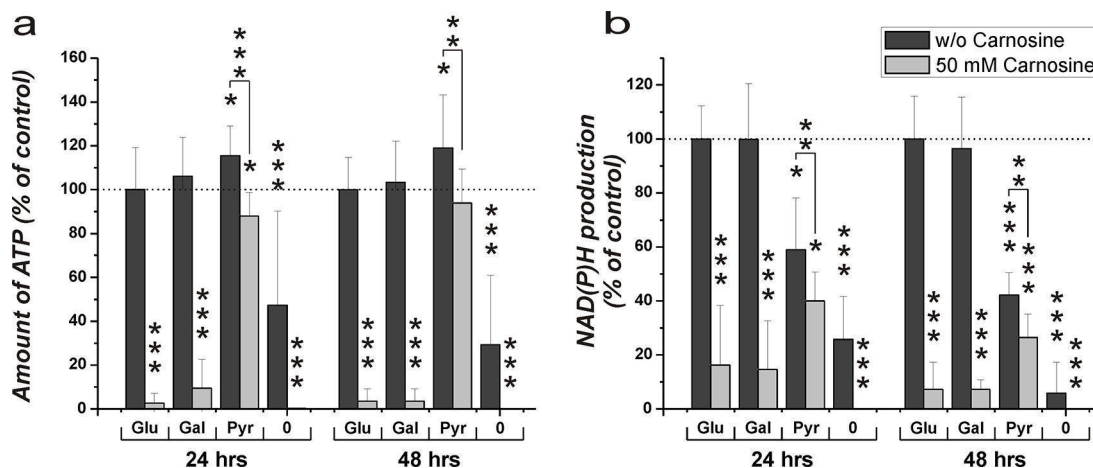

Figure 2: Amount of ATP in cell lysates and NAD(P)H production in the line U87 under the influence of glucose, galactose or pyruvate and carnosine after pre-starvation. Cells from the line U87 were seeded at a density of 5000 cells per well in 96-well microplates and were incubated for 20 hours in medium without glucose, galactose or pyruvate and without FBS and GlutaMax. After 20 hours, medium was substituted for medium with different supplements: glucose (Glu), galactose (Gal), pyruvate (Pyr): 25 mM, no supplement (0); and with or without 50 mM carnosine. 24 and 48 hours later CellTiter-Glo and CellTiter-Blue assays were employed to determine ATP in cell lysates and NAD(P)H production in intact cells. In order to compare the effects of glucose, galactose and pyruvate in the presence and absence of carnosine, results are grouped into data sets with regard to the amount of ATP in cell lysates (**A**) and dehydrogenase activity (**B**). Results are represented as mean and standard deviation of 6 wells from three independent experiments for each condition normalized to signals recorded from cells cultivated in the presence of glucose and the absence of carnosine (set as 100%). Statistical significance was determined by Student's t-test with: *$p < 0.05$; **$p < 0.005$; ***$p < 0.0005$.

Table 1: Cell viability in the presence of different nutritional compounds and inhibitors

	Glucose	Pyruvate	Glucose + Pyruvate
Control	94.30 ± 4.56%	98.54 ± 0.29%	98.63 ± 1.38%
Carnosine	0.00 ± 0.00%	99.25 ± 0.54%	95.58 ± 2.03%
CPI-613	93.79 ± 3.40%	27.41 ± 11.15%	99.18 ± 0.04%
Carnosine + CPI-613	0.47 ± 0.47%	2.72 ± 0.81%	98.37 ± 0.81%
DNP	97.13 ± 0.71%	21.06 ± 3.03%	96.48 ± 3.84%
Carnosine + DNP	1.65 ± 2.32%	1.95 ± 2.29%	98.03 ± 1.34%

Number of viable cells in the presence of different nutrients and inhibitors as determined by Calcein AM/PI staining from the experiments depicted in Figure 5 to 7 expressed in % of cells stained with Calcein AM compared to the total number of cells.

Figure 4 demonstrates that in all three lines the inhibitory effect of carnosine on cell viability in the presence of glucose is strongly attenuated by the addition of pyruvate. Only at the highest concentration of carnosine (IC80) a significantly reduced amount of ATP in the presence of glucose and pyruvate is observed. In fact, cells from the line U87 grown in the presence of glucose and 50 mM carnosine exhibit an almost complete loss of viability after a 24 hour exposure to the dipeptide. Cells, which received pyruvate in addition, were as healthy as cells cultivated in the absence of carnosine (Figure 7; Table 1). At this point it also has to be noted that the amount of ATP in the presence of glucose and pyruvate compared to glucose alone was ~2-fold higher in LN405 and comparable in U87 cells (1.3-fold higher). The amount of ATP in cells from the line T98G was ~10-fold higher in the presence of pyruvate and glucose compared to glucose alone. This underscores that ATP production from pyruvate via the
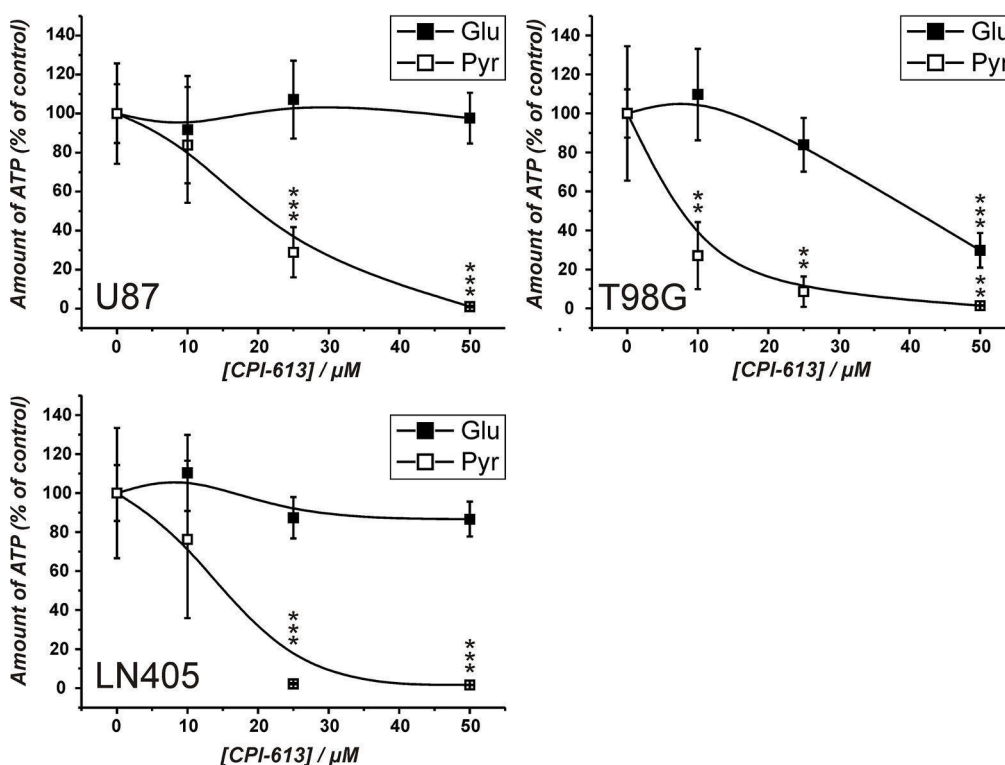

Figure 3: Amount of ATP in cell lysates of cells from the lines U87, T98G and LN405 under the influence of the pyruvate dehydrogenase inhibitor CPI-613. Cells were seeded at a density of 5000 cells per well in 96-well microplates before they received medium without glucose, galactose or pyruvate and without FBS and GlutaMax. 20 hours later fresh medium was added with different concentrations of CPI-613 (0 µM, 10 µM, 25 µM, 50 µM) in the presence of either glucose (Glu; 25 mM) or pyruvate (Pyr; 5 mM). 24 hours later ATP amount in cell lysates was determined using the CellTiter-Glo assay. ATP amount in cell lysates in the absence of inhibitor was set as 100%. Results are represented as mean and standard deviation of 6 wells for each condition. Statistical significance was determined by Student's *t*-test with: **$p < 0.005$ and ***$p < 0.0005$.

TCA cycle significantly contributes to ATP production in cells from the line T98G, but also demonstrates that ATP can also be produced by OxPhos in the other cell lines. Comparing this data to the results in the preceding section, this reveals a different response of cells to the supply with nutrients. Cells from the line T98G exhibit much higher amounts of ATP when both glucose and pyruvate are supplied than with either nutrient alone. This indicates that in these cells excessive ATP production by OxPhos also drives glycolytic ATP production - most likely via regeneration of NAD^+, resulting in an overall synergistic effect on total ATP production in these cells.

Amount of ATP and viability of U87 glioblastoma cells in the presence of glucose and pyruvate under the influence of carnosine and CPI-613

The experiments presented in Figure 4 indicated that pyruvate attenuates the inhibitory effect of carnosine on ATP production and viability in cells cultivated in glucose alone. As ATP production from pyruvate requires its entry into the TCA cycle, we asked whether the combined block of glycolysis by carnosine and of pyruvate dehydrogenase by CPI-613 does completely block ATP production in U87 cells. The result of a corresponding experiment is presented in Figure 5. This experiment demonstrates that the combination of carnosine and CPI-613 almost completely blocks ATP production in the presence of either glucose ($1.5 \pm 0.2\%$) or pyruvate alone ($5.9 \pm 5.1\%$). The viability of cells as determined by Calcein AM/PI staining was reduced to $0.5 \pm 0.5\%$ (glucose) and to $2.7 \pm 0.8\%$ (pyruvate) (see Figure 7 and Table 1). CPI-613 alone did only slightly reduce the amount of ATP determined in the presence of glucose ($91.1 \pm 6.5\%$; $p < 0.05$) and viability determined by Calcein AM/PI was $93.8 \pm 3.4\%$ compared to $94.3 \pm 4.6\%$ in the absence of CPI-613. When cells cultivated in pyruvate received CPI-613 alone, the amount of ATP was reduced from $126 \pm 21\%$ to $48 \pm 10\%$ and cell viability determined by Calcein AM/PI was reduced from $98.5 \pm 0.3\%$ to $27.4 \pm 11.2\%$ ($p < 0.02$; Figure 7; Table 1). Therefore, the cells were still able to produce some ATP and were not completely killed during the 24 hours incubation time. Most importantly, although viability was strongly reduced when only glucose or only pyruvate were supplied in the presence of carnosine and CPI-613, viability in the presence of both, glucose and pyruvate, was completely restored ($98.4 \pm 0.8\%$). Correspondingly, ATP production was restored, although significantly lower amounts were detected ($77.1 \pm 5.3\%$; $p < 0.0005$) than in cells cultivated in the presence of glucose and pyruvate without the inhibitors ($112.5 \pm 19.9\%$).
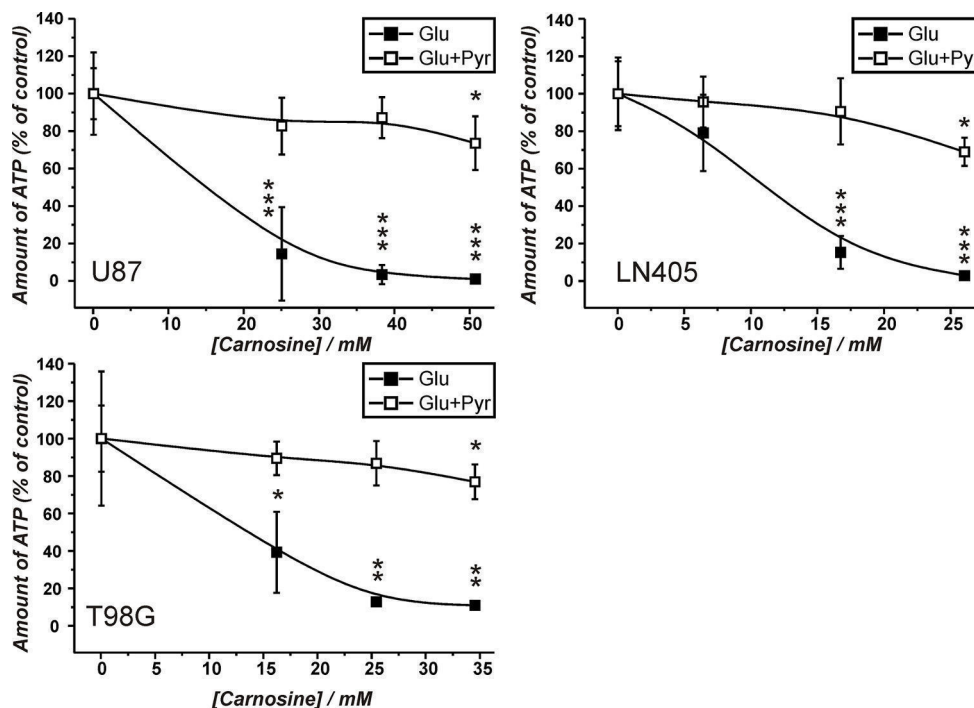

Figure 4: Amount of ATP in cell lysates of the lines U87, T98G and LN405 under the influence of different concentrations of carnosine in the presence of glucose and glucose plus pyruvate. Cells were seeded at a density of 5000 cells per well in 96-well microplates and received medium without glucose, galactose or pyruvate and without FBS and GlutaMax. After 20 hours, fresh medium was added with either glucose (Glu; 25 mM) or a mixture of 25 mM glucose and 5 mM pyruvate (Glu+Pyr) and cell line dependent inhibitory concentrations of carnosine (see Supplementary Data S2). 24 hours later the amount of ATP in cell lysates was determined using the CellTiter-Glo assay. The amount of ATP in the absence of carnosine was set as 100%. Results are represented as mean and standard deviation of 6 wells for each condition. Statistical significance was determined by Student's t-test with: *$p < 0.05$; **$p < 0.005$; ***$p < 0.0005$.

Viability and amount of ATP in U87 glioblastoma cells in the presence of glucose and pyruvate under the influence of carnosine and 2,4-dinitrophenol

The experiments in the previous section revealed that the combination of carnosine and CPI-613 in the presence of pyruvate and glucose does not kill the cells. This observation is in contrast to the notion that pyruvate's attenuation of the inhibitory effect of carnosine is dependent on ATP production from pyruvate via TCA cycle and OxPhos. However, as we observed viable cells in the presence of pyruvate alone and CPI-613 (27.4 ± 11.2%) and also a significant amount of ATP in cell lysates (48 ± 10%) (Figure 5), we decided to block ATP production additionally at the level of OxPhos using 2,4-dinitrophenol (DNP). DNP inhibits mitochondrial ATP production by uncoupling electron transport from phosphorylation [26]. In the experiment in Figure 6 cells from the line U87 were incubated with combinations of carnosine, DNP, glucose and pyruvate. In cells fed with glucose, DNP did not reduce the amount of ATP (122 ± 7.9% compared to 100 ± 9% in cells without the inhibitor). The viability determined by Calcein AM/PI was 97.1 ± 0.7% compared to 94.3 ± 4.6% (without DNP) (Figure 7; Table 1). Cells fed with pyruvate exhibited a strong reduction of ATP when incubated in the presence of DNP (0.5 ± 0.1% compared to cells in the absence of the inhibitor 138.5 ± 9%). The viability determined by Calcein AM/PI was reduced from 98.5 ± 0.3% to 21.1 ± 3% (Figure 7; Table 1). This demonstrates that DNP completely blocks ATP

production from pyruvate, but also shows that a fraction of cells is able to survive at least after 24 hours of exposure to DNP. Therefore, it is tempting to speculate that survival of some cells is independent from ATP production. Cells cultivated in glucose only exhibited a strong reduction of ATP when cultivated in carnosine (0.8 ± 0.2%; Figure 6) as already shown in Figure 5. Cells receiving pyruvate as nutrient exhibited a comparable amount of ATP in the presence of carnosine (95.5 ± 11.1%) as cells cultivated in glucose without it (100 ± 9.1%). As also seen in Figure 5 and Figure 2A, cells receiving pyruvate produced more ATP in the absence of inhibitors than cells cultivated in glucose (138.5 ± 9%). As the addition of carnosine always reduces ATP production in the presence of pyruvate alone, carnosine does obviously also inhibit mitochondrial ATP production, although to a lesser extent than it effects glycolytic ATP production. Most importantly, in the presence of both, pyruvate and glucose, the amount of ATP determined in the presence of carnosine and DNP (103.7 ± 7.0%) was comparable to that of cells grown in glucose without any inhibitor (100 ± 9.1%). In addition, viability determined by Calcein AM/PI was 98.0 ± 1.3% (Figure 7; Table 1). This demonstrates that the attenuation of the anti-neoplastic effect of carnosine by pyruvate is independent from the production of ATP via the TCA cycle and OxPhos.

DISCUSSION

We investigated how the anti-neoplastic effect of carnosine is influenced by the nutritional supply of tumor cells and how glycolysis, the TCA cycle and OxPhos
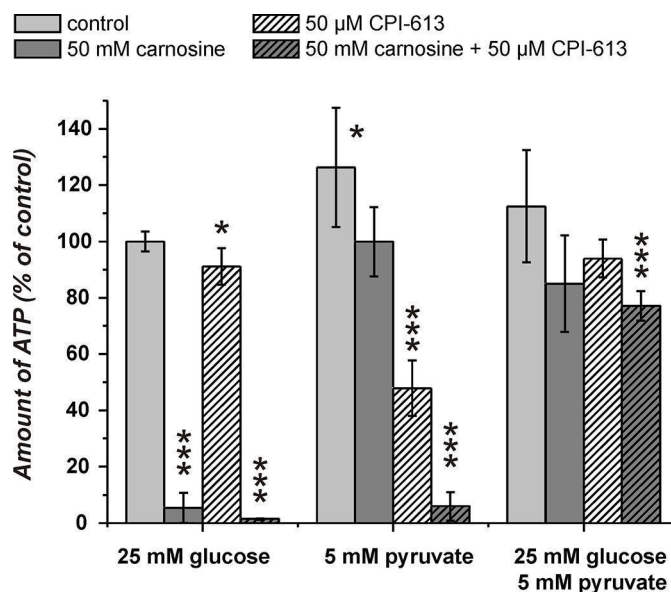

Figure 5: Amount of ATP in cell lysates of the line U87 under the influence of carnosine and CPI-613. Cells from the line U87 were seeded at a density of 5000 cells per well in 96-well microplates and received medium without glucose, galactose or pyruvate and without GlutaMax and FBS for 20 hours. Then, fresh medium was added with 25 mM glucose, 5 mM pyruvate or a combination of both nutrients. In addition, cells received 50 mM carnosine and/or 50 μM CPI-613. 24 hours later the amount of ATP in cell lysates was determined. Results are represented as mean and standard deviation of 6 wells for each condition normalized to cells cultivated in the presence of glucose (set as 100%). Statistical significance was determined by Student's t-test with: *$p < 0.05$; ***$p < 0.0005$.

contribute to tumor cell survival. It was previously shown that pyruvate inhibits the anti-neoplastic effect of carnosine [19]. We were thus interested to study, whether this can also be seen in glioblastoma tumor cells and whether the production of ATP via TCA cycle and OxPhos are responsible for this effect.

The results of the experiments presented in Figure 5 to Figure 7 and in Table 1 are summarized and interpreted in Figure 8. In (A1) of Figure 8 the situation is depicted in which glucose is supplied as the only nutrient and in the absence of inhibitors. In this case the amount of ATP determined in cell lysates is set as 100% and living cells are illustrated by the green color. Adding carnosine (A2) results in a complete loss of ATP production and the cells are dead as shown by Calcein AM/PI staining. In accordance with our previously published data [5] no signs of apoptosis were detected and cells obviously died due to necrosis. Neither CPI-613 (A3) nor DNP (A4) decrease viability in the presence of glucose. Therefore, viability in the presence of glucose is almost independent from mitochondrial ATP production. However, adding CPI-613 to cells cultivated in glucose results in a small loss of ATP (A3 compared to A1), indicating that a small amount of pyruvate produced by glycolysis is used for mitochondrial ATP production. The slightly enhanced production of ATP in the presence of DNP (A4) demonstrates enhanced glycolytic production of ATP, when OxPhos is blocked by DNP. A comparable, recent observation by Bhatt *et al*. describes a rise of glycolytic ATP production in the cerebral glioma cell line BMG-1 and other cells when

they were treated with DNP [27]. The addition of CPI-613 (A5) or DNP (A6) to cells in the presence of glucose and carnosine results in the same loss of ATP and viability as in (A2). When pyruvate is the only nutrient, ATP is even higher than in the presence of glucose alone (B1 compared to A1). Therefore, U87 cells can efficiently use pyruvate for ATP synthesis in the absence of glucose. A significant drop ($p < 0.05$) of ATP is observed when cells cultivated in pyruvate received carnosine (B2 compared to B1 and B5 compared to B3). Hence, carnosine does also inhibit mitochondrial ATP production. This inhibition is less pronounced than that on glycolysis and it is in agreement with recent observations of Shen and co-workers *et al*. These authors showed that carnosine is able to inhibit mitochondrial ATP-linked respiration in gastric cancer cells [1]. In addition, we have previously demonstrated that carnosine enhances the expression of pyruvate dehydrogenase kinase 4 (PDK4) [23], although, in further experiments (which were done in the presence of FBS and GlutaMax) we did not detect a change of pyruvate dehydrogenase activity under the influence of carnosine (unpublished data). Another result is the apparent incomplete inhibition of ATP production by CPI-613 when pyruvate is supplied, but glucose is absent (B3). This observation of the experiments presented in Figure 5 (and repetitions of it) is in contrast to the data presented in Figure 3 in which a concentration of 50 μM CPI-613 severely diminished the amount of ATP. It is tempting to speculate that this variation in the quantitative effect of CPI-613 on ATP is associated with the effect of CPI-613
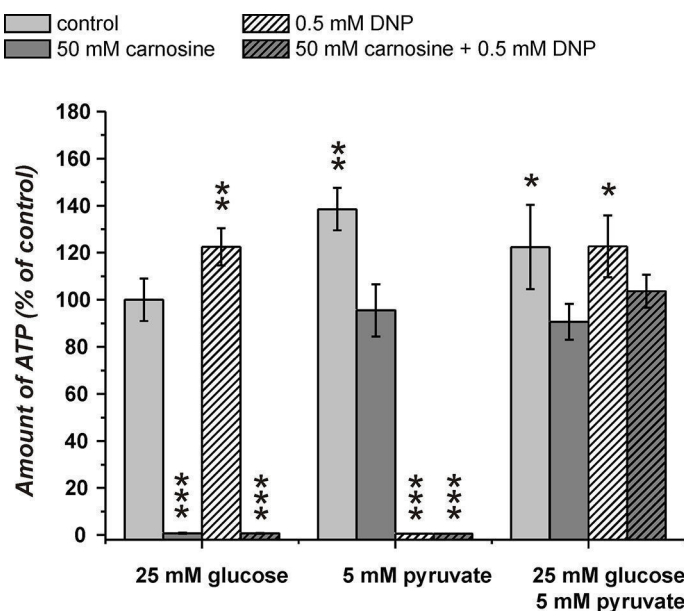

Figure 6: Amount of ATP in cell lysates of the line U87 under the influence of carnosine and 2,4-dinitrophenol (DNP). Cells from the line U87 were seeded at a density of 5000 cells per well in 96-well microplates and received medium without glucose, galactose or pyruvate and without GlutaMax and FBS for 20 hours. Then, fresh medium was added with 25 mM glucose, 5 mM pyruvate or a combination of both nutrients. In addition, cells received 50 mM carnosine and/or 0.5 mM DNP. 24 hours later the amount of ATP in cell lysates was determined. Results are represented as mean and standard deviation of 6 wells for each condition normalized to cells cultivated in the presence of glucose (set as 100%). Statistical significance was determined by Student's *t*-test with: *$p < 0.05$; **$p < 0.005$; ***$p < 0.0005$.

on 2-oxoglutarate dehydrogenase. This would also disrupt mitochondrial metabolism [28], dependent on the current status of the oxidative defense systems of the cell. Moreover, the lipoate derivative CPI-613 could possibly also inhibit other mitochondrial enzyme complexes that require lipoate as coenzyme, e.g. the branched-chained alpha-ketoacid dehydrogenase complex [29]. However, these interpretations are speculative and CPI-613 at a concentration of 50 µM may simply not always completely block the pyruvate dehydrogenase activity. In fact, as demonstrated in the experiments of Zachar *et al.* [25], the IC50 for most of the cell lines tested was in the range between 120 and 280 µM. Despite the fact, their experiments are difficult to compare, as the authors used additional media supplements. In the presence of DNP

(B4) the pyruvate supplied in the medium is not able to contribute to ATP production. Although, almost no ATP was determined in cell lysates (0.58 ± 0.06%; compared to pyruvate without inhibitor), up to 21% of the cells were still alive (Figure 7, yellow color in Figure 8, Table 1). Therefore, a strict correlation between ATP and viability has to be questioned. Nevertheless, full ATP production is important for 100% survival. It also has to be noted that the cells stained by Calcein AM had a severely changed morphology, indicating that they were also dying (data not shown). No cells are stained by Calcein AM in the presence of pyruvate and DNP when carnosine was added (B6 compared to B4). This indicates that carnosine also inhibits other biochemical pathways required for survival even in the absence of ATP production. This supports the
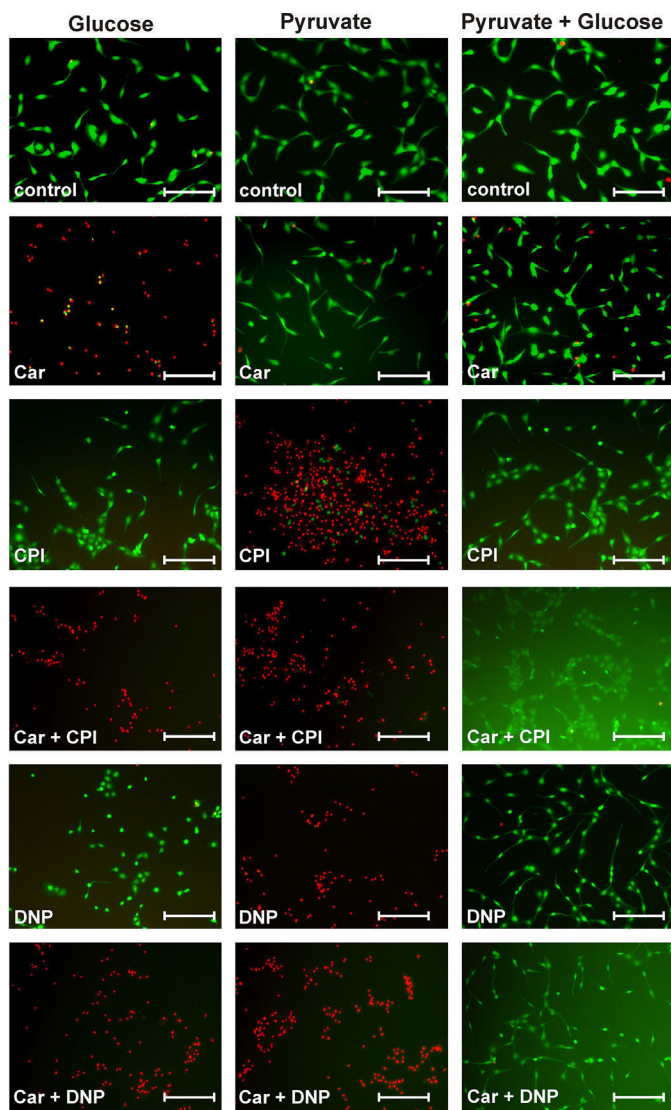

Figure 7: Viability of U87 cells under the influence of carnosine in the presence of glucose, pyruvate, carnosine (Car), 2,4-dinitrophenol (DNP) and CPI-613 (CPI). U87 cells were seeded at a density of 5000 cells per well in 96-well microplates and received medium without glucose, galactose or pyruvate and without FBS and GlutaMax. After 20 hours, fresh medium was added with either glucose (25 mM), pyruvate (5 mM) or both nutrients and in addition cells received carnosine (50 mM), CPI-613 (50 µM) or DNP (0.5 mM) or mixtures of these supplements. After 24 hours living cells were stained using Calcein AM (green) and dead cells were stained using propidium iodide (red). Fluorescence images were captured by microscopy. Scale bars: 200 µm. For quantification see Table 1.

notion that carnosine does in fact have pleiotropic effects [30]. The restoration of viability and ATP production in the experiments (C5) and (C6) whereby glucose and pyruvate are combined, demonstrates that exogenous pyruvate attenuates or even inhibits the effect of carnosine on glycolytic breakdown of glucose. We currently do not know at which step carnosine inhibits the glycolytic breakdown of glucose. This would require a detailed metabolomics study, and corresponding follow-up experiments, e.g. Western Blots, qRT-PCR and enzyme assays. Pyruvate could possibly restore NAD$^+$ which is consumed in the glycolytic step from glyceraldehyde-3-phosphate to 1,3-bisphosphoglycerate. This presupposes that carnosine reduces the availability of NAD$^+$. In that case, the concentrations of glycolytic triose phosphates (glyceraldehyde-3-phosphate and dihydroxyacetone-phosphate) will increase. In turn, the concentration of methylglyoxal will increase, which would result in protein and mitochondrial dysfunction [31]. This can explain the anti-neoplastic effects that cannot solely be attributed to the impairment of ATP production. However, this assumption is in contrast to the observation that carnosine inhibits the
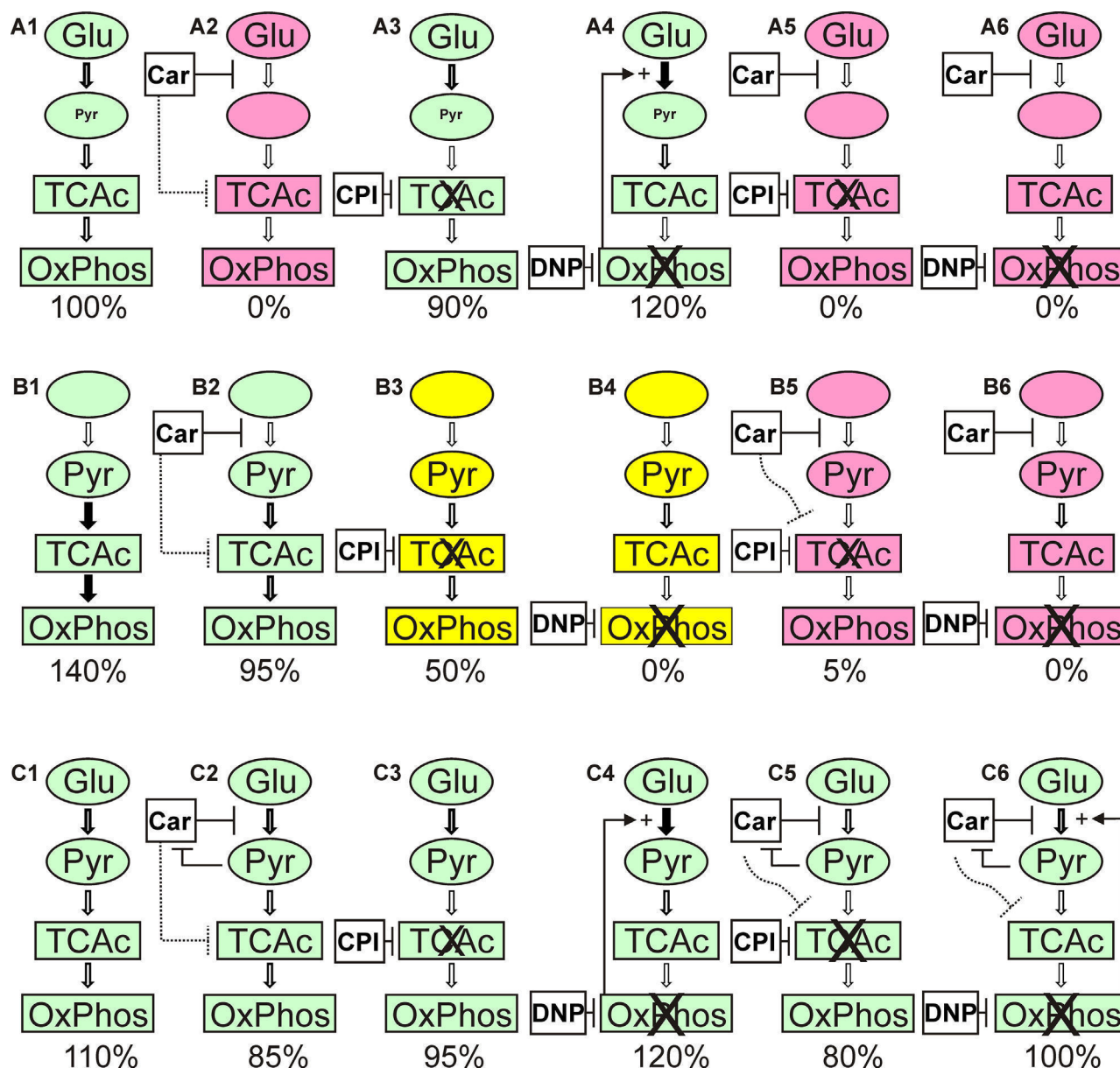

Figure 8: Overview of the results from the experiments presented in Figure 5 to Figure 7 and Table 1. A1 to A6 depict the experiments in the presence of glucose (Glu), B1 to B6 the experiments in the presence of pyruvate (Pyr) and C1 to C6 those with both, glucose and pyruvate. The numbers below denote the amount of ATP determined in cell lysates under each condition (rounded to be presented in intervals of 5). Colors denote: red: cells are dead; green: cells were alive; yellow: viable cells were detectable (20 to 30%; compare Table 1). Car denotes the use of carnosine, CPI denotes the use of CPI-613 and DNP the use of 2,4-dinitrophenol. The thickness of the arrows indicates the estimated flux of metabolites. For further details refer to the text.

deleterious effects accompanied by enhanced production of methylglyoxal [32]. In addition, carnosine's abatement on senescence and increase of life-span in normal cells and healthy organisms argue against the assumption that carnosine has a general effect on the availability of NAD^+ [33]. Hence, the hypothesis that carnosine reduces the availability of NAD^+ will only make sense if the effect is tumor-cell specific. A second possibility is a reduced availability of pyruvate from the glycolytic breakdown of glucose under the influence of carnosine. This will also suppress the regeneration of NAD^+ for ongoing glycolysis. It is known that carnosine does react with aldehydes [34], or as other histidine containing dipeptides, with carbonyl groups in general [35]. Therefore, it may react with one or several metabolites in the glycolytic pathway. However, as pyruvate attenuates the effect of carnosine even at a concentration ten times lower than that of the dipeptide, a competitive inhibition by pyruvate appears to be unlikely. Although the mechanisms by which pyruvate restores tumor cell viability in the presence of carnosine remain unknown, the hypothesis can be excluded that pyruvate inhibits the anti-neoplastic effect of carnosine by increased mitochondrial production of ATP [19].

Our data may appear to diminish the hope that carnosine could be used as an anti-cancer drug. Nevertheless, it should be taken into account that carnosine's effect on glycolysis is one aspect of its anti-neoplastic activity [36]. Results obtained with other cancer models demonstrated that carnosine does also influence signal transduction pathways such as HIF-1alpha [37] or Akt/mTOR/p70S6K [2]. In addition, effects on manganese superoxide dismutase and cyclin B1 expression have been reported [38]. At this point, it should be noted that previous experiments demonstrated that carnosine has long term effects on tumor cell growth *in vitro* [5] and *in vivo* [7] even in the presence of pyruvate and FBS. In conclusion, the results presented bear the challenge to enhance the anti-neoplastic effect of the dipeptide by an inhibition of mechanisms which attenuate its inhibition of glycolysis.

MATERIALS AND METHODS

Reagents

Unless otherwise stated, all chemicals were purchased from Sigma Aldrich (Taufkirchen, Germany) including the carnosine employed in this study (Cat.-Nr.: C9625/ Lot: BCBK4678V).

Long-term cell culture

All cells were propagated in 250 ml culture flasks (Sarstedt AG & Co., Nümbrecht, Germany) using 10 ml of standard culture medium (SCM: DMEM / 4.5 g/l glucose, without pyruvate (Life Technologies, Darmstadt, Germany) supplemented with 10% fetal bovine serum (FBS superior, Biochrom, Berlin, Germany), 2 mM GlutaMax

(Life Technologies) and Penicillin-Streptomycin (Life Technologies)) at 37°C and 5% CO_2 in humidified air in an incubator. The human glioblastoma multiforme (GBM) cell lines T98G and U87 were obtained from ATCC (Manassas, USA) and the line LN405 from the German collection of microorganisms and cell cultures (DSMZ, Braunschweig, Germany). All cells were genotyped (Genolytic GmbH, Leipzig, Germany) and their identity confirmed.

Cell culture experiments

For the experiments, cells were used from culture flasks at 70 to 90% confluency. Cells were first washed with 6 ml of Hanks (without Ca^{2+} / Mg^{2+}: 137 mM NaCl; 5.4 mM KCl; 0.33 mM Na_2HPO_4 × 2 H_2O; 0.44 mM KH_2PO_4; 2 mM Hepes (pH 7.4)) and then detached for 5 min in an incubator at 37°C using 2 ml Accutase (Life Technologies). Then, pre-warmed SCM (4 ml) was added and the cells were transferred to a centrifuge tube and collected by centrifugation (5 min; 125 × g). After aspiration of old medium, fresh SCM was added and $0.5x10^6$ cells were equally spread in 10 ml of SCM into new culture flasks (250 ml). After 72 hours cells were again harvested as described above and seeded at a density of 5000 cells per well in 96-well plates (μClear, Greiner Bio One, Frickenhausen, Germany) in SCM for 3 hours before they received fresh medium without glucose, galactose or pyruvate and without GlutaMax and FBS. Then cells were incubated for 20 or 24 hours (see individual experiment) before they received new medium with the supplements indicated in each experiment.

Cell-based assays

For the determination of the amount of ATP in cell lysates the CellTiter-Glo Assay (CTG), for the determination of NAD(P)H production the CellTiter-Blue Assay (CTB) and for the determination of extracellular lactate dehydrogenase (LDH) activity (measuring loss of membrane integrity due to necrosis) the CytoTox-ONE Assay (all from Promega, Mannheim, Germany) were employed according to the instructions of the manufacturer and as described previously [39]. Briefly, the CellTiter-Glo Assay was performed by adding 100 μl of the CellTiter-Glo Assay reagent to the cells cultivated in 100 μl medium. Cells were lysed within the solution for 10 minutes and then luminescence was recorded using a Mithras LB 940 Multimode Microplate reader (Berthold Technologies, Bad Wildbad, Germany). The CellTiter-Blue assay was started by adding 20 μl of CellTiter-Blue reagent to the cells cultivated in 100 μl of medium. Ninety minutes later fluorescence was recorded at an excitation wavelength of 560 nm and an emission wavelength of 590 nm using a Spectra Max M5 reader (Molecular Devices, Biberach, Germany). At this point it may also be important to note that the presence of test compounds in the medium did not interfere with the assays (data not shown).

Live cell imaging and cell counting

In order to determine viability at the microscopic level viable cells were stained with Calcein AM (Invitrogen, Darmstadt, Germany) and dead cells with propidium iodide (PI). Briefly, a mixture containing 20 µM Calcein AM and 120 µM propidium iodide (5 µl) was added to cells cultivated in 100 µl culture medium in a well of a 96-well plate (µClear black, Greiner Bio One). After an incubation of 10 minutes at 37°C, fluorescence images were captured using a Leica DM IRBE inverted fluorescence microscope (Leica microsystems, Wetzlar, Germany). Cells were counted using ImageJ scripts [40] and cell viability was determined by comparing the total cell number of cells to the number of living cells stained by Calcein AM and dead cells stained with propidium iodide.

Statistical analysis

For the determination of mean and standard deviation as well as statistical significance by student's *t*-test (unpaired two-sample test with unequal variances) of single experiments the algorithms implemented in Excel (Microsoft, Richmond, USA) were used. Data obtained from more than one experiment were processed as followed: Raw data of each independent experiment was normalized by the sum of all corresponding data points [41]. Then, the mean and the standard deviation of all normalized data points for each condition were calculated and statistical significance determined by the algorithms implemented in Excel. For the calculation of inhibitory concentration (IC) data points were fitted to the Boltzmann function to plot a sigmoidal curve using Origin 8 (OriginLab Corporation, Northampton, USA).

CONFLICTS OF INTEREST

The authors declare that they have no potential conflicts of interest.

REFERENCES

1. Shen Y, Yang J, Li J, Shi X, Ouyang L, Tian Y, Lu J. Carnosine inhibits the proliferation of human gastric cancer SGC-7901 cells through both of the mitochondrial respiration and glycolysis pathways. PLoS ONE. 2014; 9:e104632.

2. Zhang Z, Miao L, Wu X, Liu G, Peng Y, Xin X, Jiao B, Kong X. Carnosine Inhibits the Proliferation of Human Gastric Carcinoma Cells by Retarding Akt/mTOR/p70S6K Signaling. J Cancer. 2014; 5:382–389.

3. Iovine B, Iannella ML, Nocella F, Pricolo MR, Baldi MR, Bevilacqua MA. Carnosine inhibits KRas-mediated HCT-116 proliferation by affecting ATP and ROS production. Cancer Lett. 2011; 315:122–128.

4. Mikuła-Pietrasik J, Książek K. L-Carnosine Prevents the Pro-cancerogenic Activity of Senescent Peritoneal Mesothelium Towards Ovarian Cancer Cells. Anticancer Res. 2016; 36:665–671.

5. Renner C, Seyffarth A, Garcia de Arriba S, Meixensberger J, Gebhardt R, Gaunitz F. Carnosine Inhibits Growth of Cells Isolated from Human Glioblastoma Multiforme. Int J Pept Res Ther. 2008; 14:127–135.

6. Nagai K, Suda T. Antineoplastic effects of carnosine and beta-alanine--physiological considerations of its antineoplastic effects. J Physiol Soc Jpn. 1986; 48:741–747.

7. Renner C, Zemitzsch N, Fuchs B, Geiger KD, Hermes M, Hengstler J, Gebhardt R, Meixensberger J, Gaunitz F. Carnosine retards tumor growth *in vivo* in an NIH3T3-HER2/neu mouse model. Mol Cancer. 2010; 9:2.

8. Gaunitz F, Hipkiss AR. Carnosine and cancer: a perspective. Amino Acids. 2012; 43:135–142.

9. Hipkiss AR, Gaunitz F. Inhibition of tumour cell growth by carnosine: some possible mechanisms. Amino Acids. 2014; 46:327–337.

10. Gaunitz F, Oppermann H, Hipkiss AR. Carnosine and Cancer. In: V. R. Preedy (ed.). Imidazole Dipeptides, pp. 372–392. Cambridge. 2015.

11. Renner C, Asperger A, Seyffarth A, Meixensberger J, Gebhardt R, Gaunitz F. Carnosine inhibits ATP production in cells from malignant glioma. Neurol Res. 2010; 32:101–105.

12. Bensinger SJ, Christofk HR. New aspects of the Warburg effect in cancer cell biology. Semin Cell Dev Biol. 2012; 23:352–361.

13. Koppenol WH, Bounds PL, Dang CV. Otto Warburg's contributions to current concepts of cancer metabolism. Nat Rev Cancer. 2011; 11:325–337.

14. Frezza C, Gottlieb E. Mitochondria in cancer: Not just innocent bystanders. Semin Cancer Biol. 2009; 19:4–11.

15. Christofk HR, Vander Heiden MG, Harris MH, Ramanathan A, Gerszten RE, Wei R, Fleming MD, Schreiber SL, Cantley LC. The M2 splice isoform of pyruvate kinase is important for cancer metabolism and tumour growth. Nature. 2008; 452:230–233.

16. Sousa CM, Biancur DE, Wang X, Halbrook CJ, Sherman MH, Zhang L, Kremer D, Hwang RF, Witkiewicz AK, Ying H, Asara JM, Evans RM, Cantley LC et al. Pancreatic stellate cells support tumour metabolism through autophagic alanine secretion. Nature. 2016; 536:479–483.

17. Hay N. Reprogramming glucose metabolism in cancer: can it be exploited for cancer therapy? Nat Rev Cancer. 2016; 16:635–649.

18. Asgari Y, Zabihinpour Z, Salehzadeh-Yazdi A, Schreiber F, Masoudi-Nejad A. Alterations in cancer cell metabolism: the Warburg effect and metabolic adaptation. Genomics. 2015; 105:275–281.

19. Holliday R, McFarland GA. Inhibition of the growth of transformed and neoplastic cells by the dipeptide carnosine. Br J Cancer. 1996; 73:966–971.

20. Ostrom QT, Gittleman H, Fulop J, Liu M, Blanda R, Kromer C, Wolinsky Y, Kruchko C, Barnholtz-Sloan JS. CBTRUS Statistical Report: Primary Brain and Central Nervous System Tumors Diagnosed in the United States in 2008–2012. Neuro-Oncology. 2015; 17 Suppl 4:iv1-iv62.

21. Louis DN, Perry A, Reifenberger G, Deimling A von, Figarella-Branger D, Cavenee WK, Ohgaki H, Wiestler OD, Kleihues P, Ellison DW. The 2016 World Health Organization Classification of Tumors of the Central Nervous System: a summary. Acta Neuropathologica. 2016; 131:803–820.

22. Stupp R, Mason WP, van den Bent,M. J., Weller M, Fisher B, Taphoorn MJB, Belanger K, Brandes AA, Marosi C, Bogdahn U, Curschmann J, Janzer RC, Ludwin SK et al. Radiotherapy plus concomitant and adjuvant temozolomide for glioblastoma. New England Journal of Medicine. 2005; 352:987–996.

23. Letzien U, Oppermann H, Meixensberger J, Gaunitz F. The antineoplastic effect of carnosine is accompanied by induction of PDK4 and can be mimicked by L-histidine. Amino Acids. 2014.

24. Oppermann H, Ding Y, Sharma J, Bernd-Paetz M, Meixensberger J, Gaunitz F, Birkemeyer C. Metabolic response of glioblastoma cells associated with glucose withdrawal and pyruvate substitution as revealed by GC-MS. Nutrition & Metabolism. 2016.

25. Zachar Z, Marecek J, Maturo C, Gupta S, Stuart SD, Howell K, Schauble A, Lem J, Piramzadian A, Karnik S, Lee K, Rodriguez R, Shorr R et al. Non-redox-active lipoate derivates disrupt cancer cell mitochondrial metabolism and are potent anticancer agents *in vivo*. J Mol Med (Berl). 2011; 89:1137–1148.

26. Loomis WF, Lipmann F. Reversible inhibition of the coupling between phosphorylation and oxidation. J Biol Chem. 1948; 173:807.

27. Bhatt AN, Chauhan A, Khanna S, Rai Y, Singh S, Soni R, Kalra N, Dwarakanath BS. Transient elevation of glycolysis confers radio-resistance by facilitating DNA repair in cells. BMC Cancer. 2015; 15:335.

28. Stuart SD, Schauble A, Gupta S, Kennedy AD, Keppler BR, Bingham PM, Zachar Z. A strategically designed small molecule attacks alpha-ketoglutarate dehydrogenase in tumor cells through a redox process. Cancer Metab. 2014; 2:4.

29. Fujiwara K, Takeuchi S, Okamura-Ikeda K, Motokawa Y. Purification, characterization, and cDNA cloning of lipoate-activating enzyme from bovine liver. J Biol Chem. 2001; 276:28819–28823.

30. Boldyrev AA, Aldini G, Derave W. Physiology and pathophysiology of carnosine. Physiol Rev. 2013; 93: 1803–1845.

31. Hipkiss AR. Aging, Proteotoxicity, Mitochondria, Glycation, NAD and Carnosine: Possible Inter-Relationships and Resolution of the Oxygen Paradox. Front Aging Neurosci. 2010; 2:10.

32. Hipkiss AR, Chana H. Carnosine protects proteins against methylglyoxal-mediated modifications. Biochem Biophys Res Commun. 1998; 248:28–32.

33. Hipkiss AR. NAD(+) and metabolic regulation of age-related proteoxicity: A possible role for methylglyoxal? Exp Gerontol. 2010; 45:395–399.

34. Xie Z, Baba SP, Sweeney BR, Barski OA. Detoxification of aldehydes by histidine-containing dipeptides: From chemistry to clinical implications. Enzymology and Molecular Biology of Carbonyl Metabolism 16. 2013; 202:288–297.

35. Vistoli G, Colzani M, Mazzolari A, Maddis DD, Grazioso G, Pedretti A, Carini M, Aldini G. Computational approaches in the rational design of improved carbonyl quenchers: focus on histidine containing dipeptides. Future Med Chem. 2016; 8:1721–1737.

36. Hipkiss AR, Gaunitz F. Inhibition of tumour cell growth by carnosine: some possible mechanisms. Amino Acids. 2013.

37. Iovine B, Guardia F, Irace C, Bevilacqua MA. l-carnosine dipeptide overcomes acquired resistance to 5-fluorouracil in HT29 human colon cancer cells via downregulation of HIF1-alpha and induction of apoptosis. Biochimie. 2016; 127:196–204.

38. Rybakova YS, Kalen AL, Eckers JC, Fedorova TN, Goswami PC, Sarsour EH. Increased manganese superoxide dismutase and cyclin B1 expression in carnosine-induced inhibition of glioblastoma cell proliferation. Biomed Khim. 2015; 61:510–518.

39. Gaunitz F, Heise K. HTS compatible assay for antioxidative agents using primary cultured hepatocytes. Assay.Drug Dev. Technol. 2003; 1:469–477.

40. Schneider CA, Rasband WS, Eliceiri KW. NIH Image to ImageJ: 25 years of image analysis. Nat Methods. 2012; 9:671–675.

41. Degasperi A, Birtwistle MR, Volinsky N, Rauch J, Kolch W, Kholodenko BN. Evaluating strategies to normalise biological replicates of Western blot data. PLoS ONE. 2014; 9:e87293.

In summary, we confirmed the hypothesis that carnosine inhibits glycolysis, possibly by affecting one or more steps between the breakdown of glucose to pyruvate. Furthermore, we showed that the attenuation of the anti-neoplastic effect of carnosine by pyruvate is not performed by switching from aerobe glycolysis to oxidative phosphorylation for ATP production.

In order to get a more detailed view into the mechanisms responsible for the effect of carnosine on glycolysis further experiments were performed. As Hipkiss and co-workers demonstrated that carnosine prevents protein glycation induced by DHAP (Hipkiss et al. 1995) and as the dipeptide is in general able to react with ketones (Hipkiss 2000), it was suggested that the depletion of DHAP by carnosine could be responsible for its effect on glycolytic ATP production (Boldyrev et al. 2013; Holliday and McFarland 2000). In our next study (Oppermann et al. 2019d) we therefore analysed the influence of carnosine on the abundances of glycolytic intermediates and the corresponding connected metabolic pathways such as the PPP and the TCA cycle (see Figure 3) in three glioblastoma cell lines. To do that, we employed the GC-MS method previously used by us to investigate the central carbon metabolism of glioblastoma cells (Oppermann et al. 2016a). In addition, we used mass spectrometry to identify possible reaction products of metabolites and carnosine and we analysed whether we could also detect a direct influence on OxPhos by the dipeptide by measuring the oxygen consumption rate.

ORIGINAL ARTICLE

WILEY

Non-enzymatic reaction of carnosine and glyceraldehyde-3-phosphate accompanies metabolic changes of the pentose phosphate pathway

Henry Oppermann[1] (iD) | Claudia Birkemeyer[2] (iD) | Jürgen Meixensberger[1] | Frank Gaunitz[1] (iD)

[1]Klinik und Poliklinik für Neurochirurgie, Universitätsklinikum Leipzig AöR, Leipzig, Germany

[2]Institut für Analytische Chemie, Universität Leipzig, Leipzig, Germany

Correspondence
Henry Oppermann, Klinik und Poliklinik für Neurochirurgie, Universitätsklinikum Leipzig, Forschungslabore, Liebigstraße 19, 04103 Leipzig, Germany.
Email: henry.oppermann@medizin.uni-leipzig.de

Abstract

Objectives: Carnosine (β-alanyl-L-histidine) is a naturally occurring dipeptide that selectively inhibits cancer cell growth, possibly by influencing glucose metabolism. As its precise mode of action and its primary targets are unknown, we analysed carnosine's effect on metabolites and pathways in glioblastoma cells.

Materials and methods: Glioblastoma cells, U87, T98G and LN229, were treated with carnosine, and metabolites were analysed by gas chromatography coupled with mass spectrometry. Furthermore, mitochondrial ATP production was determined by extracellular flux analysis and reaction products of carnosine were investigated using mass spectrometry.

Results: Carnosine decreased the intracellular abundance of several metabolites indicating a reduced activity of the pentose phosphate pathway, the malate-aspartate shuttle and the glycerol phosphate shuttle. Mitochondrial respiration was reduced in U87 and T98G but not in LN229 cells, independent of whether glucose or pyruvate was used as substrate. Finally, we demonstrate non-enzymatic reaction of carnosine with dihydroxyacetone phosphate and glyceraldehyde-3-phosphate. However, glycolytic flux from glucose to L-lactate appeared not to be affected by the reaction of carnosine with the metabolites.

Conclusions: Carnosine reacts non-enzymatically with glycolytic intermediates reducing the activity of the pentose phosphate pathway which is required for cell proliferation. Although the activity of the malate-aspartate and the glycerol phosphate shuttle appear to be affected, reduced mitochondrial ATP production under the influence of the dipeptide is cell-specific and appears to be independent of the effect on the shuttles.

1 | INTRODUCTION

In 1900, Gulewitsch and Amiradžibi characterized the first naturally occurring dipeptide carnosine (β-alanyl-L-histidine), which was isolated from Liebig's meat extract.[1] In human skeletal muscle, carnosine reaches a median concentration of about 20.0 ± 4.7 mmol per kg dry weight.[2] Albeit human brain tissue contains more homocarnosine (0.16 mmol per kg dry weight[3]) than carnosine, the latter

is found with higher concentrations (2.2 mmol per kg dry weight[4]) in the olfactory bulb. In the human body, carnosine levels are controlled by three genes. Human serum carnosinase (CNDP1) and cytosolic non-specific dipeptidase (CNDP2) degrade the dipeptide, whereas carnosine synthase 1 (CARNS1), which is highly expressed in skeletal muscle, catalyses the formation of carnosine from β-alanine and L-histidine.[5] Surprisingly, although the dipeptide is known since more than 100 years, its physiological role has not completely been resolved. Among the physiological functions described are pH-buffering, chelation of heavy metal ions, scavenging of reactive oxygen species, protection from advanced glycation end-products and protection from lipid peroxidation-related cell damage (for a comprehensive review see Boldyrev et al[6]). In 1986, Nagai and Suda demonstrated that carnosine aside from "normal" physiological functions inhibits tumour growth in a mouse in vivo model.[7] We and other groups confirmed this anti-neoplastic effect using different types of cancer models, including glioblastoma, in vivo[8,9] and in vitro.[10-13] Since the anti-neoplastic effect has been studied in more detail, a number of possibly involved signalling pathways have been suggested. Some reports point towards an inhibition of Akt phosphorylation [12,14] and HIF-1α signalling,[10] and G1 and G2/M cell cycle arrest has been detected.[15,16] Furthermore, we and others reported that carnosine inhibits glucose-dependent ATP production in glioblastoma cells.[11,17] However, the mechanisms responsible for carnosine's anti-neoplastic effect are far from being understood. Additionally, a primary target has not been identified which especially pertains to carnosine's effect on glucose metabolism. Here, we analysed the metabolic profiles of tumour cells treated with or without carnosine in order to reveal whether primary targets of the dipeptide can be identified.

We decided to use glioblastoma cells in our study as this is the most frequent malignant tumour of the human brain[18] with an incident of 3.21 new cases per 100 000 inhabitants in the United States. Under standard therapy consisting of maximal safe resection of the tumour, radiotherapy and adjuvant chemotherapy with temozolomide, median survival of patients is only 12-15 months.[19] Thus, there is an urgent need for additional therapeutic options to treat this highly malignant tumour of the central nervous system. Understanding the mechanisms by which carnosine exerts its anti-neoplastic effect could well pave the way for the development of new therapeutic options.

2 | MATERIALS AND METHODS

2.1 | Chemicals and reagents

If not stated otherwise, all chemicals were purchased from Sigma-Aldrich. Carnosine was kindly provided by Flamma S.p.A.

2.2 | Cell culture

U87, T98G and LN229 cells were originally obtained from the ATCC and cultured in T-75 culture flasks (Sarstedt AG & Co.) in DMEM/25 mM glucose, without pyruvate (Thermo Fisher Scientific), supplemented with 10% foetal bovine serum (FBS superior, Biochrom), 2 mM L-alanyl-L-glutamine and antibiotics (Thermo Fisher Scientific) (further designated as "culture medium") at 37°C and 5% CO_2 in humidified air in an incubator. In order to confirm identity over long culture periods, cells were genotyped by STR analysis at the Genolytic GmbH using a PowerPlex® 21 System (Promega) and cells were confirmed as the U87MG cell line from the ATCC.[20]

2.3 | Growth rate determination

About 150 000 cells were seeded in culture medium (5 mL) in nine T-25 culture flasks (Sarstedt). After 24 hours of incubation, cells in three flasks were detached using StemPro Accutase (Thermo Fisher Scientific) and cells were counted. Then, remaining cells were washed once with Hank's balanced salt solution (HBSS; 2 mL; 137 mM NaCl, 5.4 mM HCl, 0.41 mM $MgSO_4$, 0.49 mM $MgCl_2$, 0.126 mM $CaCl_2$, 0.33 mM Na_2HPO_4, 0.44 mM KH_2PO_4, 2 mM HEPES, pH 7.4), followed by an incubation time of 72 hours in DMEM (1 mL) containing 25 mM glucose, 2 mM l-alanyl-l-glutamine, N2 supplement (further designated DMEM N2) and supplemented with or without 50 mM carnosine. Then, cells were detached and counted, and the doubling time was calculated.

2.4 | Determination of L-lactate production rate

About 10^6 cells were seeded in culture medium (2 mL) per well into 6-well plates. After 24 hours of incubation, cells were washed once with HBSS (1 mL) and then further incubated with DMEM N2 and supplemented with or without 50 mM carnosine. After 0, 3, 6, 12, 24 and 32 hours, medium (5 µL) was collected and stored at −80°C until further use. L-lactate was determined as described before.[21] Absolute amounts of L-lactate were calculated using a standard curve, and L-lactate production rate was determined by calculating the L-lactate production between three and six hours of incubation. In order to validate the significance of the data obtained, repeated measures one-way ANOVA was performed using all time points.

2.5 | Determination of glucose uptake rate

A total of 10 000 cells were seeded in culture medium (200 µL) in 96-well plates (µClear, Greiner Bio-One). After 24 hours of incubation, cells were washed once with HBSS (200 µL) and then further incubated with DMEM N2 and supplemented with or without 50 mM carnosine for 6 hours. Then, DMEM (30 µL) containing Hoechst 33 342 (10 ng/mL; Thermo Fisher Scientific) was added to each well and cells were counted using a Celigo Imaging Cytometer (Nexcelom Bioscience LLC) after an incubation for 30 minutes at 37°C. Afterwards, cells were washed once with HBSS (100 µL) and further incubated in the presence of 1 mM 2-desoxy-D-glucose for 10 minutes. Formed 2-desoxy-D-glucose-6-phosphate was determined using the glucose uptake Glo assay (Promega) according to the manufactures recommendations.

2.6 | Metabolic profiling via GC-MS

Metabolic profiling was performed as described previously.[21] Briefly, 10^6 cells were seeded in culture medium (2 mL) per well into 6-well plates. After 24 hours of incubation, cells were washed once with HBSS (1 mL) and then further incubated with DMEM N2 (1 mL), supplemented with 0, 12.5, 25 or 50 mM carnosine. After incubation (see individual experiments for details), cell supernatants (10 µL) were collected from each well and immediately frozen at –80°C until further use. For the determination of intracellular metabolites, cells were placed on ice and briefly washed with ice-cold HBSS. Immediately after washing, ice-cold methanol (1 mL) was added to each well and metabolites were extracted for 24 hours on an orbital shaker at 8°C. Then, extracts were collected and wells were rinsed once with methanol. Afterwards, samples were evaporated to dryness using a speed vac (Maxi-Dry Lyo, Heto-Holten) and stored at –80°C until further use. Derivatization, gas chromatography coupled with mass spectrometry (GC-MS) analysis and data evaluation were performed as described before.[21,22] If not stated otherwise, the abundance of a metabolite is defined by the peak area determined from the selected ion chromatogram of an experiment normalized to total cellular protein (µg).

2.7 | Quantification of glyceraldehyde-3-phosphate and dihydroxyacetone phosphate

In order to investigate a possible reaction of carnosine with glyceraldehyde-3-phosphate (GA3P) and dihydroxyacetone phosphate (DHAP), GA3P (625 µM) or DHAP (625 µM) was incubated at 37°C for 4 hours in the presence of 0, 0.625, 1.25, 6.25 or 62.5 mM carnosine in triethanolamine buffer (50 mM triethanolamine; 5 mM $MgCl_2$; pH 7.6; total volume: 75 µL). Then, the amounts of GA3P or DHAP were quantified according to Bergmeyer.[23] Briefly, 1.5 µL of NADH solution (20 mM) was added to each reaction and the initial extinction at 340 nm was determined. Afterwards, enzyme mix (3.5 µL) was added to detect GA3P (1 U/µL triosephosphate isomerase; 0.085 U/µL glycerol-3-phosphate dehydrogenase diluted in triethanolamine buffer) or DHAP (0.085 U/µL glycerol-3-phosphate dehydrogenase, diluted in triethanolamine buffer). After an incubation of 30 minutes at 37°C, extinction at 340 nm was determined and the absolute amounts of GA3P and DHAP were calculated using a standard curve.

2.8 | MS-based analysis of carnosine reaction products

In order to identify a possible reaction product of carnosine and GA3P, GA3P (7.5 mM) was incubated in the presence or absence of carnosine (7.5 mM) in NH_4^+/CH_3COO^- buffer (5 mM, pH 7.6) for 4 hours at 37°C. Then, the reaction mixture was diluted 1:12.5 in 30% acetonitrile/H_2O and analysed by flow injection analysis on an ESI-TOF micrOTOF (Bruker Daltonik) in positive mode (negative mode for GA3P detection) with an Agilent

1100 AS autosampler and otofControl 3.4 and HyStar 3.2-LC/MS. Injection was performed with the following parameters: nebulizer (26.1 psi), dry gas flow (6 L/min), dry gas temperature (220°C), injection volume (5 µL), flow rate (0.1 mL/min) and eluent (methanol containing 0.1% formic acid). Mass selective detector was used with the following settings: mass range m/z 50-1500, capillary exit 100 V, skimmer 1 50 V, hexapole 1 23 V, hexapole RF 70 Vpp, skimmer 2 23 V, lens 1 transfer 70 µs and lens 1 pre-pulse storage 8 µs.

2.9 | Determination of oxygen consumption rate (OCR) and extracellular acidification rates (ECAR)

For the determination of the OCR and the ECAR, 10 000 cells were seeded in 80 µL of culture medium in an XF96 cell culture microplate (Seahorse Bioscience). After 19 hours, cells were washed once with HBSS (1 mL) and then further incubated with DMEM (80 µL) containing 25 mM glucose, 2 mM L-alanyl-L-glutamine, N2 supplement and 0 or 50 mM carnosine. After additional 6 hours of incubation, cells were washed twice with HBSS, followed by 1 h incubation at 37°C in 180 µL of Seahorse XF DMEM containing 25 mM glucose and 2 mM L-alanyl-L-glutamine and 0 or 50 mM carnosine, or 180 µL HBSS containing 25 mM glucose or 5 mM pyruvate and supplemented with 0 or 50 mM carnosine. Then, Seahorse XF Cell Mito Stress Test was performed using an XF96 Extracellular Flux Analyzer according to the manufacturer. Briefly, after baseline determination, OCR was determined after the sequential addition of oligomycin A, FCCP and rotenone/antimycin A (each 1 µM). After the final measurement, Seahorse XF DMEM (30 µL) containing Hoechst 33342 (10 ng/mL) was added to each well and cells were counted using a Celigo Imaging Cytometer after an incubation of 30 minutes at 37°C. Data were analysed using the Seahorse Wave Desktop Software; OCR is reported as unit nanomole per minute and 10^6 cells, and ECAR is reported as unit mpH per minute and 10^3 cells.

2.10 | Statistical analysis

Statistical analysis was carried out using SPSS (IBM; Version: 24.0.0.2 64-bit). False discovery rate (FDR) was calculated according to Benjamini and Hochberg.[24] For pairwise comparisons, a t test was performed. For multiple comparisons, a one-way ANOVA with the Games-Howell post hoc test was used. Principal component analysis (data were normalized to untreated control and auto-scaled) and metabolite pathway analysis (settings: Over Representation Analysis: Hypergeometric Test; Pathway Topology Analysis: Relative-betweenness Centrality; Pathway Database: Homo sapiens The Small Molecule Pathway Database) were performed using MetaboAnalyst.[25] If not stated otherwise, experiments were carried out in 6-tuplicate (independent experiments) and data are presented as mean ± standard deviation. Non-overlapping confidence intervals (CI 95%), P-value < .05 or FDR < 0.05 were presumed to be statistically significant.

3 | RESULTS

3.1 | Carnosine affects metabolic pathways connected to glycolysis

Previous studies indicated that carnosine affects cancer cell metabolism by influencing the glycolytic pathway.[11,26] As neither its mode of action nor targets of carnosine were known, we employed a targeted method using GC-MS to study metabolites and pathways connected to glycolysis. Therefore, U87 glioblastoma cells were treated with FBS-free medium containing different concentrations of carnosine (0, 12.5, 25 and 50 mM), followed by metabolite extraction and GC-MS analysis after 6 hours of incubation. First, we asked whether the dipeptide has a general effect on cancer cell metabolism. Performing a principal component analysis (Figure 1A), we observed a significantly different metabolic profile already at a concentration of 12.5 mM carnosine. Increasing its concentrations for treatment resulted in an even better separation compared to the control cells, but confidence intervals of scores between cells treated with different concentrations of carnosine overlap, indicating a similarity between metabolic profiles under carnosine treatment. In order to distinguish between cell-specific and general effects of the dipeptide, we also analysed intra- and extracellular metabolites in the glioblastoma cell lines T98G and LN229 treated with 50 mM carnosine for 6 hours. Similar to U87 cells, treatment of T98G and LN229 cells resulted in a clear separation in principal component analysis (Figure 1B,C). Next, we investigated which metabolic pathways are affected by the dipeptide using MetaboAnalyst. Therefore, abundances of intra- and extracellular metabolites of cells treated with 0 and 50 mM carnosine were compared by using a t test (for each cell line individually) and metabolites whose abundances exhibited an FDR < 0.05 were subjected to a pathway analysis (Figure 1D).

The metabolite set enrichment analysis revealed effects on several pathways, such as glycine and serine metabolism and lysine degradation with different probability among the cell lines. More important, four pathways, namely pentose phosphate pathway (PPP), malate-aspartate shuttle, glycerol phosphate shuttle and Warburg effect (summarizes glycolysis, PPP and citric acid cycle), were significantly ($P < .05$) enriched in all three cell lines after carnosine treatment. The relative intracellular abundances of the detected metabolites of the corresponding pathways are shown in Figure 1F (for the complete results of the metabolic profiling see Figure S1).

The influence of carnosine on the PPP is highly interesting, as this pathway plays a critical role for proliferation, providing 5-phosphoribosyl diphosphate for DNA and RNA biosynthesis.[27] In accordance, treatment with 50 mM carnosine significantly increased the doubling time of U87, T98G and LN229 glioblastoma cells (Figure 1E).

In addition, the influence of carnosine on the glycerol phosphate shuttle and the malate-aspartate shuttle suggests an inhibitory effect of carnosine on cellular redox homeostasis, as the malate-aspartate shuttle contributes ~20% to the total respiratory rate, and its inhibition leads to reduced production of glutamate from glucose.[28]
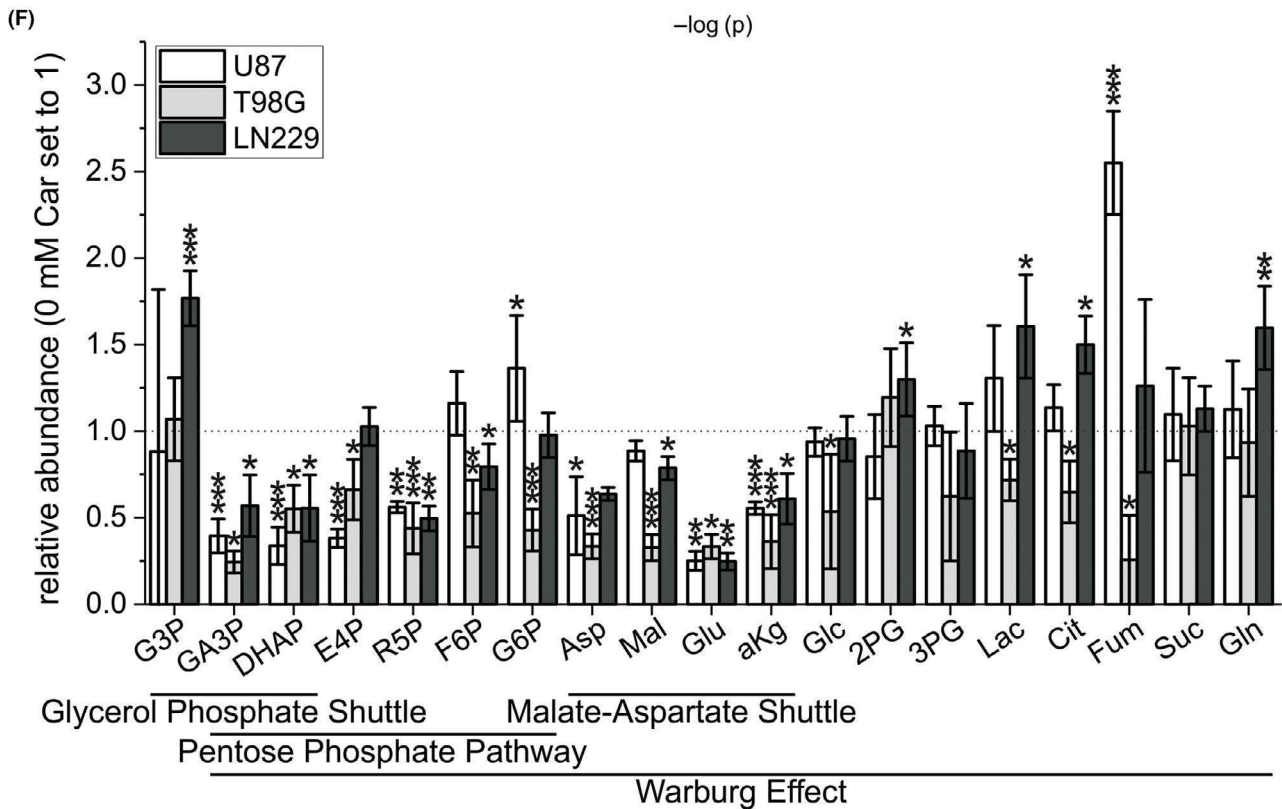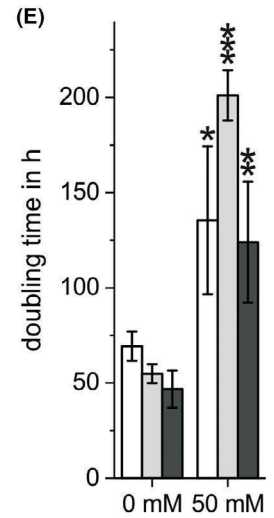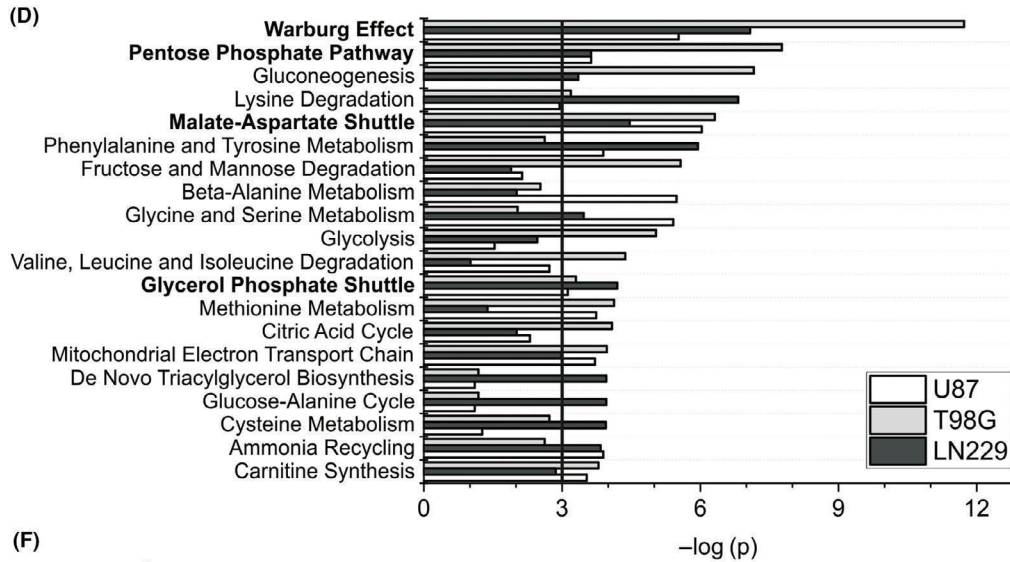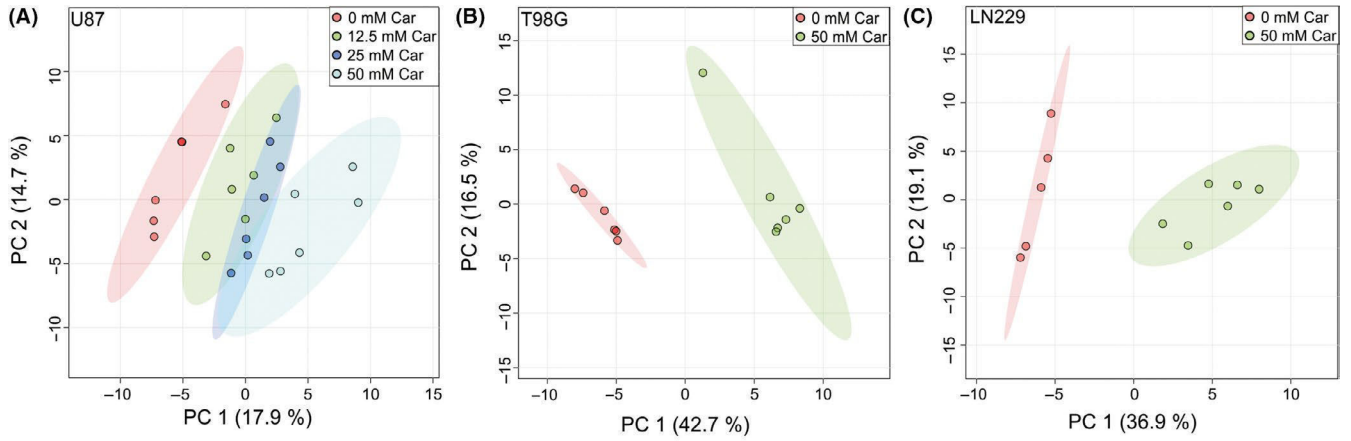
3.2 | Carnosine inhibits mitochondrial respiration independent of the malate-aspartate and the glycerol phosphate shuttle

Our results suggest an inhibitory effect of carnosine on the glycerol phosphate shuttle and the malate-aspartate shuttle which are required for mitochondrial ATP production. Hence, we investigated the influence of carnosine on mitochondrial respiration using a Seahorse XF analyser. In this experiment (Figure 2A,C,E; see also Figure S2), treatment with 50 mM carnosine significantly reduced the ATP-linked oxygen consumption rate (OCR) of U87 and T98G cells but not that of LN229 cells (assayed in DMEM containing 25 mM glucose and 2 mM L-alanyl-L-glutamine). Although reduced ATP-linked OCR in U87 and T98G is in agreement with the assumption that it is caused by the dipeptide's influence on the aforementioned shuttles, the observation made in LN229 argues against this idea. Therefore, we determined the OCR in HBSS with pyruvate as the only substrate, as mitochondrial ATP production from pyruvate is independent of the malate-aspartate shuttle and the glycerol phosphate shuttle.[29] As seen in Figure 2B,D,F, ATP-linked OCR was significantly higher in the presence of 5 mM pyruvate than in the presence of 25 mM glucose in all three cell lines. More important, we also observed reduced ATP-linked OCR under the influence of pyruvate in U87 and T98G but not in LN229 (for the complete analysis of data obtained from the Seahorse experiments see Figure S3). Therefore, we conclude that carnosine's impact on mitochondrial respiration is cell-specific and not necessarily dependent on its influence on the shuttle systems.

3.3 | Glucose consumption and L-lactate production

In view of the observation that the abundances of DHAP and GA3P (Figure 1F) are reduced under the influence of the

FIGURE 1 Impact of carnosine on glioblastoma cell metabolism. Principal component analysis of the metabolic profiles obtained from (A) U87 cells treated for 6 h with 0 mM (red), 12.5 mM (green), 25 mM (blue) or 50 mM (cyan) carnosine (Car) and (B) T98G and (C) LN229 cells treated for 6 h with 0 mM (red), 50 mM (green) Car. D, Pathway analysis using metabolites whose abundances were significantly (FDR < 0.05) changed by 50 mM Car. Bold line indicates a P-value = .05. E, Doubling time of U87, T98G and LN229 cells treated with or without 50 mM Car (n = 3). F, Significantly, changed abundances of metabolites which belong to the metabolic pathways shown in (D). Data are presented as fold-change compared to 0 mM Car (n = 6). 2PG, 2-phosphoglycerate; 3PG, 3-phosphoglycerate; aKg, α-ketoglutarate; Asp, aspartate; Cit, citrate; DHAP, dihydroxyacetone phosphate; E4P, erythrose-4-phosphate; F6P, fructose-6-phosphate; Fum, fumarate; G3P, glycerol-3-phosphate; G6P, glucose-6-phosphate; GA3P, glyceraldehyde-3-phosphate; Glc, glucose; Gln, glutamine; Glu, glutamate; Lac, lactate; Mal, malate; R5P, ribose-5-phosphate; Suc, succinate. Level of significance is indicated as: ***$P < .0005$; **$P < .005$; *$P < .05$ vs. 0 mM Car
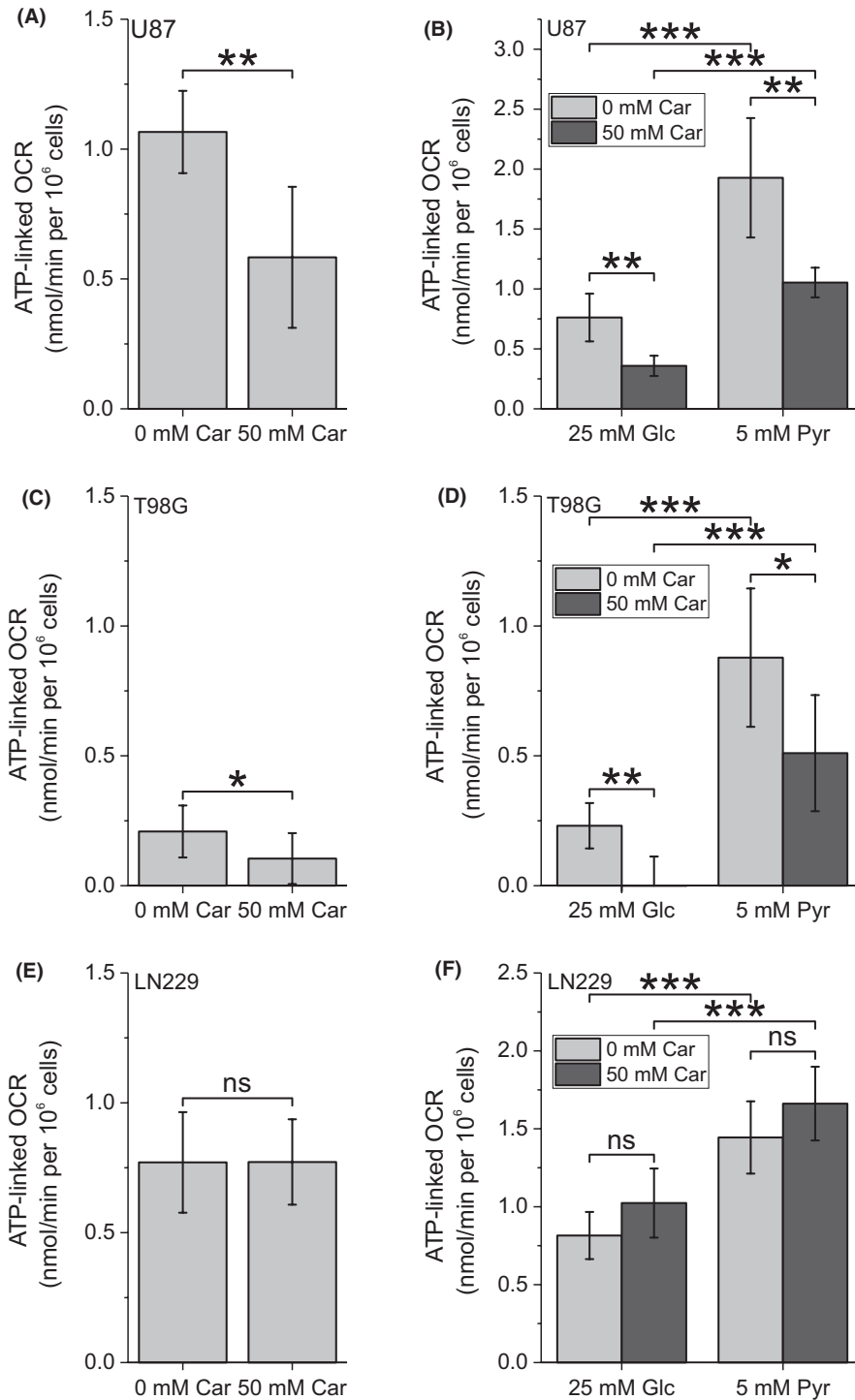
FIGURE 2 Carnosine inhibits mitochondrial ATP production in U87 and T98G cells. Determination of the ATP-linked oxygen consumption rate (OCR) in (A) U87, (C) T98G or (E) LN229 cells treated with or without 50 mM carnosine (Car) for 6 h in the presence of DMEM with 25 mM glucose (Glc) and 2 mM L-alanyl-L-glutamine (Ala-Gln). Determination of the ATP-linked oxygen consumption rate (OCR) in (B) U87, (D) T98G or (F) LN229 cells in HBSS containing 25 mM Glc or 5 mM pyruvate (Pyr) as the only energy source after 6 h treatment with 0 or 50 mM Car (n = 6-10). Level of significance is indicated as: ***$P < .0005$; **$P < .005$; *$P < .05$; ns: $P > .05$

dipeptide, we wondered whether the flux from glucose to L-lactate is also affected. Therefore, we determined glucose uptake rate (Figure 3A) and L-lactate production rate (Figure 3B) under the influence of 50 mM carnosine. As can be seen in Figure 3A,B, uptake of 2-desoxy-D-glucose was significantly reduced only in LN229 cells and L-lactate production significantly reduced only in T98G cells (repeated measures one-way ANOVA over all time points: $P = .065$, .0026 and .055 for U87, T98G and LN229, respectively).

3.4 | Carnosine reduces the intracellular abundance of GA3P by a direct reaction with the metabolite

Next, we investigated whether reaction of carnosine with DHAP and GA3P may be responsible for their decreased abundance in the presence of the dipeptide. Therefore, both triose phosphates were incubated in vitro in the presence of the dipeptide (Figure 4A). We observed that equimolar concentrations of carnosine resulted

FIGURE 3 Influence of carnosine on glucose uptake and L-lactate production. A, Cells were treated with or without 50 mM carnosine (Car) for 6 h. Then, 2-desoxy-D-glucose (2DG) uptake was determined as a measure for the glucose uptake rate (n = 6). B, Cells were treated with or without 50 mM Car and extracellular L-lactate was determined after 3 and 6 h to calculate L-lactate production rate (n = 6). Level of significance is indicated as: ***$P < .0005$; **$P < .005$; ns: $P > .05$
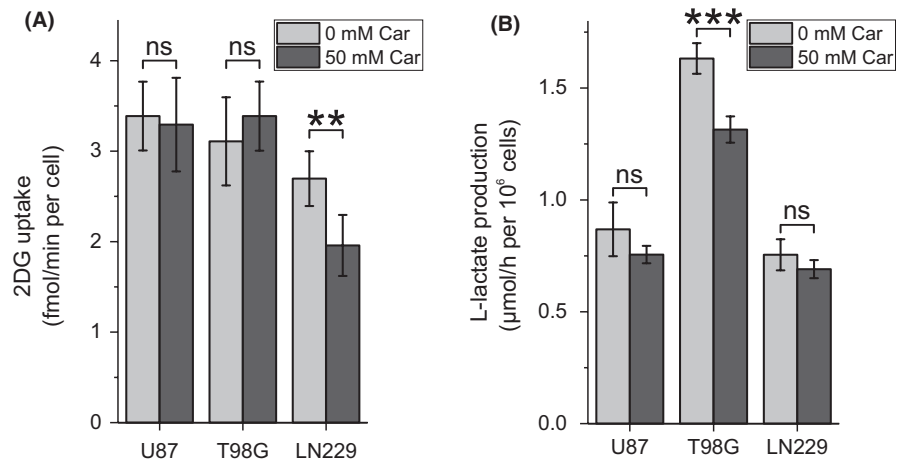
in a 1.3-fold reduction of the GA3P concentration, and a ten-fold higher concentration of the dipeptide resulted in a 36.5-fold reduction of GA3P. We also observed a reduced concentration of DHAP in the presence of carnosine, but a 1.1-fold reduction of DHAP required a ten-fold molar excess of carnosine. This indicates that a non-enzymatic reaction of carnosine with GA3P is responsible for the reduced abundance of the triose phosphates. To confirm a reaction of carnosine with GA3P, mass spectrometry was performed which detected two peaks with a mass of 379.1011 and 401.0829 (Figure 4D,E) referring to a reaction product of GA3P and carnosine ionized with H^{+} or Na^{+} (calculated mass: 379.1013 and 401.0833, respectively). Interestingly, we also detected the reaction product of methylglyoxal (MGO) and carnosine (Figure 4F,G), which was identified by the exact mass of 281.1264 (H^{+} ionization; calculated mass: 281.1244) and 303.1036 (Na^{+} ionization; calculated mass: 303.1064).

4 | DISCUSSION

The naturally occurring dipeptide carnosine reduces tumour growth in vivo[8,9] and in vitro.[10-13] However, as pointed out in the introduction, neither the exact mechanisms behind this observation nor the primary targets of carnosine have been identified. Using mass spectrometry, we detected that carnosine non-enzymatically reacts with GA3P in vitro similar to its previously described reaction with methylglyoxal.[30] As we also see reduced intracellular abundances of GA3P and DHAP in cultured cells, we presume this reaction to be responsible for the reduced abundances of these triose phosphates. Surprisingly, the reduced abundance of these metabolites was not unequivocally accompanied by a decreased glucose uptake rate or by a decreased lactate release rate. Although one has to note that a precise determination of the glycolytic flux would require more powerful methods, such as ^{13}C-based metabolic flux analysis, this is an indication that the overall glycolytic flux is not decreased by the presence of the dipeptide. More importantly, the reduced abundances of GA3P and DHAP

are accompanied by reduced abundances of metabolites associated with the PPP, the glycerol phosphate shuttle and the malate-aspartate shuttle. The PPP is especially important for tumour cells as it provides nucleotides for nucleic acid synthesis and NADPH required for fatty acid synthesis and scavenging of reactive oxygen species (for review see[31]). Therefore, a decreased activity of this pathway will impair proliferation and defence against oxidative stress, and it has been discussed that the PPP could be in fact a potential target for cancer therapy.[32]

In previous investigations, the anti-neoplastic of carnosine was shown to be associated with decreased ATP production. However, there have been different reports either pointing towards an effect on glycolysis, mitochondrial respiration or on both, depending on the cell type investigated.[11,15,17,18] As we observed a reduction of metabolites of the malate-aspartate shuttle and the glycerol phosphate shuttle in all three cell lines, it is straightforward to assume that this observation is responsible for reduced mitochondrial ATP production as these pathways deliver cytosolic NADH to mitochondrial oxidation. However, using pyruvate as substrate, only cells from the lines U87 and T98G responded to the presence of the dipeptide with reduced ATP-linked OCR but not cells from the line LN229. As LN229 cells do not respond with reduced ATP production even in the presence of glucose (Figure S3), aside from a predicted impairment of the shuttles, we assume that the shuttles may also be of less importance for ATP production in U87 and T98G cells. In addition, the cell-specific response of mitochondrial ATP production to the presence of carnosine is highly interesting, pointing towards the possibility of a tumour-specific reactivity. A cell-specific response was also reported by Bao et al[17] who demonstrated that carnosine inhibits the enzymatic activity of electron transport chain complexes in HeLa cells but not in SiHa cells. Therefore, future work should carefully evaluate in which cells carnosine affects ATP-linked OCR to reveal the mechanisms behind this phenomenon. Nonetheless, carnosine impairs proliferation in all three lines examined. This in turn indicates that decreased mitochondrial ATP production is not as important for the anti-neoplastic effect of the dipeptide as a decreased activity of the PPP.
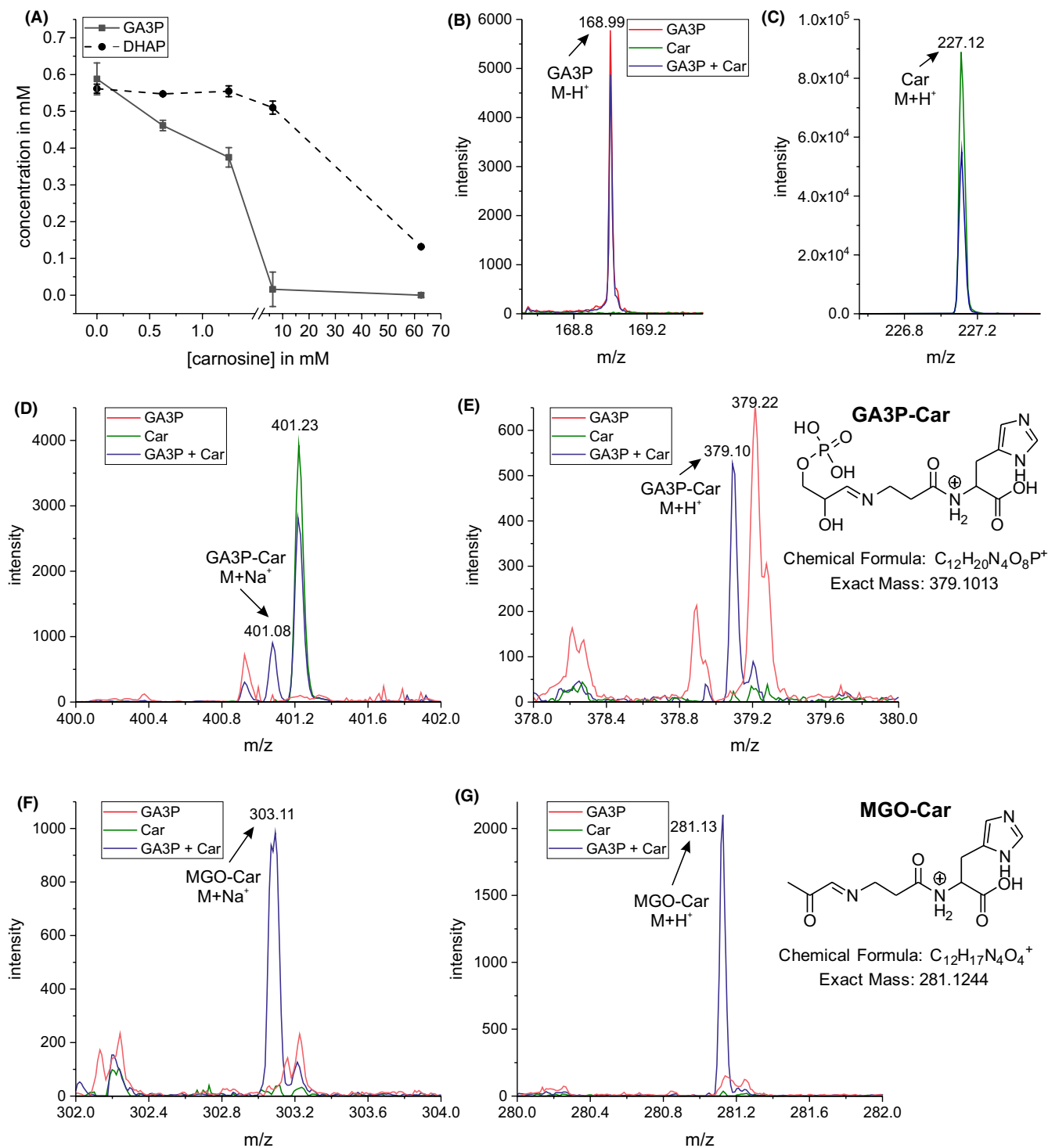
FIGURE 4 Carnosine reacts with glyceraldehyde-3-phosphate. A, Carnosine (Car) non-enzymatically reacts with glyceraldehyde-3-phosphate (GA3P) and dihydroxyacetone phosphate (DHAP) (4 h of incubation; n = 3). Mass spectrometric analysis of reaction products of carnosine with GA3P and methylglyoxal (MGO). Intensity of (B) GA3P, (C) car, (D, E) GA3P-Car, (F, G) MGO-Car. Numbers indicate the corresponding *m/z*

Up to now, several suggestions have been made on how carnosine may influence tumour cell growth (for a review see[33]). A recent report analysing a potential role of the PI3K/Akt/mTOR signalling pathway in U87 and T98G cells demonstrated that the inhibitory effect of carnosine is independent of this pathway, although cells from the line U87 exhibited a decreased phosphorylation of Akt under the influence of the dipeptide.[14] Whether the effect on Akt is caused by the influence of carnosine on metabolites

or mitochondrial respiration is difficult to resolve as these interactions are highly complex (for review see[34]). At this point, it should also be emphasized that care has to be taken to compare the dipeptide's effect on different cancer cell types. Whereas in glioblastoma cells no effect on mTOR signalling was detected,[14] Zhang et al reported an inhibitory effect on mTOR/p70S6K-signalling in gastric carcinoma.[12] As increased GA3P levels lead to activation of mTOR,[35] a reduction of GA3P could be responsible for an inhibitory effect. To solve the riddle why glioblastoma cells behave differently with regard to mTOR signalling would require further investigations on how phosphorylation/dephosphorylation of mTOR is controlled in different cells. However, both observations taken together argue against the notion that mTOR is a direct target of carnosine, pointing towards an upstream target such as GA3P.

As it is reported that carnosine suppresses HIF-1α signalling,[10,36] it is also tempting to speculate that inhibition of this pathway, which controls the expression of glycolytic enzymes, is responsible for the effects observed in this study. However, there are also reports that the dipeptide may increase HIF-1α activity accompanied by reduced tumour growth and extracellular acidification.[37] In order to resolve whether HIF-1α signalling is involved in carnosine's anti-neoplastic effect certainly requires further investigations. At this point, it should also be noted that the influence of metabolites on signalling is still far from being understood.[38]

Our observation that all three lines responded to the presence of carnosine with decreased activity of the PPP and with decreased proliferation when supplied with glucose is in agreement with more recent interpretations of the Warburg effect. Warburg's observation that cancer cells exhibit a high rate of glycolysis even in the presence of oxygen (aerobic glycolysis) has long been debated. Today, the most accepted interpretation trying to explain this phenomenon is that aerobic glycolysis, despite its low efficiency in ATP yield per molecule glucose, strongly supports macromolecular synthesis (for review see[39]). Therefore, the reduced abundances of metabolites such as GA3P, DHAP, E4P or R5P can be interpreted as a direct effect of carnosine on the Warburg effect. Noteworthy, our results also demonstrate that the cells from all three lines are able to produce ATP in the presence of pyruvate and in the absence of glucose confirming that mitochondria are not defective in their ability to carry out oxidative phosphorylation (OXPHOS). However, as carnosine interferes with OXPHOS in U87 and T98G cells but not in LN229 cells, mitochondrial physiology may be different in different cells. This can even be the case within one tumour. Janiszewska et al, for example, demonstrated that especially glioblastoma cancer stem cells strongly appear to be dependent on OXPHOS but not on glycolysis.[40] As there is now emerging evidence that cancer cells can acquire a high metabolic plasticity by their hybrid glycolysis/OXPHOS phenotype,[41] and it is interesting that carnosine is able to interfere with both pathways. Hence, our observations strongly demand further research into carnosine's effect on OXPHOS, as metabolic plasticity may be associated with metastasis and therapy-resistance.

Considering using carnosine for the therapy of glioblastoma or other types of cancer, the question has to be answered whether intracellular concentrations of carnosine could be reached that are able to inhibit the PPP by reaction with GA3P. The experiments presented in Figure 4A demonstrate that a concentration of >1 mM carnosine should be reached to reduce the available amount of GA3P to <50%. This is at least in the range of carnosine concentrations determined in kidney tissue of CN1 transgenic mice which were supplemented with a bolus of 200 mg carnosine.[42] In these experiments, carnosine concentrations reached ~0.5 mmol/kg 8 hours after supplementation. More interestingly, the authors could also demonstrate that in mice receiving a CN1 inhibitor, tissue concentrations increased ~7-fold, which is an interesting aspect considering carnosine as a therapeutic. In this context, one should also be aware that in the experiments of Qiu et al,[42] carnosine was supplemented only once and tissue concentrations were determined 8 hours later. However, in a clinical set-up carnosine might be supplemented repeatedly. As demonstrated by the experiments of Blancquaert et al,[43] daily administration of the carnosine moieties β-alanine and L-histidine over 23 days results in a continuous increase in muscle carnosine concentrations. This observation points towards the possibility that the dipeptide's tissue concentration might continuously be increased after repeated supplementation during cancer therapy.

In conclusion, our investigation demonstrates that carnosine's anti-neoplastic effect is accompanied by reduced abundances of several metabolites associated with glycolysis and pathways dependent on it. We suggest that a non-enzymatic reaction of GA3P with the dipeptide is responsible for its reduced abundance that in turn leads to a decreased activity of the pentose phosphate pathway required for proliferation. However, we also observed an inhibitory effect on mitochondrial ATP production which is cell-specific and independent of carnosine's effect on glycolytic metabolites.

CONFLICT OF INTEREST

The authors declare that they have no potential conflict of interest.

AUTHOR CONTRIBUTIONS

HO performed the experiments and analysed the data. CB carried out the mass spectrometry measurements and identified the reaction products. JM revised the manuscript. HO and FG designed the

study and wrote the manuscript. All authors reviewed and approved the manuscript.

ORCID

Henry Oppermann https://orcid.org/0000-0001-9216-5918

Claudia Birkemeyer https://orcid.org/0000-0002-8538-8838

Frank Gaunitz https://orcid.org/0000-0001-6628-0605

REFERENCES

1. Gulewitsch WL, Amiradžibi S. Ueber das Carnosin, eine neue organische Base des Fleischextractes. *Ber Dtsch Chem Ges.* 1900;33(2):1902-1903.
2. Mannion AF, Jakeman PM, Dunnett M, Harris RC, Willan PL. Carnosine and anserine concentrations in the quadriceps femoris muscle of healthy humans. *Eur J Appl Physiol Occup Physiol.* 1992;64:47-50.
3. Abraham D, Pisano JJ, Uendriend S. The distribution of homocarnosine in mammals. *Arch. Biochem. Biophys.* 1962;99:210-213.
4. Margolis FL. Carnosine in the primary olfactory pathway. *Science.* 1974;184(4139):909-911.
5. Bellia F, Vecchio G, Rizzarelli E. Carnosinases, their substrates and diseases. *Molecules.* 2014;19(2):2299-2329.
6. Boldyrev AA, Aldini G, Derave W. Physiology and pathophysiology of carnosine. *Physiol. Rev.* 2013;93:1803-1845.
7. Nagai K, Suda T. Antineoplastic effects of carnosine and beta-alanine—physiological considerations of its antineoplastic effects. *Nihon Seirigaku Zasshi.* 1986;48:741-747.
8. Renner C, Zemitzsch N, Fuchs B, et al. Carnosine retards tumor growth in vivo in an NIH3T3-HER2/neu mouse model. *Mol Cancer.* 2010;9(1):2.
9. Horii Y, Shen J, Fujisaki Y, Yoshida K, Nagai K. Effects of ʟ-carnosine on splenic sympathetic nerve activity and tumor proliferation. *Neurosci Lett.* 2012;510(1):1-5.
10. Iovine B, Oliviero G, Garofalo M, et al. The anti-proliferative effect of ʟ-carnosine correlates with a decreased expression of hypoxia inducible factor 1 alpha in human colon cancer cells. *PLoS ONE.* 2014;9(5):e96755.
11. Oppermann H, Schnabel L, Meixensberger J, Gaunitz F. Pyruvate attenuates the anti-neoplastic effect of carnosine independently from oxidative phosphorylation. *Oncotarget.* 2016;7(52):85848-85860.
12. Zhang Z, Miao L, Wu X, et al. Carnosine inhibits the proliferation of human gastric carcinoma cells by retarding Akt/mTOR/p70S6K signaling. *J. Cancer.* 2014;5(5):382-389.
13. Renner C, Seyffarth A, de Arriba SG, Meixensberger J, Gebhardt R, Gaunitz F. Carnosine inhibits growth of cells isolated from human glioblastoma multiforme. *Int J Pept Res Ther.* 2008;14(2):127-135.
14. Oppermann H, Faust H, Yamanishi U, Meixensberger J, Gaunitz F. Carnosine inhibits glioblastoma growth independent from PI3K/Akt/mTOR signaling. *PLoS ONE.* 2019;14(6):e0218972.
15. Rybakova YS, Kalen AL, Eckers JC, Fedorova TN, Goswami PC, Sarsour EH. Increased manganese superoxide dismutase and cyclin B1 expression in carnosine-induced inhibition of glioblastoma

cell proliferation. *Biochem (Moscow) Suppl Ser B: Biomed Chem.* 2015;9(1):63-71.
16. Bao Y, Ding S, Cheng J, et al. Carnosine inhibits the proliferation of human cervical gland carcinoma cells through inhibiting both mitochondrial bioenergetics and glycolysis pathways and retarding cell cycle progression. *Integr Cancer Ther.* 2018;17(1):80-91.
17. Shen Y, Yang J, Li J, et al. Carnosine inhibits the proliferation of human gastric cancer SGC-7901 cells through both of the mitochondrial respiration and glycolysis pathways. *PLoS ONE.* 2014;9(8):e104632.
18. Ostrom QT, Gittleman H, Truitt G, Boscia A, Kruchko C, Barnholtz-Sloan JS. CBTRUS statistical report: primary brain and other central nervous system tumors diagnosed in the United States in 2011–2015. *Neuro-Oncology.* 2018;20(suppl_4):iv1-iv86.
19. Stupp R, Mason WP, van den Bent MJ, et al. Radiotherapy plus concomitant and adjuvant temozolomide for glioblastoma. *N Engl J Med.* 2005;352(10):987-996.
20. Allen M, Bjerke M, Edlund H, Nelander S, Westermark B. Origin of the U87MG glioma cell line: good news and bad news. *Sci Transl Med.* 2016;8(354):354re3-354re3.
21. Oppermann H, Ding Y, Sharma J, et al. Metabolic response of glioblastoma cells associated with glucose withdrawal and pyruvate substitution as revealed by GC-MS. *Nutrition & Metabolism.* 2016;13(13). Articel No: 70.
22. Hutschenreuther A, Kiontke A, Birkenmeier G, Birkemeyer C. Comparison of extraction conditions and normalization approaches for cellular metabolomics of adherent growing cells with GC-MS. *Anal Methods.* 2012;4(7):1953.
23. Bergmeyer HU, editor. *Methods of Enzymatic Analysis.* Weinheim, Germany: Verlag Chemie; 1974.
24. Benjamini Y, Hochberg Y. Controlling the false discovery rate: a practical and powerful approach to multiple testing. *J R Stat Soc Ser B-Methodol.* 1995;57:289-300.
25. Xia J, Wishart DS. Using MetaboAnalyst 3.0 for comprehensive metabolomics data analysis. *Curr Protoc Bioinformatics.* 2016;55:14.10.1-14.10.91.
26. Renner C, Asperger A, Seyffarth A, Meixensberger J, Gebhardt R, Gaunitz F. Carnosine inhibits ATP production in cells from malignant glioma. *Neurol Res.* 2010;32(1):101-105.
27. Ramos-Montoya A, Lee W-N, Bassilian S, et al. Pentose phosphate cycle oxidative and nonoxidative balance: a new vulnerable target for overcoming drug resistance in cancer. *Int J Cancer.* 2006;119(12):2733-2741.
28. Thornburg JM, Nelson KK, Clem BF, et al. Targeting aspartate aminotransferase in breast cancer. *Breast Cancer Res.* 2008;10(10). Article number: R84.
29. Orr AL, Ashok D, Sarantos MR, et al. Novel inhibitors of mitochondrial sn-glycerol 3-phosphate dehydrogenase. *PLoS ONE.* 2014;9(2):e89938.
30. Vistoli G, Colzani M, Mazzolari A, et al. Quenching activity of carnosine derivatives towards reactive carbonyl species: focus on α−(methylglyoxal) and β−(malondialdehyde) dicarbonyls. *Biochem Biophys Res Comm.* 2017;492(3):487-492.
31. Patra KC, Hay N. The pentose phosphate pathway and cancer. *Trends Biochem Sci.* 2014;39(8):347-354.
32. Cho ES, Cha YH, Kim HS, Kim NH, Yook JI. The pentose phosphate pathway as a potential target for cancer therapy. *Biomolecules & Therapeutics.* 2018;26(1):29-38.
33. Gaunitz F, Oppermann H, Hipkiss A. Carnosine and Cancer. In: Preedy VR, editor. *Imidazole Dipeptides.* Cambridge, UK: Royal Society of Chemistry; 2015:(Ch. 20, 372-392).
34. Coloff JL, Rathmell JC. Metabolic regulation of Akt: roles reversed. *J Cell Biol.* 2006;175:845-847.

35. Lee MN, Ha SH, Kim J, et al. Glycolytic flux signals to mTOR through glyceraldehyde-3-phosphate dehydrogenase-mediated regulation of Rheb. *Mol Cell Biol.* 2009;29(14):3991-4001.

36. Forsberg EA, Botusan IR, Wang J, et al. Carnosine decreases IGFBP1 production in db/db mice through suppression of HIF-1. *J Endocrinol.* 2015;225(3):159-167.

37. Ditte Z, Ditte P, Labudova M, et al. Carnosine inhibits carbonic anhydrase IX-mediated extracellular acidosis and suppresses growth of HeLa tumor xenografts. *BMC Cancer.* 2014;14(1). Article number: 358.

38. Metallo CM, Vander Heiden MG. Metabolism strikes back: metabolic flux regulates cell signaling. *Genes Dev.* 2010;24(24):2717-2722.

39. Lunt SY, Vander Heiden MG. Aerobic glycolysis: meeting the metabolic requirements of cell proliferation. *Annu Rev Cell Dev Biol.* 2011;27(1):441-464.

40. Janiszewska M, Suva ML, Riggi N, et al. Imp2 controls oxidative phosphorylation and is crucial for preserving glioblastoma cancer stem cells. *Genes Dev.* 2012;26(17):1926-1944.

41. Jia D, Park J, Jung K, Levine H, Kaipparettu B. Elucidating the metabolic plasticity of cancer: mitochondrial reprogramming and hybrid metabolic states. *Cells.* 2018;7(3):21.

42. Qiu J, Hauske SJ, Zhang S, et al. Identification and characterisation of carnostatine (SAN9812), a potent and selective carnosinase (CN1) inhibitor with in vivo activity. *Amino Acids.* 2019;51(1):7-16.

43. Blancquaert L, Everaert I, Missinne M, et al. Effects of histidine and β-alanine supplementation on human muscle carnosine storage. *Med Sci Sports Exerc.* 2017;49(3):602-609.

SUPPORTING INFORMATION

Additional supporting information may be found online in the Supporting Information section at the end of the article.

In summary, our results suggest that carnosine's effect on glioblastoma cell viability mainly results from a non-enzymatic reaction of the dipeptide with GA3P that in turn diminishes the supply of precursors for the biosynthesis of macromolecules, e.g. via the PPP. In fact, the PPP has already been considered to have a vital role in tumorigenesis (Patra and Hay 2014).

At this point it is interesting to add that using mass spectrometry we observed that the identified carnosine-GA3P adduct exhibited only a minor abundance (signal) compared to the carnosine-methylglyoxal adduct. This indicates that GA3P-carnosine is an intermediate and not the end-product of carnosine dependent GA3P reduction. Using nuclear magnetic resonance spectroscopy, we observed that the dipeptide reduces the amounts of GA3P without being consumed. Further analysis revealed that carnosine catalyses the degradation of GA3P to methylglyoxal (unpublished results). Interestingly, the dipeptide also catalyses the oligomerisation of methylglyoxal (Weigand et al. 2018) which could be a subsequent reaction and possibly explains the detection of the carnosine-methylglyoxal adduct in our experiments. More important, the observation that carnosine can act as a catalyser opens a new aspect of the molecular properties of the dipeptide and deserves further investigation.

2.5 Carnosine's effect on Glioblastoma cell viability and migration

Infiltration and formation of metastasis is in addition to rapid growth a hallmark of cancer (Hanahan and Weinberg 2011). Especially gliomas grow highly infiltrative and glioma cells can be found throughout the whole brain (Sahm et al. 2012). According to the "go or growth" hypothesis, cancer cells either exhibit a proliferative or an invasive phenotype (Hatzikirou et al. 2012). Therefore, a drug that inhibits cancer cell proliferation, such as carnosine, could possibly induce invasion which is accompanied with a poor prognosis for patients (Evdokimova et al. 2009). Therefore, we investigated carnosine's influence on glioblastoma cell migration with a newly developed cell co-culture model (Oppermann et al. 2018). In our model, glioblastoma cells were seeded inside of a cloning ring and patient-derived fibroblasts were placed outside of the ring. After removal of the ring, co-cultures were cultivated in the presence or absence of carnosine over four weeks. In order to assess glioblastoma colony formation, an immunofluorescent staining was employed to distinguished fibroblasts from glioblastoma cells. This allowed us to investigate the infiltrative growth of glioblastoma cells in a non-neoplastic cell layer.

Cancer Cell International

PRIMARY RESEARCH

Open Access

CrossMark

Carnosine selectively inhibits migration of IDH-wildtype glioblastoma cells in a co-culture model with fibroblasts

Henry Oppermann[1†], Johannes Dietterle[1†], Katharina Purcz[1], Markus Morawski[2], Christian Eisenlöffel[3], Wolf Müller[3], Jürgen Meixensberger[1] and Frank Gaunitz[1*] iD

Abstract

Background: Glioblastoma (GBM) is a tumor of the central nervous system. After surgical removal and standard therapy, recurrence of tumors is observed within 6–9 months because of the high migratory behavior and the infiltrative growth of cells. Here, we investigated whether carnosine (β-alanine-ʟ-histidine), which has an inhibitory effect on glioblastoma proliferation, may on the opposite promote invasion as proposed by the so-called "go-or-grow concept".

Methods: Cell viability of nine patient derived primary (isocitrate dehydrogenase wildtype; IDH1R132H non mutant) glioblastoma cell cultures and of eleven patient derived fibroblast cultures was determined by measuring ATP in cell lysates and dehydrogenase activity after incubation with 0, 50 or 75 mM carnosine for 48 h. Using the glioblastoma cell line T98G, patient derived glioblastoma cells and fibroblasts, a co-culture model was developed using 12 well plates and cloning rings, placing glioblastoma cells inside and fibroblasts outside the ring. After cultivation in the presence of carnosine, the number of colonies and the size of the tumor cell occupied area were determined.

Results: In 48 h single cultures of fibroblasts and tumor cells, 50 and 75 mM carnosine reduced ATP in cell lysates and dehydrogenase activity when compared to the corresponding untreated control cells. Co-culture experiments revealed that after 4 week exposure to carnosine the number of T98G tumor cell colonies within the fibroblast layer and the area occupied by tumor cells was reduced with increasing concentrations of carnosine. Although primary cultured tumor cells did not form colonies in the absence of carnosine, they were eliminated from the co-culture by cell death and did not build colonies under the influence of carnosine, whereas fibroblasts survived and were healthy.

Conclusions: Our results demonstrate that the anti-proliferative effect of carnosine is not accompanied by an induction of cell migration. Instead, the dipeptide is able to prevent colony formation and selectively eliminates tumor cells in a co-culture with fibroblasts.

Keywords: Glioblastoma, Migration assay, Fibroblast ring co-culture, Carnosine

*Correspondence: Frank.Gaunitz@medizin.uni-leipzig.de
†Henry Oppermann and Johannes Dietterle contributed equally to this work
[1] Department of Neurosurgery, University Hospital Leipzig, Liebigstraße 20, 04103 Leipzig, Germany
Full list of author information is available at the end of the article

Oppermann *et al. Cancer Cell Int (2018) 18:111*

Page 2 of 10

Background

Isocitrate dehydrogenase (IDH)-wildtype glioblastoma is the most malignant brain tumor of the adult brain and designated as Grade IV tumor by the World Health Organization (WHO) [1]. All tumors used in this study were IDH1R132H-non-mutant glioblastoma of elderly patients and, for reasons of simplicity, will further be referred to as GBM. Aside from a high mitotic activity and its ability to vascularize, GBM, as all diffuse glioma, has a high potential to infiltrate into intact brain tissue which makes it virtually impossible for the surgeon to completely remove the tumor. Cells able to migrate within intact tissue are considered to be the main cause of tumor recurrence which is generally observed within 6–9 month after surgery and standard therapy [2]. Therefore, any therapeutic approach has to consider that it may not be enough to inhibit the proliferation of cells, but should although prevent their spreading into intact tissue. Moreover, as Giese et al. [3] pointed out already more than 20 years ago, proliferation and migration appear to be mutually exclusive behaviors. The concept of a dichotomy of proliferation/migration has been observed by many groups and has coined the term "go or grow" [4]. Having this dichotomy in mind it is important that a substance that inhibits proliferation does not at the same time trigger migration and invasive behavior. This is the case for the dipeptide L-carnosine (β-alanyl-L-histidine). This naturally occurring dipeptide has been discovered in 1900 by Gulewitsch and Amiradzibi [5]. Aside from a number of physiological roles attributed to it, such as pH-buffering or the chelation of metal ions (for review see [6]), it is discussed as a potential drug for the treatment of tumors (for reviews see [7, 8]). After the first observations made by Nagai and Suda [9] and the rediscovery of its anti-neoplastic effect by Holliday and McFarland [10], carnosine's anti-tumor effect has been shown in vitro for a variety of cells derived from different tumors. This, for instance, includes gastric cancer cells [11], colon cancer cells [12] and, with special emphasis to this work, cells derived from glioblastoma [13]. Unfortunately, the exact mechanisms by which the dipeptide exerts its anti-neoplastic effect are still unknown but appear to be pleiotropic and dependent on the tumor cells investigated (for review see [14]).

Although previous experiments pointed towards the possibility that carnosine also reduces migration and infiltration via inhibition of Matrix Metalloproteinase-9 in SK-Hep-1 hepatoma cells [15] and in oxygen–glucose deprived reactive rat astrocytes [16] tumor cell invasion in these experiments was determined using trans well chamber assays, which cannot answer the question whether migration into tissue or a layer of cells will also be inhibited by the dipeptide. The same is the case with recently published experiments performed with HCT-116 human colon cancer cells which also indicated that the invasion ability of these cells is significantly inhibited already at a concentration 0.5 mM carnosine [17]. Therefore, we analyzed the infiltrative capacity of IDH-wildtype glioblastoma cells in the presence of carnosine in a newly developed co-culture model. In our model glioblastoma cells were seeded inside a cloning ring placed in the well of a 12 well plate, seeding patient-derived fibroblasts outside the cloning rings. The rings were removed after the cells had attached to the culture dishes and the cells were incubated for different periods of time in the absence and presence of different concentrations of carnosine. Finally, the infiltrative potential of the tumor cells was analyzed by determining the number of colonies formed within the fibroblast layer and the area they covered.

Materials and methods
Reagents

Unless stated otherwise, all chemicals were purchased from Sigma Aldrich (Taufkirchen, Germany). Carnosine was kindly provided by Flamma (Flamma s.p.a. Chignolo d'Isola, Italy).

Cell lines and primary cell cultures

The GBM cell line T98G, negative for IDH1R132H-mutation and *O*-6-methylguanine-DNA methyltransferase (MGMT) promoter methylation, was obtained from the ATCC, genotyped using a PowerPlex 21 System (Promega; Mannheim; Germany) by the Genolytic GmbH (Leipzig, Germany) and authenticated by comparison to data at the ATCC and the DSMZ. T98G cells were used at passage 5–7 after genotyping and authentication. Both, primary GBM cultures and primary fibroblast cultures were established from tissue samples obtained during standard surgery performed at the Neurosurgery Department of the University Hospital Leipzig during 2015 and 2016. All patients provided written informed consent according to the German laws as confirmed by the local committee. When possible, one primary GBM cell culture and one primary fibroblast culture was established from tissue samples obtained from each patient (Additional file 1: Table S1). All GBM samples were diagnosed and have been approved by the Neuropathology Department of the Leipzig University Hospital. IDH 1 status has been determined using immunohistochemistry and pyrosequencing, MGMT promoter methylation status was determined using nucleic acid amplification followed by pyrosequencing.

For cultivation, tissue specimens from the tumor, from galea or from periost were cut into approximately 1 mm^3 large pieces and then separately placed into 25 mm^2 culture flasks (TPP, Trasadingen, Switzerland)

Oppermann *et al. Cancer Cell Int* (2018) 18:111

Page 3 of 10

until tumor cells or fibroblasts grew out. When more than 90% confluence was reached specimens were removed and primary cell cultures were transferred into 75 mm^2 culture flasks (TPP) for further cultivation. Cell cultures were maintained in high glucose DMEM (4.5 g glucose/ml) supplemented with 2 mM Glutamax™, 1% penicillin/streptomycin (all from Gibco Life Technologies, now Thermo Fisher Scientific, Darmstadt, Germany) and 10% FBS (Biochrom GmbH, Berlin, Germany), further referred to as "standard medium", and kept in incubators (37 °C, 5% CO$_2$/95% air).

Cell viability assays

For cell viability assays, cells were counted and seeded into sterile 96-well plates (μClear, Greiner Bio One, Frickenhausen, Germany) at a density of 5000 cells/well in 200 μl standard medium. After 24 h of cultivation (37 °C, 5% CO$_2$/95% air) the medium was aspirated and fresh medium supplemented with or without carnosine was added (100 μl/well) and the cells were incubated for additional 48 h. Then, the CellTiter-Glo Luminescent Cell Viability Assay (CTG, Promega, Mannheim, Germany) was employed to determine viable cells by measuring ATP in cell lysates and the CellTiter-Blue Cell Viability Assay (CTB, Promega) was used to quantify the cell's metabolic capacity in living cells. All assays were carried out according to manufacturer's protocols. Luminescence and fluorescence were measured using a SpectraMax M5 multilabel reader (Molecular Devices, Biberach, Germany).

Co-cultivation of GBM cells and fibroblasts (ring-cultures)

When cells reached more than 90% confluence in 75 cm^2 cell culture flasks they were detached using accutase (Thermo Fisher), counted and diluted for co-cultivation. The ring-cultures were established in 12-well plates. Therefore, sterile cloning rings (steel, 6 mm inner; 8 mm outer diameter, Hartenstein, Würzburg, Germany) usually used for the isolation of clones, were placed in the middle of each well dividing it into an inner-ring and an outer-ring part. Then, 2500 tumor cells suspended in standard medium (112 μl) were seeded inside the ring. Afterwards, 50,000 fibroblasts (in 658 μl standard medium) were seeded outside of the ring (Additional file 2: Figure S1). Co-cultures with cloning rings were incubated for 4 h (37 °C, 5% CO$_2$/95% air) before the rings were carefully removed using sterile forceps. Medium was exchanged immediately after ring removal containing various

concentrations of carnosine. On the following days medium was exchanged twice a week.

Carnosine co-culture experiments

Carnosine was diluted in 0.7% NaCl solution and carnosine experiments were performed with concentrations of 0 mM, 10 mM, 25 mM, 50 mM and 75 mM. All ring-culture experiments were prepared as described above. Control experiments with T98G cells inside the ring and without fibroblasts in the outer part were kept for over 2 weeks. Ring co-cultures with T98G and fibroblasts (P0385) and with GBM cells and fibroblasts of the same patient (P0383 with P0385 and P0431 with P0433) were cultivated for 4 weeks. Throughout cultivation, cell growth and dissemination were monitored by bright field microscopy. After 4 weeks all co-cultures were fixated in 4.5% paraformaldehyde and stored in 1% sodium azide solution at 4 °C until microscopic analysis.

Immunostaining

Immunofluorescent staining was carried out to discriminate between tumor cells and fibroblasts using anti-fibroblast TE-7 (CBL271, Merck Millipore, Darmstadt, Germany), anti-nestin (AB5922, Merck Millipore) and secondary antibodies (ab6563, ab150081, abcam, Cambridge, UK). Briefly, for the detection of TE-7 the fixated co-cultures were permeabilized with 0.1% TritonX-100 at room temperature (RT) for 5 min. After blocking with 10% goat serum for 15 min, samples were incubated with anti-fibroblast TE-7 primary antibodies (dilution 1:100) at 5 °C overnight, washed with TBS (20 mM Tris, 134 mM NaCl) and subsequently incubated with the secondary antibody (1:250; ab6563) for 45 min at RT. For the detection of nestin, fixated cell cultures were permeabilized with 0.1% TritonX-100 in TBS for 1 h at RT, blocked for 15 min with 10% goat serum and then incubated with an anti-nestin antibody (dilution 1:250) for 1 h at RT. Afterwards, cultures were washed with TBS and incubated with a dilution of secondary antibody (1:250; ab150081) for 45 min at RT. Finally, nuclei were counterstained with DAPI (4 μg/ml) and cell cultures were preserved in 10% sodium azide solution at 4 °C until microscopy.

Microscopy

For microscopic analysis a Zeiss Axiovert 200M microscope (Zeiss, Oberkochen, Germany) equipped with a motorized stage (Märzhäuser, Wetzlar, Germany) with MosaiX software and by means of a CCD camera (Zeiss MRC) connected to an AxioVision 4.8.2 image analysis system (Zeiss) was used to create tile pictures. Each tile picture is composed of 285 single microscopic images

Oppermann *et al. Cancer Cell Int (2018) 18:111*

Page 4 of 10

taken at a magnification of 50 and represents a whole well of a 12-well plate. As denoted in the figure legend to Fig. 2 ImageJ images in this figure have been graphically enhanced for representation purposes using the Corel Draw Graphics Suite 2017 (Corel Corporation, Ottawa, Canada).
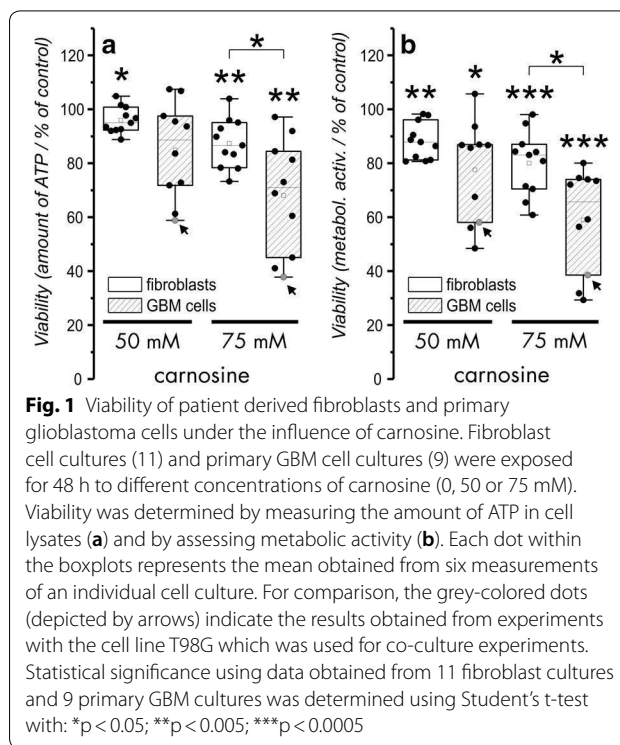
Quantitative and statistical analysis

The number of colonies in ring co-culture experiments was determined using ImageJ after a color threshold and a common pixel size were defined. All pictures used for the analysis were taken at the same magnification and had the same size. Statistical analysis was performed using the algorithm for t-test implemented in Microsoft Excel 2010.

Results

Viability of patient derived fibroblasts and GBM cells under the influence of carnosine

In order to figure out how fibroblasts isolated from patients who underwent surgery for GBM do respond to the presence of carnosine, 11 primary fibroblast cultures derived from galea or periost were exposed to different concentrations of carnosine. Viability was determined by measuring the amount of ATP in cell lysates and by the analysis of metabolic activity, as reflected by dehydrogenase activity. In order to compare the effect of the dipeptide on fibroblasts, we performed the same experiment with 9 primary GBM cell cultures derived from patients and cells from the GBM cell line T98G. All cells were seeded at a density of 5000 cells into the wells of 96-well plates and exposed to carnosine for 48 h. The result of the experiment is presented in Fig. 1. At a concentration of 50 mM carnosine, the amounts of ATP and the metabolic activity in fibroblasts were significantly reduced compared to untreated control cells (metabolic activity: $89.4\% \pm 7.53$, $p < 0.005$; ATP: $96.6\% \pm 5.08\%$. $p < 0.05$). We also observed a significant reduction of metabolic activity in primary GBM cells treated with 50 mM carnosine (compared to untreated control: $79.7\% \pm 18.51\%$, $p < 0.05$). However, although the amounts of ATP were decreased at 50 mM carnosine ($87.8\% \pm 16.35\%$ compared to the untreated control) this effect was not significant ($p = 0.056$). Increasing the concentration of carnosine to 75 mM leads to a significant reduction of metabolic activity and a decrease in the amounts of ATP in both, primary GBM cells (metabolic activity: $61.2\% \pm 18.96$, $p < 0.0005$; ATP: $71.5\% \pm 19.68\%$. $p < 0.005$) and fibroblasts (metabolic activity: $81.5\% \pm 12.03$, $p < 0.0005$; ATP: $88.4\% \pm 5.07\%$. $p < 0.005$) compared to the untreated control. Furthermore, in the presence of

Fig. 1 Viability of patient derived fibroblasts and primary glioblastoma cells under the influence of carnosine. Fibroblast cell cultures (11) and primary GBM cell cultures (9) were exposed for 48 h to different concentrations of carnosine (0, 50 or 75 mM). Viability was determined by measuring the amount of ATP in cell lysates (**a**) and by assessing metabolic activity (**b**). Each dot within the boxplots represents the mean obtained from six measurements of an individual cell culture. For comparison, the grey-colored dots (depicted by arrows) indicate the results obtained from experiments with the cell line T98G which was used for co-culture experiments. Statistical significance using data obtained from 11 fibroblast cultures and 9 primary GBM cultures was determined using Student's t-test with: $*p < 0.05$; $**p < 0.005$; $***p < 0.0005$
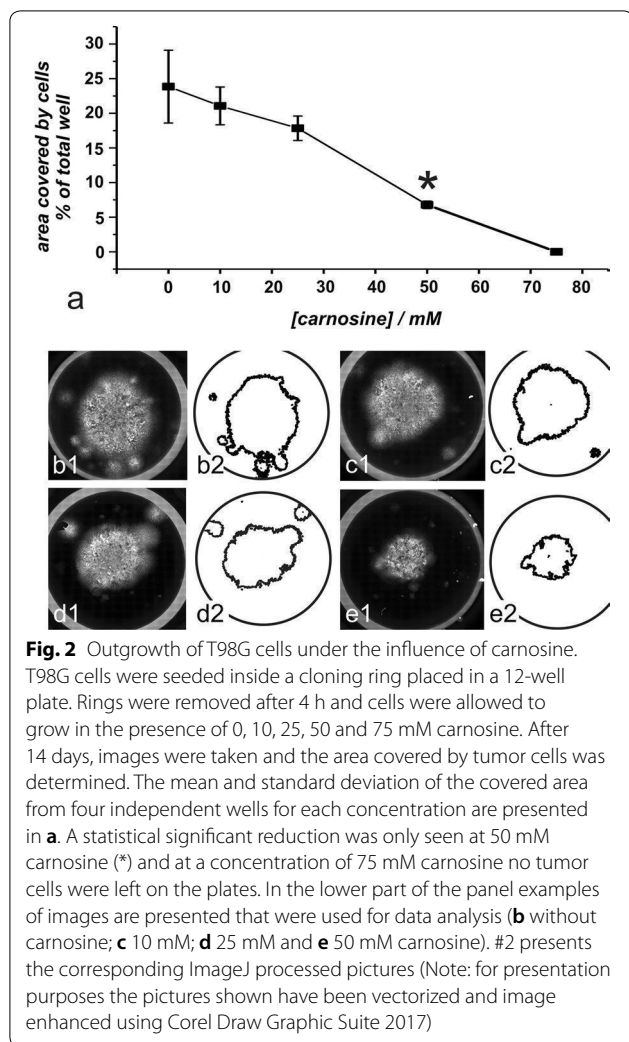
75 mM carnosine, viability of primary GBM cells was significantly stronger reduced than in fibroblasts (metabolic activity: $p < 0.05$; ATP: $p < 0.05$).

Please also note, that for statistical analysis data obtained from experiments with the cell line T98G were excluded.

Outgrowth of cells from a ring culture without co-cultivated fibroblasts

Next, we asked how carnosine influences the growth of glioblastoma cells over a longer period of time when they start to grow after being seeded inside of a cloning ring and removal of it in the absence of other cells. Therefore, 2500 cells from the glioblastoma cell line T98G were seeded inside a cloning ring placed in a 12-well plate. Four hours later the rings were removed and the cells were allowed to grow for 2 weeks in the absence and presence of carnosine (10 mM, 25 mM, 50 mM and 75 mM). Medium was exchanged twice a week. After fixation of cells, 285 tiled images were taken from each well for each concentration employed (in quadruplicate) and the area covered by tumor cells was determined using ImageJ. The result of the experiment is presented in Fig. 2. As can be seen, the tumor cell covered area is continuously decreasing with increasing concentrations of carnosine although the effect becomes significant only at a concentration of 50 mM carnosine. At a concentration of 75 mM carnosine, no tumor cells were remaining on the plates, demonstrating that this concentration

Oppermann *et al. Cancer Cell Int (2018) 18:111*

Page 5 of 10

Fig. 2 Outgrowth of T98G cells under the influence of carnosine. T98G cells were seeded inside a cloning ring placed in a 12-well plate. Rings were removed after 4 h and cells were allowed to grow in the presence of 0, 10, 25, 50 and 75 mM carnosine. After 14 days, images were taken and the area covered by tumor cells was determined. The mean and standard deviation of the covered area from four independent wells for each concentration are presented in **a**. A statistical significant reduction was only seen at 50 mM carnosine (*) and at a concentration of 75 mM carnosine no tumor cells were left on the plates. In the lower part of the panel examples of images are presented that were used for data analysis (**b** without carnosine; **c** 10 mM; **d** 25 mM and **e** 50 mM carnosine). #2 presents the corresponding ImageJ processed pictures (Note: for presentation purposes the pictures shown have been vectorized and image enhanced using Corel Draw Graphic Suite 2017)

do survive for 2 weeks when seeded at a density of 2500 cells inside a cloning ring and are incubated at carnosine concentrations of 50 mM or below.
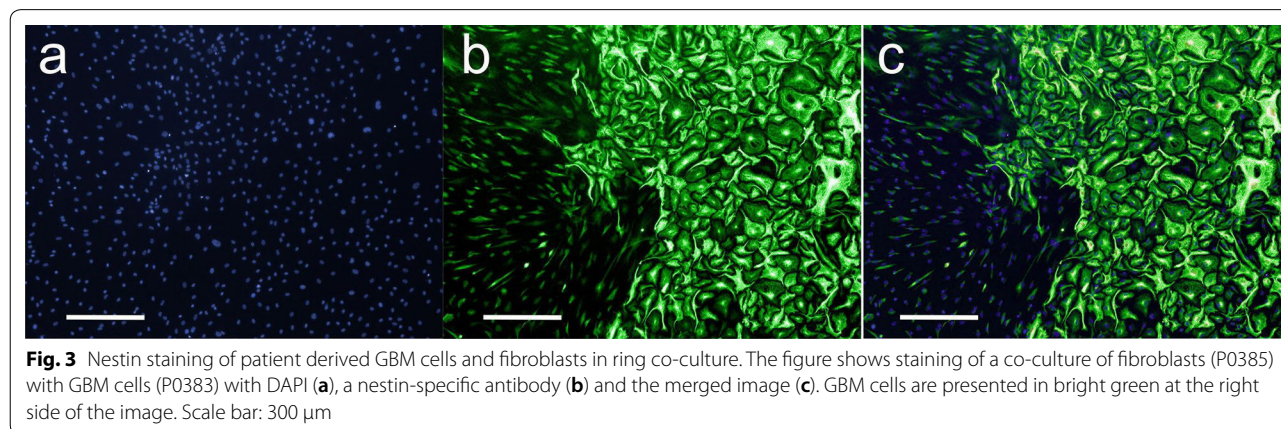
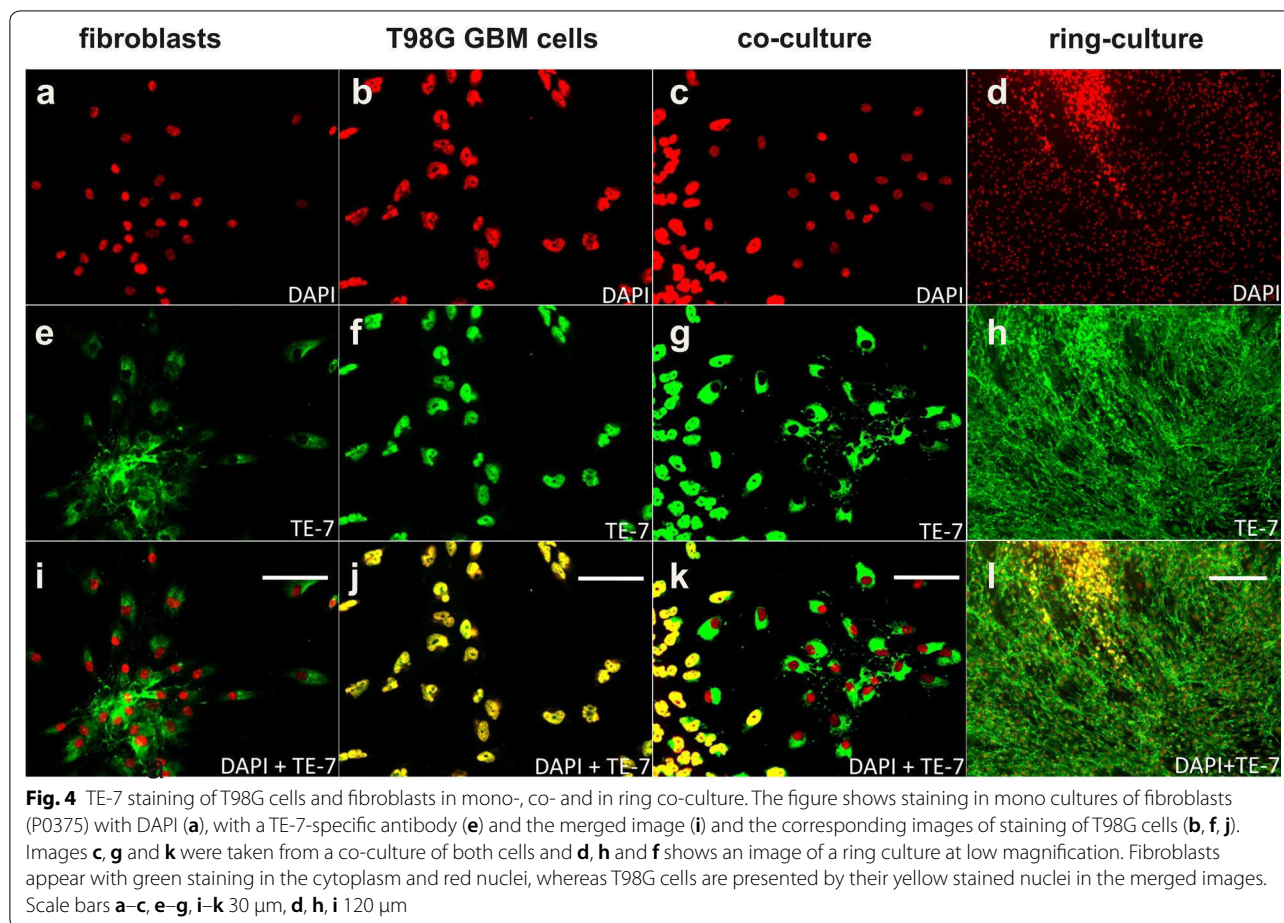**Fluorescent discrimination of tumor cells and fibroblasts in co-culture**

In order to perform co-culture experiments with GBM cells and fibroblasts, we had to establish a method by which both types of cells can be discriminated. Using patient derived fibroblasts (P0385) and primary glioblastoma cells (P0383) we were able to discriminate both types of cells using an antibody directed against nestin (Fig. 3). Although both types of cells were detected by the anti-nestin specific antibody, staining was significantly more intense on GBM cells allowing discrimination between both types of cells as demonstrated by the images presented in Fig. 3.

Unfortunately, discrimination between fibroblasts and cells from the glioblastoma cell line T98G was not possible using the nestin-specific antibody. We found a solution, using an anti-body directed against TE-7 which stains an unknown antigen specific for fibroblasts [18]. As demonstrated in Fig. 4 the TE-7 specific anti-body did also stain the nuclei of T98G cells, but did not detect antigen in their cytoplasm. Therefore, counterstaining with DAPI (color-coded in red) and TE-7 (color-coded in green) results in a yellow color of T98G nuclei and fibroblasts appear in green (cytosol) with red nuclei. At this point it should also be noted that the TE-7 specific antibody did also stain cells in primary GBM cultures which is the reason why this antibody had not been used for co-cultures with primary cells.

Colony formation of T98G tumor cells in ring culture with fibroblasts under the influence of carnosine
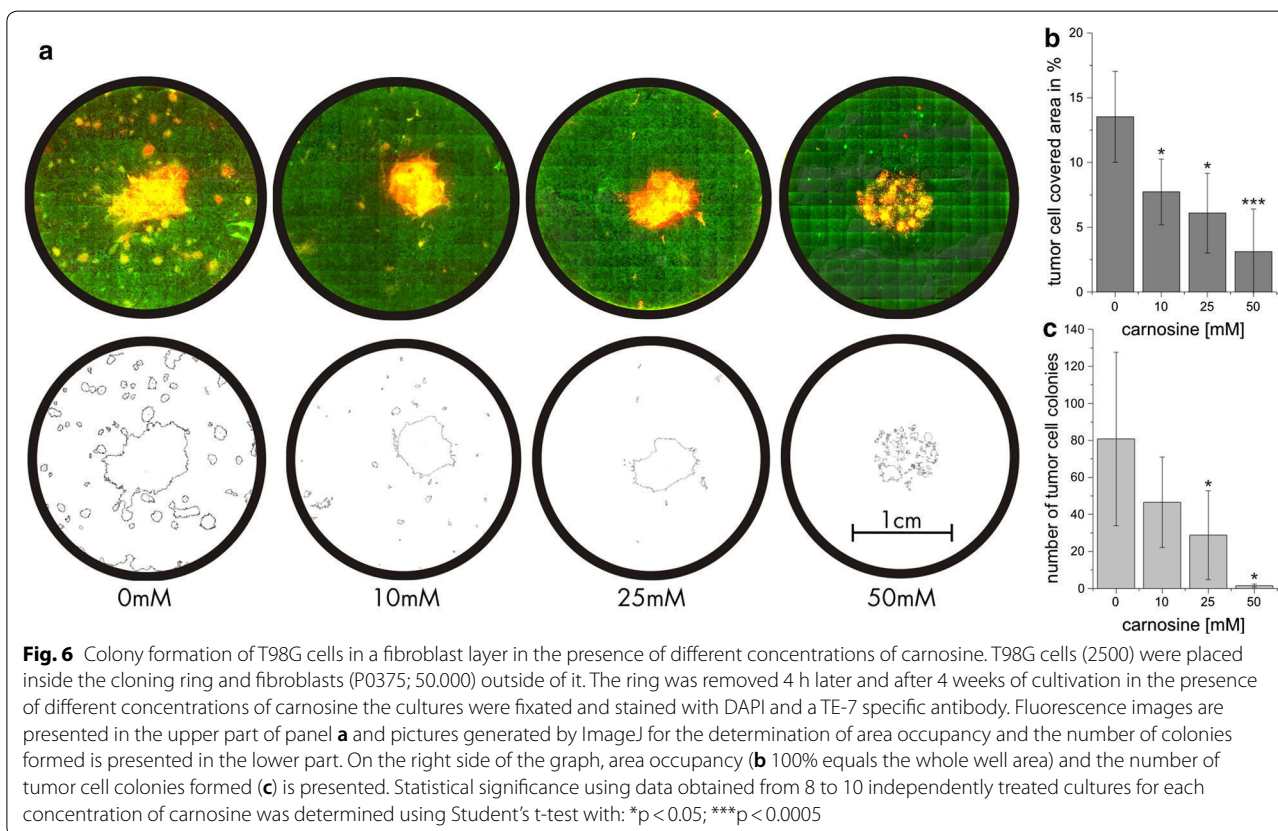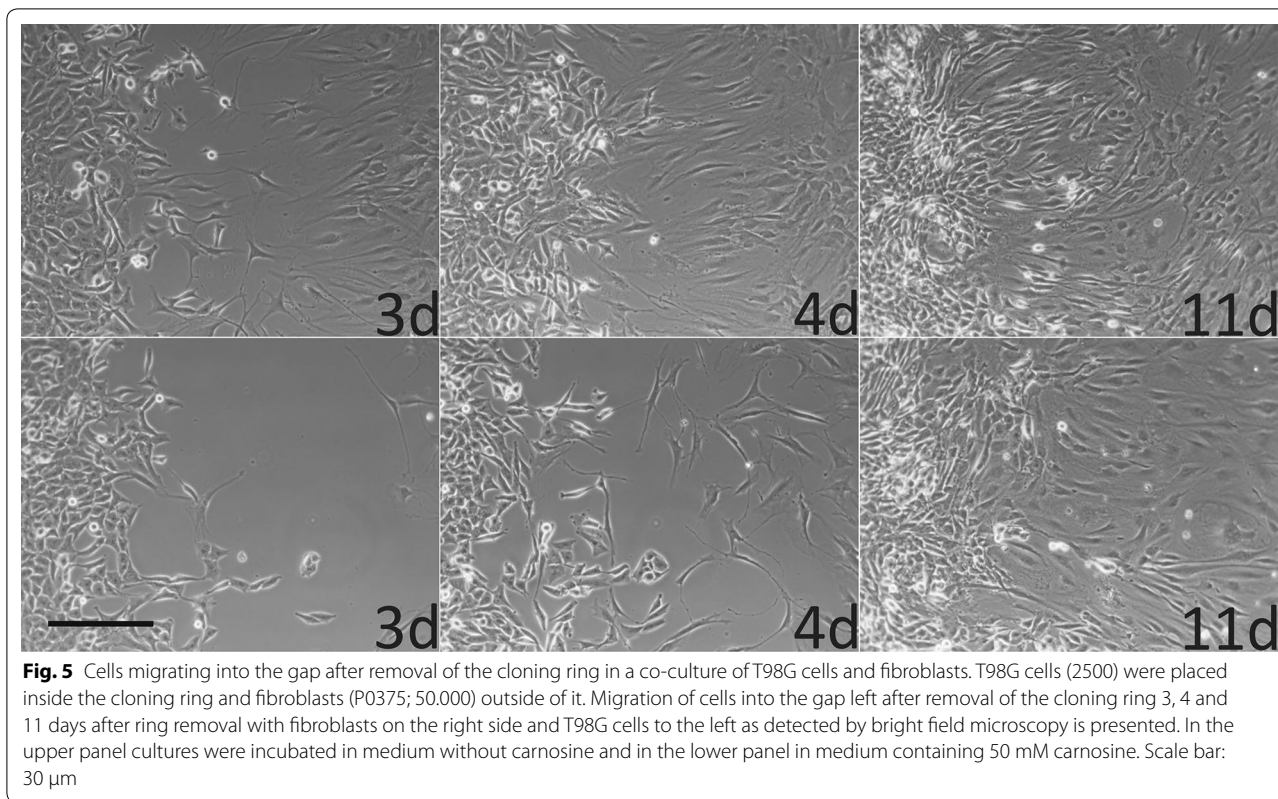
Next we asked whether T98G cells seeded inside a cloning ring can migrate into a surrounding layer of

does not only inhibit proliferation but also eliminates the tumor cells when exposed to the dipeptide for 2 weeks. In conclusion, the experiment demonstrates that the cells

Fig. 3 Nestin staining of patient derived GBM cells and fibroblasts in ring co-culture. The figure shows staining of a co-culture of fibroblasts (P0385) with GBM cells (P0383) with DAPI (**a**), a nestin-specific antibody (**b**) and the merged image (**c**). GBM cells are presented in bright green at the right side of the image. Scale bar: 300 μm

Oppermann *et al. Cancer Cell Int* (2018) 18:111

Page 6 of 10

Fig. 4 TE-7 staining of T98G cells and fibroblasts in mono-, co- and in ring co-culture. The figure shows staining in mono cultures of fibroblasts (P0375) with DAPI (**a**), with a TE-7-specific antibody (**e**) and the merged image (**i**) and the corresponding images of staining of T98G cells (**b**, **f**, **j**). Images **c**, **g** and **k** were taken from a co-culture of both cells and **d**, **h** and **f** shows an image of a ring culture at low magnification. Fibroblasts appear with green staining in the cytoplasm and red nuclei, whereas T98G cells are presented by their yellow stained nuclei in the merged images. Scale bars **a**–**c**, **e**–**g**, **i**–**k** 30 μm, **d**, **h**, **i** 120 μm

fibroblasts and whether migration and development of tumor cell colonies inside the fibroblast layer is influenced by carnosine. Therefore, ring co-cultures were established with T98G cells inside the cloning ring and fibroblasts (P0375) outside of it. After removal of the ring, cells first have to migrate towards each other filling the gap left after ring removal. As presented in Fig. 5 cells are migrating to fill the gap within 4–11 days. As can be seen, both, fibroblasts (right side) and T98G cells are able to migrate towards each other, filling the gap between day 4 and day 11 in the absence of carnosine. In the presence of 50 mM carnosine migration is impaired in both types of cells as shown in the image taken after 4 days. At day 11 the gap gets filled, too, but it seems that mainly fibroblasts are located in the previous gap (Note: This experiment resembles a classical scratch assay). In a following series of experiments ring co-cultures of T98G cells and fibroblasts (P0375) incubated for 4 weeks in different concentrations of carnosine (0, 10, 25 and 50 mM) were fixated and stained with DAPI and the TE-7 specific antibody. After fluorescence microscopy the number of colonies formed by T98G cells and the area occupied by

tumor cells was analyses using ImageJ. In Fig. 6a example fluorescence images of cultures and their corresponding ImageJ derived images are presented as well as the result of the determination of area occupancy (Fig. 6b) and the measurement of the number of colonies formed (Fig. 6c). As can be seen, the size of the area occupied by tumor cells and the number of colonies are decreasing with increasing concentrations of carnosine. In the absence of carnosine tumor cells occupied $13.5\% \pm 3.5\%$ of the plate. Already in the presence of 10 mM carnosine area occupancy was significantly decreased to $7.7\% \pm 2.5\%$ ($p < 0.05$) and diminished further by increasing concentrations of carnosine (25 mM: $6.0\% \pm 3.0\%$, $p < 0.05$; 50 mM: $3.1\% \pm 3.3\%$, $p < 0.0005$). In addition, the number of colonies decreased with increasing concentrations from 80.8 ± 46.8 colonies in the absence of carnosine to 46.6 ± 24.4 colonies (10 mM; not significant), 28.8 ± 24.0 (25 mM, $p < 0.05$) and to 1.5 ± 0.8 colonies (50 mM, $p < 0.05$). This clearly demonstrates that carnosine inhibits the potential of T98G cells to infiltrate the fibroblast layer.

Fig. 5 Cells migrating into the gap after removal of the cloning ring in a co-culture of T98G cells and fibroblasts. T98G cells (2500) were placed inside the cloning ring and fibroblasts (P0375; 50.000) outside of it. Migration of cells into the gap left after removal of the cloning ring 3, 4 and 11 days after ring removal with fibroblasts on the right side and T98G cells to the left as detected by bright field microscopy is presented. In the upper panel cultures were incubated in medium without carnosine and in the lower panel in medium containing 50 mM carnosine. Scale bar: 30 μm

Fig. 6 Colony formation of T98G cells in a fibroblast layer in the presence of different concentrations of carnosine. T98G cells (2500) were placed inside the cloning ring and fibroblasts (P0375; 50.000) outside of it. The ring was removed 4 h later and after 4 weeks of cultivation in the presence of different concentrations of carnosine the cultures were fixated and stained with DAPI and a TE-7 specific antibody. Fluorescence images are presented in the upper part of panel **a** and pictures generated by ImageJ for the determination of area occupancy and the number of colonies formed is presented in the lower part. On the right side of the graph, area occupancy (**b** 100% equals the whole well area) and the number of tumor cell colonies formed (**c**) is presented. Statistical significance using data obtained from 8 to 10 independently treated cultures for each concentration of carnosine was determined using Student's t-test with: *p < 0.05; ***p < 0.0005

Oppermann *et al. Cancer Cell Int* (2018) 18:111

Page 8 of 10

Colony formation of primary glioblastoma cells in ring culture with fibroblasts under the influence of carnosine

In order to verify that the effect of carnosine is not restricted to a cell line but can also be seen with tumor cells derived from a patient, we also performed ring co-culture experiments with two patient-derived tumor cell cultures (P0383 and P0431) and fibroblasts from the same patient (P0385 and P0433, respectively). Again, tumor cells were seeded inside the cloning ring and fibroblasts outside of it. After 4 weeks of cultivation cells were stained with DAPI and a nestin-specific antibody and analyzed using ImageJ. Surprisingly, we did not detect colony formation inside the fibroblast layer even in the absence of carnosine. On the other hand, the tumor occupied area was significantly reduced already at a concentration of 10 mM carnosine. As the two primary cultured glioblastoma cells occupied different areas in the absence of carnosine, we set the area occupied in the absence of carnosine for each cell culture as 100% in order to compare the effect of carnosine and to determine an average. We found a reduction of the occupied area to $68.1\% \pm 11.3\%$ ($p < 0.05$) at a concentration of 10 mM carnosine, to $70.6\% \pm 3.1\%$ ($p < 0.0005$) at 25 mM and to $18.7\% \pm 3.0\%$ ($p < 0.0005$) at 50 mM. Comparable to the experiments with T98G cells and fibroblasts presented in Fig. 6, the space previously occupied by tumor cells becomes occupied by the fibroblasts. (For comparison: setting the occupied area to 100% in the experiment with T98G cells the reduction is $57.0\% \pm 18.5\%$ at 10 mM, $44.4\% \pm 22.2\%$ at 25 mM and $23.0\% \pm 24.4\%$ at 50 mM carnosine).

Discussion

As outlined in the introduction, we and others have shown that the naturally occurring dipeptide carnosine inhibits the growth of cancer cells in vitro and in vivo [14], whereas beneficial effects have been observed in cultured human fibroblasts [19]. Using a colorimetric assay (tetrazolium compound [3-(4,5-dimethylthiazol-2-yl)-5-(3-carboxymethoxyphenyl)-2-(4-sulfophenyl)-2H-tetrazolium, inner salt; MTS]) and human dermal fibroblasts, Ansurudeen et al. also demonstrated a greater number of viable cells in the presence of 50 mM carnosine after 24 h incubation [20]. Unfortunately, it is not traceable whether the fibroblasts used by Ansurudeen et al. were from juvenile foreskin or from adult skin. In addition, the experiments performed by Holliday and McFarland were done by using a fibroblast cell line established from human foreskin of a newborn male (HFF-1) and a second cell line established from lung tissue of a male at 14 weeks gestation (MRC-5). Considering using carnosine for the treatment of elderly patients the question had to be answered whether fibroblasts isolated

from adults or even senescent patients may behave different to fibroblasts isolated from fetal or newborn human tissue. In our experiments presented in Fig. 1 we did not see a measurable beneficial effect of carnosine on fibroblast viability, although it is interesting to note, that fibroblasts cultivated in 50 mM carnosine appeared to be rejuvenated compared to fibroblasts cultivated in the absence of carnosine in accordance to the observations of McFarland and Holiday [21]. We also did not see any correlation between age of the patient, the tissue of origin or gender, though it has to be realized that the number of samples may be too low for such an analysis and most of our patients have been of comparable age. More importantly, a prolonged cultivation of fibroblasts as in the co-culture experiments demonstrates that the fibroblasts are alive and able to occupy the space left by dying glioblastoma cells even under the highest concentration of carnosine employed (50 mM). It is also very interesting to note that we observed complete cell death of T98G tumor cells in long term culture incubating the cells at a concentration of 75 mM carnosine (Fig. 2). In previous experiments, cells were usually kept in the presence of carnosine for 24, 48 or 96 h [13] but not for 2 weeks. This is interesting, as shorter exposure times in previous experiments resulted in reduced proliferation but not complete elimination of tumor cells. Which processes are responsible for reduced tumor cell proliferation are under the influence of carnosine are still unknown [14]. However, it is an interesting question whether the processes which reduce proliferation after short term exposure may finally lead to cell death when the tumor cells are exposed to carnosine for a longer period of time.

In order to discriminate tumor cells from fibroblasts in ring co-culture experiments several markers were tested including glial fibrillary acidic protein (GFAP) which did also stained fibroblasts in accordance with observations made by others [22]. We finally identified that nestin-staining was suitable to discriminate primary cultured tumor cells from patient-derived fibroblasts. Nestin is a class VI intermediate filament protein and a marker for neural stem cells. In addition, it has been reported as a cancer stem cell-specific marker [23] and a recent meta-analysis performed by Lv et al. [24] demonstrated that increased expression of nestin is positively associated with higher histological grade in glioma patients. This analysis also indicated that patients with higher nestin expression are prone to recurrence and glioma cell infiltration into intact brain tissue. Surprisingly, in our ring co-culture experiments T98G cells, which did not express nestin, as previously reported by other investigators [25, 26], gave rise to many colonies in the surrounding fibroblast layer which was not the case when primary cultures with a high expression of nestin were cultivated

Oppermann *et al. Cancer Cell Int* (2018) 18:111

Page 9 of 10

with fibroblasts. Although speculative, one interpretation could be that the primary cultures we used were of very early passages (Passage 1 and 5) and not as rapidly growing as T98G cells which is also reflected by their higher resistance towards carnosine (Fig. 1) as carnosine exerts its action mainly on metabolic highly active tumor cells [27]. Nonetheless, the results presented in Fig. 6 clearly demonstrate that colony formation is significantly inhibited when invasively grown glioblastoma cells are treated with carnosine. In the last years, a so-called "go or grow concept" has been discussed, assuming that proliferation and migration are mutually exclusive phenomena in cancer cells [4]. Studies confirming this hypothesis are for example observations made in breast cancer cell lines in which overexpression of Homeobox Protein C9 (HOXC9) resulted in increased invasiveness but at the same time inhibited proliferation [28]. Another example is the observation that enforced expression of Y-box binding protein-1 (YB-1) in non-invasive breast epithelial cells induces an epithelial–mesenchymal transition (EMT) resulting in an enhanced metastatic potential but at the same time reduces proliferation [29]. Unfortunately, the exact mechanisms and down-stream targets responsible for either proliferation or invasion mediated by HOXC9 or YB-1 signaling are still unknown. More importantly, our results demonstrate that carnosine does not inversely influence proliferation and invasion. Up to now, the mechanisms responsible for the dipeptides antiproliferative effect, which has been confirmed in several studies with different types of cancer cells [11–13, 30] are still not understood. With regard to carnosine's effect on migration and invasion it has been discussed that it involves regulation of matrix metalloproteinases (MMPs) [15], but more experiments are certainly needed to properly address this question.

Conclusions

This study demonstrates that carnosine's anti-proliferative effect is not accompanied by increased invasion as suggested by the so-called "go-or-grow" concept. In fact, the dipeptide can inhibit tumor cell migration, which is especially important for the treatment of highly infiltrating and metastasizing tumors such as IDH-wildtype glioblastoma. In addition, the co-culture model presented is a valuable alternative to the commonly used scratch or Boyden chamber assays.

Additional files

Additional file 1: Table S1. Patients and patient derived cell cultures.

Additional file 2. Setup of ring-cultures.

Abbreviations

CTB: CellTiter-Blue Cell Viability Assay; CTG: CellTiter-Glo Luminescent Cell Viability Assay; GBM: IDH1R132H-non-mutant glioblastoma; GFAP: glial fibrillary acidic protein; HOXC9: Homeobox Protein C9; IDH: isocitrate dehydrogenase; MGMT: O-6-methylguanine-DNA methyltransferase; MTS: 3-(4,5-dimethylthiazol-2-yl)-5-(3-carboxymethoxyphenyl)-2-(4-sulfophenyl)-2H-tetrazolium, inner salt; YB-1: Y-box binding protein-1; WHO: World Health Organization.

Authors' contributions
JD performed most of the experiments with contributions of HO and KP. MM and CE assisted at microscopy and immuno-histochemistry. WM and CE performed the pathologic classification of tumors. JM did the surgery and revised the manuscript. HO, JD and FG designed the experiments and contributed conceptually. HO and FG coordinated the experiments. JD and FG mainly wrote the manuscript but all authors contributed to its writing. All authors read and approved the final manuscript.

Author details
[1] Department of Neurosurgery, University Hospital Leipzig, Liebigstraße 20, 04103 Leipzig, Germany. [2] Medical Faculty, Paul-Flechsig-Institute of Brain Research, University of Leipzig, Leipzig, Germany. [3] Department of Neuropathology, University Hospital Leipzig, Leipzig, Germany.

Publisher's Note
Springer Nature remains neutral with regard to jurisdictional claims in published maps and institutional affiliations.

References

1. Louis DN, Ohgaki H, Wiestler OD, Cavenee WK. WHO classification of tumours of the central nervous system. 4th ed. Lyon: International Agency for Research on Cancer; 2016.
2. Mallick S, Benson R, Hakim A, Rath GK. Management of glioblastoma after recurrence: a changing paradigm. J Egypt Natl Cancer Inst. 2016;28:199–210. https://doi.org/10.1016/j.jnci.2016.07.001.
3. Giese A, Loo MA, Tran N, Haskett D, Coons SW, Berens ME. Dichotomy of astrocytoma migration and proliferation. Int J Cancer. 1996;67:275–82.

Oppermann *et al. Cancer Cell Int* (2018) 18:111

Page 10 of 10

https://doi.org/10.1002/(SICI)1097-0215(19960717)67:2%3c275:AID-IJC20%3e3.0.CO;2-9.

4. Hatzikirou H, Basanta D, Simon M, Schaller K, Deutsch A. 'Go or grow': the key to the emergence of invasion in tumour progression? Math Med Biol. 2012;29:49–65. https://doi.org/10.1093/imammb/dqq011.

5. Gulewitsch W, Amiradzibi S. Ueber das Carnosin, eine neue organische Base des Fleischextraktes. Ber Dtsch Chem Ges. 1900;33:1902–3.

6. Boldyrev AA, Aldini G, Derave W. Physiology and pathophysiology of carnosine. Physiol Rev. 2013;93:1803–45. https://doi.org/10.1152/physrev.00039.2012.

7. Gaunitz F, Hipkiss AR. Carnosine and cancer: a perspective. Amino Acids. 2012;43:135–42. https://doi.org/10.1007/s00726-012-1271-5.

8. Hipkiss AR, Gaunitz F. Inhibition of tumour cell growth by carnosine: some possible mechanisms. Amino Acids. 2014;46:327–37.

9. Nagai K, Suda T. Antineoplastic effects of carnosine and beta-alanine—physiological considerations of its antineoplastic effects. J Physiol Soc Jpn. 1986;48:741–7.

10. Holliday R, McFarland GA. Inhibition of the growth of transformed and neoplastic cells by the dipeptide carnosine. Br J Cancer. 1996;73:966–71.

11. Shen Y, Yang J, Li J, Shi X, Ouyang L, Tian Y, Lu J. Carnosine inhibits the proliferation of human gastric cancer SGC-7901 cells through both of the mitochondrial respiration and glycolysis pathways. PLoS ONE. 2014;9:e104632. https://doi.org/10.1371/journal.pone.0104632.

12. Iovine B, Oliviero G, Garofalo M, Orefice M, Nocella F, Borbone N, et al. The anti-proliferative effect of L-carnosine correlates with a decreased expression of hypoxia inducible factor 1 alpha in human colon cancer cells. PLoS ONE. 2014;9:e96755. https://doi.org/10.1371/journal.pone.0096755.

13. Renner C, Seyffarth A, de Arriba S, Meixensberger J, Gebhardt R, Gaunitz F. Carnosine inhibits growth of cells isolated from human glioblastoma multiforme. Int J Pept Res Ther. 2008;14:127–35. https://doi.org/10.1007/s10989-007-9121-0.

14. Gaunitz F, Oppermann H, Hipkiss AR. Carnosine and cancer. In: Preedy VR, editor. Imidazole dipeptides. Cambridge: The Royal Society of Chemistry; 2015. p. 372–92.

15. Chuang C-H, Hu M-L. L-Carnosine inhibits metastasis of SK-Hep-1 cells by inhibition of matrix metaoproteinase-9 expression and induction of an antimetastatic gene, nm23-H1. Nutr Cancer. 2008;60:526–33. https://doi.org/10.1080/01635580801911787.

16. Ou-Yang L, Liu Y, Wang B-Y, Cao P, Zhang J-J, Huang Y-Y, et al. Carnosine suppresses oxygen–glucose deprivation/recovery-induced proliferation and migration of reactive astrocytes of rats in vitro. Acta Pharmacol Sin. 2018;39:24–34. https://doi.org/10.1038/aps.2017.126.

17. Lai P-Y, Hsieh S-C, Wu C-C, Hsieh S-L. ID: 1029 Effects of carnosine on regulation of migration and invasion in human colorectal cancer cells. Biomed Res Ther. 2017;4:104. https://doi.org/10.15419/bmrat.v4iS.305.

18. Goodpaster T, Legesse-Miller A, Hameed MR, Aisner SC, Randolph-Habecker J, Coller HA. An immunohistochemical method for identifying fibroblasts in formalin-fixed, paraffin-embedded tissue. J Histochem Cytochem. 2008;56:347–58. https://doi.org/10.1369/jhc.7A7287.2007.

19. Holliday R, McFarland GA. A role for carnosine in cellular maintenance. Biochemistry (Mosc). 2000;65:843–8.

20. Ansurudeen I, Sunkari VG, Grünler J, Peters V, Schmitt CP, Catrina S-B, et al. Carnosine enhances diabetic wound healing in the db/db mouse model of type 2 diabetes. Amino Acids. 2012;43:127–34. https://doi.org/10.1007/s00726-012-1269-z.

21. McFarland GA, Holliday R. Further evidence for the rejuvenating effects of the dipeptide L-carnosine on cultured human diploid fibroblasts. Exp Gerontol. 1999;34:35–45.

22. Hainfellner JA, Voigtländer T, Ströbel T, Mazal PR, Maddalena AS, Aguzzi A, Budka H. Fibroblasts can express glial fibrillary acidic protein (GFAP) in vivo. J Neuropathol Exp Neurol. 2001;60:449–61.

23. Neradil J, Veselska R. Nestin as a marker of cancer stem cells. Cancer Sci. 2015;106:803–11. https://doi.org/10.1111/cas.12691.

24. Lv D, Lu L, Hu Z, Fei Z, Liu M, Wei L, Xu J. Nestin expression is associated with poor clinicopathological features and prognosis in glioma patients: an association study and meta-analysis. Mol Neurobiol. 2017;54:727–35. https://doi.org/10.1007/s12035-016-9689-5.

25. Kurihara H, Zama A, Tamura M, Takeda J, Sasaki T, Takeuchi T. Glioma/glioblastoma-specific adenoviral gene expression using the nestin gene regulator. Gene Ther. 2000;7:686–93. https://doi.org/10.1038/sj.gt.3301129.

26. Hong X, Chedid K, Kalkanis SN. Glioblastoma cell line-derived spheres in serum-containing medium versus serum-free medium: a comparison of cancer stem cell properties. Int J Oncol. 2012;41:1693–700. https://doi.org/10.3892/ijo.2012.1592.

27. Oppermann H, Schnabel L, Meixensberger J, Gaunitz F. Pyruvate attenuates the anti-neoplastic effect of carnosine independently from oxidative phosphorylation. Oncotarget. 2016;7:85848–60. https://doi.org/10.18632/oncotarget.13039.

28. Hur H, Lee J-Y, Yang S, Kim JM, Park AE, Kim MH. HOXC9 induces phenotypic switching between proliferation and invasion in breast cancer cells. J Cancer. 2016;7:768–73. https://doi.org/10.7150/jca.13894.

29. Evdokimova V, Tognon C, Ng T, Ruzanov P, Melnyk N, Fink D, et al. Translational activation of snail1 and other developmentally regulated transcription factors by YB-1 promotes an epithelial–mesenchymal transition. Cancer Cell. 2009;15:402–15. https://doi.org/10.1016/j.ccr.2009.03.017.

30. Zhang Z, Miao L, Wu X, Liu G, Peng Y, Xin X, et al. Carnosine inhibits the proliferation of human gastric carcinoma cells by retarding Akt/mTOR/p70S6K signaling. J Cancer. 2014;5:382–9. https://doi.org/10.7150/jca.8024.

In summary, the experiments performed demonstrate that carnosine inhibits both colony formation and proliferation of glioblastoma cells. Thus, the anti-proliferative effect of carnosine is not accompanied by increased invasion as suggested by the "go or growth" concept. Furthermore, we also demonstrate that prolonged exposure to carnosine reduces glioblastoma growth also at lower concentrations (10 mM) than at those employed investigating the dipeptides anti-neoplastic effect in short term experiments (50 mM and higher) (Asperger et al. 2011; Iovine et al. 2012; Lee et al. 2018). Moreover, fibroblasts remained vital even in the presence of the highest carnosine concentration employed.

2.6 Carnosine does not interfere with standard therapy for glioblastoma

Considering using carnosine for the treatment of glioblastoma patients, possible interactions with the current standard therapy need to be taken into account. According to the European Association for Neuro-Oncology, treatment of newly diagnosed glioblastoma consist of microsurgical resection of the tumour followed by radiotherapy and adjuvant chemotherapy with TMZ ((Weller et al. 2014) and see 1.1 Glioblastoma). TMZ is a pro-drug which is dependent on pH non-enzymatically converted to 5-(3-methyltriazen-1-yl)imidazole-4-carboxamide (MTIC). MTIC yields diazomethane which spontaneously produces a methyldiazonium cation leading to the formation of methyl adducts at the guanine residue of DNA (Bonmassar et al. 2013). Although carnosine exhibits potent pH puffer capabilities, it is unknown whether the dipeptide affects MTIC formation from TMZ. However, it was reported that carnosine mitigates genotoxicity induced by the alkylating agent cyclophosphamide (Naghshvar et al. 2012). The biological effect of IR is conducted by the formation of reactive oxygen and nitrogen species leading to DNA damage, changes in redox signalling and disruption of metabolic processes (Spitz and Hauer-Jensen 2014). As carnosine is capable of scavenging free radicals and has even been shown to attenuate IR induced damage (Guney et al. 2006), the dipeptide may attenuate the effect of IR which is indispensable for an improved outcome of glioblastoma patients (Laperriere et al. 2002). The study of Dietterle et al. (Dietterle et al. 2019) addresses the question whether carnosine attenuates the effects of IR and TMZ in glioblastoma. Therefore, we determined the influence of carnosine on cell viability in combination with IR and TMZ in primary glioblastoma cultures.

Carnosine increases efficiency of temozolomide and irradiation treatment of isocitrate dehydrogenase-wildtype glioblastoma cells in culture

Johannes Dietterle[‡,1], Henry Oppermann[‡,1], Annegret Glasow[2], Karsten Neumann[3], Jürgen Meixensberger[1] & Frank Gaunitz*[,1] (iD)

[1]Department of Neurosurgery, University Hospital Leipzig, Leipzig, Germany
[2]Department of Radiooncology, University of Leipzig, Leipzig, Germany
[3]Department of Pathology, Medical Clinic Dessau, Germany
*Author for correspondence: Tel.: +49 341 971 7544; Fax: +49 341 971 7509; Frank.Gaunitz@medizin.uni-leipzig.de
[‡] Authors contributed equally

Aim: The naturally occurring dipeptide carnosine (CAR) has been considered for glioblastoma therapy. As CAR also protects against ionizing irradiation (IR), we investigated whether it may counteract standard therapy consisting of postsurgery IR and treatment with temozolomide (TMZ). **Materials & methods:** Four isocitrate dehydrogenase-wildtype primary cell cultures were exposed to different doses of IR and different concentrations of TMZ and CAR. After exposure, viability under the different conditions and combinations of them was determined. **Results:** All cultures responded to treatment with TMZ and IR with reduced viability. CAR further decreased viability when TMZ and IR were combined. **Conclusion:** Treatment with CAR does not counteract glioblastoma standard therapy. As the dipeptide also protects nontumor cells from IR, it may reduce deleterious side effects of treatment.

*Isocitrate dehydrogenas*e (*IDH*)-wildtype glioblastoma (GBM) is a brain-derived tumor classified as WHO grade IV based on histologic criteria, including high vascularization, high mitotic activity and invasion of adjacent brain structures [1]. GBM is the most common of all malignant brain and other CNS tumors (47.7%) and accompanied with very poor prognosis for patients (1-year survival: $39.7 \pm 0.5\%$; 2-year survival: $17.2 \pm 0.4\%$) [2]. Standard treatment consists of microsurgical resection and adjuvant radiochemotherapy consisting of up to 60 Gray (Gy) x-irradiation (IR) with concomitant temozolomide (TMZ) treatment followed by six cycles of the TMZ treatment alone [3]. Although technical aspects of neurosurgery, including intraoperative magnetic resonance imaging [4], mapping of brain functions [5] or awake craniotomy [6] have improved to provide maximum safe resection, pharmacological therapy options remain poor [7]. In 2007, anti-angiogenic therapy with bevacizumab has been approved for the treatment of recurrent GBM by the US FDA [8], yet meta-analysis did not show statistically significant extension of overall survival [9]. Presently, the most promising new option to treat GBM are tumor-treating fields that have shown to extent overall survival in large clinical trials by around 2–3 months [10] but are not included into European guidelines for glioblastoma treatment until the present day [3]. As these new treatment options are also far from being satisfying there is still urgent need to find new treatment strategies and compounds that are able to selectively eliminate GBM tumor cells after surgical resection.

In a number of preclinical investigations, the naturally occurring dipeptide carnosine (CAR; β-alanyl-L-histidine) was suggested as a potential new anticancer drug, also for the treatment of GBM [11]. The dipeptide was originally discovered in 1900 by Gulewitsch and Amiradžibi [12], but its physiological role is still not fully understood. It has been suggested that it has pH-buffering functions [13] and could act as a modulator of intracellular calcium [14]. It is also able to act as a metal chelator [15], a scavenger of radical oxygen species [16], and as a protector against lipid

Table 1. Primary cell cultures used for the experiments.					
Culture label	Gender	Age at date of surgery in years	MGMT promoter methylation status (%)	IDH1-status (codon 132)	IDH2-status (codon 172)
Number 1	Female	53	46%	WT	WT
Number 2	Male	69	<10	WT	WT
Number 3	Female	64	96%	WT	WT
Number 4	Male	60	96%	WT	WT

Gender (male/female) and age of the patient at surgery are indicated along with the *MGMT* promoter methylation status and the i*socitrate dehydrogenase1/2* mutation status (all WT) determined in the culture.
IDH: Isocitrate dehydrogenase; MGMT: O-6-methylguanine-DNA methyltransferase; WT: Wildtype.

peroxidation, hypochlorite anions and reactive nitrogen species [17]. As it exhibits antineoplastic effects *in vitro* and *in vivo* against a range of cancer cells, including GBM [18], colon [19,20], gastric [21] and cervix carcinoma [22] cells, it has been discussed as potential drug for the treatment of malignant diseases [23].

On the other hand, it is known since many years that the dipeptide has radioprotective properties [24–26]. In fact, this effect could be exploited as suggested for the CAR-containing drug polaprezinc (Zeria Pharmaceutical Co., Tokyo, Japan) [27] which has already been used in clinical trials [28]. However, it has to be asked whether the radioprotective properties may become a problem when standard therapy of GBM including TMZ and especially IR would be combined with CAR treatment.

Therefore, we investigated whether CAR interferes with standard therapy using four primary GBM cell cultures.

Materials & methods
Reagents
If not stated otherwise, all chemicals were purchased from Sigma-Aldrich (Taufkirchen, Germany), Merck (Darmstadt, Germany) or Carl Roth (Karlsruhe, Germany). CAR was kindly provided by Flamma s.p.a. (Chignolo d'Isola, Italy).

Primary glioblastoma cell cultures
Primary GBM cultures were derived from tissue samples obtained during standard surgery performed at the Department of Neurosurgery of the University of Leipzig Medical Center between 2005 and 2009 (Table 1). Written informed consent from all patients was obtained according to the German laws as confirmed by the local committee (144/08-ek). All samples were diagnosed at the Department of Neuropathology of the University of Leipzig Medical Center. After cell cultures were established as described in detail before [29], cell suspensions containing one million cells in 1 ml freezing medium (Dulbecco's modified Eagle medium supplemented with 15% fetal bovine serum and 10% dimethyl sulfoxide) were slowly cooled down to -80°C (Nalgene Mr. Frosty, Thermo Fisher Scientific, Darmstadt, Germany) and finally stored at -174°C in liquid nitrogen (Air Liquide, Düsseldorf, Germany).

For cultivation, cell suspensions were warmed up at room temperature and transferred into 75 mm^2 culture flasks (TPP, Trasadingen, Switzerland). Cell cultures were maintained in high glucose Dulbecco's modified Eagle medium (4.5 g glucose/l) supplemented with 1% penicillin/streptomycin, GlutaMax (both, Thermo Fisher Scientific) and 10% fetal bovine serum (Biochrom GmbH, Berlin, Germany), further referred to as 'standard medium,' and kept in incubators (37°C, 5% CO_2/95% air), further referred to as 'standard condition.' After unfreezing, *IDH1/2* mutation status and O-6-methylguanine-DNA methyltransferase (*MGMT*) promoter methylation of all cell cultures were determined using immunohistochemistry and pyrosequencing or nucleic acid amplification followed by pyrosequencing (PyroMark Q24 System and the PyroMark Q24 CpG *MGMT* kit; Qiagen, Hilden, Germany), respectively (Table 1).

Irradiation
A 150 kV x-ray machine (DARPAC 150-MC, RayTech) with a dose rate of 0.86 Gy/min was used for IR.

Cell-based assays
Primary GBM cells were seeded into 96-well plates (μClear, Greiner Bio One, Frickenhausen, Germany) at a density of 2500 cells per well in 200 μl standard medium. After 24 h incubation, cells received fresh medium
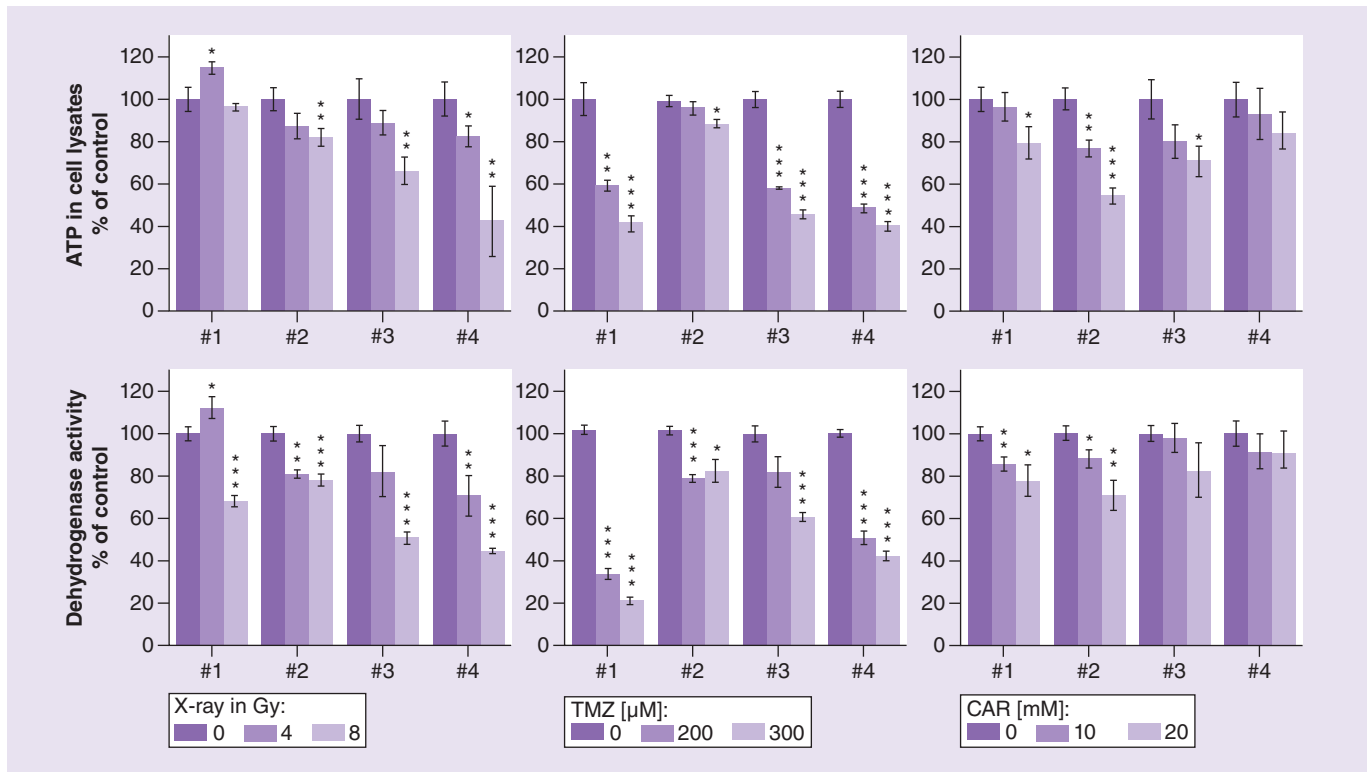
Figure 1.   Viability of glioblastoma cells under the influence of irradiation, temozolomide and carnosine. Cells were treated with 4 or 8 Gy (left panels), 200 and 300 μM TMZ (central panels) and 10 and 20 mM CAR (right panels). Viability was determined by measuring ATP in cell lysates (upper panels) or dehydrogenase activity in living cells (lower panels). Experiments have been performed in sextuplicate and asterisks denote significance compared with untreated control cells as determined by one-way ANOVA with Games–Howell post hoc test ($*p < 0.05$; $**p < 0.005$; $***p < 0.0005$).
ANOVA: Analysis of variance; CAR: Carnosine; TMZ: Temozolomide.

containing the test compounds CAR and/or TMZ. IR was applied 24 h later and cell viability was assessed after incubation for another 5 days under standard conditions (for details see single experiments).

In order to assess tumor cell viability, ATP in cell lysates and dehydrogenase activity in living cells were determined using the CellTiter-Glo Luminescent Cell Viability Assay (CTG) and the CellTiter-Blue Cell Viability Assay (CTB), respectively (both from Promega, Mannheim, Germany). Luminescence and fluorescence were measured using SpectraMax M5 Microplate Reader (Molecular Devices, Biberach, Germany).

Statistical analysis
Statistical analysis was carried out using SPSS (IBM, NY, USA; version: 24.0.0.2 64-bit). For multiple comparisons, a one-way analysis of variance (ANOVA) with Games–Howell post hoc test was used. p-values below 0.05 were considered statistically significant.

Results
In a first series of experiments, we determined the effect of each compound and of IR on tumor cell viability in four primary GBM cultures. Therefore, cells either received a single dose of 4 or 8 Gy, 200 or 300 μM TMZ and 10 or 20 mM CAR and cell viability was determined after 5 days. The results to the experiments are depicted in Figure 1. Aside from a surprising slight significant increase of viability observed when cells from culture number 1 were exposed to 4 Gy (CTB: 112.2 ± 5.2%; CTG: 114.9 ± 22.9%; p > 0.05) all cultures responded to IR with decreased viability, which was highly significant with both assays at 8 Gy (with the exception of culture number 1 with regard to CTG). We also observed a reduction of viability at 4 Gy in all cultures except for culture number 1 but statistical significance was not reached in all cases. Exposing the cells to 300 μM TMZ significantly reduced viability in all cell cultures with both assays. At a concentration of 200 μM TMZ all cultures except
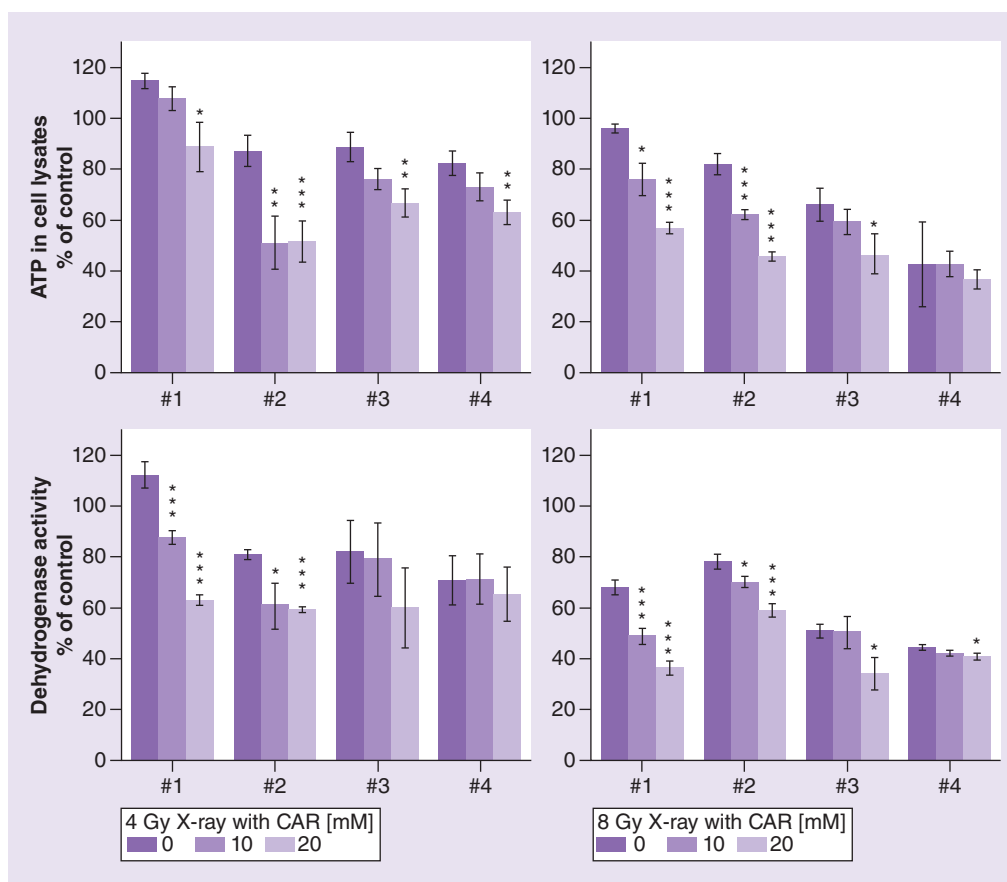
Figure 2.   Viability of glioblastoma cells under the influence of irradiation combined with carnosine. Cells were treated with 4 Gy (left panels) or 8 Gy (right panels) in combination with 10 and 20 mM CAR. Viability was determined by measuring ATP in cell lysates (upper panels) or dehydrogenase activity in living cells (lower panels). Experiments have been performed in sextuplicate and asterisks denote significance compared with untreated control cells as determined by one-way ANOVA with Games–Howell post hoc test: *p < 0.05; **p < 0.005; ***p < 0.0005. CAR: Carnosine.

culture number 2 responded with reduced ATP in cell lysates. Although a response of this culture was seen with regard to dehydrogenase activity, this culture in general exhibited a weak response towards TMZ. This is in fact not surprising as this culture exhibited very low *MGMT* promoter methylation (Table 1) which confers resistance toward TMZ [30]. At the concentrations employed, the effect of CAR on tumor cell viability was obvious and more pronounced in the presence of 20 mM than in the presence of 10 mM CAR, although the effect did not reach statistical significance in all cases. Only culture number 4 does appear to have a very low response to the presence of the dipeptide.

Next, we combined CAR treatment with IR (Figure 2) or with TMZ treatment (Figure 3). In both figures, statistical significance is depicted with regard to treatment with 4/8 Gy or 200/300 mM TMZ without CAR. As can be seen in Figure 2, treatment with CAR further decreased viability of cells exposed to IR even in culture number 1 which exhibited higher viability when exposed to 4 Gy alone. Almost no effect of CAR on irradiated cells was seen in culture number 4 which is in agreement with the results presented in Figure 1. Analyzing the effect of CAR on treatment with TMZ (Figure 3) all cultures responded to the presence of CAR with a further decrease in viability when exposed to TMZ as revealed by the CTG assay. However, although the CTB also demonstrated a tendency toward lower viability with increasing concentrations of CAR, this effect was weak and reached statistical significance only in a few cases. More important, both experiments in Figures 2 & 3 demonstrate that CAR does not counteract the effects of TMZ or IR on cell viability.

Finally, we asked whether CAR may counteract the effect of combined treatment with IR and TMZ, mimicking glioblastoma standard therapy. Therefore, we applied 4 Gy together with 200 μM TMZ and compared viability
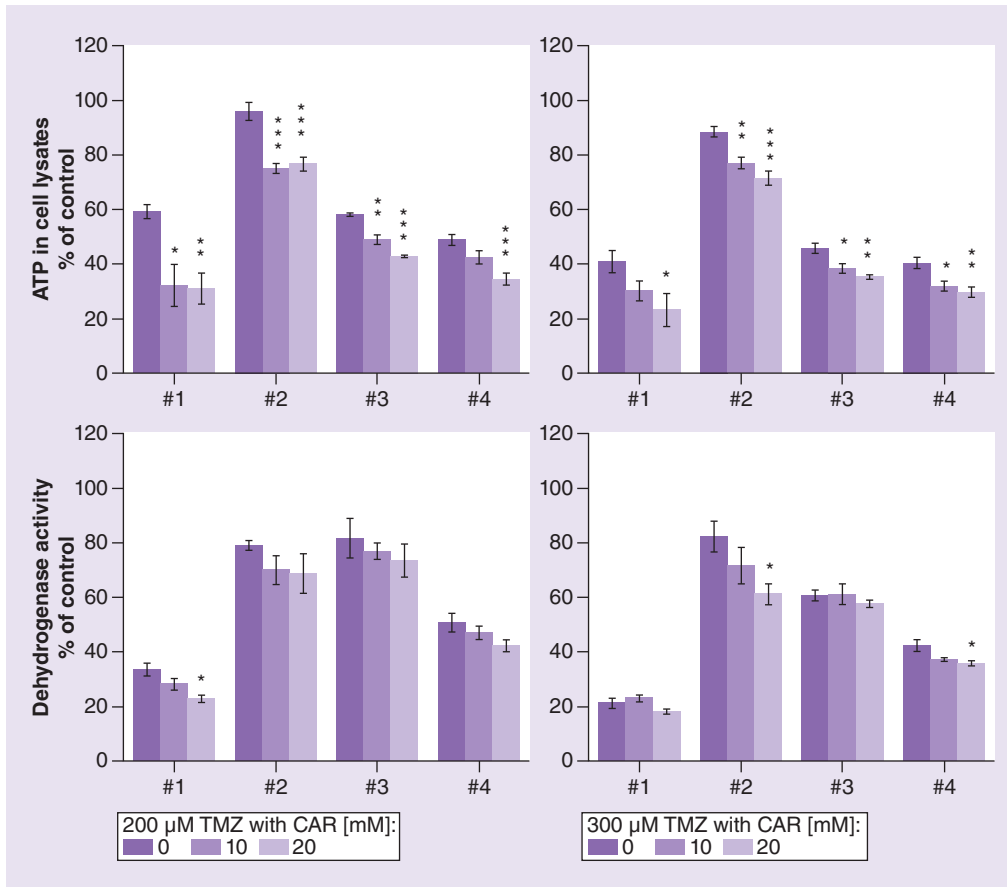
Figure 3.   Viability of glioblastoma cells under the influence of temozolomide combined with carnosine. Cells were treated with 200 μM (left panels) or 300 μM TMZ (right panels) in combination with 10 and 20 mM CAR. Viability was determined by measuring ATP in cell lysates (upper panels) or dehydrogenase activity in living cells (lower panels). Experiments have been performed in sextuplicate and asterisks denote significance compared with untreated control cells as determined by one-way ANOVA with Games–Howell post hoc test: *p < 0.05; **p < 0.005; ***p < 0.0005. CAR: Carnosine; TMZ: Temozolomide.

of cells without CAR and with 20 mM CAR to untreated control cells (Figure 4). As can be seen, CAR had no counter-effect on combined treatment with TMZ and IR but did even further decrease viability in all cell cultures. The additional viability reduction was statistically significant in three of the four cultures employed (numbers 1–3).

Discussion

Although CAR appears to be a promising candidate for the treatment of different malignant diseases [23], including GBM, one has to be aware that it is also able to protect against IR. Severin *et al.*, who investigated the influence of CAR (50–200 mg/kg/day for 20 days) on the survival of albino rats subjected to 5 Gy whole body IR, observed an increased survival rate by 45–65% [24]. Comparable observations were made by other groups [25,26,31] and it was suggested that CAR could be used to alleviate symptoms due to IR-induced lung injury in patients treated for lung cancer [32]. Just recently, Doi *et al.* [28] collected data from clinical studies in which polaprezinc, an orally bioavailable chelate composed of zinc and CAR, was applied together with IR therapy demonstrating potential beneficial effects. As the biological effects of IR are mediated by the production of reactive oxygen and nitrogen species [33], the well-described antioxidant activity of CAR [16] appears to be responsible for its IR-protective effects. However, IR-induced production of reactive oxygen species in the tumor is required for the clinical efficiency of IR. As demonstrated by Bairati *et al.* in the case of patients treated by radiation therapy for head and neck cancer, supplementation of antioxidant vitamins can significantly increase mortality rates [34]. Therefore, it could not be precluded, that the antineoplastic effects of CAR may be counteracted by protection against IR applied in the course of cancer treatment. As demonstrated by the results presented in this manuscript, this does not seem to be
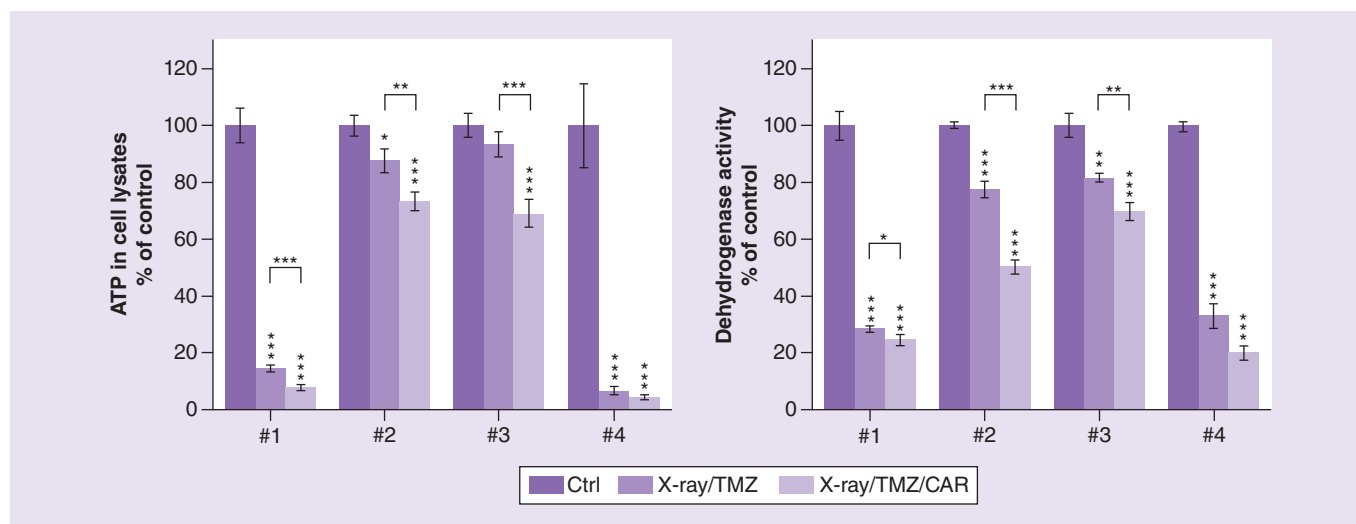
Figure 4.   Viability of glioblastoma cells under the influence of temozolomide combined with irradiation and of temozolomide plus irradiation combined with carnosine. Cells were treated with 200 μM TMZ in combination IR 4 Gy and additionally with CAR (20 mM). Viability was determined by measuring ATP in cell lysates (left panel) or dehydrogenase activity in living cells (right panel).
Experiments have been performed in sextuplicate and asterisks denote significance compared with untreated control cells as determined by one-way ANOVA with Games–Howell post hoc test: *p < 0.05; **p < 0.005; ***p < 0.0005.
CAR: Carnosine; TMZ: Temozolomide.

the case. CAR, employed at concentrations of 10 and 20 mM, did neither counteract the effect of IR (4 and 8 Gy) on GBM cell viability nor that of TMZ (200 and 300 µM). More important, CAR employed at a concentration of 20 mM together with TMZ and IR (200 µM and 4 Gy) did further decrease the viability of GBM cells compared with cells treated only with a combination of TMZ and IR.

Regarding a potential therapeutic use of CAR, the question has to be answered whether the concentrations used in our experiments are therapeutically feasible. In nonsupplemented humans, it reaches a median concentration of about 20.0 ± 4.7 mmol/kg dry weight in skeletal muscle [35], but can be increased by 50% (soleus) by a daily administration of the CAR moieties β-alanine and L-histidine over 23 days [36]. Although less abundant in other tissues, Qui *et al.* demonstrated that in kidney tissue of *CNDP1* transgenic mice supplemented with a bolus of 200 mg CAR concentrations of approximately 0.5 mmol/kg were observed 8 h after supplementation [37]. More interesting, the authors could also demonstrate that in mice receiving a CN1 inhibitor, tissue concentrations increased sevenfold, which is an interesting aspect considering CAR as a therapeutic. At this point, it is also interesting to note that CAR appears to be nontoxic to nontumor cells even at concentrations up to 50 mM as demonstrated already in 1994 by McFarland and Holiday [38]. In addition, aside from a rare and mild dysesthesia reported after oral ingestion of CAR no other side effects have been described in a number of small clinical trials supplementing CAR for the treatment of other diseases [39,40].

The next step that should be performed is to address, how cancer stem cells respond to combined treatment, as these cells are generally more resistant to IR than their more mature progeny, exhibiting lower levels of reactive oxygen species associated with increased expression of free radical scavenging systems [41]. In addition, experiments should be performed to investigate whether the protective effects of CAR described in the literature could be exploited for GBM standard therapy, protecting nontumor cells. These experiments could possibly be done with ectopic GBM mouse models.

Conclusion

The experiments presented demonstrate that it seems to be safe to combine CAR with IR and TMZ for GBM therapy and most likely also for other cancer therapies. As CAR was shown to protect animals from deleterious side effects of IR and as up to now no deleterious side effects on nontumor cells have been observed, the dipeptide or its zinc chelate could become a valuable supplement for the treatment of different malignancies.

Future perspective

Deleterious side effects of ionizing IR caused by radiotherapy of cancer are a serious problem causing acute and late morbidities. Up to now, most radioprotectors tested had limited success and also the FDA-approved and currently used radioprotector amifostine, which has been used with success, has side effects such as allergic reactions, hypotension, nausea and vomiting. CAR, which is long known to have radioprotective effects, is a naturally occurring compound without known side effects. As it also has antineoplastic activity, the compound or drugs derived from it, such as polaprezinc, may become a valuable adjuvant to radiotherapy not only in the case of glioblastoma.

Executive summary

- Glioblastoma is the most common *de novo* brain malignancy and accompanied with very poor prognosis for patients.
- Current standard therapy of glioblastoma consists of tumor removal by surgery, followed by radiotherapy combined with temozolomide (TMZ) treatment.
- Median survival of patients undergoing standard therapy is poor with a 5-year survival rate of 5.5% after diagnosis.
- The naturally occurring dipeptide carnosine (CAR) was shown to have antineoplastic effects *in vitro* and *in vivo* in a number of animal and cell culture models, including glioblastoma.
- CAR is known to have radioprotective functions due to its ability to scavenge reactive oxygen and nitrogen species.
- CAR does not counteract the effects of radiation or TMZ treatment in *isocitrate dehydrogenase*-wildtype glioblastoma cell cultures.
- CAR further reduces cell viability when combined with radiation and TMZ treatment.
- CAR or drugs derived from it, such as polaprezinc, may become a valuable adjuvant to radiotherapy not only in the case of glioblastoma.

References

1. Louis DN, Ohgaki H, Wiestler OD, Cavenee WK. *WHO Classification of Tumours of the Central Nervous System (4th Revised Edition)*. International Agency for Research on Cancer, Lyon, France (2016).

2. Ostrom QT, Gittleman H, Truitt G, Boscia A, Kruchko C, Barnholtz-Sloan JS. CBTRUS statistical report: primary brain and other central nervous system tumors diagnosed in the United States in 2011–2015. *Neuro Oncol.* 20(Suppl. 4), iv1–iv86 (2018).

3. Weller M, van den Bent M, Tonn JC *et al.* European Association for Neuro-Oncology (EANO) guideline on the diagnosis and treatment of adult astrocytic and oligodendroglial gliomas. *Lancet Oncol.* 18(6), e315–e329 (2017).

4. Marongiu A, D'Andrea G, Raco A. 1.5-T field intraoperative magnetic resonance imaging improves extent of resection and survival in glioblastoma removal. *World Neurosurg.* 98, 578–586 (2017).

5. Sanai N, Mirzadeh Z, Berger MS. Functional outcome after language mapping for glioma resection. *N. Engl. J. Med.* 358(1), 18–27 (2008).

6. Hervey-Jumper SL, Li J, Lau D *et al.* Awake craniotomy to maximize glioma resection: methods and technical nuances over a 27-year period. *J. Neurosurg.* 123(2), 325–339 (2015).

7. Mooney J, Bernstock JD, Ilyas A *et al.* Current approaches and challenges in the molecular therapeutic targeting of glioblastoma. *World Neurosurg.* doi:10.1016/j.wneu.2019.05.205 (2019) (Epub ahead of print).

8. Cohen MH, Shen YL, Keegan P, Pazdur R. FDA drug approval summary: bevacizumab (Avastin) as treatment of recurrent glioblastoma multiforme. *Oncologist* 14(11), 1131–1138 (2009).

9. Kim MM, Umemura Y, Leung D. Bevacizumab and glioblastoma: past, present, and future directions. *Cancer J.* 24(4), 180–186 (2018).

10. Fabian D, Guillermo Prieto Eibl MDP, Alnahhas I *et al.* Treatment of glioblastoma (GBM) with the addition of tumor-treating fields (TTF): a review. *Cancers* 11(2), 1–12 (2019).

11. Renner C, Seyffarth A, de Arriba S, Meixensberger J, Gebhardt R, Gaunitz F. Carnosine inhibits growth of cells isolated from human glioblastoma multiforme. *Int. J. Pept. Res. Ther.* 14, 127–135 (2008).

12. Gulewitsch W, Amiradžibi S. Ueber das Carnosin, eine neue organische Base des Fleischextraktes. *Ber. Dtsch. Chem. Ges.* 33, 1902–1903 (1900).

13. Smith EC. The buffering of muscle in rigor; protein, phosphate and carnosine. *J. Physiol.* 92(3), 336–343 (1938) 16994977.

14. Zaloga GP, Roberts PR, Black KW *et al.* Carnosine is a novel peptide modulator of intracellular calcium and contractility in cardiac cells. *Am. J. Physiol.* 272(1 Pt 2), H462–8 (1997).

15. Baran EJ. Metal complexes of carnosine. *Biochemistry (Mosc.)* 65(7), 789–797 (2000) 10951097.

16. Kohen R, Yamamoto Y, Cundy KC, Ames BN. Antioxidant activity of carnosine, homocarnosine, and anserine present in muscle and brain. *Proc. Natl Acad. Sci. USA* 85(9), 3175–3179 (1988) 3362866.

17. Boldyrev AA, Aldini G, Derave W. Physiology and pathophysiology of carnosine. *Physiol. Rev.* 93(4), 1803–1845 (2013).

18. Renner C, Zemitzsch N, Fuchs B *et al.* Carnosine retards tumor growth *in vivo* in an NIH3T3-HER2/neu mouse model. *Mol. Cancer* 9, 2 (2010).

19. Horii Y, Shen J, Fujisaki Y, Yoshida K, Nagai K. Effects of l-carnosine on splenic sympathetic nerve activity and tumor proliferation. *Neurosci. Lett.* 510(1), 1–5 (2012).

20. Iovine B, Oliviero G, Garofalo M *et al.* The anti-proliferative effect of L-carnosine correlates with a decreased expression of hypoxia inducible factor 1 alpha in human colon cancer cells. *PLoS ONE* 9(5), e96755 (2014).

21. Shen Y, Yang J, Li J *et al.* Carnosine inhibits the proliferation of human gastric cancer SGC-7901 cells through both of the mitochondrial respiration and glycolysis pathways. *PLoS ONE* 9(8), e104632 (2014).

22. Ditte Z, Ditte P, Labudova M *et al.* Carnosine inhibits carbonic anhydrase IX-mediated extracellular acidosis and suppresses growth of HeLa tumor xenografts. *BMC Cancer* 14, 358 (2014).

23. Gaunitz F, Hipkiss AR. Carnosine and cancer: a perspective. *Amino Acids* 43(1), 135–142 (2012).

24. Severin SE, Boldyrev AA, Stvolinsky SL *et al.* On radioprotective efficacy of carnosine. *Radiobiologiia* 30(6), 765–768 (1990).

25. Kurella EG, Maltzeva VV, Seslavina LS, Stvolinsky SL. Stimulating action of carnosine on hematopoietic stem-cells. *Biull. Eksp. Biol. Med.* 112(7), 966–968 (1991).

26. Naumova OV, Goncharenko EN, Deev LI. [The effect of carnosine on the liver enzyme system in the irradiated body]. *Biokhimiia* 57(9), 1373–1377 (1992).

27. Odawara S, Doi H, Shikata T *et al.* Polaprezinc protects normal intestinal epithelium against exposure to ionizing radiation in mice. *Mol. Clin. Oncol.* 5(4), 377–381 (2016).

28. Doi H, Kuribayashi K, Kijima T. Utility of polaprezinc in reducing toxicities during radiotherapy: a literature review. *Future Oncol.* 14(19), 1977–1988 (2018).

29. Oppermann H, Dietterle J, Purcz K *et al.* Carnosine selectively inhibits migration of IDH-wildtype glioblastoma cells in a co-culture model with fibroblasts. *Cancer Cell Int.* 18, 111 (2018).

30. Hegi ME, Diserens A-C, Gorlia T *et al.* MGMT gene silencing and benefit from temozolomide in glioblastoma. *N. Engl. J. Med.* 352(10), 997–1003 (2005).

31. Zainal TA, Srinivasan V, Whitnall MH. Evaluation of carnosine as a radiation countermeasure agent. *Free Rad. Biol. Med.* 43, S133 (2007).

32. Guney Y, Turkcu UO, Hicsonmez A *et al.* Carnosine may reduce lung injury caused by radiation therapy. *Med. Hypotheses* 66(5), 957–959 (2006).

33. Spitz DR, Hauer-Jensen M. Ionizing radiation-induced responses: where free radical chemistry meets redox biology and medicine. *Antioxid. Redox Signal.* 20(9), 1407–1409 (2014).

34. Bairati I, Meyer F, Jobin E *et al.* Antioxidant vitamins supplementation and mortality: a randomized trial in head and neck cancer patients. *Int. J. Cancer* 119(9), 2221–2224 (2006).

35. Mannion AF, Jakeman PM, Dunnett M, Harris RC, Willan PL. Carnosine and anserine concentrations in the quadriceps femoris muscle of healthy humans. *Eur. J. Appl. Physiol. Occup. Physiol.* 64(1), 47–50 (1992).

36. Blancquaert L, Everaert I, Missinne M *et al.* Effects of histidine and β-alanine supplementation on human muscle carnosine storage. *Med. Sci. Sports Exerc.* 49(3), 602–609 (2017).

37. Qiu J, Hauske SJ, Zhang S *et al.* Identification and characterisation of carnostatine (SAN9812), a potent and selective carnosinase (CN1) inhibitor with *in vivo* activity. *Amino Acids* 51(1), 7–16 (2019).

38. McFarland GA, Holliday R. Retardation of the senescence of cultured human diploid fibroblasts by carnosine. *Exp. Cell Res.* 212(2), 167–175 (1994).

39. Baraniuk JN, El-Amin S, Corey R, Rayhan R, Timbol C. Carnosine treatment for Gulf War illness: a randomized controlled trial. *GJHS* 5(3), 69–81 (2013).

40. Chez MG, Buchanan CP, Aimonovitch MC *et al.* Double-blind, placebo-controlled study of L-carnosine supplementation in children with autistic spectrum disorders. *J. Child Neurol.* 17(11), 833–837 (2002).

41. Diehn M, Cho RW, Lobo NA *et al.* Association of reactive oxygen species levels and radioresistance in cancer stem cells. *Nature* 458(7239), 780–783 (2009).

3 Summary and Outlook

Glioblastoma is the most common primary malignancy of the human brain in adults. Despite patients undergo a harsh therapeutic regime consisting of microsurgical resection aiming at total gross resection of the tumour, radiotherapy and adjuvant chemotherapy with TMZ, only ~17% of patients survive two years after diagnosis (Ostrom et al. 2018). Furthermore, side effects of the therapy, such as myelosuppression, nausea and alopecia, strongly affect the quality of life of patients (Davis 2016). Hence, new therapeutic approaches are urgently needed to improve outcome and quality of life of patients. Carnosine is a natural occurring dipeptide which was first isolated more than a century ago. Since its discovery several health promoting effects have been ascribed to carnosine, such as scavenging of reactive oxygen species, chelation of heavy metal ions, Ca^{2+} regulation and protection against advanced glycation end products and lipid peroxidation (see 1.3 Carnosine in health and disease). Therefore, the dipeptide or the carnosine containing drug polaprezinc has already been clinically evaluated for the mitigation of side effects of radio-/chemotherapy (Suzuki et al. 2016; Yehia et al. 2019). Moreover, we and others demonstrated that carnosine inhibits proliferation and migration of cancer cells originating from different tissues ((Oppermann et al. 2018) and see 1.3.2 Carnosine and cancer). Understanding the molecular mechanisms of carnosine's effects on tumour cells could pave the way for the design of new drugs exploiting the protective and anti-neoplastic effects of the dipeptide. Up to now, several suggestions have been made on how carnosine may inhibit tumour cell growth. Among them are the induction of cell cycle arrest at G1 (Huijie Jia et al. 2009) and G2/M (Rybakova et al. 2015), suppression of HIF (Iovine et al. 2014) and PI3K/Akt/mTORC1 (Zhang et al. 2014) signalling and inhibition of glycolytic (Renner et al. 2010a) and mitochondrial (Bao et al. 2018) ATP production. Despite those numerous reports, the mode of action of carnosine's anti-neoplastic effect has not been completely resolved. Especially, controversial observations made investigating different cancer cell types, for example the expression of HIF in colon (Iovine et al. 2014) and cervical (Ditte et al. 2014) cancer cells under the influence of the dipeptide, hamper the identification of carnosine's primary target. In the present work we investigated carnosine's impact on glioblastoma cell signalling and metabolism, in order to shed light into its mode of action. We demonstrated that carnosine's anti-neoplastic effect does not correlate with its influence on PI3K/Akt/mTORC1 signalling in glioblastoma (Oppermann et al. 2019b). We suggest that its effect on transcription is in part mediated by influencing histone acetylation (Oppermann et al. 2019a). To our knowledge, the latter study for the first time demonstrated that carnosine induces gene expression by an epigenetic mechanism. Therefore, identifying further genes which expression is influenced by the

dipeptide, by combining chromatin immunoprecipitation with whole transcriptome sequencing, could potentially contribute to the understanding to carnosine's anti-neoplastic and physiological effects. In order to examine the impact of carnosine on cell metabolism, we first investigated the metabolic plasticity of glioblastoma cells. With a metabolomics approach we showed that glioblastoma cells are using both glycolysis and mitochondrial respiration for energy production and are able to switch their metabolic program dependent on the supply of nutrients (Oppermann et al. 2016a). We disproved the theory that pyruvate attenuates the anti-neoplastic effect of carnosine by anaplerosis of TCA cycle intermediates and subsequent ATP generation via OxPhos (Holliday and McFarland 1996; Oppermann et al. 2016b). More important, we proved the suggestion that carnosine reacts with the glycolytic intermediates GA3P and DHAP (Holliday and McFarland 2000). Moreover, this effect was accompanied with reduced amounts of PPP intermediates which suggests the inhibition of proliferation by retarding nucleotide biosynthesis, rather than only by inhibiting ATP production (Oppermann et al. 2019d). As carnosine more effectively reduces the amount of GA3P than that of DHAP, we suggest that the non-enzymatic reaction of carnosine with GA3P is of higher importance for its anti-neoplastic effect. In further studies the impact of this effect on non-neoplastic cells, such as erythrocytes which rely on glycolytic ATP production and NADPH generation via PPP, needs to be evaluated.

Considering carnosine for the clinical application in glioblastoma therapy, we contributed to the pharmacological evaluation of the dipeptide. Carnosine is taken up by three different transporters of the POT family which mRNA expression is increased in glioblastoma tissue compared to normal brain tissue (Oppermann et al. 2019e). Furthermore, we demonstrated that cleavage of carnosine to L-histidine and β-alanine is not required to deploy its anti-neoplastic effect. Consequently, delivery of intact carnosine to the target cells should be maximised for an optimal effect. Despite the observation that the dipeptide is effective as a drug when administered orally (Baraniuk et al. 2013; Mehrazad-Saber et al. 2018; Yehia et al. 2019), carnosine is rapidly degraded by CN1 which considerably reduces its tissue availability (Qiu et al. 2019)(Qiu et al. 2019). In order to overcome this obstacle, different approaches were suggested, including the co-administration of the CN1 inhibitor carnostatine (Qiu et al. 2019)(Qiu et al. 2019), development of CN1-resistant mimics of carnosine (Anderson et al. 2018)(Anderson et al. 2018) and intra-nasal administration of the dipeptide (Hipkiss et al. 2013)(Hipkiss et al. 2013). Despite these promising approaches for the clinical administration of carnosine, the impact and enrichment of carnosine in glioblastoma tissue relevant for patients can only be evaluated by a clinical trial. Keeping in mind that carnosine protects from IR induced damage (Guney et al. 2006), we tested whether the dipeptide may attenuate the effects of radiotherapy which is needed for an improved outcome of glioblastoma patients. Instead of attenuation, we could observe that carnosine further

decreased glioblastoma cell viability in combination with IR. The same observation was made, when carnosine was combined with TMZ or TMZ and IR (Dietterle et al. 2019). Hence, as carnosine amplifies the effect of glioblastoma standard therapy, rather than attenuating it, we conclude that treatment with the dipeptide will be safe for glioblastoma therapy.

In conclusion, the natural occurring dipeptide carnosine inhibits proliferation and invasion of glioblastoma cells. We demonstrated for the first time that carnosine influences transcription via an epigenetic mechanism. Furthermore, we identified GA3P as a molecular target reacting non-enzymatically with the dipeptide resulting in decreased amounts of PPP intermediates. Important for the clinical application, we proved that in glioblastoma cells the dipeptide can be taken up by three different transporters and that the delivery of carnosine to the target cells does not require its degradation. Finally, the administration of carnosine does not negatively affect standard therapy in culture but even amplifies the effects of TMZ and IR. Therefore, we encourage the clinical evaluation of carnosine for the treatment of glioblastoma patients.

4 References

Abraham D, Pisano JJ, Uendriend S (1962) The distribution of homocarnosine in mammals. Arch. Biochem. Biophys. 99:210–213

Ackermann D, Timpe O, Poller K (1929) Über das Anserin, einen neuen Bestandteil der Vogelmuskulatur. Hoppe-Seyler´s Zeitschrift für physiologische Chemie 183:1–10. doi: 10.1515/bchm2.1929.183.1-2.1

Ait-Ghezala G, Hassan S, Tweed M, Paris D, Crynen G, Zakirova Z, Crynen S, Crawford F (2016) Identification of Telomerase-activating Blends From Naturally Occurring Compounds. Altern Ther Health Med 22 Suppl 2:6–14

Aldini G, Carini M, Beretta G, Bradamante S, Facino RM (2002) Carnosine is a quencher of 4-hydroxy-nonenal: through what mechanism of reaction? Biochem. Biophys. Res. Commun. 298:699–706. doi: 10.1016/S0006-291X(02)02545-7

Altman BJ, Stine ZE, Dang CV (2016) From Krebs to clinic: glutamine metabolism to cancer therapy. Nat Rev Cancer 16:619–634. doi: 10.1038/nrc.2016.71

Anderson EJ, Vistoli G, Katunga LA, Funai K, Regazzoni L, Monroe TB, Gilardoni E, Cannizzaro L, Colzani M, Maddis D de, Rossoni G, Canevotti R, Gagliardi S, Carini M, Aldini G (2018) A carnosine analog mitigates metabolic disorders of obesity by reducing carbonyl stress. J Clin Invest 128:5280–5293. doi: 10.1172/JCI94307

Ansurudeen I, Sunkari VG, Grünler J, Peters V, Schmitt CP, Catrina S-B, Brismar K, Forsberg EA (2012) Carnosine enhances diabetic wound healing in the db/db mouse model of type 2 diabetes. Amino Acids 43:127–134. doi: 10.1007/s00726-012-1269-z

Antonov A, Agostini M, Morello M, Minieri M, Melino G, Amelio I (2014) Bioinformatics analysis of the serine and glycine pathway in cancer cells. Oncotarget 5:11004–11013. doi: 10.18632/oncotarget.2668

Argilés JM, Busquets S, Stemmler B, López-Soriano FJ (2014) Cancer cachexia: understanding the molecular basis. Nat Rev Cancer 14:754–762. doi: 10.1038/nrc3829

Artioli GG, Gualano B, Smith A, Stout J, Lancha AH, JR (2010) Role of beta-alanine supplementation on muscle carnosine and exercise performance. Med Sci Sports Exerc 42:1162–1173. doi: 10.1249/MSS.0b013e3181c74e38

Asperger A, Renner C, Menzel M, Gebhardt R, Meixensberger J, Gaunitz F (2011) Identification of factors involved in the anti-tumor activity of carnosine on glioblastomas using a proteomics approach. Cancer Invest. 29:272–281. doi: 10.3109/07357907.2010.550666

Bagley SJ, Desai AS, Linette GP, June CH, O'Rourke DM (2018) CAR T-cell therapy for glioblastoma: recent clinical advances and future challenges. Neuro-oncology 20:1429–1438. doi: 10.1093/neuonc/noy032

Baguet A, Koppo K, Pottier A, Derave W (2010) Beta-alanine supplementation reduces acidosis but not oxygen uptake response during high-intensity cycling exercise. Eur J Appl Physiol 108:495–503. doi: 10.1007/s00421-009-1225-0

Bairati I, Meyer F, Jobin E, Gelinas M, Fortin A, Nabid A, Brochet F, Tetu B (2006) Antioxidant vitamins supplementation and mortality: a randomized trial in head and neck cancer patients. Int J Cancer 119:2221–2224. doi: 10.1002/ijc.22042

Bao Y, Ding S, Cheng J, Liu Y, Wang B, Xu H, Shen Y, Lyu J (2018) Carnosine Inhibits the Proliferation of Human Cervical Gland Carcinoma Cells Through Inhibiting Both Mitochondrial Bioenergetics and

Glycolysis Pathways and Retarding Cell Cycle Progression. Integr Cancer Ther 17:80–91. doi: 10.1177/1534735416684551

Baran EJ (2000) Metal complexes of carnosine. Biochemistry Mosc. 65:789–797

Baran EJ, Parajón-Costa BS, Rojo T, Sáez-Puche R, Fernández F, Tótaro RM, Apella MC, Etcheverry SB, Torre MH (1995) Spectroscopic, magnetic, and electrochemical behavior of the copper(II) complex of carnosine. Journal of Inorganic Biochemistry 58:279–289. doi: 10.1016/0162-0134(94)00061-E

Baraniuk JN, El-Amin S, Corey R, Rayhan R, Timbol C (2013) Carnosine treatment for gulf war illness: a randomized controlled trial. Glob J Health Sci 5:69–81

Barrès R, Yan J, Egan B, Treebak JT, Rasmussen M, Fritz T, Caidahl K, Krook A, O'Gorman DJ, Zierath JR (2012) Acute exercise remodels promoter methylation in human skeletal muscle. Cell Metab. 15:405–411. doi: 10.1016/j.cmet.2012.01.001

Bauer K (2005) Carnosine and homocarnosine, the forgotten, enigmatic peptides of the brain. Neurochem Res 30:1339–1345. doi: 10.1007/s11064-005-8806-z

Bellia F, Vecchio G, Rizzarelli E (2014) Carnosinases, their substrates and diseases. Molecules 19:2299–2329. doi: 10.3390/molecules19022299

Bermúdez M-L, Skelton MR, Genter MB (2018) Intranasal carnosine attenuates transcriptomic alterations and improves mitochondrial function in the Thy1-aSyn mouse model of Parkinson's disease. Mol Genet Metab. doi: 10.1016/j.ymgme.2018.08.002

Bharadwaj LA, Davies GF, Xavier IJ, Ovsenek N (2002) l-carnosine and verapamil inhibit hypoxia-induced expression of hypoxia inducible factor (HIF-1 alpha) in H9c2 cardiomyoblasts. Pharmacol. Res. 45:175–181. doi: 10.1006/phrs.2001.0911

Boldyrev A, Fedorova T, Stepanova M, Dobrotvorskaya I, Kozlova E, Boldanova N, Bagyeva G, Ivanova-Smolenskaya I, Illarioshkin S (2008) Carnosine [corrected] increases efficiency of DOPA therapy of Parkinson's disease: a pilot study. Rejuvenation Res 11:821–827. doi: 10.1089/rej.2008.0716

Boldyrev AA, Gallant SC, Sukhich GT (1999) Carnosine, the protective, anti-aging peptide. Biosci Rep 19:581–587. doi: 10.1023/a:1020271013277

Boldyrev AA, Aldini G, Derave W (2013) Physiology and pathophysiology of carnosine. Physiol. Rev. 93:1803–1845

Bonfanti L, Peretto P, Marchis S de, Fasolo A (1999) Carnosine-related dipeptides in the mammalian brain. Prog Neurobiol 59:333–353

Bonmassar L, Marchesi F, Pascale E, Franzese O, Margison GP, Bianchi A, D'Atri S, Bernardini S, Lattuada D, Bonmassar E, Aquino A (2013) Triazene compounds in the treatment of acute myeloid leukemia: a short review and a case report. Curr Med Chem 20:2389–2401. doi: 10.2174/0929867311320190001

Bouatra S, Aziat F, Mandal R, Guo AC, Wilson MR, Knox C, Bjorndahl TC, Krishnamurthy R, Saleem F, Liu P, Dame ZT, Poelzer J, Huynh J, Yallou FS, Psychogios N, Dong E, Bogumil R, Roehring C, Wishart DS (2013) The human urine metabolome. PLoS ONE 8:e73076. doi: 10.1371/journal.pone.0073076

Brown CE, Alizadeh D, Starr R, Weng L, Wagner JR, Naranjo A, Ostberg JR, Blanchard MS, Kilpatrick J, Simpson J, Kurien A, Priceman SJ, Wang X, Harshbarger TL, D'Apuzzo M, Ressler JA, Jensen MC, Barish ME, Chen M, Portnow J, Forman SJ, Badie B (2016) Regression of Glioblastoma after Chimeric Antigen Receptor T-Cell Therapy. N Engl J Med 375:2561–2569. doi: 10.1056/NEJMoa1610497

References

Cartwright SP, Bill RM, Hipkiss AR (2012) L-carnosine affects the growth of Saccharomyces cerevisiae in a metabolism-dependent manner. PLoS ONE 7:e45006. doi: 10.1371/journal.pone.0045006

Chaleckis R, Murakami I, Takada J, Kondoh H, Yanagida M (2016) Individual variability in human blood metabolites identifies age-related differences. Proc Natl Acad Sci U S A 113:4252–4259. doi: 10.1073/pnas.1603023113

Chang HT, Olson LK, Schwartz KA (2013) Ketolytic and glycolytic enzymatic expression profiles in malignant gliomas: implication for ketogenic diet therapy. Nutr Metab (Lond) 10:47. doi: 10.1186/1743-7075-10-47

Chavez JC, Bachmeier C, Kharfan-Dabaja MA (2019) CAR T-cell therapy for B-cell lymphomas: clinical trial results of available products. Ther Adv Hematol 10. doi: 10.1177/2040620719841581

Cheng J-Y, Yang J-B, Liu Y, Xu M, Huang Y-Y, Zhang J-J, Cao P, Lyu J-X, Shen Y (2019) Profiling and targeting of cellular mitochondrial bioenergetics: inhibition of human gastric cancer cell growth by carnosine. Acta Pharmacol Sin 40:938–948. doi: 10.1038/s41401-018-0182-8

Chengappa, K N Roy, Turkin SR, DeSanti S, Bowie CR, Brar JS, Schlicht PJ, Murphy SL, Hetrick ML, Bilder R, Fleet D (2012) A preliminary, randomized, double-blind, placebo-controlled trial of L-carnosine to improve cognition in schizophrenia. Schizophr. Res. 142:145–152. doi: 10.1016/j.schres.2012.10.001

Chez MG, Buchanan CP, Aimonovitch MC, Becker M, Schaefer K, Black C, Komen J (2002) Double-blind, placebo-controlled study of L-carnosine supplementation in children with autistic spectrum disorders. J. Child Neurol. 17:833–837

Chuang C-H, Hu M-L (2008) L-carnosine inhibits metastasis of SK-Hep-1 cells by inhibition of matrix metaoproteinase-9 expression and induction of an antimetastatic gene, nm23-H1. Nutr Cancer 60:526–533. doi: 10.1080/01635580801911787

Corona C, Frazzini V, Silvestri E, Lattanzio R, La Sorda R, Piantelli M, Canzoniero LMT, Ciavardelli D, Rizzarelli E, Sensi SL (2011) Effects of dietary supplementation of carnosine on mitochondrial dysfunction, amyloid pathology, and cognitive deficits in 3xTg-AD mice. PLoS ONE 6:e17971. doi: 10.1371/journal.pone.0017971

Crown SB, Marze N, Antoniewicz MR (2015) Catabolism of Branched Chain Amino Acids Contributes Significantly to Synthesis of Odd-Chain and Even-Chain Fatty Acids in 3T3-L1 Adipocytes. PLoS ONE 10:e0145850. doi: 10.1371/journal.pone.0145850

Daniel H, Kottra G (2004) The proton oligopeptide cotransporter family SLC15 in physiology and pharmacology. Pflugers Arch 447:610–618. doi: 10.1007/s00424-003-1101-4

Davis ME (2016) Glioblastoma: Overview of Disease and Treatment. Clin J Oncol Nurs 20:S2-8. doi: 10.1188/16.CJON.S1.2-8

Dawson R, Biasetti M, Messina S, Dominy J (2002) The cytoprotective role of taurine in exercise-induced muscle injury. Amino Acids 22:309–324. doi: 10.1007/s007260200017

DeBerardinis RJ, Mancuso A, Daikhin E, Nissim I, Yudkoff M, Wehrli S, Thompson CB (2007) Beyond aerobic glycolysis: transformed cells can engage in glutamine metabolism that exceeds the requirement for protein and nucleotide synthesis. Proc. Natl. Acad. Sci. U.S.A. 104:19345–19350. doi: 10.1073/pnas.0709747104

del Rio RM, Orensanz Muñoz LM, DeFeudis FV (1977) Contents of beta-alanine and gamma-aminobutyric acid in regions of rat CNS. Exp Brain Res 28:225–227. doi: 10.1007/bf00235704

Deng YH, Deng ZH, Hao H, Wu XL, Gao H, Tang SH, Tang H (2018) MicroRNA-23a promotes colorectal cancer cell survival by targeting PDK4. Exp Cell Res 373:171–179. doi: 10.1016/j.yexcr.2018.10.010

References

Dietterle J, Oppermann H, Glasow A, Neumann K, Meixensberger J, Gaunitz F (2019) Carnosine increases efficiency of temozolomide and irradiation treatment of isocitrate dehydrogenase-wildtype glioblastoma cells in culture. Future Oncol. doi: 10.2217/fon-2019-0447

Ding Q, Tanigawa K, Kaneko J, Totsuka M, Katakura Y, Imabayashi E, Matsuda H, Hisatsune T (2018) Anserine/Carnosine Supplementation Preserves Blood Flow in the Prefrontal Brain of Elderly People Carrying APOE e4. Aging Dis 9:334–345. doi: 10.14336/AD.2017.0809

Ditte Z, Ditte P, Labudova M, Simko V, Iuliano F, Zatovicova M, Csaderova L, Pastorekova S, Pastorek J (2014) Carnosine inhibits carbonic anhydrase IX-mediated extracellular acidosis and suppresses growth of HeLa tumor xenografts. BMC Cancer 14:358. doi: 10.1186/1471-2407-14-358

Dobbie H, Kermack WO (1955) Complex-formation between polypeptides and metals. 2. The reaction between cupric ions and some dipeptides. Biochem. J. 59:246–257. doi: 10.1042/bj0590246

Dodd KM, Yang J, Shen MH, Sampson JR, Tee AR (2015) mTORC1 drives HIF-1α and VEGF-A signalling via multiple mechanisms involving 4E-BP1, S6K1 and STAT3. Oncogene 34:2239–2250. doi: 10.1038/onc.2014.164

Drozak J, Veiga-da-Cunha M, Vertommen D, Stroobant V, van Schaftingen E (2010) Molecular identification of carnosine synthase as ATP-grasp domain-containing protein 1 (ATPGD1). J Biol Chem 285:9346–9356. doi: 10.1074/jbc.M109.095505

Drozak J, Piecuch M, Poleszak O, Kozlowski P, Chrobok L, Baelde HJ, Heer E de (2015) UPF0586 Protein C9orf41 Homolog Is Anserine-producing Methyltransferase. J. Biol. Chem. 290:17190–17205. doi: 10.1074/jbc.M115.640037

Dunnett M, Harris RC (1999) Influence of oral beta-alanine and L-histidine supplementation on the carnosine content of the gluteus medius. Equine Vet J Suppl:499–504

Dutka TL, Lamboley CR, McKenna MJ, Murphy RM, Lamb GD (2012) Effects of carnosine on contractile apparatus Ca^{2+} sensitivity and sarcoplasmic reticulum Ca^{2+} release in human skeletal muscle fibers. J Appl Physiol (1985) 112:728–736. doi: 10.1152/japplphysiol.01331.2011

Elsakka AMA, Bary MA, Abdelzaher E, Elnaggar M, Kalamian M, Mukherjee P, Seyfried TN (2018) Management of Glioblastoma Multiforme in a Patient Treated With Ketogenic Metabolic Therapy and Modified Standard of Care: A 24-Month Follow-Up. Front. Nutr. 5:20. doi: 10.3389/fnut.2018.00020

Evdokimova V, Tognon C, Ng T, Ruzanov P, Melnyk N, Fink D, Sorokin A, Ovchinnikov LP, Davicioni E, Triche TJ, Sorensen PHB (2009) Translational activation of snail1 and other developmentally regulated transcription factors by YB-1 promotes an epithelial-mesenchymal transition. Cancer Cell 15:402–415. doi: 10.1016/j.ccr.2009.03.017

Fagerberg L, Hallström BM, Oksvold P, Kampf C, Djureinovic D, Odeberg J, Habuka M, Tahmasebpoor S, Danielsson A, Edlund K, Asplund A, Sjöstedt E, Lundberg E, Szigyarto CA-K, Skogs M, Takanen JO, Berling H, Tegel H, Mulder J, Nilsson P, Schwenk JM, Lindskog C, Danielsson F, Mardinoglu A, Sivertsson A, Feilitzen K von, Forsberg M, Zwahlen M, Olsson I, Navani S, Huss M, Nielsen J, Ponten F, Uhlén M (2014) Analysis of the human tissue-specific expression by genome-wide integration of transcriptomics and antibody-based proteomics. Mol Cell Proteomics 13:397–406. doi: 10.1074/mcp.M113.035600

Fan J, Ye J, Kamphorst JJ, Shlomi T, Thompson CB, Rabinowitz JD (2014) Quantitative flux analysis reveals folate-dependent NADPH production. Nature 510:298–302. doi: 10.1038/nature13236

Farrell CJ, Plotkin SR (2007) Genetic causes of brain tumors: neurofibromatosis, tuberous sclerosis, von Hippel-Lindau, and other syndromes. Neurol Clin 25:925-46, viii. doi: 10.1016/j.ncl.2007.07.008

References

Fonteh AN, Harrington RJ, Tsai A, Liao P, Harrington MG (2007) Free amino acid and dipeptide changes in the body fluids from Alzheimer's disease subjects. Amino Acids 32:213–224. doi: 10.1007/s00726-006-0409-8

Forsberg EA, Botusan IR, Wang J, Peters V, Ansurudeen I, Brismar K, Catrina SB (2015) Carnosine decreases IGFBP1 production in db/db mice through suppression of HIF-1. J Endocrinol 225:159–167. doi: 10.1530/JOE-14-0571

Furuta S, Toyama S, Miwa M, Itabashi T, Sano H, Yoneta T (1995) Residence time of polaprezinc (zinc L-carnosine complex) in the rat stomach and adhesiveness to ulcerous sites. Jpn J Pharmacol 67:271–278. doi: 10.1254/jjp.67.271

Gaggelli E, Valensin G (1990) 1 H and 13 C NMR relaxation investigation of the calcium complex of β-alanyl- L -histidine (carnosine) in aqueous solution. J. Chem. Soc., Perkin Trans. 2 184:401–406. doi: 10.1039/P29900000401

Gardner ML, Illingworth KM, Kelleher J, Wood D (1991) Intestinal absorption of the intact peptide carnosine in man, and comparison with intestinal permeability to lactulose. J. Physiol. (Lond.) 439:411–422. doi: 10.1113/jphysiol.1991.sp018673

Garofalo M, Iovine B, Kuryk L, Capasso C, Hirvinen M, Vitale A, Yliperttula M, Bevilacqua MA, Cerullo V (2016) Oncolytic Adenovirus Loaded with L-carnosine as Novel Strategy to Enhance the Antitumor Activity. Mol Cancer Ther 15:651–660. doi: 10.1158/1535-7163.MCT-15-0559

Gaunitz F, Hipkiss AR (2012) Carnosine and cancer: a perspective. Amino Acids 43:135–142. doi: 10.1007/s00726-012-1271-5

Gaunitz F, Oppermann H, Hipkiss A (2015) CHAPTER 20. Carnosine and Cancer. In: Preedy VR (ed) Imidazole Dipeptides. Royal Society of Chemistry, Cambridge, pp 372–392

Gautam P, Nair SC, Gupta MK, Sharma R, Polisetty RV, Uppin MS, Sundaram C, Puligopu AK, Ankathi P, Purohit AK, Chandak GR, Harsha HC, Sirdeshmukh R (2012) Proteins with altered levels in plasma from glioblastoma patients as revealed by iTRAQ-based quantitative proteomic analysis. PLoS ONE 7:e46153. doi: 10.1371/journal.pone.0046153

Gayova E, Kron I, Suchozova K, Pavlisak V, Fedurco M, Novakova B (1999) Karnozín u pacientov s diabetes mellitus typu I (Carnosine in patients with type I diabetes mellitus). Bratisl Lek Listy 100:500–502

Gilbert MR, Dignam JJ, Armstrong TS, Wefel JS, Blumenthal DT, Vogelbaum MA, Colman H, Chakravarti A, Pugh S, Won M, Jeraj R, Brown PD, Jaeckle KA, Schiff D, Stieber VW, Brachman DG, Werner-Wasik M, Tremont-Lukats IW, Sulman EP, Aldape KD, Curran WJ, Mehta MP (2014) A randomized trial of bevacizumab for newly diagnosed glioblastoma. N. Engl. J. Med. 370:699–708. doi: 10.1056/NEJMoa1308573

Gulewitsch W (1911) Zur Kenntnis der Extraktivstoffe der Muskeln. XII. Mitteilung. Über die Konstitution des Carnosins. Hoppe-Seyler´s Zeitschrift für physiologische Chemie 73:434–446. doi: 10.1515/bchm2.1911.73.6.434

Gulewitsch W, Amiradžibi S (1900) Ueber das Carnosin, eine neue organische Base des Fleischextractes. Ber. Dtsch. Chem. Ges. 33:1902–1903. doi: 10.1002/cber.19000330275

Guney Y, Turkcu UO, Hicsonmez A, Andrieu MN, Guney HZ, Bilgihan A, Kurtman C (2006) Carnosine may reduce lung injury caused by radiation therapy. Med Hypotheses 66:957–959. doi: 10.1016/j.mehy.2005.11.023

Hajizadeh-Zaker R, Ghajar A, Mesgarpour B, Afarideh M, Mohammadi M-R, Akhondzadeh S (2018) l-Carnosine As an Adjunctive Therapy to Risperidone in Children with Autistic Disorder: A Randomized, Double-Blind, Placebo-Controlled Trial. J Child Adolesc Psychopharmacol 28:74–81. doi: 10.1089/cap.2017.0026

References

Hanahan D, Weinberg RA (2011) Hallmarks of cancer: the next generation. Cell 144:646–674. doi: 10.1016/j.cell.2011.02.013

Hatzikirou H, Basanta D, Simon M, Schaller K, Deutsch A (2012) 'Go or grow': the key to the emergence of invasion in tumour progression? Math Med Biol 29:49–65. doi: 10.1093/imammb/dqq011

Hegi ME, Diserens A-C, Gorlia T, Hamou M-F, Tribolet N de, Weller M, Kros JM, Hainfellner JA, Mason W, Mariani L, Bromberg JEC, Hau P, Mirimanoff RO, Cairncross JG, Janzer RC, Stupp R (2005) MGMT gene silencing and benefit from temozolomide in glioblastoma. N Engl J Med 352:997–1003. doi: 10.1056/NEJMoa043331

Herrera-Ruiz D, Wang Q, Gudmundsson OS, Cook TJ, Smith RL, Faria TN, Knipp GT (2001) Spatial expression patterns of peptide transporters in the human and rat gastrointestinal tracts, Caco-2 in vitro cell culture model, and multiple human tissues. AAPS PharmSci 3:E9

Hipkiss AR (1998a) Carnosine, a protective, anti-ageing peptide? Int. J. Biochem. Cell Biol. 30:863–868

Hipkiss AR (2000) Carnosine and protein carbonyl groups: a possible relationship. Biochemistry Mosc. 65:771–778

Hipkiss AR, Michaelis J, Syrris P (1995) Non-enzymatic glycosylation of the dipeptide L-carnosine, a potential anti-protein-cross-linking agent. FEBS Lett. 371:81–85

Hipkiss AR (1998b) Carnosine, a protective, anti-ageing peptide? Int. J. Biochem. Cell Biol. 30:863–868. doi: 10.1016/S1357-2725(98)00060-0

Hipkiss AR (2005) Glycation, ageing and carnosine: are carnivorous diets beneficial? Mech Ageing Dev 126:1034–1039. doi: 10.1016/j.mad.2005.05.002

Hipkiss AR (2009) On the enigma of carnosine's anti-ageing actions. Exp. Gerontol. 44:237–242. doi: 10.1016/j.exger.2008.11.001

Hipkiss AR (2010) Aging, Proteotoxicity, Mitochondria, Glycation, NAD and Carnosine: Possible Inter-Relationships and Resolution of the Oxygen Paradox. Front Aging Neurosci 2:10. doi: 10.3389/fnagi.2010.00010

Hipkiss AR, Gaunitz F (2014) Inhibition of tumour cell growth by carnosine: some possible mechanisms. Amino Acids 46:327–337. doi: 10.1007/s00726-013-1627-5

Hipkiss AR, Cartwright SP, Bromley C, Gross SR, Bill RM (2013) Carnosine: can understanding its actions on energy metabolism and protein homeostasis inform its therapeutic potential? Chem Cent J 7:38. doi: 10.1186/1752-153X-7-38

Hobson RM, Saunders B, Ball G, Harris RC, Sale C (2012) Effects of β-alanine supplementation on exercise performance: a meta-analysis. Amino Acids 43:25–37. doi: 10.1007/s00726-011-1200-z

Hoffmann AM, Bakardjiev A, Bauer K (1996) Carnosine-synthesis in cultures of rat glial cells is restricted to oligodendrocytes and carnosine uptake to astrocytes. Neuroscience Letters 215:29–32. doi: 10.1016/S0304-3940(96)12937-2

Holliday R, McFarland GA (1996) Inhibition of the growth of transformed and neoplastic cells by the dipeptide carnosine. Br. J. Cancer 73:966–971

Holliday R, McFarland GA (2000) A role for carnosine in cellular maintenance. Biochemistry Mosc. 65:843–848

Horii Y, Shen J, Fujisaki Y, Yoshida K, Nagai K (2012) Effects of L-carnosine on splenic sympathetic nerve activity and tumor proliferation. Neurosci. Lett. 510:1–5. doi: 10.1016/j.neulet.2011.12.058

Hou C, Yamaguchi S, Ishi Y, Terasaka S, Kobayashi H, Motegi H, Hatanaka KC, Houkin K (2019) Identification of PEPT2 as an important candidate molecule in 5-ALA-mediated fluorescence-

guided surgery in WHO grade II/III gliomas. J Neurooncol 143:197–206. doi: 10.1007/s11060-019-03158-3

Hsieh S-L, Hsieh S, Lai P-Y, Wang J-J, Li C-C, Wu C-C (2019) Carnosine Suppresses Human Colorectal Cell Migration and Intravasation by Regulating EMT and MMP Expression. Am J Chin Med 47:477–494. doi: 10.1142/S0192415X19500241

Hu Y, Xie Y, Keep RF, Smith DE (2014) Divergent developmental expression and function of the proton-coupled oligopeptide transporters PepT2 and PhT1 in regional brain slices of mouse and rat. J Neurochem 129:955–965. doi: 10.1111/jnc.12687

Huijie Jia, Xiaodan Qi, Shaohong Fang, Yuhong Jin, Xiaoying Han, Yi Wang, Aimin Wang, Hongbo Zhou (2009) Carnosine inhibits high glucose-induced mesangial cell proliferation through mediating cell cycle progression. Regulatory Peptides. doi: 10.1016/j.regpep.2008.12.004

Iovine B, Iannella ML, Nocella F, Pricolo MR, Bevilacqua MA (2012) Carnosine inhibits KRAS-mediated HCT116 proliferation by affecting ATP and ROS production. Cancer Lett. 315:122–128. doi: 10.1016/j.canlet.2011.07.021

Iovine B, Oliviero G, Garofalo M, Orefice M, Nocella F, Borbone N, Piccialli V, Centore R, Mazzone M, Piccialli G, Bevilacqua MA (2014) The anti-proliferative effect of L-carnosine correlates with a decreased expression of hypoxia inducible factor 1 alpha in human colon cancer cells. PLoS ONE 9:e96755. doi: 10.1371/journal.pone.0096755

Jackson MC, Kucera CM, Lenney JF (1991) Purification and properties of human serum carnosinase. Clinica Chimica Acta 196:193–205. doi: 10.1016/0009-8981(91)90073-L

Jeong JY, Jeoung NH, Park K-G, Lee I-K (2012) Transcriptional regulation of pyruvate dehydrogenase kinase. Diabetes Metab J 36:328–335. doi: 10.4093/dmj.2012.36.5.328

Judel GK (2003) Die Geschichte von Liebigs Fleischextrakt: Zur populärsten Erfindung des berühmten Chemikers. Spiegel der Forschung:6–17

Kalyankar GD, Meister A (1959) Enzymatic synthesis of carnosine and related beta-alanyl and gamma-aminobutyryl peptides. J. Biol. Chem. 234:3210–3218

Kamal MA, Jiang H, Hu Y, Keep RF, Smith DE (2009) Influence of genetic knockout of Pept2 on the in vivo disposition of endogenous and exogenous carnosine in wild-type and Pept2 null mice. Am J Physiol Regul Integr Comp Physiol 296:R986-91. doi: 10.1152/ajpregu.90744.2008

Kang JH, Kim KS (2003) Enhanced oligomerization of the alpha-synuclein mutant by the Cu,Zn-superoxide dismutase and hydrogen peroxide system. Mol Cells 15:87–93

Kim JA, Choi DK, Min JS, Kang I, Kim JC, Kim S, Ahn JK (2018) VBP1 represses cancer metastasis by enhancing HIF-1α degradation induced by pVHL. FEBS J 285:115–126. doi: 10.1111/febs.14322

Kinlaw WB, Baures PW, Lupien LE, Davis WL, Kuemmerle NB (2016) Fatty Acids and Breast Cancer: Make Them on Site or Have Them Delivered. J Cell Physiol 231:2128–2141. doi: 10.1002/jcp.25332

Kleihues P, Soylemezoglu F, Schäuble B, Scheithauer BW, Burger PC (1995) Histopathology, classification, and grading of gliomas. Glia 15:211–221. doi: 10.1002/glia.440150303

Kohen R, Yamamoto Y, Cundy KC, Ames BN (1988) Antioxidant activity of carnosine, homocarnosine, and anserine present in muscle and brain. Proc. Natl. Acad. Sci. U.S.A. 85:3175–3179

Kuhajda FP, Jenner K, Wood FD, Hennigar RA, Jacobs LB, Dick JD, Pasternack GR (1994) Fatty acid synthesis: a potential selective target for antineoplastic therapy. Proc. Natl. Acad. Sci. U.S.A. 91:6379–6383. doi: 10.1073/pnas.91.14.6379

Kurabe N, Hayasaka T, Ogawa M, Masaki N, Ide Y, Waki M, Nakamura T, Kurachi K, Kahyo T, Shinmura K, Midorikawa Y, Sugiyama Y, Setou M, Sugimura H (2013) Accumulated phosphatidylcholine

References

(16:0/16:1) in human colorectal cancer; possible involvement of LPCAT4. Cancer Science 104:1295–1302. doi: 10.1111/cas.12221

Kusakabe T, Maeda M, Hoshi N, Sugino T, Watanabe K, Fukuda T, Suzuki T (2000) Fatty acid synthase is expressed mainly in adult hormone-sensitive cells or cells with high lipid metabolism and in proliferating fetal cells. J Histochem Cytochem 48:613–622. doi: 10.1177/002215540004800505

Kwon H-S, Huang B, Unterman TG, Harris RA (2004) Protein kinase B-alpha inhibits human pyruvate dehydrogenase kinase-4 gene induction by dexamethasone through inactivation of FOXO transcription factors. Diabetes 53:899–910

Kwon H-S, Huang B, Ho Jeoung N, Wu P, Steussy CN, Harris RA (2006) Retinoic acids and trichostatin A (TSA), a histone deacetylase inhibitor, induce human pyruvate dehydrogenase kinase 4 (PDK4) gene expression. Biochim. Biophys. Acta 1759:141–151. doi: 10.1016/j.bbaexp.2006.04.005

Labuschagne CF, van den Broek, Niels J F, Mackay GM, Vousden KH, Maddocks ODK (2014) Serine, but not glycine, supports one-carbon metabolism and proliferation of cancer cells. Cell Rep 7:1248–1258. doi: 10.1016/j.celrep.2014.04.045

Laperriere N, Zuraw L, Cairncross G (2002) Radiotherapy for newly diagnosed malignant glioma in adults: a systematic review. Radiotherapy and Oncology 64:259–273. doi: 10.1016/s0167-8140(02)00078-6

Laplante M, Sabatini DM (2013) Regulation of mTORC1 and its impact on gene expression at a glance. J Cell Sci 126:1713–1719. doi: 10.1242/jcs.125773

Lee J, Park J-R, Lee H, Jang S, Ryu S-M, Kim H, Kim D, Jang A, Yang S-R (2018) L-carnosine induces apoptosis/cell cycle arrest via suppression of NF-κB/STAT1 pathway in HCT116 colorectal cancer cells. In Vitro Cell Dev Biol Anim. doi: 10.1007/s11626-018-0264-4

Letzien U, Oppermann H, Meixensberger J, Gaunitz F (2014) The antineoplastic effect of carnosine is accompanied by induction of PDK4 and can be mimicked by l-histidine. Amino Acids 46:1009–1019. doi: 10.1007/s00726-014-1664-8

Liau LM, Ashkan K, Tran DD, Campian JL, Trusheim JE, Cobbs CS, Heth JA, Salacz M, Taylor S, D'Andre SD, Iwamoto FM, Dropcho EJ, Moshel YA, Walter KA, Pillainayagam CP, Aiken R, Chaudhary R, Goldlust SA, Bota DA, Duic P, Grewal J, Elinzano H, Toms SA, Lillehei KO, Mikkelsen T, Walbert T, Abram SR, Brenner AJ, Brem S, Ewend MG, Khagi S, Portnow J, Kim LJ, Loudon WG, Thompson RC, Avigan DE, Fink KL, Geoffroy FJ, Lindhorst S, Lutzky J, Sloan AE, Schackert G, Krex D, Meisel H-J, Wu J, Davis RP, Duma C, Etame AB, Mathieu D, Kesari S, Piccioni D, Westphal M, Baskin DS, New PZ, Lacroix M, May S-A, Pluard TJ, Tse V, Green RM, Villano JL, Pearlman M, Petrecca K, Schulder M, Taylor LP, Maida AE, Prins RM, Cloughesy TF, Mulholland P, Bosch ML (2018) First results on survival from a large Phase 3 clinical trial of an autologous dendritic cell vaccine in newly diagnosed glioblastoma. J Transl Med 16:142. doi: 10.1186/s12967-018-1507-6

Liu P, Ge X, Ding H, Jiang H, Christensen BM, Li J (2012) Role of glutamate decarboxylase-like protein 1 (GADL1) in taurine biosynthesis. J. Biol. Chem. 287:40898–40906. doi: 10.1074/jbc.M112.393728

Liu Z, Chen X, Wang Y, Peng H, Wang Y, Jing Y, Zhang H (2014) PDK4 protein promotes tumorigenesis through activation of cAMP-response element-binding protein (CREB)-Ras homolog enriched in brain (RHEB)-mTORC1 signaling cascade. J Biol Chem 289:29739–29749. doi: 10.1074/jbc.M114.584821

Loomis WF, Lipmann F (1948) Reversible inhibition of the coupling between phosphorylation and oxidation. J. Biol. Chem. 173:807

Louis DN, Suva ML, Burger PC, Perry A, Kleihues P, Aldape KD, Brat DJ, Biernat W, Bigner DD, Nakazato Y, Plate KH, Giangaspero F, Ohgaki H, Cavenee WK, Wick W, Barnholtz-Sloan J,

Rosenblum MK, Hegi M, Stupp R, Hawkins C, Verhaak RGW, Ellison DW, von Deimling A (2016) Glioblastoma, IDH-wildtype. In: Louis DN, Ohgaki H, Wiestler OD, Cavenee WK (eds) WHO classification of tumours of the central nervous system, Revised 4th edition. International Agency for Research on Cancer, Lyon, pp 28–45

Louis DN, Ohgaki H, Wiestler OD, Cavenee WK, Burger PC, Jouvet A, Scheithauer BW, Kleihues P (2007) The 2007 WHO classification of tumours of the central nervous system. Acta Neuropathol. 114:97–109. doi: 10.1007/s00401-007-0243-4

Lu W (2012) Adsorptive-mediated brain delivery systems. Curr Pharm Biotechnol 13:2340–2348. doi: 10.2174/138920112803341851

Lunt SY, Vander Heiden MG (2011) Aerobic glycolysis: meeting the metabolic requirements of cell proliferation. Annu. Rev. Cell Dev. Biol. 27:441–464. doi: 10.1146/annurev-cellbio-092910-154237

Mannion AF, Jakeman PM, Dunnett M, Harris RC, Willan PL (1992) Carnosine and anserine concentrations in the quadriceps femoris muscle of healthy humans. Eur J Appl Physiol Occup Physiol 64:47–50

Marchis S de, Modena C, Peretto P, Migheli A, Margolis FL, Fasolo A (2000) Carnosine-related dipeptides in neurons and glia. Biochemistry Mosc. 65:824–833

Margolis FL (1974) Carnosine in the primary olfactory pathway. Science 184:909–911. doi: 10.1126/science.184.4139.909

Masoud GN, Li W (2015) HIF-1α pathway: role, regulation and intervention for cancer therapy. Acta Pharm Sin B 5:378–389. doi: 10.1016/j.apsb.2015.05.007

Matsukura T, Tanaka H (2000) Applicability of zinc complex of L-carnosine for medical use. Biochemistry Mosc. 65:817–823

Mattaini KR, Sullivan MR, Vander Heiden MG (2016) The importance of serine metabolism in cancer. J Cell Biol 214:249–257. doi: 10.1083/jcb.201604085

McFate T, Mohyeldin A, Lu H, Thakar J, Henriques J, Halim ND, Wu H, Schell MJ, Tsang TM, Teahan O, Zhou S, Califano JA, Jeoung NH, Harris RA, Verma A (2008) Pyruvate dehydrogenase complex activity controls metabolic and malignant phenotype in cancer cells. J. Biol. Chem. 283:22700–22708. doi: 10.1074/jbc.M801765200

Mehrazad-Saber Z, Kheirouri S, Noorazar S-G (2018) Effects of l-Carnosine Supplementation on Sleep Disorders and Disease Severity in Autistic Children: A Randomized, Controlled Clinical Trial. Basic Clin Pharmacol Toxicol 123:72–77. doi: 10.1111/bcpt.12979

Momcilovic M, Shackelford DB (2018) Imaging Cancer Metabolism. Biomol Ther (Seoul) 26:81–92. doi: 10.4062/biomolther.2017.220

Morgan LL (2015) The epidemiology of glioma in adults: a "state of the science" review. Neuro-oncology 17:623–624. doi: 10.1093/neuonc/nou358

Morita M, Sato T, Nomura M, Sakamoto Y, Inoue Y, Tanaka R, Ito S, Kurosawa K, Yamaguchi K, Sugiura Y, Takizaki H, Yamashita Y, Katakura R, Sato I, Kawai M, Okada Y, Watanabe H, Kondoh G, Matsumoto S, Kishimoto A, Obata M, Matsumoto M, Fukuhara T, Motohashi H, Suematsu M, Komatsu M, Nakayama KI, Watanabe T, Soga T, Shima H, Maemondo M, Tanuma N (2018) PKM1 Confers Metabolic Advantages and Promotes Cell-Autonomous Tumor Cell Growth. Cancer Cell 33:355-367.e7. doi: 10.1016/j.ccell.2018.02.004

Muoio DM, MacLean PS, Lang DB, Li S, Houmard JA, Way JM, Winegar DA, Corton JC, Dohm GL, Kraus WE (2002) Fatty acid homeostasis and induction of lipid regulatory genes in skeletal muscles of peroxisome proliferator-activated receptor (PPAR) alpha knock-out mice. Evidence for

compensatory regulation by PPAR delta. J Biol Chem 277:26089–26097. doi: 10.1074/jbc.M203997200

Nagai K, Suda T (1986) [Antineoplastic effects of carnosine and beta-alanine--physiological considerations of its antineoplastic effects]. Nihon Seirigaku Zasshi 48:741–747

Nagai K, Suda T, Kawasaki K, Mathuura S (1986) Action of carnosine and beta-alanine on wound healing. Surgery 100:815–821

Nagai K, Tanida M, Niijima A, Tsuruoka N, Kiso Y, Horii Y, Shen J, Okumura N (2012) Role of l-carnosine in the control of blood glucose, blood pressure, thermogenesis, and lipolysis by autonomic nerves in rats: involvement of the circadian clock and histamine. Amino Acids 43:97–109. doi: 10.1007/s00726-012-1251-9

Naghshvar F, Abianeh SM, Ahmadashrafi S, Hosseinimehr SJ (2012) Chemoprotective effects of carnosine against genotoxicity induced by cyclophosphamide in mice bone marrow cells. Cell Biochem Funct 30:569–573. doi: 10.1002/cbf.2834

Nicoletti VG, Santoro AM, Grasso G, Vagliasindi LI, Giuffrida ML, Cuppari C, Purrello VS, Stella AMG, Rizzarelli E (2007) Carnosine interaction with nitric oxide and astroglial cell protection. J Neurosci Res 85:2239–2245. doi: 10.1002/jnr.21365

Nobusawa S, Watanabe T, Kleihues P, Ohgaki H (2009) IDH1 mutations as molecular signature and predictive factor of secondary glioblastomas. Clin. Cancer Res. 15:6002–6007. doi: 10.1158/1078-0432.CCR-09-0715

Numata Y, Terui T, Okuyama R, Hirasawa N, Sugiura Y, Miyoshi I, Watanabe T, Kuramasu A, Tagami H, Ohtsu H (2006) The Accelerating Effect of Histamine on the Cutaneous Wound-Healing Process Through the Action of Basic Fibroblast Growth Factor. Journal of Investigative Dermatology 126:1403–1409. doi: 10.1038/sj.jid.5700253

Ocheltree SM, Shen H, Hu Y, Xiang J, Keep RF, Smith DE (2004) Role of PEPT2 in the choroid plexus uptake of glycylsarcosine and 5-aminolevulinic acid: studies in wild-type and null mice. Pharm Res 21:1680–1685. doi: 10.1023/b:pham.0000041465.89254.05

O'Dowd A, Miller DJ (1998) Analysis of an H1 receptor-mediated, zinc-potentiated vasoconstrictor action of the histidyl dipeptide carnosine in rabbit saphenous vein. Br J Pharmacol 125:1272–1280. doi: 10.1038/sj.bjp.0702184

O'Dowd JJ, Robins DJ, Miller DJ (1988) Detection, characterisation, and quantification of carnosine and other histidyl derivatives in cardiac and skeletal muscle. Biochimica et Biophysica Acta (BBA) - General Subjects 967:241–249. doi: 10.1016/0304-4165(88)90015-3

Ogihara H, Saito H, Shin BC, Terado T, Takenoshita S, Nagamachi Y, Inui K, Takata K (1996) Immuno-localization of H+/peptide cotransporter in rat digestive tract. Biochem Biophys Res Commun 220:848–852

Ohgaki H, Kleihues P (2005) Epidemiology and etiology of gliomas. Acta Neuropathologica 109:93–108. doi: 10.1007/s00401-005-0991-y

Ohgaki H, Kleihues P (2013) The definition of primary and secondary glioblastoma. Clin. Cancer Res. 19:764–772. doi: 10.1158/1078-0432.CCR-12-3002

Ohgaki H, Dessen P, Jourde B, Horstmann S, Nishikawa T, Di Patre P-L, Burkhard C, Schüler D, Probst-Hensch NM, Maiorka PC, Baeza N, Pisani P, Yonekawa Y, Yasargil MG, Lütolf UM, Kleihues P (2004) Genetic pathways to glioblastoma: a population-based study. Cancer Res. 64:6892–6899. doi: 10.1158/0008-5472.CAN-04-1337

Ohgaki H, Burger P, Kleihues P (2014) Definition of primary and secondary glioblastoma--response. Clin. Cancer Res. 20:2013. doi: 10.1158/1078-0432.CCR-14-0238

References

Ohgaki H, Kleihues P, von Deimling A, Louis DN, Reifenberger G, Yan H, Weller M (2016) Glioblastoma, IDH-mutant. In: Louis DN, Ohgaki H, Wiestler OD, Cavenee WK (eds) WHO classification of tumours of the central nervous system, Revised 4th edition. International Agency for Research on Cancer, Lyon, pp 52–56

Oku T, Ando S, Tsai H-C, Yamashita Y, Ueno H, Shiozaki K, Nishi R, Yamada S (2012) Purification and identification of two carnosine-cleaving enzymes, carnosine dipeptidase I and Xaa-methyl-His dipeptidase, from Japanese eel (Anguilla japonica). Biochimie 94:1281–1290. doi: 10.1016/j.biochi.2012.02.016

Okumura N, Takao T (2017) The zinc form of carnosine dipeptidase 2 (CN2) has dipeptidase activity but its substrate specificity is different from that of the manganese form. Biochem Biophys Res Commun 494:484–490. doi: 10.1016/j.bbrc.2017.10.100

Oppermann H, Ding Y, Sharma J, Berndt Paetz M, Meixensberger J, Gaunitz F, Birkemeyer C (2016a) Metabolic response of glioblastoma cells associated with glucose withdrawal and pyruvate substitution as revealed by GC-MS. Nutr Metab (Lond) 13:519. doi: 10.1186/s12986-016-0131-9

Oppermann H, Schnabel L, Meixensberger J, Gaunitz F (2016b) Pyruvate attenuates the anti-neoplastic effect of carnosine independently from oxidative phosphorylation. Oncotarget. doi: 10.18632/oncotarget.13039

Oppermann H, Dietterle J, Purcz K, Morawski M, Eisenlöffel C, Müller W, Meixensberger J, Gaunitz F (2018) Carnosine selectively inhibits migration of IDH-wildtype glioblastoma cells in a co-culture model with fibroblasts. Cancer Cell Int 18:199. doi: 10.1186/s12935-018-0611-2

Oppermann H, Alvanos A, Seidel C, Meixensberger J, Gaunitz F (2019a) Carnosine influences transcription via epigenetic regulation as demonstrated by enhanced histone acetylation of the pyruvate dehydrogenase kinase 4 promoter in glioblastoma cells. Amino Acids 51:61–71. doi: 10.1007/s00726-018-2619-2

Oppermann H, Faust H, Yamanishi U, Meixensberger J, Gaunitz F (2019b) Carnosine inhibits glioblastoma growth independent from PI3K/Akt/mTOR signaling. PLoS ONE 14:e0218972. doi: 10.1371/journal.pone.0218972

Oppermann H, Purcz K, Birkemeyer C, Baran-Schmidt R, Meixensberger J, Gaunitz F (2019c) Carnosine's inhibitory effect on glioblastoma cell growth is independent of its cleavage. Amino Acids 51:761–772. doi: 10.1007/s00726-019-02713-6

Oppermann H, Birkemeyer C, Meixensberger J, Gaunitz F (2019d) Non-enzymatic reaction of carnosine and glyceraldehyde-3-phosphate accompanies metabolic changes of the pentose phosphate pathway. Cell Prolif 33:1902. doi: 10.1111/cpr.12702

Oppermann H, Heinrich M, Birkemeyer C, Meixensberger J, Gaunitz F (2019e) The proton-coupled oligopeptide transporters PEPT2, PHT1 and PHT2 mediate the uptake of carnosine in glioblastoma cells. Amino Acids. doi: 10.1007/s00726-019-02739-w

Ostrom QT, Bauchet L, Davis FG, Deltour I, Fisher JL, Langer CE, Pekmezci M, Schwartzbaum JA, Turner MC, Walsh KM, Wrensch MR, Barnholtz-Sloan JS (2014) The epidemiology of glioma in adults: a "state of the science" review. Neuro-oncology 16:896–913. doi: 10.1093/neuonc/nou087

Ostrom QT, Gittleman H, Truitt G, Boscia A, Kruchko C, Barnholtz-Sloan JS (2018) CBTRUS Statistical Report: Primary Brain and Other Central Nervous System Tumors Diagnosed in the United States in 2011-2015. Neuro-oncology 20:iv1-iv86. doi: 10.1093/neuonc/noy131

Park YJ, Volpe SL, Decker EA (2005) Quantitation of carnosine in humans plasma after dietary consumption of beef. J Agric Food Chem 53:4736–4739. doi: 10.1021/jf047934h

Patra KC, Hay N (2014) The pentose phosphate pathway and cancer. Trends Biochem Sci 39:347–354. doi: 10.1016/j.tibs.2014.06.005

Patra KC, Wang Q, Bhaskar PT, Miller L, Wang Z, Wheaton W, Chandel N, Laakso M, Muller WJ, Allen EL, Jha AK, Smolen GA, Clasquin MF, Robey B, Hay N (2013) Hexokinase 2 is required for tumor initiation and maintenance and its systemic deletion is therapeutic in mouse models of cancer. Cancer Cell 24:213–228. doi: 10.1016/j.ccr.2013.06.014

Pavlov AR, Revina AA, Dupin AM, Boldyrev AA, Yaropolov AI (1993) The mechanism of interaction of carnosine with superoxide radicals in water solutions. Biochimica et Biophysica Acta (BBA) - General Subjects 1157:304–312. doi: 10.1016/0304-4165(93)90114-N

Peng H, Du B, Jiang H, Gao J (2016) Over-expression of CHAF1A promotes cell proliferation and apoptosis resistance in glioblastoma cells via AKT/FOXO3a/Bim pathway. Biochem Biophys Res Commun 469:1111–1116. doi: 10.1016/j.bbrc.2015.12.111

Perel'man MI, Kornilova ZK, Paukova VS, Boikov AK, Priimak AA, Bulargina TV, Severin SE, Tikhonova GN (1989) Effect of carnosine on healing of lung wounds. Bull Exp Biol Med 108:1329–1333. doi: 10.1007/BF00839483

Perry TL, Hansen S, Stedman D, Love D (1968) Homocarnosine in human cerebrospinal fluid: an age-dependent phenomenon. J. Neurochem. 15:1203–1206. doi: 10.1111/j.1471-4159.1968.tb06838.x

Peters V, Jansen EEW, Jakobs C, Riedl E, Janssen B, Yard BA, Wedel J, Hoffmann GF, Zschocke J, Gotthardt D, Fischer C, Köppel H (2011) Anserine inhibits carnosine degradation but in human serum carnosinase (CN1) is not correlated with histidine dipeptide concentration. Clin. Chim. Acta 412:263–267. doi: 10.1016/j.cca.2010.10.016

Peters V, Klessens CQF, Baelde HJ, Singler B, Veraar KAM, Zutinic A, Drozak J, Zschocke J, Schmitt CP, Heer E de (2015) Intrinsic carnosine metabolism in the human kidney. Amino Acids 47:2541–2550. doi: 10.1007/s00726-015-2045-7

Pfeiffer T, Schuster S, Bonhoeffer S (2001) Cooperation and competition in the evolution of ATP-producing pathways. Science 292:504–507. doi: 10.1126/science.1058079

Psychogios N, Hau DD, Peng J, Guo AC, Mandal R, Bouatra S, Sinelnikov I, Krishnamurthy R, Eisner R, Gautam B, Young N, Xia J, Knox C, Dong E, Huang P, Hollander Z, Pedersen TL, Smith SR, Bamforth F, Greiner R, McManus B, Newman JW, Goodfriend T, Wishart DS (2011) The human serum metabolome. PLoS ONE 6:e16957. doi: 10.1371/journal.pone.0016957

Puthanveetil P, Wang Y, Wang F, Kim MS, Abrahani A, Rodrigues B (2010) The increase in cardiac pyruvate dehydrogenase kinase-4 after short-term dexamethasone is controlled by an Akt-p38-forkhead box other factor-1 signaling axis. Endocrinology 151:2306–2318. doi: 10.1210/en.2009-1072

Qiu J, Hauske SJ, Zhang S, Rodriguez-Niño A, Albrecht T, Pastene DO, van den Born J, van Goor H, Ruf S, Kohlmann M, Teufel M, Krämer BK, Hammes H-P, Peters V, Yard BA, Kannt A (2019) Identification and characterisation of carnostatine (SAN9812), a potent and selective carnosinase (CN1) inhibitor with in vivo activity. Amino Acids 51:7–16. doi: 10.1007/s00726-018-2601-z

Rajanikant GK, Zemke D, Senut M-C, Frenkel MB, Chen AF, Gupta R, Majid A (2007) Carnosine is neuroprotective against permanent focal cerebral ischemia in mice. Stroke 38:3023–3031. doi: 10.1161/STROKEAHA.107.488502

Rauen U, Klempt S, Groot H de (2007) Histidine-induced injury to cultured liver cells, effects of histidine derivatives and of iron chelators. Cell Mol Life Sci 64:192–205. doi: 10.1007/s00018-006-6456-1

References

Reardon DA, Omuro A, Brandes AA, Rieger J, Wick A, Sepulveda J, Phuphanich S, Souza P de, Ahluwalia MS, Lim M, Vlahovic G, Sampson J (2017) OS10.3 Randomized Phase 3 Study Evaluating the Efficacy and Safety of Nivolumab vs Bevacizumab in Patients With Recurrent Glioblastoma: CheckMate 143. Neuro-oncology 19:iii21-iii21. doi: 10.1093/neuonc/nox036.071

Reitman ZJ, Yan H (2010) Isocitrate dehydrogenase 1 and 2 mutations in cancer: alterations at a crossroads of cellular metabolism. J Natl Cancer Inst 102:932–941. doi: 10.1093/jnci/djq187

Renner C, Seyffarth A, de Arriba, Susana Garcia, Meixensberger J, Gebhardt R, Gaunitz F (2008) Carnosine Inhibits Growth of Cells Isolated from Human Glioblastoma Multiforme. Int J Pept Res Ther 14:127–135. doi: 10.1007/s10989-007-9121-0

Renner C, Asperger A, Seyffarth A, Meixensberger J, Gebhardt R, Gaunitz F (2010a) Carnosine inhibits ATP production in cells from malignant glioma. Neurol. Res. 32:101–105. doi: 10.1179/016164109X12518779082237

Renner C, Zemitzsch N, Fuchs B, Geiger KD, Hermes M, Hengstler J, Gebhardt R, Meixensberger J, Gaunitz F (2010b) Carnosine retards tumor growth in vivo in an NIH3T3-HER2/neu mouse model. Mol. Cancer 9:2. doi: 10.1186/1476-4598-9-2

Rieger J, Bahr O, Maurer GD, Hattingen E, Franz K, Brucker D, Walenta S, Kammerer U, Coy JF, Weller M, Steinbach JP (2014) ERGO: a pilot study of ketogenic diet in recurrent glioblastoma. Int J Oncol 44:1843–1852. doi: 10.3892/ijo.2014.2382

Rohrig F, Schulze A (2016) The multifaceted roles of fatty acid synthesis in cancer. Nat Rev Cancer. doi: 10.1038/nrc.2016.89

Ross K, Jones RJ (2017) Immune checkpoint inhibitors in renal cell carcinoma. Clin Sci (Lond) 131:2627–2642. doi: 10.1042/CS20160894

Rybakova Y, Akkuratov E, Kulebyakin K, Brodskaya O, Dizhevskaya A, Boldyrev A (2013) Receptor-mediated Oxidative Stress in Murine Cerebellar Neurons is Accompanied by Phosphorylation of MAP (ERK 1/2) Kinase. CAS 5:225–230. doi: 10.2174/1874609811205030009

Rybakova YS, Boldyrev AA (2012) Effect of carnosine and related compounds on proliferation of cultured rat pheochromocytoma PC-12 cells. Bull. Exp. Biol. Med. 154:136–140

Rybakova YS, Kalen AL, Eckers JC, Fedorova TN, Goswami PC, Sarsour EH (2015) Increased manganese superoxide dismutase and cyclin B1 expression in carnosine-induced inhibition of glioblastoma cell proliferation. Biochem. Moscow Suppl. Ser. B 9:63–71. doi: 10.1134/S1990750815010096

Sahm F, Capper D, Jeibmann A, Habel A, Paulus W, Troost D, Deimling A von (2012) Addressing diffuse glioma as a systemic brain disease with single-cell analysis. Arch Neurol 69:523–526. doi: 10.1001/archneurol.2011.2910.

Sakata K, Yamashita T, Maeda M, Moriyama Y, Shimada S, Tohyama M (2001) Cloning of a lymphatic peptide/histidine transporter. Biochem J 356:53–60

Sale C, Saunders B, Harris RC (2010) Effect of beta-alanine supplementation on muscle carnosine concentrations and exercise performance. Amino Acids 39:321–333. doi: 10.1007/s00726-009-0443-4

Sanderink GJ, Artur Y, Siest G (1988) Human aminopeptidases: a review of the literature. J Clin Chem Clin Biochem 26:795–807

Sant M, Minicozzi P, Lagorio S, Børge Johannesen T, Marcos-Gragera R, Francisci S (2012) Survival of European patients with central nervous system tumors. Int J Cancer 131:173–185. doi: 10.1002/ijc.26335

Sasawatari S, Okamura T, Kasumi E, Tanaka-Furuyama K, Yanobu-Takanashi R, Shirasawa S, Kato N, Toyama-Sorimachi N (2011) The solute carrier family 15A4 regulates TLR9 and NOD1 functions in

References

the innate immune system and promotes colitis in mice. Gastroenterology 140:1513–1525. doi: 10.1053/j.gastro.2011.01.041

Sassoè-Pognetto M, Cantino D, Panzanelli P, Di Verdun Cantogno L, Giustetto M, Margolis FL, Biasi S de, Fasolo A (1993) Presynaptic co-localization of carnosine and glutamate in olfactory neurones. Neuroreport 5:7–10. doi: 10.1097/00001756-199310000-00001

Saxton RA, Sabatini DM (2017) mTOR Signaling in Growth, Metabolism, and Disease. Cell 168:960–976. doi: 10.1016/j.cell.2017.02.004

Schön M, Mousa A, Berk M, Chia WL, Ukropec J, Majid A, Ukropcová B, Courten B de (2019) The Potential of Carnosine in Brain-Related Disorders: A Comprehensive Review of Current Evidence. Nutrients 11. doi: 10.3390/nu11061196

Schug ZT, Peck B, Jones DT, Zhang Q, Grosskurth S, Alam IS, Goodwin LM, Smethurst E, Mason S, Blyth K, McGarry L, James D, Shanks E, Kalna G, Saunders RE, Jiang M, Howell M, Lassailly F, Thin MZ, Spencer-Dene B, Stamp G, van den Broek NJF, Mackay G, Bulusu V, Kamphorst JJ, Tardito S, Strachan D, Harris AL, Aboagye EO, Critchlow SE, Wakelam MJO, Schulze A, Gottlieb E (2015) Acetyl-CoA synthetase 2 promotes acetate utilization and maintains cancer cell growth under metabolic stress. Cancer Cell 27:57–71. doi: 10.1016/j.ccell.2014.12.002

Seiki M, Ueki S, Tanaka Y, Soeda M, Hori Y, Aita H, Yoneta T, Morita H, Tagashira E, Okabe S (1990) Studies on anti-ulcer effects of a new compound, zinc L-carnosine (Z-103). Nippon Yakurigaku Zasshi 95:257–269. doi: 10.1254/fpj.95.5_257

Shen Y, Yang J, Li J, Shi X, Ouyang L, Tian Y, Lu J (2014) Carnosine inhibits the proliferation of human gastric cancer SGC-7901 cells through both of the mitochondrial respiration and glycolysis pathways. PLoS ONE 9:e104632. doi: 10.1371/journal.pone.0104632

Smith EC (1938) The buffering of muscle in rigor; protein, phosphate and carnosine. J. Physiol. (Lond.) 92:336–343

Smith DE, Clémençon B, Hediger MA (2013) Proton-coupled oligopeptide transporter family SLC15: physiological, pharmacological and pathological implications. Mol Aspects Med 34:323–336. doi: 10.1016/j.mam.2012.11.003

Son DO, Satsu H, Kiso Y, Totsuka M, Shimizu M (2008) Inhibitory effect of carnosine on interleukin-8 production in intestinal epithelial cells through translational regulation. Cytokine 42:265–276. doi: 10.1016/j.cyto.2008.02.011

Spitz DR, Hauer-Jensen M (2014) Ionizing Radiation-Induced Responses: Where Free Radical Chemistry Meets Redox Biology and Medicine. Antioxid Redox Signal 20:1407–1409. doi: 10.1089/ars.2013.5769

Stein WH, Moore S (1954) The free amino acids of human blood plasma. J. Biol. Chem. 211:915–926

Stummer W, Pichlmeier U, Meinel T, Wiestler OD, Zanella F, Reulen H-J (2006) Fluorescence-guided surgery with 5-aminolevulinic acid for resection of malignant glioma: a randomised controlled multicentre phase III trial. The Lancet Oncology 7:392–401. doi: 10.1016/S1470-2045(06)70665-9

Stupp R, Taillibert S, Kanner A, Read W, Steinberg DM, Lhermitte B, Toms S, Idbaih A, Ahluwalia MS, Fink K, Di Meco F, Lieberman F, Zhu J-J, Stragliotto G, Tran DD, Brem S, Hottinger AF, Kirson ED, Lavy-Shahaf G, Weinberg U, Kim C-Y, Paek S-H, Nicholas G, Burna J, Hirte H, Weller M, Palti Y, Hegi ME, Ram Z (2017) Effect of Tumor-Treating Fields Plus Maintenance Temozolomide vs Maintenance Temozolomide Alone on Survival in Patients With Glioblastoma: A Randomized Clinical Trial. JAMA 318:2306–2316

Suyama M, Maruyama M (1969) Identification of methylated beta-alanylhistidine in the muscles of snake and dolphin. J Biochem 66:405–407. doi: 10.1093/oxfordjournals.jbchem.a129159

References

Suzuki A, Kobayashi R, Shakui T, Kubota Y, Fukita M, Kuze B, Aoki M, Sugiyama T, Mizuta K, Itoh Y (2016) Effect of polaprezinc on oral mucositis, irradiation period, and time to discharge in patients with head and neck cancer. Head Neck 38:1387–1392. doi: 10.1002/hed.24446

Szcześniak D, Budzeń S, Kopeć W, Rymaszewska J (2014) Anserine and carnosine supplementation in the elderly: Effects on cognitive functioning and physical capacity. Arch Gerontol Geriatr 59:485–490. doi: 10.1016/j.archger.2014.04.008

Szwergold BS (2005) Carnosine and anserine act as effective transglycating agents in decomposition of aldose-derived Schiff bases. Biochem. Biophys. Res. Commun. 336:36–41. doi: 10.1016/j.bbrc.2005.08.033

Takahashi S, Nakashima Y, Toda K-I (2009) Carnosine facilitates nitric oxide production in endothelial f-2 cells. Biol Pharm Bull 32:1836–1839. doi: 10.1248/bpb.32.1836

Tamba M, Torreggiani A (1998) A pulse radiolysis study of carnosine in aqueous solution. Int J Radiat Biol 74:333–340. doi: 10.1080/095530098141474

Tardito S, Oudin A, Ahmed SU, Fack F, Keunen O, Zheng L, Miletic H, Sakariassen PØ, Weinstock A, Wagner A, Lindsay SL, Hock AK, Barnett SC, Ruppin E, Mørkve SH, Lund-Johansen M, Chalmers AJ, Bjerkvig R, Niclou SP, Gottlieb E (2015) Glutamine synthetase activity fuels nucleotide biosynthesis and supports growth of glutamine-restricted glioblastoma. Nat Cell Biol 17:1556–1568. doi: 10.1038/ncb3272

Tehrani MHH, Bamoniri A, Gholibeikian M (2018) The toxicity study of synthesized inverse carnosine peptide analogues on HepG2 and HT-29 cells. Iran J Basic Med Sci 21:39–46. doi: 10.22038/IJBMS.2017.23153.5852

Teufel M, Saudek V, Ledig J-P, Bernhardt A, Boularand S, Carreau A, Cairns NJ, Carter C, Cowley DJ, Duverger D, Ganzhorn AJ, Guenet C, Heintzelmann B, Laucher V, Sauvage C, Smirnova T (2003) Sequence identification and characterization of human carnosinase and a closely related non-specific dipeptidase. J. Biol. Chem. 278:6521–6531. doi: 10.1074/jbc.M209764200

Tiedje KE, Stevens K, Barnes S, Weaver DF (2010) Beta-alanine as a small molecule neurotransmitter. Neurochem Int 57:177–188. doi: 10.1016/j.neuint.2010.06.001

Ueda J-i, Ozawa T, Miyazaki M, Fujiwara Y (1993) SOD-like activity of complexes of nickel(II) ion with some biologically important peptides and their novel reactions with hydrogen peroxide. Inorganica Chimica Acta 214:29–32. doi: 10.1016/S0020-1693(00)87522-2

Vander Heiden MG, Cantley LC, Thompson CB (2009) Understanding the Warburg effect: the metabolic requirements of cell proliferation. Science 324:1029–1033. doi: 10.1126/science.1160809

Warburg O, Wind F, Negelein E (1927) THE METABOLISM OF TUMORS IN THE BODY. J Gen Physiol 8:519–530

Warburg O (1956) On the origin of cancer cells. Science 123:309–314

Wasternack C (1978) Degradation of Pyrimidines — Enzymes, Localization and Role in Metabolism. Biochemie und Physiologie der Pflanzen 173:467–499. doi: 10.1016/S0015-3796(17)30527-9

Watanabe T, Ishihara M, Matsuura K, Mizuta K, Itoh Y (2010) Polaprezinc prevents oral mucositis associated with radiochemotherapy in patients with head and neck cancer. Int J Cancer 127:1984–1990. doi: 10.1002/ijc.25200

Watson J, Degnan B, Degnan S, Kromer JO (2014) Determining the biomass composition of a sponge holobiont for flux analysis. Methods Mol Biol 1191:107–125. doi: 10.1007/978-1-4939-1170-7_7

Weigand T, Singler B, Fleming T, Nawroth P, Klika KD, Thiel C, Baelde H, Garbade SF, Wagner AH, Hecker M, Yard BA, Amberger A, Zschocke J, Schmitt CP, Peters V (2018) Carnosine Catalyzes the

Formation of the Oligo/Polymeric Products of Methylglyoxal. Cell Physiol Biochem 46:713–726. doi: 10.1159/000488727

Weller M, van den Bent M, Hopkins K, Tonn JC, Stupp R, Falini A, Cohen-Jonathan-Moyal E, Frappaz D, Henriksson R, Balana C, Chinot O, Ram Z, Reifenberger G, Soffietti R, Wick W (2014) EANO guideline for the diagnosis and treatment of anaplastic gliomas and glioblastoma. The Lancet Oncology 15:e395-e403. doi: 10.1016/S1470-2045(14)70011-7

Wen PY, Kesari S (2008) Malignant gliomas in adults. N. Engl. J. Med. 359:492–507. doi: 10.1056/NEJMra0708126

Wende AR, Huss JM, Schaeffer PJ, Giguère V, Kelly DP (2005) PGC-1alpha coactivates PDK4 gene expression via the orphan nuclear receptor ERRalpha: a mechanism for transcriptional control of muscle glucose metabolism. Mol Cell Biol 25:10684–10694. doi: 10.1128/MCB.25.24.10684-10694.2005

Westphal M, Heese O, Steinbach JP, Schnell O, Schackert G, Mehdorn M, Schulz D, Simon M, Schlegel U, Senft C, Geletneky K, Braun C, Hartung JG, Reuter D, Metz MW, Bach F, Pietsch T (2015) A randomised, open label phase III trial with nimotuzumab, an anti-epidermal growth factor receptor monoclonal antibody in the treatment of newly diagnosed adult glioblastoma. Eur J Cancer 51:522–532. doi: 10.1016/j.ejca.2014.12.019

Wise DR, DeBerardinis RJ, Mancuso A, Sayed N, Zhang X-Y, Pfeiffer HK, Nissim I, Daikhin E, Yudkoff M, McMahon SB, Thompson CB (2008) Myc regulates a transcriptional program that stimulates mitochondrial glutaminolysis and leads to glutamine addiction. Proc Natl Acad Sci U S A 105:18782–18787. doi: 10.1073/pnas.0810199105

Yamashita S, Sato M, Matsumoto T, Kadooka K, Hasegawa T, Fujimura T, Katakura Y (2018) Mechanisms of carnosine-induced activation of neuronal cells. Biosci Biotechnol Biochem 82:683–688. doi: 10.1080/09168451.2017.1413325

Yanase K, Funaguchi N, Iihara H, Yamada M, Kaito D, Endo J, Ito F, Ohno Y, Tanaka H, Itoh Y, Minatoguchi S (2015) Prevention of radiation esophagitis by polaprezinc (zinc L-carnosine) in patients with non-small cell lung cancer who received chemoradiotherapy. Int J Clin Exp Med 8:16215–16222

Yates AJ, Thompson DK, Boesel CP, Albrightson C, Hart RW (1979) Lipid composition of human neural tumors. J Lipid Res 20:428–436

Yehia R, Saleh S, El Abhar H, Saad AS, Schaalan M (2019) L-Carnosine protects against Oxaliplatin-induced peripheral neuropathy in colorectal cancer patients: A perspective on targeting Nrf-2 and NF-κB pathways. Toxicol Appl Pharmacol 365:41–50. doi: 10.1016/j.taap.2018.12.015

Yeung SJ, Pan J, Lee M-H (2008) Roles of p53, MYC and HIF-1 in regulating glycolysis - the seventh hallmark of cancer. Cell. Mol. Life Sci. 65:3981–3999. doi: 10.1007/s00018-008-8224-x

Yoshikawa T, Naito Y, Tanigawa T, Yoneta T, Kondo M (1991) The antioxidant properties of a novel zinc-carnosine chelate compound, N-(3-aminopropionyl)-l-histidinato zinc. Biochimica et Biophysica Acta (BBA) - General Subjects 1115:15–22. doi: 10.1016/0304-4165(91)90005-2

Zachar Z, Marecek J, Maturo C, Gupta S, Stuart SD, Howell K, Schauble A, Lem J, Piramzadian A, Karnik S, Lee K, Rodriguez R, Shorr R, Bingham PM (2011) Non-redox-active lipoate derivates disrupt cancer cell mitochondrial metabolism and are potent anticancer agents in vivo. J. Mol. Med. 89:1137–1148. doi: 10.1007/s00109-011-0785-8

Zhang L, Yao K, Fan Y, He P, Wang X, Hu W, Chen Z (2012) Carnosine protects brain microvascular endothelial cells against rotenone-induced oxidative stress injury through histamine H_1 and H_2 receptors in vitro. Clin Exp Pharmacol Physiol 39:1019–1025. doi: 10.1111/1440-1681.12019

Zhang Z, Miao L, Wu X, Liu G, Peng Y, Xin X, Jiao B, Kong X (2014) Carnosine Inhibits the Proliferation of Human Gastric Carcinoma Cells by Retarding Akt/mTOR/p70S6K Signaling. J Cancer 5:382–389. doi: 10.7150/jca.8024

Zhao W, Prijic S, Urban BC, Tisza MJ, Zuo Y, Li L, Tan Z, Chen X, Mani SA, Chang JT (2016) Candidate Antimetastasis Drugs Suppress the Metastatic Capacity of Breast Cancer Cells by Reducing Membrane Fluidity. Cancer Res 76:2037–2049. doi: 10.1158/0008-5472.CAN-15-1970

Zuccoli G, Marcello N, Pisanello A, Servadei F, Vaccaro S, Mukherjee P, Seyfried TN (2010) Metabolic management of glioblastoma multiforme using standard therapy together with a restricted ketogenic diet: Case Report. Nutr Metab (Lond) 7:33. doi: 10.1186/1743-7075-7-33

5 Appendix

5.1 Eidesstattliche Erklärungen zur vorgelegten Habilitationsschrift

Hiermit erkläre ich an Eides statt,

1. dass die vorliegende Habilitationsordnung der Medizinischen Fakultät der Universität Leipzig anerkannt wird;

2. dass die Habilitationsschrift in dieser oder ähnlicher Form an keiner anderen Stelle zum Zweck eines Graduierungsverfahrens vorgelegt wurde (ggf. eine Erklärung über frühere Habilitationsversuche unter Angabe von Ort, Zeit, Fakultät sowie Titel der Schrift);

3. dass die Habilitationsschrift selbstständig verfasst und keine anderen als die angegebenen Quellen und Hilfsmittel benutzt wurden;

4. dass die Einhaltung der „Satzung der Universität Leipzig zur Sicherung guter wissenschaftlicher Praxis" in der Erstfassung vom 17. April 2015 Grundlage der Forschungstätigkeit war.

....

Datum   Unterschrift

5.3 Danksagung